Lehrstuhl für Steuerungs- und Regelungstechnik
Technische Universität München
Univ.-Prof. Dr.-Ing./Univ. Tokio Martin Buss

Interactive Maneuver Prediction and Planning for Highly Automated Driving Functions

Mohammad Bahram

Vollständiger Abdruck der von der Fakultät für Elektrotechnik und Informationstechnik der Technischen Universität München zur Erlangung des akademischen Grades eines

Doktor-Ingenieurs (Dr.-Ing.)

genehmigten Dissertation.

Vorsitzender:	Prof. Dr.-Ing. Eckehard Steinbach

Prüfer der Dissertation:

1. Prof. Dr.-Ing. habil. Dirk Wollherr
2. Prof. Dr.-Ing. Fritz Busch

Die Dissertation wurde am 04.10.2016 bei der Technischen Universität München eingereicht und durch die Fakultät für Elektrotechnik und Informationstechnik am 22.02.2017 angenommen.

Foreword

This thesis summarizes the results of three years research as a doctoral student at the BMW Group Research and Technology in Munich.

My sincere thanks go to Prof. Dr.-Ing. habil. Dirk Wollherr from the Chair of Automatic Control Engineering (LSR) of the Technische Universität München for supervising my doctoral thesis and for all his valuable advice. Furthermore, special thanks go to Dr. Werner Huber, who initiated this thesis at the BMW Group Research and Technology and who supported me in all aspects during these three years.

Certainly, this thesis would not have been possible without the supervision and support of Michael Aeberhard and Sebastian Rauch, who encouraged me in numerous discussions, meetings and test drives. Moreover, I would like to thank all colleagues for their helpfulness and for providing a great working atmosphere.

Additionally, I want to thank Anton Wolf, Artur Lohrer, Jasper Friedrichs, Constantin Hubmann, Zahra Ghandeharioun, Erbatur Cagatay, Fabian Hanke, Yupeng Wu and Dominik Bayerl, who supported me by means of their theses and internships in our department.

Finally, I would like to express my deep gratitude to my parents and to Gelareh who always had faith in me and supported me particularly in critical phases. Without their strong affection, understanding and unconditional love, this work would not have been possible.

May no more traffic accidents take away family happiness.

Munich, August 2016 Mohammad Bahram

تقدیم به صاحب چشمانی که آرامش قلب من است و صدایش دلنشین‌ترین ترانه من است

تقدیم به تنها عشق زندگیم

آرزو

Contents

Notations

Abbreviations

ACC	Active Cruise Control system
ADAS	Advanced Driver Assistance Systems
AGV	Automated Guided Vehicles
AUC	Area Under Curve
BMW	Bayerische Motoren Werke
CO	Combinatorial Optimization
DAMN	Distributed Architecture for Mobile Navigation
DARPA	Defense Advanced Research Projects Agency
DHA	Discrete Hybrid Automaton
EG	Event Generator
FPR	False Positive Rate
FSM	Finite State Machine
GM	General Motors Company
GPS	Global Positioning System
HAD	Highly Automated Driving
HAV	Highly Automated Vehicles
HMI	Human-Machine-Interaction
HYSDEL	HYbrid System DEscription Language
IDM	Intelligent Driver Model
LCL	Lane Change to Left
LCR	Lane Change to Right
LK	Lane Keeping
LP	Linear Program
MIQP	Mixed-Integer Quadratic Program
MLD	Mixed Logical Dynamical System
MOMDP	Mixed Observability Markov Decision Processes
MPC	Model Predictive Control
MS	Mode Selector
POMDP	Partially Observable Markov Decision Process
PWA	Piecewise Affine System
QP	Quadratic Program
ROC	Receiver Operating Characteristic
ROS	Robot Operation System
SAE	The Society of Automotive Engineers
SAS	Switched Affine System

SIL	Software in the Loop
StVO	German Traffic Regulations (*Straßenverkehrs-Ordnung*)
TAP	Temporary Auto Pilot
TET	Time Exposed Time to collision
TIV	Intervehicular Time
TIT	Time Integrated Time to collision
TOR	(Driver) Take Over Request
TPR	True Positive Rate
TTC	Time To Collision

Most Relevant Symbols

Interaction-aware Traffic Scene Prediction

$a_{\text{decel,max}}$	Maximum deceleration
$a_{\text{decel,min}}$	Minimum deceleration
$\mathbf{c}_v^t$	Contextual state vector of the evaluated vehicle
d_0	Distance to the target object at the moment of crossing the lane markings
$d(t)$	Distance to the target object at the discrete time step t
d_{decel}	Distance to the target object at the beginning of braking
δ_t	Prediction time
Δ_t	Prediction step size
Δv_{decel}	Speed difference between the host vehicle and the target object at the beginning of braking
$\mathbf{f}_v^t$	Interaction-aware acceleration (resp. deceleration)
F_1	F_1 score
$\mathcal{F}_v$	Multidimensional conditionally dependent feature vector
$\hat{\mathcal{F}}_v$	Multidimensional conditionally independent feature vector
$\mathcal{I}_v^{t:t+T}$	Predicted non-observable future driver intention of the evaluated vehicle
$\mathbf{k}$	Dynamic constraints vector
λ_i	Weighting factors of cost functions
$m_{\text{lat},v}$	Lateral motion of the evaluated vehicle
$m_{\text{long},v}$	Longitudinal motion of the evaluated vehicle
$m_{j,v}^t$	j-th basic maneuver of the v-th vehicle at the discrete time step t
$\mathcal{M}_v^t$	Finite set of basic maneuvers which belongs to the evaluated vehicle
$\mathcal{M}_{\text{lat}}$	Discrete set of feasible lateral movements on highways
$\mathcal{M}_{\text{long}}$	Discrete set of feasible longitudinal movements on highways
$\boldsymbol{\pi}_v$	Predicted maneuver sequence of the evaluated vehicle
$\mathbf{\Pi}_v$	Finite set of maneuver sequences of the evaluated vehicle
$\mathbf{X}_v^{t-n:t}$	Last n measured dynamic states up to the current time t of the evaluated vehicle
$\mathcal{X}^{t-n:t}$	Finite set of last n measured dynamic states of all vehicles in the current traffic scene up to the current time t
$P_{\pm1,\text{max}}$	Maximum joint probability for the lane change maneuvers
$P_{\pm1,\text{min}}$	Minimum joint probability for the lane change maneuvers

$\bar{P}_{\mathrm{LC}}$	Average of interaction-aware lane change joint probabilities over all the test samples
$\bar{P}_{\mathrm{LCL}}$	Average of interaction-aware lane change to the left joint probabilities over all the test samples
$\bar{P}_{\mathrm{LCR}}$	Average of interaction-aware lane change to the right joint probabilities over all the test samples
T	Prediction horizon
$\mathbf{U}_v^t(x,y)$	Spatio-temporal cost map in the two-dimensional Cartesian space at the predicted time step t
u_i	Corresponding cost function
v'	Relevant traffic from the perspective of the evaluated vehicle
$\mathbf{x}_v^t$	Multivariate normally distributed state vector of the evaluated vehicle at the time step t

Basic Behavioral Strategy

$a_{\mathrm{long},v}^{k+j\|k}$	Interaction-aware longitudinal acceleration of the v-th vehicle at the corresponding prediction step
Δt_{p_j}	Interval in seconds between the prediction instances
g_{TFC}	The dynamic model of the traffic
g_{Host}	The dynamic model of the host vehicle
H_c	Control horizon
H_p	Prediction horizon
$\mathcal{I}_v^{k+j\|k}$	Interaction-aware lateral maneuver intention of the v-th vehicle at the corresponding prediction step
j	Prediction instance
$l_{\max}$	Maximum number of lanes
Φ	Objective function
$\pi_1^{*k+j\|k}$	Optimal maneuver at the corresponding prediction step
$\pi_2^{*k+j\|k}$	Optimal velocity at the corresponding prediction step
Π^{*k}	Optimal policy sequence (resp. driving goals)
$r_{\mathrm{ttc/tiv}}^{k+j\|k}$	Risk based on the TTC and TIV
$\boldsymbol{\mathcal{U}}_{\mathrm{Host}}^{k+j\|k}$	Feasible solution space of the host control input
v_{des}	Desired speed of the host vehicle
$\mathbf{x}_v^{k+j\|k}$	The j-th predicted state vector of the v-th vehicle at the k-th replanning time instance
y_{des}	Lateral position of the desired lane

Cooperative Behavioral Strategy

Γ	The quintuple which defines the interactive maneuver planning based on extensive-form game
I	The information sets
$\mathcal{M}$	Finite set of basic maneuvers
π_{Host}^{*T}	Interactive maneuver sequence (resp. driving goals) of the host vehicle

Π_v^t	The set of maneuver sequences of the v-th vehicle over several time steps
$\mathcal{P}_{\text{Host}}^t$	The set of prediction scenes
$\mathcal{P}_{x,\pi_{\text{Host}}}^t$	The set of host-dependent prediction scenes of the traffic participant x
$\mathcal{P}_{\text{Host}\setminus v}^t$	The set of predicted scenes from the perspective of the host vehicle, excluding the evaluated vehicle v
$P_{\nleftrightarrow}(.)$	The interaction-unaware a priori maneuver probability
$P_{\leftrightarrow}(.)$	The interaction-aware maneuver probability
$\mathcal{S}_{\pi_{\text{Host}}}^t$	The set of planning scenes
R	Conditional collision risk of different maneuvers
T	Planning horizon
U^t	The set of payoffs belonging to each maneuver sequence of the host vehicle

Driver Take Over Behavioral Strategy

d_{TOR}	Traveled distance during TOR phase
S_{Auto}	Automated driving mode
S_{TOR}	The state of the vehicle during the TOR phase
S_{Safe}	The safe state of the vehicle
S_{Manuel}	The state for the manual driving mode
T_{TOR}	TOR time interval
$t_{\text{TOR,s}}$	Start time of the TOR phase
$t_{\text{TOR,e}}$	End time of the TOR phase

Abstract

Advances in computational power and sensor technology have changed the way technical systems work during the last century. Today, "intelligent systems" are affecting almost every aspect of our lives. The transportation systems are no exception to this trend. The increasing automation of driver assistance and active safety systems facilitates driver support in critical situations even today. At this, highly automated driving offers entirely new possibilities.

In this thesis, a novel interactive maneuver prediction and planning for highly automated driving functions for highways is presented. The main contributions of this thesis are multiple. First, a novel *hierarchical decision network* is presented which implements the continuous decision-making process of a human driver by determining a discrete set of different *behavioral strategies*. Each behavior implements a suitable *model predictive maneuver planning* for the specific traffic situation. Second in order to enable proactive maneuver planning, a robust and computationally efficient maneuver prediction of all the traffic participants is required. This novel interaction-aware maneuver prediction framework is implemented based on a combined model- and learning-based approach.

The functional architecture of the tactical decision-making process, the novel traffic scene prediction framework and the different behavioral strategies based on model predictive maneuver planning provide together the complex artificial intelligence framework of the automated driving functions. This novel approach offers benefits in terms of flexible and modular functional development and allowing distributed computing. Further improvements of the intelligence can be done by defining a new behavior and adapting its decision-making process to handle its specific requirements and objectives.

Finally, a novel framework for impact assessment based on *microscopic traffic simulation* is developed which allows simulative study of the questions about the overall impact of automated driving on traffic safety and traffic efficiency.

Zusammenfassung

Die Fortschritte in der Rechenleistung und Sensortechnik im letzten Jahrhundert haben die Art und Weise wie die technischen Systeme funktionieren grundlegend verändert. Heute beeinflussen "intelligente Systeme" fast jeden Aspekt unseres Lebens. Die Transportsysteme sind keine Ausnahme von diesem Trend. Die zunehmende Automatisierung von Fahrerassistenz- und aktive Sicherheitssystemen unterstützt immer mehr die Fahrer in kritischen Situationen, hierbei bietet das hochautomatisierte Fahren völlig neue Einsatzmöglichkeiten.

Im Rahmen dieser Dissertation wird eine neuartige interaktive Manöverprädiktion und Manöverplanung für das hochautomatisierte Fahren auf Autobahnen vorgestellt. Die wichtigsten Beiträge dieser Arbeit sind daher vielfältig. Zunächst wird ein neuartiges *hierarchisches Entscheidungsnetzwerk* vorgestellt, welches den kontinuierlichen Entscheidungsfindungsprozess eines menschlichen Fahrers anhand der diskreten *Verhaltensstrategien* realisiert. Jede Verhaltensstrategie implementiert eine geeignete *modellprädiktive Manöverplanung* für die gegebene Verkehrssituation. Um die vorausschauende Manöverplanung zu ermöglichen, ist eine robuste und effiziente Manöverprädiktion

aller umgebenden Verkehrsteilnehmer erforderlich. In dieser Arbeit wird das neuartige Manöverprädiktion-Framework auf der Basis eines kombinierten modell- und lernbasierten Ansatzes implementiert.

Die funktionale Architektur des taktischen Entscheidungsfindungsprozesses, das neuartige Manöverprädiktion-Framework und die unterschiedlichen Verhaltensstrategien auf Basis der modellprädiktiven Manöverplanung ermöglichen zusammen die komplexe künstliche Intelligenz der automatisierten Fahrfunktion. Dieser neuartige Ansatz bietet viele Vorteile in Bezug auf Flexibilität und modulare Funktionsentwicklung sowie verteilte Rechenleistung. Eine weitere Erweiterung der Intelligenz kann anhand der Definition einer neuen Verhaltensstrategie und der Anpassung dessen Entscheidungsfindungsprozess realisiert werden.

Zum Schluss wird ein neues Framework für die Folgenabschätzung der automatisierten Fahrfunktion auf Basis von *mikroskopischer Verkehrssimulation* entwickelt. Das Framework ermöglicht u. a. die simulative Untersuchung der Auswirkungen des automatisierten Fahrens auf die Verkehrssicherheit und Verkehrseffizienz.

List of Figures

List of Tables

1 Introduction

Advances in computational power and sensor technology have changed the way technical systems work during the last century. Today, "intelligent systems" are affecting almost every aspect of our lives. The transportation systems are no exception to this trend. Since the 1930s, automated driving has been a vision for future mobility. Norman Bel Geddes, one of the most prominent U.S. pioneers for automated mobility concepts, presented in 1939 at the New York World's Fair his ideas for future traffic systems in 1959 [50]. The exhibit, called *Futurama*, was sponsored by the General Motors Company (GM). Figure 1.1 shows parts of his huge model, where two 14-lane highways are crossing with driver-less vehicles controlled via radio. He also predicted big things for cars 20 years later [58]:

"*These cars of 1960 and the highways on which they drive will have in them devices which will correct the faults of human beings as drivers. They will prevent the driver from committing errors. They will prevent his turning out into traffic except when he should. They will aid him in passing through intersections without slowing down or causing anyone else to do so and without endangering himself or others.*"

Although Gedde's vision never became true, it was the beginning of countless projects in this research field around the world until to the present day.

The objective of automated driving is approached mainly from two different directions. On the one hand, the automotive industry tries to reach this goal from the practical and economical point of views. Starting with basic driver assistance systems like a simple cruise control in the late 1950s [181], the automotive industry is continuously increasing the degree of automation by development of various *advanced driver assistance systems* (ADAS). These systems thus became one of the fast-growing segments in automotive electronics [131]. On the other hand, the robotic researchers, who are working on algorithms

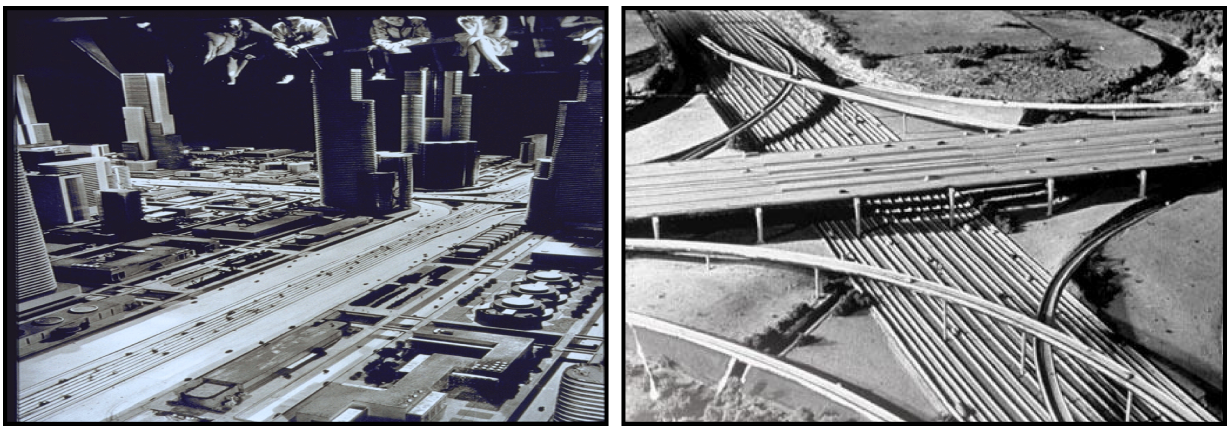

Fig. 1.1: Two parts of the GM Exhibit, *Futurama*, at the New York World's Fair in 1939. Image source: [173]

dealing with environment perception and artificial intelligence, try to realize different applications of autonomous systems beside driver-less transportation systems. Therefore, one of the big challenges nowadays is to combine the best of these two worlds.

Besides the ADAS in most of the production vehicles, such as anti-lock braking system (ABS), electronic stability control (ESC), brake assistant or lane change assistant [181], highly automated driving (HAD) is attracting the most attention in recent years. The functions, such as automatic parking, traffic jam assistant or emergency stop assistant have in common, that some parts of individual vehicle controls are accomplished by the system. The introduction of automated driving currently finds itself in a critical time, where the technology is able to take over control, in theory, of all driving control inputs (steering, brakes, gas, blinker, etc.), but in practice the systems are still in their infancy and must heavily rely on the driver in situations where a system limit is reached. Unlike ACC or traffic jam assistant, where the driver is continuously in control, automated driving systems may give the driver the impression that the vehicle can drive completely autonomously, even though there are still many limits.

In Germany, the Federal Highway Research Institute (*Bundesanstalt für Straßenwesen* (BASt)) [147], and internationally the Society of Automotive Engineers (SAE) [135], have defined various levels of vehicle automation in order to differentiate the responsibilities between the driver and an automated driving system.

Considering the SAE terminology, at the lowest Level 0 is "No Automation", or manual driving, where the human driver has complete control and responsibility of all aspects of the driving task. Level 1, "Driver Assistance", refers to a system that performs either the steering *or* the acceleration/deceleration and the human driver is responsible for all other aspects of the driving task. ACC, which controls only the longitudinal aspect of driving, is an example of a Level 1 system. The next level, Level 2 "Partial Automation", takes things a bit further by defining a system which can execute both the steering *and* acceleration/deceleration of the vehicle, with the exception that the human driver has the responsibility of continuously monitoring the system and the outside environment. It is assumed that driver must be able to immediately take over control of the system and identify system errors on his/her own in case the system reaches a limit. Level 3 automation, named "Conditional Automation", is similar to Level 2 in that the system takes control of *both* steering and acceleration/deceleration with one very important difference to Level 2: the system is now responsible for monitoring the driving environment and must inform the driver *ahead of time* in case the driver must take over control. The driver, however, must still be available and is required to respond to a take over request. In Level 4, "High Automation", the system must additionally also serve as the fallback in case the driver fails to respond to a take over request. At the highest level, Level 5, "Full Automation", the vehicle is able to drive autonomously in all situations without any intervention from the driver whatsoever. The SAE levels of automation and their respective restrictions / responsibilities for the system and driver, as defined in [135], is shown in Table 1.1.

Besides fully autonomous driving, today's automotive industry shows great interest in the field of highly automated driving. It corresponds to the third and fourth automation level of the previously discussed SAE definitions. The standardization of HAD for highway applications will be one of the most challenging goals for the next years [32].

Tab. 1.1: Overview of automation levels as defined by the SAE [135].

Automation Level	Name	Execution of steering and acceleration/deceleration	Monitoring of the driving environment	Fallback for driving task	System capability
0	No Automation	Driver	Driver	Driver	N/A
1	Assisted	Driver/system	Driver	Driver	Some driving modes
2	Partial Automation	System	Driver	Driver	Some driving modes
3	Conditional Automation	System	System	Driver	Some driving modes
4	High Automation	System	System	System	Some driving modes
5	Full Automation	System	System	System	All driving modes

1.1 Motivation

The German Highway Research Institute reported in 2013 that 89.7% of traffic accidents in Germany were caused due to failure or inability of human drivers [31]. In 2012, the number of road fatalities in Europe was 28.138 [36]. Thus, the European Commission sets the objective to reduce the number of traffic fatalities significantly until 2020. In order to achieve this, a "Roadmap to a Single European Transport Area" has been elaborated in 2011 [35]. In point 2.5 (9), it states:

"*By 2050, move close to zero fatalities in road transport. In line with this goal, the EU aims at halving road casualties by 2020.*"

The use of intelligent transportation systems is one of the major topics within this roadmap. Through the use of HAD, the number of accidents caused by inattentive drivers in monotonous situations could be significantly reduced. The reason is that specific hazardous situations can be recognized faster by the system than most human drivers, so that overall safety is significantly improved [22]. Additionally, if the driver is no longer able to drive (e.g. due to a sudden heart attack), the function can completely take over the driving task and find a safe way to stop the car [79]. Another important benefit from the new mobility concepts is that driving is also made possible for elderly and disabled people. In 2012, for instance, Google's self driving car gave the legally-blind Steve Mahan, the CEO of the Santa Clara Valley Blind Center, a ride to Taco Bell [91].

The steady increase in the degree of automation can also lead to improved traffic flow and reduced fuel consumption thanks to the harmonization effect of traffic [190]. Consequently, this has a positive effect on the achievable motorway capacity as well.

Furthermore, as the autonomous car takes over from the driver in situations where driving is not much fun, such as in traffic jam situations, it gives real added quality to time spent out on the road. Shared cars or driverless taxis may be safer, cheaper, and more efficient than personal vehicles. All these benefits could make driving a totally different experience and can have a tremendous economic impact on our society.

To sum it up, the highly automated driving has a positive impact on the traffic in different ways and offers unimaginable opportunities for the future of individual mobility. Before discussing the problem formulation and the main challenges of this thesis, significant

milestones of autonomous and highly automated driving are presented in the next section.

1.2 Major Milestones of Autonomous Driving

After the vision of *Futurama* has been presented to the public, General Motors developed the first prototype of an autonomous vehicle *Firebird III* in 1958 (Figure 1.2). It used a magnetic field by power cable implemented in the smart "highway" for heading and velocity control.

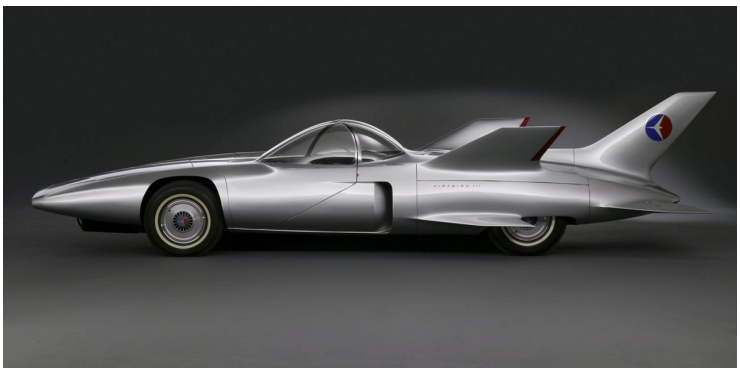

Fig. 1.2: "Want to sit back and relax? Well then, set in the speed you want to fly and switch over to automatic guidance. Release the stick, and Firebird III is on its own." - *Firebird III* advertisement, late 1950s [173]. The *Firebird III* experimental show car mixed practicality and fantasy. While the protruding fins would have menaced pedestrians, the ability to self-drive on automated highways was actually being tested on ordinary GM cars. Image source: [1]

By the 1960s, researchers of artificial intelligence (AI) on computers began dreaming of cars smart enough to navigate ordinary streets on their own. The challenges were daunting - essentially to reverse-engineer the relevant systems in a moving animal-like:

- Sensing
- Processing: modeling the outside world and decision-making process
- Reacting, with appropriate movement

The first and last steps were feasible with known technology. The unknown part at this time was the processing, the machine intelligence needed in between. Due to the increase of situational complexity, in which the autonomous driving system will be used, all three fields are still active areas of research. Then as now, much of that challenge was about interpretation. Early AI pioneers dreamed of breakthroughs that would bring human-like robots by the millennium. But real progress was more incremental than revolutionary.

In the 1980s, German pioneer Ernst Dickmanns developed the vehicle *VaMoRs* at the Bundeswehr University in Munich. The Mercedes van used a camera and an imaging system for its positioning and was therefore not depending on exogenous signals. The prototype (Figure 1.3) drove hundreds of kilometers autonomously on highways, a tremendous feat especially with the computing power of the time. At the final presentation of the

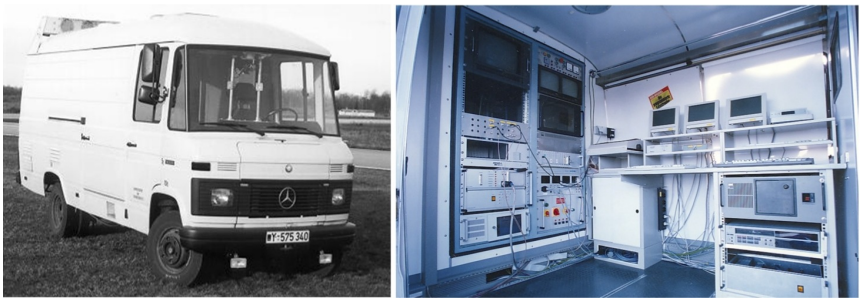

Fig. 1.3: Ernst Dickmanns' VaMoRs Mercedes van, Bundeswehr University Munich, 1986-2003. Dickmanns' laboratory substantially pioneered practical self-driving technology; this van tested three generations of systems. Image source: [173]

EU-project EUREKA-PROMETHEUS in 1993, Prof. Dickmanns presented further functionalities with his second test vehicle *VaMP* (Figure 1.4). With this vehicle he managed to drive 1000 km autonomously with a velocity of 130 $\frac{\text{km}}{\text{h}}$ on a three-lane highway in Paris. This vehicle additionally performed automated lane change maneuvers after the driver's approval.

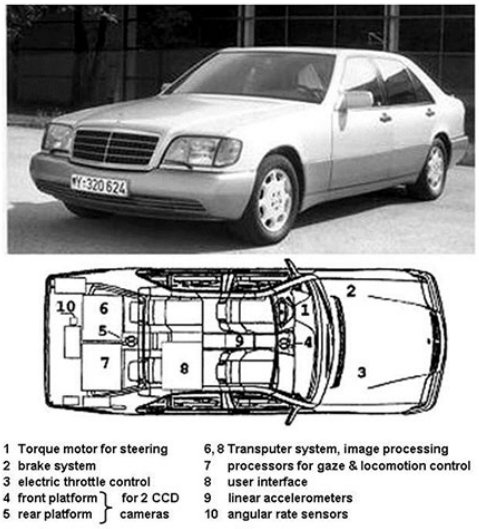

Fig. 1.4: Dickmanns' 1993 VaMP Mercedes sedan would cover thousands of kilometers in traffic at up to 130 $\frac{\text{km}}{\text{h}}$ as part of the massive Eureka PROMETHEUS project. Image source: [173]

Around the world, dozens of other pioneers added their own improvements. In 1996 the team of Artificial Vision and Intelligent Systems Laboratory (VisLab) of the University of Parma managed to drive more than 94% of a 2000 km long track around Italy autonomously with its test vehicle *ARGO* (Figure 1.5). The car was able to distinguish traffic lanes, identify ahead vehicles and other interference to its path, without requiring any special road infrastructure.

In 2004, the U.S. Defense Advanced Research Projects Agency (DARPA) introduced its Grand Challenge (Figure 1.6). International teams were assembled to enter autonomous

Fig. 1.5: ARGO Project, Universities of Parma and Pavia. An offshoot of the European PROMETHEUS project, the ARGO team drove their car about 2000 km around Italy in 1996, 94% of the time in autonomous mode. The special feature of this vehicle was the small number of sensors. With merely two black/white cameras the team achieved their goal. Image source: [173]

vehicles that raced off-road in depopulated suburbs. In 2007, the DARPA Urban challenge was held on a course that ran through a city-like setting. While European researchers had laid the groundwork in self-driving, the U.S. was now a serious contender.

Fig. 1.6: DARPA Grand Challenge winner Stanley (left), runner-ups Sandstorm (right) and Highlander (middle). The winning Stanley VW Touareg team was headed by Stanford Artificial Intelligence Laboratory professor Sebastian Thrun. Image source: [173]

Many major automotive manufacturers, including General Motors, Ford, Mercedes Benz, Volkswagen, Audi, Nissan, Toyota, Volvo and BMW, are testing driverless car systems as of 2015. In 2010, Italy's VisLab from the University of Parma ran the VisLab Intercontinental Autonomous Challenge, a 15.900 km test run which marked the first intercontinental land journey completed by autonomous vehicles. Four driverless electric vans (Figure 1.7) successfully completed the 100-day journey, leaving Parma, Italy, on 20 July 2010, and arriving at the Shanghai Expo in China on 28 October [167]. In the same year, Audi sent a driverless Audi TTS to the top of Pike's Peak at close to race speeds [146]. Furthermore, the Institute of Control Engineering of the Technische Universität Braunschweig demonstrated the first autonomous driving on public streets in Germany with the research vehicle *Leonie* [179].

BMW (Figure 1.8) has been testing automated vehicles on the highways around Munich,

Fig. 1.7: The VisLab Intercontinental Autonomous Challenge. Image sources: [167]

(a) **(b)** **(c)**

Fig. 1.8: Various highly automated driving projects from the BMW Group Research and Technology. (a): cockpit of the actual BMW highly automated test vehicle. (b): BMW TrackTrainer on the Nürburgring Nordschleife. (c): Bird's-eye view of an emergency stop maneuver on a highway. Image sources: [11, 152, 189]

Fig. 1.9: Inside GM's EN-V "Jiao" model. EN-V incorporates GPS, distance sensing technologies and vehicle-to-vehicle communication to react with its surrounding environment. Image source: [149]

Germany since around 2011 [23, 81, 189]. This project is a successor of the BMW Track Trainer [171] and BMW Emergency Stop Assistant [82] projects, where core technologies of those projects were integrated and further developed. In 2011, GM introduced the *EN-V* (Electric Networked-Vehicle), a 2-seat urban electric concept car (Figure 1.9). The most significant feature of the vehicles is autonomous operation. The *EN-V* can detect and avoid obstacles - including other vehicles - park themselves and come to you when called

by phone [149]. The Freie Universität Berlin developed in the same time two autonomous cars to drive in the innercity traffic of Berlin in Germany. Led by the AutoNOMOS group, the two vehicles *Spirit of Berlin* and *MadeInGermany* handled intercity traffic, traffic lights and roundabouts between International Congress Centrum and Brandenburg Gate. It was financed by the German Federal Ministry of Education and Research [15].

Fig. 1.10: Test vehicle Mercedes-Benz S 500 INTELLIGENT DRIVE. Image source: [108]

In 2012, Volkswagen began testing a "Temporary Auto Pilot" (TAP) system that will allow a car to drive itself at speeds of up to 130 $\frac{\text{km}}{\text{h}}$ on the highway [168]. In the same time Ford has also conducted extensive research into driverless systems and vehicular communication systems during past years [52]. In May 2012, a 22 km driving test was administered to a Google self-driving car by Nevada motor vehicle examiners in a test route in the city of Las Vegas, Nevada. The autonomous car passed the test, but was not tested at roundabouts, no-signal railroad crossings, or school zones [75].

In January 2013, Toyota demonstrated a partially self-driving car with numerous sensors and communication systems [19]. In August 2013, Daimler R&D with Karlsruhe Institute of Technology/FZI, made a Mercedes-Benz S-Class vehicle (Figure 1.10) with close-to-production stereo cameras and radars drive completely autonomously for about 100 km from Mannheim to Pforzheim, Germany, following the historic Bertha Benz Memorial Route [188].

In May 2014, Google presented a new concept for their driverless car that had neither a steering wheel nor pedals, [129] and unveiled a fully functioning prototype in December of that year that they planned to test on San Francisco Bay Area roads beginning in 2015 (Figure 1.11). Google plans to make these cars available to the public in 2020 [155]. In October 2014 Tesla Motors announced its first version of AutoPilot. Model S cars equipped with this system are capable of lane control with autonomous steering, braking and speed limit adjustment based on signals image recognition. The system also provide autonomous parking and is able to receive software updates to improve skills over time [151]. However, this systems currently does not provide any tactical decision-making task.

As of March 2015, Tesla has been testing the autopilot system on the highway between San Francisco and Seattle with a driver but letting the car operate almost unassisted [150]. Volvo plans for 2017 to take the test of self-driving cars to a new level that will enable the vehicle to do all of the work required to operate safely in highway traffic with ordinary people behind the wheel [34].

Fig. 1.11: Google's new self-driving car. Image source: [129]

As of 2015, four U.S. states have passed laws permitting autonomous cars: Nevada, Florida, California, and Michigan. In Europe, cities in Belgium, France, Italy and the UK are planning to operate transport systems for driverless cars and Germany, the Netherlands, and Spain have allowed testing robotic cars in traffic [138].

1.3 Problem Formulation and Challenges

As automated mobile platforms find their ways from research areas into real applications in human populated environments, more and more safety requirements must be fulfilled. Nevertheless, the benefits of automation of transportation systems are conclusive by means of comfort, energy efficiency and safety [22, 190]. Automated driving on highways with close-to-series sensors is one of the most challenging aspects in the upcoming industrialization of this technology. The main objective is to perform the complete driving task autonomously with maximum comfort and safety. However, if a critical situation occurs, which can not be automatically resolved by the system, the driver must be brought back into the driving task within an appropriate time interval. At the same time the system should always ensure a "safe state", if the driver does not take over the driving task within the given time [63, 194].

Regarding the above-mentioned objectives, safe *maneuver planning* in dynamic environments is one of the key challenges in the domains of mobile robotics, autonomous and highly-automated driving. The task is to *plan* the most comfortable and safe maneuvers in populated environments with only partial knowledge about future trajectories of the other (human) traffic participants. Such knowledge can be acquired from real data by learning or from a model of human behavior. This knowledge is then used to *predict* the future human motion in the environment as accurately as possible, with growing uncertainty over time. This uncertainty is explicitly modelled in probabilistic approaches, which assign likelihoods to various motion options. In other words, maneuver planning can not be treated separately from the environment prediction.

The task of maneuver planning (resp. *tactical decision-making*) is thus equivalent to the *action selection problem* [144], a way of characterizing the most basic problem of intelligent systems: **what to do next?** The first step for understanding action selection is determining the level of abstraction used for specifying an "act". In this thesis, the

action of the cognitive vehicle is defined as its planned maneuvers for the next consecutive time steps.

To accomplish the tactical decision-making and ensure a comfortable and safe maneuver planning, following main requirements has to be fulfilled:

- The cognitive vehicle (agent) mostly acts in real time; therefore it must make decisions in a timely fashion.
- The cognitive vehicle must select its action in dynamic and partly unpredictable environments.
- The environment, the cognitive vehicle operates in, include human traffic participants, who may make things more difficult for the agent (either intentionally or by attempting to assist). Thus, the cognitive vehicle has to predict its environment, which is quite complicated.
- The tactical decision-making should allow execution of various tasks with possible different objectives which may conflict with resource allocation.
- The action selection itself must be controllable and transparent in order to increase the system acceptance.

1.4 Main Contributions and Outline of the Dissertation

The main contributions of this thesis are multiple. In Chapter 2, the functional architecture of the tactical decision-making process is presented. It is realized through the developed *hierarchical decision network*. The complexity of the continuous driving task is thus reduced by determining a discrete set of different *behavioral strategies*. Each behavior implements a suitable model-predictive maneuver planning for the specific highway traffic situation, regarding the certain requirements and objectives of the behavioral strategy. Starting the appropriate strategy and terminating the unnecessary ones are handled by the process of *Arbitration*. The novel approach offers benefits in terms of flexible and modular functional development and allows for distributed computing. Further improvements of the intelligence can be easily done by defining a new behavior and adapting its decision-making process to handle its specific requirements and objectives.

To enable proactive maneuver planning, a robust and computationally efficient maneuver prediction of all the traffic participants is required. Chapter 3 presents the development of a combined model- and learning-based framework for interaction-aware maneuver prediction. The advantages of this novel framework are twofold. On the one hand, expert knowledge can be integrated, minimizing the amount of necessary labeled real world data. On the other hand, the difficulties due to the so-called *curse of dimensionality* can be reduced, as a reduced feature space is sufficient for supervised learning. The developed framework achieves a significant improvement in terms of the prediction horizon and precision compared to other state-of-the art approaches.

Given the current sensor measurements and the possible future traffic scenes predicted by the above-mentioned framework, optimal maneuver decisions for further automated driving has to be determined. In this thesis, three different behavioral strategies of *basic behavioral strategy* (Chapter 4), *cooperative behavioral strategy* (Chapter 5) and *driver take over behavioral strategy* (Chapter 6) for highway traffic situations are developed. On the contrary to the state-of-the-art approaches, the common core idea of the different maneuver planning methods within each behavioral strategy is based on the *receding horizon* approach. This satisfies the two important requirements for reactivity and anticipatory. Furthermore, it implicitly takes into account the uncertainties of surrounding vehicles, by applying the idea of the moving horizon.

In the case of basic behavioral strategy, two different approaches of *constrained optimization of hybrid system* and *combinatorial optimization* have been developed and are compared. The maneuver planning within the cooperative behavioral strategy captures the mutual dependence between maneuver choices of all traffic participants over multiple time steps. The replanning ability of other vehicles is thus integrated into the planning of a reasonable interactive maneuver sequence for the host vehicle. For the mathematical modeling of the problem and its solution, methods from game theory have been applied. During automated driving, a critical part of the system is the driver take over request. Little focus has been given to this important aspect in an automated driving journey. Similar to the previous behavioral strategies, the maneuver planning here is based on the model predictive approach as well. The approach is based on convex optimization problem with time-varying constraints and diminishing rather than receding horizon. The output is a one-dimensional plan for braking the cognitive vehicle into a safe state.

The functional architecture of the tactical decision-making process, the novel traffic scene prediction module and the different behavioral strategies together provides the complex artificial intelligence framework of the automated driving function for highways. During the development phase of this tactical level, the following two important issues has to be investigated:

- How can the effect of parameter changes within the tactical decision-making process be objectively evaluated?
- What is the impact of automated driving with actual implementation of its tactical level on traffic safety and traffic efficiency?

For these reasons, a novel framework for impact assessment based on *microscopic traffic simulation* is developed which allows the study of the above questions. This framework will be discussed in detail in Section 7.

Finally, the main results and a discussion concerning future directions are provided in Chapter 8.

2 Novel Tactical Decision-making Framework

2.1 Introduction and State of the Art

The entire planning task in dynamic environments can be classified into the three hierarchical levels of navigation task (*strategic level*), guidance task (*tactical level*) and stabilization task (*operational level*) [46]. All of them are necessary for successful autonomous navigation of a *cognitive agent*. Thus, the *decision-making process* for autonomous driving should consider these three tasks as well. Figure 2.1 shows these different levels of the decision-making process by a cognitive vehicle.

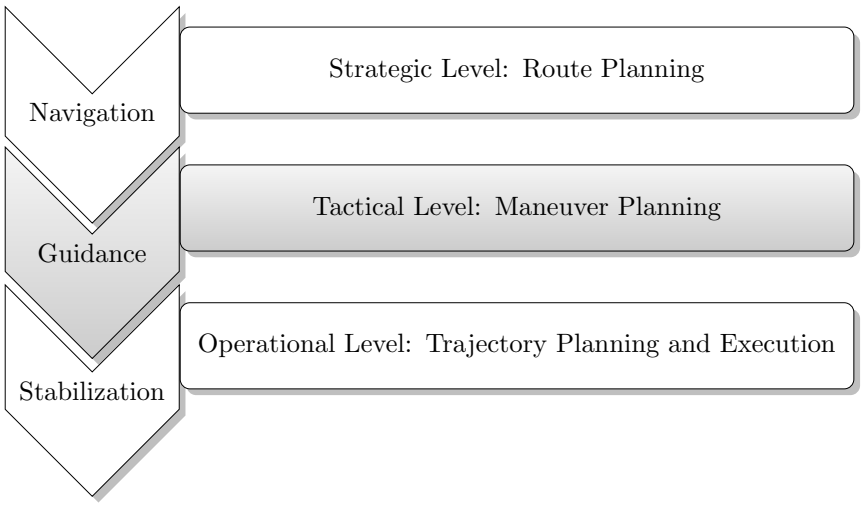

Fig. 2.1: Tactical decision-making as a sub-problem of the overall decision-making process for navigation in dynamic environments.

The navigation task selects an optimal sequence of roads and even driving lane segments to reach the driving destination based on certain predefined criteria, such as shortest travel time or fuel efficiency. This task is usually performed once at the beginning of driving. In the case of disturbances, such as accidents or construction sites, a modified route planning may be required. There are already different types of navigation devices, mostly based on A-star graph search algorithms [134], which automatically perform this task.

The actual dynamic process of the driving task is, however, performed by maintaining a continuous feedback loop between the guidance and stabilization tasks. The guidance task represents the tactical level of the autonomous driving. On this layer the cognitive vehicle has to deal with the vast variety of traffic situations and thus adapts its driving strategy continuously. Therefore, the tactical level is equivalent to a situation-dependent maneuver planning taking into account the perceived environment. On the one hand, a

reactive behavior should be ensured. On the other hand, the ability of forward-looking planning has to be realized by predicting the intention and maneuvers of the surrounding environment. With other words, the tactical level implements the artificial intelligence of the automated driving. Finally, the operational level performs the stabilization task in real time. This task includes a low-level trajectory planning and motion controller for comfortable and safe driving. In other words, this layer converts the maneuvers provided by the tactical decision-making into reliable values for steering and acceleration actuators.

Regarding the above discussion, the main challenges for automated driving remains in the tactical and operational levels. This thesis thus focuses on the realization of a novel tactical layer which fulfills certain requirements, discussed in next section. In Section 2.2, the actual implemented operational level in the BMW Group Research and Technology prototype vehicles will be briefly discussed.

Highly automated driving requires a complex artificial intelligence that makes optimal decisions based on the current measurements and information. The developed tactical level of the decision-making process in this thesis implements this intelligence through a sophisticated hierarchy of a *high-level behavioral strategy* and a *low-level maneuver planning*. Put simply, in a highway application the high-level behavioral strategy answers the questions like as: "Should the cognitive vehicle insist on its traffic rights or consider a cooperative driving behavior with a particular road users?" or "Should the cognitive vehicle request an driver take over, since a complex situation ahead cannot be handled properly by the function?". In other words, the behavioral strategies correspond to the medium-term *driving strategies* selected by the human drivers.

Whereas the low-level maneuver planing answers the questions: "Should the cognitive vehicle change the lane? and if so, when should the lane change maneuver begin?" and "At which velocities should be driven for the next seconds in order to ensure the maximum comfort and traffic safety?". Thus, the maneuver planning provides the short-term *driving goals*. The decision-making process is based on the current environment data as well as further information such as traffic rules, driver's intention, current driver state and back-end data.

The determined driving decisions will be passed to the subsequent trajectory planning which provides comfortable and physically feasible trajectories. The objective of the tactical level is thus to model the complex process of decision-making of a rational human driver in different traffic situations. It plays a central role in the automated driving function and has a great impact on the driving comfort and the overall traffic safety. Consequently, in the development of a suitable framework for the tactical decision-making certain requirements have to be considered.

The framework should allow diversity in the decision-making for various traffic situations and modular expandability of the overall intelligence. It means that the existing framework should be easily extended by new behavioral strategies to deal with further traffic situations. This enables continuous improvement of the system in the future development process. A modular design of the framework with predefined input and output interfaces allows a flexible and efficient development and testing and satisfies this requirement. In addition, such a modular architecture allows distributed computing which makes the overall decision-making even more reliable against possible hardware failure than single-server

processing systems.

The most determining requirement, however, is the safety for all traffic participants. For this reason, the decision-making process has to be controllable and robust. Besides a reactive response to changes in the dynamic environment, a deliberative component should also be considered to incorporate the future evolution of the environment in the maneuver planing. This ensures a forward-looking, human-like driving behavior, which increases the acceptance of the HAD by the passengers as well. Due to the application in a real test vehicle, the tactical decision-making has to operate in real-time. Hence, computational effort has to be addressed via modular framework and efficient implementation of planning algorithms. Moreover, the tactical decision-making must be robust against uncertainties arises from the environment perception and behavior prediction of traffic.

The main requirements for the tactical decision-making process can thus be summarized as follows:

- On-line capability
- Flexibility and modular expandability
- Robustness against uncertainties
- Predictability and transparency

In the following, the state-of-the-art in decision-making process for automated driving will be discussed. The focus lies here on the evaluation of different frameworks. The introduced approaches are part of the latest and most successful projects within this field of research. Due to the fact that none of these concepts can fulfill all previously defined requirements, a novel decision-making framework is presented in Section 2.2 that addresses the above-mentioned specific requirements of highly automated driving.

Thanks to the continuous improvement of the computing power, the research field of autonomous navigation have progressed rapidly in the past two decades. Especially the DARPA Challenges between 2004 and 2007 [39–41] put autonomous driving into the focus of many research groups around the world. In the following, a detailed review of the applied frameworks for the tactical decision-making process in some of the most important projects are given. The advantages and disadvantages of each framework will be evaluated against the requirements discussed above.

Compared with algorithms developed for the environment perception, the decision-making process is usually simplified in many previous autonomous driving projects. The most simplest approach is to calculate the required steering torque directly from the perceived lane geometry. The longitudinal control is performed independently by a standard active cruise control system (ACC) [55, 69]. Thus, the tactical level is realized here in a reactive manner without any complex artificial intelligence..

In the DARPA Grand Challenges in 2004 and 2005 a more than 200 km long course had to be accomplished. The objective was to follow a given route through mostly unstructured, rough terrain and avoid collision with only static objects [39, 40]. Similar to the previous projects, these vehicles did not require any intelligent tactical decision-making due to the fact that the main objective is keeping the vehicles on an online calculated path. Therefore,

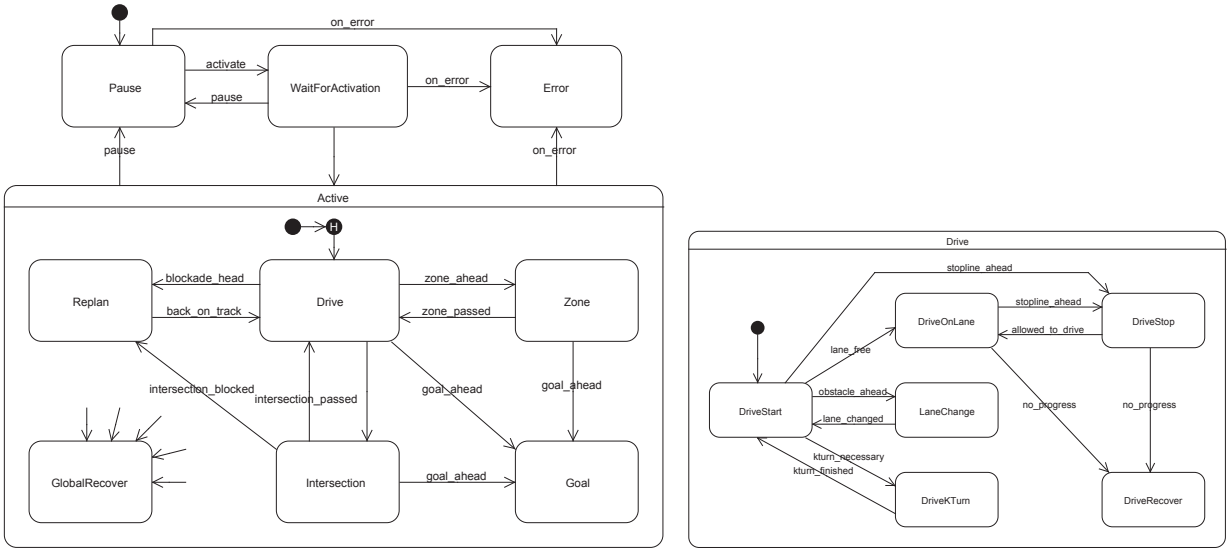

(a) State chart of the main level of the FSM. **(b)** Substate of the state *Drive*.

Fig. 2.2: UML diagram of the introduced hierarchical state machine of team *AnnieWay*. Image source: [61]

the guidance task has been simplified here to a path planing module. The vehicle *Stanley*, that won the DARPA Grand Challenge in 2005, applied such a path planning module [154]. The BMW *TrackTrainer* [171], which shows the participants the most ideal and safe path on a race track, can be also classified in this category of autonomous driving without any explicit situation-awareness.

With increasing complexity, the above mentioned approaches have limitation in handling all possible situations. In the DARPA Urban Challenge in 2007, for instance, the participants had to drive a 97 km long course through an urban environment [41]. The traffic situations considered here were thus much more complex than the previous Grand Challenges. Yielding precedence at intersections or overtaking a slower preceding vehicle on a road with multiple lanes are two example of such a complex decision-making. Consequently, applying an intelligent tactical decision-making unit was necessary. The functional framework of the tactical decision-making process in the most of successful systems in Urban Challenge [61, 80, 113, 162] is realized by deterministic hierarchical finite state machines (FSM) [169]. Here, the continuous driving task was divided into several discrete driving states, which are again continuous subsystems. The state transitions were realized by rules based on expert knowledge, which has ensured the compliance of regulations.

Figure 2.2a illustrates the hierarchical state machine for the tactical decision-making of team *AnnieWay* [61]. On the top level the framework separates between nine different states of the system. Each state contains again a state machine on a lower level which represents a specific driving behavior. Thus, every substate can be seen as a further specialization of its parent state (i.e. a nested FSM). The state *Drive* in Figure 2.2b, for instance, covers the most important driving maneuvers on a normal road. It is separated into six further substates, such as *DriveOnLane* or *LaneChange*. Finally, the reached state generates a path, which will be forwarded to the control module. This calculated path may be overridden by the low level collision avoidance system [80].

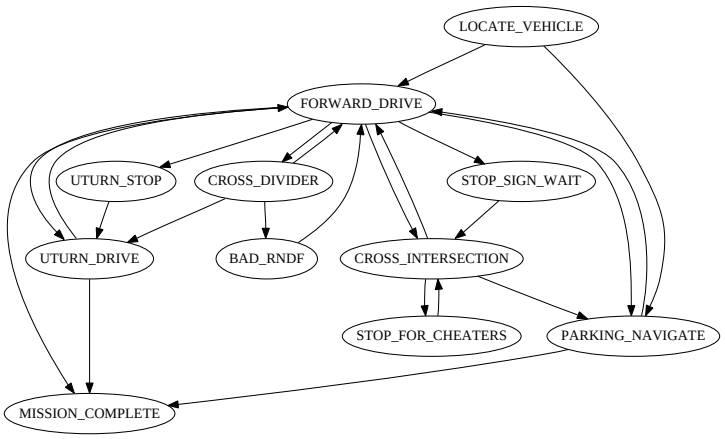

Fig. 2.3: Stanford Racing Team: *Junior's* FSM that governs its behavior. Image source: [113]

Figure 2.3 shows the FSM used by the Stanford Racing Team to switch between different discrete driving states. This team made the second place in the Urban Challenge with their car *Junior* [113]. The FSM processes a total of thirteen states and is responsible for tactical decisions such as lane changes, merging, and avoiding obstacles. At the highest level, the FSM transitions between various driving states like as *Lane_Keeping* or *Parking_Lot_Navigation*. Within a driving state, an online path planner was applied to continuous vehicle guidance. A special aspect of the Stanford architecture is its *stuckness detector*, which prevents the car from getting stuck in some specific situation by initiating transitions to low-level exceptions. It is either triggered through a timeout or through a repeated traversal in the digital map. This formulation makes the robot robust to various unexpected events, which were probable to appear at the Urban Challenge such as blocked lanes, blocked intersections, unreachable checkpoints and mapping errors.

The winner of the Urban Challenge was the Tartan Racing Team from the Carnegie Mellon University in Pittsburgh. Their car *BOSS* uses the high-level decision-making framework, which can be seen in figure 2.4a. It subdivides the continuous driving task into the three hierarchical levels of *Mission Planing*, *Behavioral Executive* and *Motion Planning* [162]. The mission planning module computes the way to the next checkpoint and publishes a *Value Function*, which maps to each waypoint an estimated time to reach. The subsequent behavioral executive creates from the Value Function so-called *Motion Goals*, e.g. "drive to end of current lane". Finally, the motion planning is responsible for the safe, comfortable and timely execution of the incremental goals provided by the behavioral executive. Figure 2.4b shows the core functionality of the behavioral executive, which is grouped into three functional contexts consisting of nine observers.

The BMW Group Research and Technology has been testing automated vehicles on Germany's highways since 2011 [170, 189]. Similar to the previous approaches, the continuous driving task is divided in this project into a finite set of discrete lateral and longitudinal guidance states, which are summarized in Table 2.1. Based on the current situation, the decision-making process selects the appropriate system states q_{lat} and q_{long}. This process is modeled via a network of concurrent finite state machines and decision-trees [11, 13].

Figure 2.5 illustrates the system structure for the decision-making process and vehicle

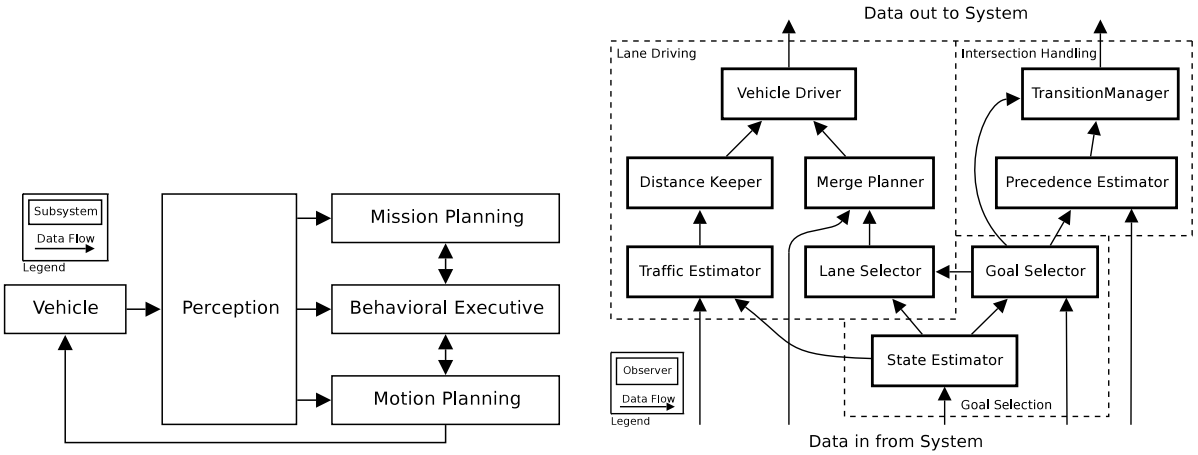

(a) *BOSS* decision-making framework: showing primary subsystems and data paths.

(b) Architecture of *BOSS's* high-level behavioral executive.

Fig. 2.4: The high-level decision-making framework of *BOSS*. Image source: [16]

control of the HAD system. The decision-making process runs through four hierarchical steps. From the evaluation of the situation, driving requests are derived. These requests are investigated concerning their feasibility in the next level and depending on the feasibility, an appropriate driving maneuver is executed [11]. The state transition in the lateral direction (from lane keeping to lane change maneuver) is realized by a utility-based approach [12]. The utility of the current lane and neighboring lanes are determined in terms of linear functions considering several criteria due to their weights. The disadvantage of this approach is, however, the large number of weighting parameters that are usually determined by time-consuming trial and error tuning.

Another recent project which applies hierarchical state machine to generate basic behaviors is *Bertha Benz driver* presented in [186, 188]. Here, the prototype vehicle follows the route from Mannheim to Pforzheim, Germany, in fully autonomous manner. Figure 2.6 shows a part of the state chart that was applied in this project for the tactical

Tab. 2.1: System states for the previous HAD prototype by BMW Group Research and Technology [11].

i \ $q_{\square}$	q_{lat}	q_{long}
0	Off	Off
1	Lane Keeping	Dynamic Cruise Control
2	Lane Change Gap Approach (left)	Active Cruise Control
3	Lane Change Gap Approach (right)	Lane Change Gap Approach
4	Lane Change (left)	Critical Control
5	Lane Change (right)	
6	Lane Change-Abortion (left)	
7	Lane Change-Abortion (right)	

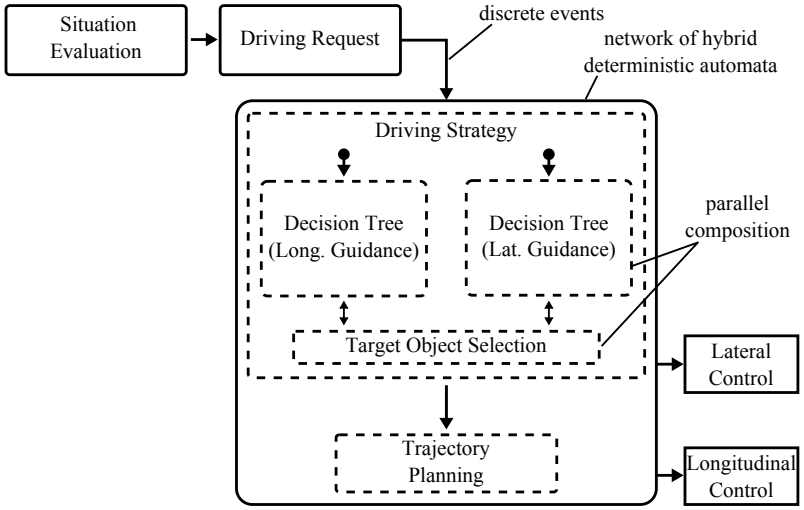

Fig. 2.5: System structure for the decision-making process and control of the previous HAD prototype by BMW Group Research and Technology. Image source: [189]

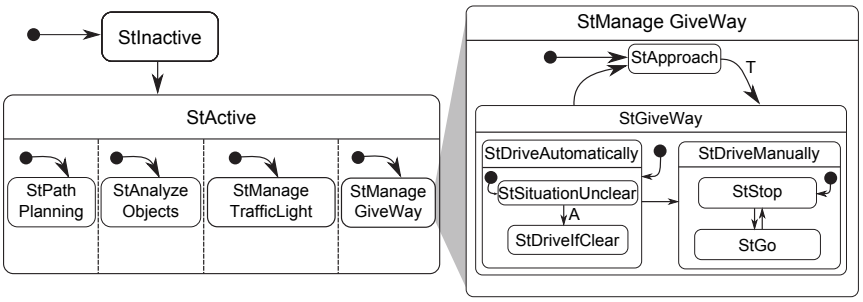

Fig. 2.6: Excerpt from the behavioral state chart used in the *Bertha Benz driver*. Image source: [186]

decision-making.

The left part of the figure illustrates the concept of concurrency. Thus, after activation the system is simultaneously running four concurrent state charts. The right part gives a more detailed overview about the state *StManageGiveWay* with the default substate *StApproach*, meaning that the vehicle is approaching an intersection and its right-of-way is still unclear. If the vehicle passes a trigger point on the digital map, which indicates that the own road doesn't have right-of-way, event T is triggered and the substate chart transitions to the state *StGiveWay*. If the vehicle is in autonomous mode, it remains in the substate *StSituationUnclear* until another event A is triggered, meaning that the vehicle has approached close enough to observe the entire intersection. When all the transitions have been made, the system takes road topology, static and dynamic objects into account and outputs geometric constraints for the next level, the trajectory planner. The trajectory planner subsequently computes a desired trajectory by solving an optimization problem concerning several aspects such as minimum jerk, offsets to road boundaries and so on.

Finite state machines allow structured and transparent modeling of reactive systems, enabling a top-down design of complex driving task. Although the above mentioned systems based proved their reliability, the decision-making processes do not seem to be well

organized. Assume the states of *Junior's* FSM in figure 2.3 would be doubled and they are correlated with each other, i.e. every state is reachable from every other one. The framework's transparency and comprehensibility would suffer significantly. Furthermore, with increasing complexity it is harder to proof the robustness of the system, since the number of transitions is increasing quadratic with the number of states. Thus, the state machine has to be designed such that the transparency of the system is guaranteed, even by decision-making in complex traffic situations.

Another approach for realization of the tactical decision-making module is based on the DAMN (Distributed Architecture for Mobile Navigation) framework [133], in which distributed task-achieving modules (resp. behaviors) cooperatively determine the final action of the system by voting for various relevant behavioral goals (see Figure 2.7). The advantage of DAMN architecture lies on the modular extensibility, as more behaviors can be added easily to the system. Depending on the current priority of the concurrent goals, an arbiter chooses corresponding weights and performs command fusion to select a decision.

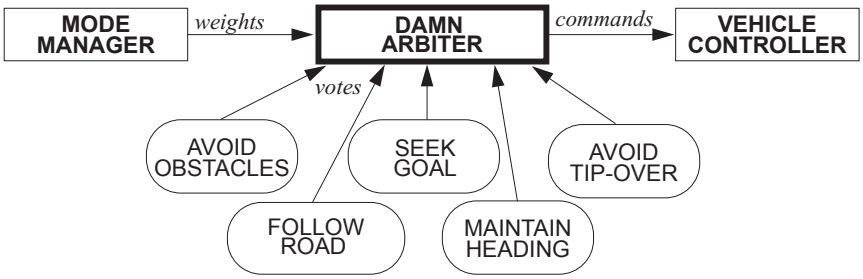

Fig. 2.7: Overall structure of DAMN. Image source: [133]

Team *CarOLO* from the Technical University of Braunschweig applies in the DARPA Urban Challenge this approach for tactical decision-making, which outputs a velocity and a curvature in every replanning step [18, 128]. The arbiter for curvature, for example, iteratively votes for all possible curvatures, follows the best scored one for one meter and performs the next voting. Together with the other arbiter for velocity, the artificial intelligence generates a trajectory, in which the discrete points on it include information about position, orientation and velocity. This trajectory is then passed to the path planner for further processing.

The project *Stadtpilot* [179] with the vehicle *Leonie*, which builds upon the experiences from team *CarOLO*, applies a similar concept of the decision unit. Here, the final driving behavior is determined by a fusion of multiple concurrent goals. The following behaviors are considered in this system: *Follow waypoints*, *Stay in lane*, *Avoid obstacles*, *Stay on roadway* and *Stay in zone*. Each of these behaviors can vote for an influence. Figure 2.8a visualizes an example of a voting process and the end result.

This architecture enables a situation adaptive driving behavior. However, due to the fact that the fusion of concurrent goal has a direct influence on the conducted driving maneuvers, it causes traceability difficulties and a non-deterministic behavior [103]. In other words, there is no clear distinction between the tactical decision-making and the operational level. As a consequence, this approach does not meet the mandatory requirements

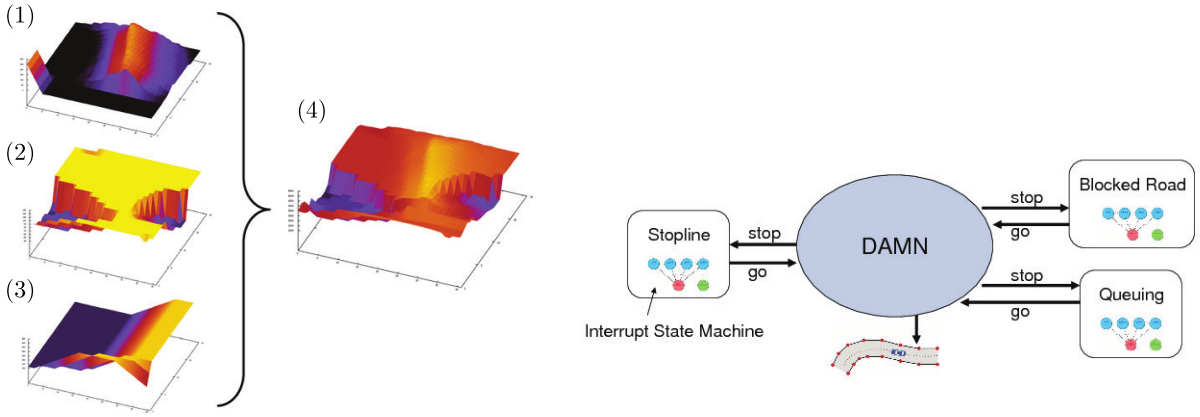

(a) Votes of (1) stay in lane, (2) avoid obstacles, (3) follow waypoints and (4) weighted sum.

(b) Extended DAMN algorithm including interrupts.

Fig. 2.8: Components of the *Stadtpilot's* tactical decision-making process. Image source: [128, 180]

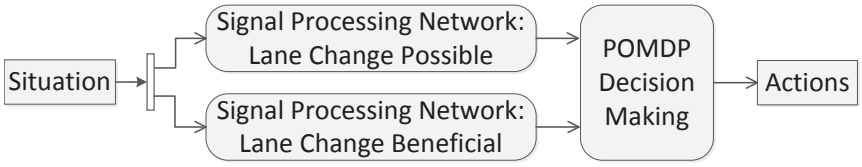

Fig. 2.9: Proposed steps for lane change decision-making within the further developed *Stadtpilot* project. Image source: [159]

of predictability and transparency.

Another approach, which is presented in the further development of the *Stadtpilot* project, is a stochastic tactical decision-making for performing lane changes in urban environments [159, 160]. It is based on an on-line capable Partially Observable Markov Decision Process (POMDP) [78, 153]. In this framework, different types of uncertainties such as uncertainties in perception and in the control effects can be modelled directly in the decision-making process. Figure 2.9 shows the signal processing flow from the approach used in [159] to decide if a lane change based on the current traffic situation is possible.

In another work [17], a Mixed Observability Markov Decision Processes (MOMDP) [121] is applied, which is a structured and more compact variant of the common POMDP. The approach proposes that intention of road users is a further uncertain variable when considering motion planning and model the intention of pedestrians to move towards a specific goal location as a further partially observable state.

A further stochastic framework to implement the situation assessment and tactical decision-making is the Bayesian inference [74, 153]. The system presented in [140] applies this approach in the context of lane change decisions on highways. In [100, 101] a Bayesian framework is introduced which enables recursive estimation of a dynamic environment model and behavior selection based on these uncertain estimates. This approach is applied here to navigate a robot through densely populated environments [99].

A major advantage of the above introduced stochastic frameworks is the consideration of different types of uncertainties within the tactical decision-making process. However, one

of the main challenges is their computational complexity. Since they are PSPACE-complete (in the cases of POMDP and MOMDP [123]) and thus in general getting computationally intractable by increasing the dimension of the state space or even considering continuous state spaces. Another disadvantage is the large number of parameters like the reward matrix, the observation and transition functions or the conditional probabilities. They are mostly determined by expert knowledge, since learning from real data (e.g. with reinforcement learning) needs a huge amount of labeled training data. A further drawback is the limitations in adapting the introduced approaches to changed conditions, since all the parameters must be re-learned for each new situation.

Another approach for the realization of the tactical decision-making process (especially modelling discrete decisions such as the lane change decision [116, 126]) is based on fuzzy logic [118]. The advantages of this framework are its transparency thanks to the linguistic formulation of the problem and computational efficiency. However, this method is less suitable when considering future events in the decision-making process. Furthermore, defining the fuzzy rules even for a small problems get quite challenging, which leads to inaccurate modelling of the decision-making process.

All the above systems do not require any vehicle-to-vehicle and vehicle-to-infrastructure communication. The Grand Cooperative Driving Challenge in 2011 [57], which was organized by Netherlands Organisation for Applied Scientific Research in Helmond, was the first international competition to implement highway platooning scenarios of cooperating vehicles. To achieve this, the vehicles had to exchange information about their actual states and future intentions via wireless communication devices. Team *AnnieWay's* vehicle shows the best cooperative driving result within this challenge against ten other teams. The tactical decision-making process was realized here as a controller which was able to stabilize a platoon of multiple vehicles [59]. Another important projects which investigate the feasibility of such networked cooperative traffic were the research projects simTD [145] and Ko-FAS [87]. In [53, 54], the authors compare different motion planning algorithms for cooperative collision avoidance of multiple networked cognitive vehicles.

The benefits of such sophisticated inter-vehicle communication systems are on the one hand "extending" of the sensor ranges and on the other hand enabling a cooperative decision-making thanks to the a priori knowledge about the future behaviors of other traffic participants, which may optimize the whole traffic flow. However, the disadvantages due to the high cost of the needed infrastructure, the scalability problem of the networks and the related security issues [125] make its industrialization very difficult. The proposed tactical decision-making processes presented in this thesis does not primarily need any type of inter-vehicle communication systems. However, it will be shown that this information can be easily integrated and used within the framework.

2.1.1 Evaluation of the Frameworks

The previous section has provided a detailed overview about the relevant deterministic and stochastic frameworks for the tactical decision-making process applied in the research field of automated driving. The analysis about the pros and cons of the contemporary frameworks clarifies that they generally do not provide suitable concepts for modular expandability. In the case of introduced FSMs, for instance, integrating a new set of states

in the existing system, to handle more complex traffic situations, is not straightforward, since all possible transitions to other states have to be formulated. This "state and transition explosion" [86] results in the deterioration of the system transparency. The approach of deterministic FSMs, however, proved to be highly suitable for mastering complexity and making the systems robust. It satisfies the requirement of on-line capability as well. Hence, the concept of deterministic concurrent FSMs are applied in this thesis to select the appropriate behavioral strategy within the tactical decision-making process. It is designed in a manner that the system transparency and flexibility is given.

In the case of the introduced probabilistic frameworks, however, adaption and extending of the decision-making means the definition of a whole new set of parameters (e.g. the ones of the reward matrix or the conditional probabilities), which is generally a challenging task. In addition, non of the earlier works proposed an approach, how arbitration between different high-level behavioral strategies can be handled. Furthermore, the dimensions of states and actions must be kept low, in order to achieve an on-line capable system. Another disadvantage of the stochastic frameworks is that they could be non-predicable. Consequently, It has a negative effect on the safety requirement of the system. The decision-making process presented in this thesis is able to deal with uncertainties in a way which minimizes the above disadvantages.

Another important drawback among the presented works is the lack of a sophisticated reasoning and prediction of other road users within the tactical decision-making process. For example in [186], an upper and a lower estimated acceleration value is used for the prediction without considering the context and interaction between the traffic participants. Due to the lack of interaction-awareness, the forward-looking decision-making is not reliable in some traffic situations.

This thesis introduces a novel tactical decision-making framework which combines a high-level *behavioral arbitration* with a low-level *model predictive maneuver planning*. Thus, it enables the system to be reactive and to simultaneously consider the future evolution of the environment regarding the interaction between traffic participants. The maneuver planning within each behavioral strategy is based on the same idea of predictive planning (receding horizon approach). However, they are implemented with different granularity regarding the specific objectives and requirements of the respective behavioral strategy. The main advantages of the proposed framework are a well-organized functional architecture and transparent behavioral selection. Compared to the previous works, it meets a higher requirement of modular expandability and flexibility.

Based on the results of this evaluation a new framework for tactical decision-making process is presented in the next chapter.

2.2 Hierarchical Decision Network

The entirety of the tactical decision-making process is realized in this thesis through the novel approach of the *hierarchical decision network*[1]. The hierarchical structure can be interpreted as an attempt to handle the complex driving task by decomposing it into smaller

[1]Parts of the results in this chapter have been pre-published in [196].

subproblems and reassembling their solutions into a "functioning" hierarchical structure. Figure 2.10 illustrates the overall structure of the proposed framework.

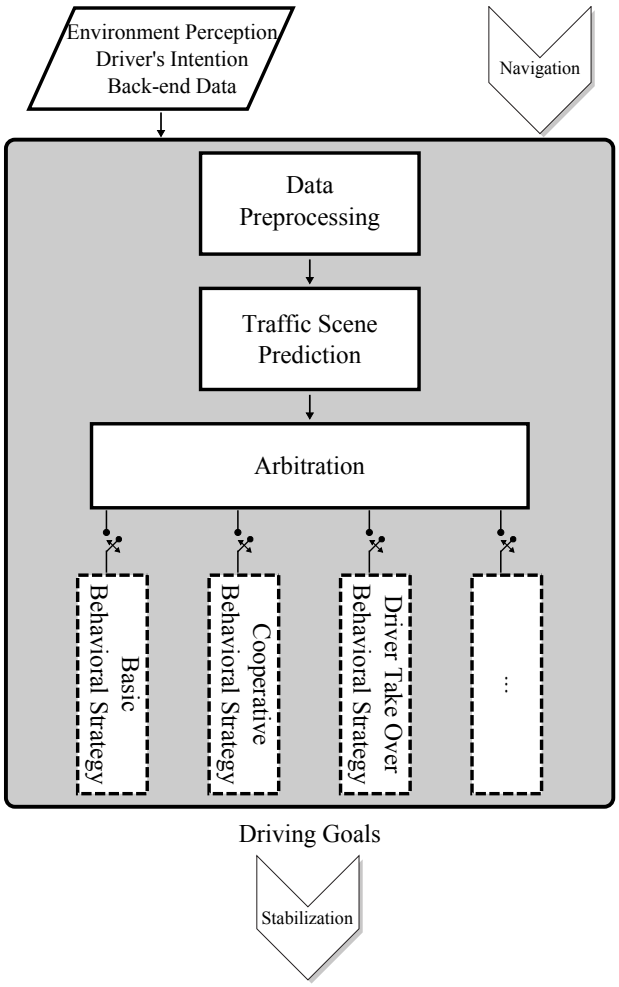

Fig. 2.10: The framework of tactical decision-making process: hierarchical decision network. Different behavioral strategies can run simultaneously, which is indicated by dashed lines.

The complexity of the continuous driving task is reduced by determining a finite set of various high-level behavioral strategies. Each one represents a subset of specific situations with its overall objective. It will be activated if the cognitive vehicle is in this corresponding traffic situation. This high-level behavior selection is inspired by the human driver's medium-term goals depend on the upcoming traffic situation. Each behavior implements a suitable model predictive maneuver planning based on its requirements defined by the respective traffic situation. For example, driving in a highway junction requires a higher level of cooperation between traffic participants. Consequently, the maneuver planning within this behavioral strategy has to consider this requirement explicitly.

From the software point of view, the maneuver planning within each behavioral strategy will be executed as an independent thread or process [172]. Starting the appropriate strategy and terminating the unnecessary ones are handled by the process of *Arbitration*. This independent layer thus corresponds to a situation classification module. The proposed

architecture meets the requirements of expandability and transparency. Further improvements of the intelligence can be easily done by defining a new behavioral strategy and adapting the maneuver planning within this to handle its specific objective. The modular design allows independent development of different behavioral strategies. Besides, the current implementation of the tactical decision-making process within the framework of Robot Operation System (ROS) [106, 132] allows distributed operation of the behavioral strategies on a heterogeneous computer cluster. The separation between the maneuver planning within the tactical level and the trajectory planning within the operational level provides a further safety redundancy of the system thanks to performing different methods of collision detection to surrounding objects.

In the following, the most important aspects of the hierarchical decision network will be discussed.

2.2.1 Input/Output Interfaces

The first step in the development of the hierarchical decision network is the definition of the input and output interfaces. As the central instance for the intelligent decision-making, various types of information should be taken into account. The input data are on the one hand the environment information such as the detected dynamic and static objects and an accurate road model to obtain a higher level understanding of the cognitive vehicle's environment [5, 72, 127]. On the other hand, the information related to the driver such as his/her intention and current state has to be considered. Further data, e.g. from a back-end server, are optional but can be easily integrated in the framework and used for the decision-making. All this data are prepared by the central *preprocessing* module. Thus, it is guaranteed that all the subsequent layers always shares the same input interface.

As a consequence of the modular design of the hierarchical decision network, it must be ensured that all the behavioral strategies provides their results through the same output interface. The output of the hierarchical decision network is hereinafter referred to as *driving goals*. It is equivalent to a sequence of optimal *policy* (i.e. optimal actions) determined by the active behavioral strategy (optimal in the sense of the defined objective function). The driving goals in this thesis consist of a two-dimensional vector of desired lanes and velocities for several discrete time steps in the future to be followed by the cognitive vehicle. To provide a flexible implementation of each behavioral strategy, the *planning horizon* is not fixed. Thus, the vector of the driving goals is in general variable-size. The determined driving goals bound the solution space of the subsequent trajectory planning which finally plans a continuous trajectory through these discrete spatio-temporal points and forwards it to the motion controller unit.

2.2.2 Traffic Scene Prediction

As discussed above, the tactical decision-making process should meet the two important requirements of reactivity and anticipatory. For this reason, the future evolution of the dynamic environment has to be predicted as accurately as possible, primarily with the on-board sensors. In this way, a forward-looking maneuver planning with early reaction to critical events, such as risky overtaking and cut-in maneuvers, is made possible. This

traffic scene prediction module has to consider the measurement uncertainties. Moreover, it must be computationally efficient in order to predict the intentions and maneuvers of all the relevant traffic participants for a predefined *prediction horizon*. The novel approach presented in Chapter 3 satisfies these requirements [192, 195]. In contrast to the previous works, this approach provides an interpretation of what other traffic participants intent to do and how they interact with the relevant traffic from their individual perspective using the game theoretic approach of *multi-agent simulation* [183]. Thus, the tactical decision-making based on this interaction-aware prediction is more reliable than the former approaches.

The encapsulation of the traffic scene prediction as an independent process within the hierarchical decision network enables a modular development of its functionality. For the subsequent layers, the output form the prediction module is a further important input data. Through the use of a vehicle-to-vehicle communication technology in future, the results of the traffic scene prediction module can be improved or even replaced by the a priori knowledge about the exact planned maneuvers of other traffic participants.

2.2.3 Arbitration

The process of *Arbitration* corresponds to the situation classification. Its tasks are one the one hand to coordinate (i.e. activating and terminating) the respective behavioral strategies based on the current and upcoming events. On the other hand, if multiple behavioral strategies are simultaneously active, this module has to provide the final driving goals. Thus, an important part of the overall intelligence of the tactical decision-making process is integrated in the arbitration process.

The coordination task is implemented in this thesis using the concept of concurrent FSMs in a way that its flexibility and transparency is guaranteed [196]. For each behavioral strategy it exists a separate state machine with only the two states of *Active* and *Inactive*. The transitions between the states within each FSM are realized by a rule-based approach. Once a state machine changes to the state *Active*, the corresponding maneuver planning process begins to calculate the driving goals at its particular rate. The final driving goals is, however, determined by the arbitration process through interpolation between possibly asynchronous driving goals of the active behavioral strategies and applying a priority based approach.

2.2.4 Behavioral Strategies

As discussed before, each behavioral strategy implements an appropriate model predictive maneuver planning which is responsible for achieving a specific medium-term behavioral goal. In this thesis, three novel strategies are developed for highly automated driving in highway applications to accomplish the most of complex traffic situations:

- Basic Behavioral Strategy: This behavioral strategy ensures a comfortable and safe driving with respect to the surrounding traffic in most of the time. The maneuver planning, discussed in Chapter 4, is realized by a nonlinear model predictive

approach [196] which is solved using two different formulations of mixed integer quadratic programming and combinatorial optimization.

- Cooperative Behavioral Strategy: In some specific situations, such as merging scenarios, a higher level of cooperation between the cognitive vehicle and the relevant traffic participants is needed. In Chapter 5, a novel maneuver planning approach based on the methods from game theory is developed, which is able to capture this complex interaction between the road users by modelling the replanning capabilities of them [193]. With this, the maneuver planning in this behavioral strategy offers cooperative driving decisions.

- Driver Take Over Behavioral Strategy: During autonomous driving, a critical part of the system is the driver take over request. A driver take over request, or TOR, can happen for various reasons and under varying circumstances. Once a TOR occurs, this behavioral strategy has to realize a comfortable TOR for the driver. In the case that driver fails to take over control, however, the cognitive vehicle has to reach a safe state at the end of TOR phase. The maneuver planning introduced in Chapter 6 satisfies these requirements. It is based on a model predictive approach with a diminishing rather than receding horizon and with time-varying constraints [194].

Further improvements of the decision-making process can be easily done by defining new behavioral strategies with certain goals and requirements and integration these into the modular structure of the proposed hierarchical decision network. Finally, the arbitration process has to be extended in order to properly manage the new behaviors.

2.3 Operational Level

The previous section gives a detailed overview about the developed tactical decision-making framework. In this section, the actual approach of the operational level implemented in the BMW Group Research and Technology prototype vehicles will be briefly discussed.

The operational level comprises the two modules of *trajectory planning* and *motion control*. The trajectory planning generates a set of collision-free trajectories with minimum jerk based on the provided driving goals from the tactical decision-making process. The approach is based on a combined optimization of lateral and longitudinal movements using discretized terminal manifolds [178]. Various optimization restrictions such as vehicular physics and detected collisions [64, 148, 187] are considered in the optimization process.

In order to facilitate velocity and distance control, a cascade control structure was developed. The structure consists of three nested control loops for acceleration, velocity and distance control. A detailed description of the introduced state adaptive control concept is presented in [4, 11]. The lateral controller is based on the control concept discussed in [177]. Since the lateral controller should be used up to a moderate dynamic range, a simplified vehicle model (e.g. single-track model) can be used for modeling the controlled system. For this purpose, a decoupling-controller is applied, which has high control accuracy, stability and comfort. The controller consists of an inner and an outer loop. The inner loop corresponds to the decoupling controller with the yaw rate as output. It ensures

that the yaw motion of the vehicle follows its desired value from the generated trajectory. The outer control loop provides the required nominal variables for the yaw rate controller through state feedback.

2.4 Conclusion and Discussion

In this chapter, the most important frameworks concerning the tactical decision-making process of automated driving have been discussed. It has been revealed that the division of the continuous driving task into a finite set of discrete driving states is the most effective way to master this complex task. However, Within the current concepts it has been shown that there is no framework that fulfills all previously defined requirements. In particular, the lack of flexibility and modular expandability are two major shortcomings of the state-of-the-art approaches.

Based on the results of this evaluation, a novel framework for the tactical decision-making process, the so-called hierarchical decision network, has been developed and presented. One of the main advantages of the proposed framework is the centralization of the interaction-aware traffic scene prediction module and applying its outcomes to ensure a reactive and anticipatory decision-making. Thus, an independent development of this module is always possible. Furthermore, introducing the concept of high-level behavioral strategies with their specific objectives and well-defined input/output interfaces simplifies the complex driving task and enables a modular expandability of the system. In addition, thanks to the arbitration layer, which performs the task of situation classification, an intelligent managing of the behavioral strategies in a distributed manner is allowed.

The proposed framework can be applied in further autonomous driving application cases (e.g. tactical decision-making in urban environments) or in general action selection problems associated with intelligent agents [183].

In the next chapter, a novel, on-line capable interaction-aware intention and maneuver prediction framework for dynamic environments is presented. As discussed before, this module is one of the major improvements compared to the previous works. The main contribution is here the combination of a model-based interaction-aware intention prediction with a maneuver-based motion prediction based on supervised learning. The proposed algorithm can be used for highly automated driving or as a prediction module for advanced driver assistance systems without the need of inter-vehicle communication.

3 Interaction-aware Traffic Scene Prediction

As discussed in the last chapter, the traffic scene prediction module is one of the most important elements of the proposed hierarchical decision network. It provides the subsequent behavioral strategies with the necessary information about the possible future states of the environment with the corresponding probabilities. In this chapter, a novel framework for interaction-aware maneuver prediction is presented, which combines the benefits of the *model-based* and the *learning-based* approaches[1]. The advantages of this framework are twofold. On the one hand, expert knowledge in the form of heuristics is integrated, which simplifies modelling of the interaction. On the other hand, the difficulties associated with the *scalability* and *data sparsity* of the algorithm due to the so-called *curse of dimensionality* can be reduced, as a reduced feature space is sufficient for supervised learning.

At the start of the algorithm, the motion intention of each driver in a traffic scene is estimated in an iterative manner using the game-theoretic idea of stochastic *multi-agent simulation*. This approach provides an interpretation of what other drivers intent to do and how they interact with surrounding traffic. By incorporating this information into a *Bayesian network classifier*, the developed framework achieves a significant improvement in terms of reliable prediction time and precision compared to other state-of-the-art approaches. By means of experimental results in real traffic on highways, the validity of the proposed concept and its on-line capability is demonstrated. Furthermore, its performance is quantitatively evaluated using appropriate statistical measures.

In this thesis, the proposed approach is presented for highway scenarios. The algorithm, however, can be adapted to further environments or be applied in other research fields such as cooperatively navigating of mobile service robots in populated environments.

3.1 Introduction and State of the Art

Safe motion planning in dynamic environments is one of the key challenges in the domains of mobile robotics, driver assistance, autonomous and highly automated driving. This can only be achieved if the future state of the environment is known to the cognitive agent as accurately as possible. Therefore, not only the actual perception, but also the future evolution of the traffic scene has to be considered in motion planning. Basically, a cognitive vehicle which is able to predict the maneuvers of other road users resembles to what humans refer to as "driving with foresight and anticipation", a way of driving which is taught to drivers already in their first driving lessons.

Most accidents on highways occur due to risky overtaking and cut-in maneuvers [33]. Through the use of a maneuver prediction system, an early response to such critical events

[1] Parts of the results in this chapter have been pre-published in [192].

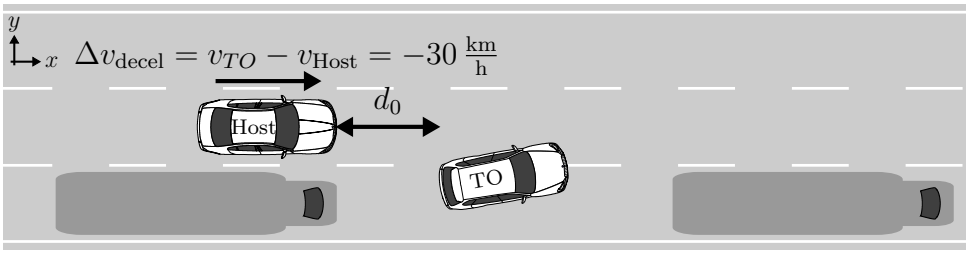

Fig. 3.1: Example of a critical cut-in situation on highway.

is made possible. Such an anticipatory tactical decision-making promises not only enhanced safety, but also advantages in comfort, fuel consumption and traffic flow [22, 190]. To show the significance of even small gains in the prediction horizon, consider the following simplified example.

Figure 3.1 sketches a critical situation on the highway. It is assumed that the host vehicle drives with a standard adaptive cruise control system (ACC), when the second vehicle suddenly starts a critical cut-in maneuver at its constant speed. The host vehicle, thus, automatically adjusts its driving speed with a maximum constant deceleration of $a_{\text{decel,max}} = -4\,\text{m/s}^2$. Let the speed difference between the host vehicle and the target object at the beginning of braking be denoted by Δv_{decel}. The distance to the target object at this moment is referred to as d_0. To ensure a collision-free driving in this situation, the relative braking distance Δd_{decel} should be less than or equal d_0, i.e.[2]

$$\Delta d_{\text{decel}} = \tfrac{1}{2} a_{\text{decel,max}} t^2 - \Delta v_{\text{decel}} t \leq d_0, \tag{3.1}$$

with

$$t = \left| \frac{\Delta v_{\text{decel}}}{a_{\text{decel,max}}} \right|. \tag{3.2}$$

In the case of today's ACC implementations the host vehicle begins to brake after the target object crosses the lane markings (see Fig. 3.1). Using these numbers, the illustrated traffic situation will remain collision-free only if the inter-vehicular distance is $d_0 \geq 8.7\,\text{m}$.

The same scenario is now considered assuming that the lane change maneuver of the target object was predicted $\delta_t = 1\,\text{s}$ in advance. The host vehicle can thus start one second earlier with decelerating (i.e. $t = \left| \frac{\Delta v_{\text{decel}}}{a_{\text{decel,max}}} \right| + \delta_t$). In order to avoid the collision, d_0 can be now as small as $d_0 \geq 6.7\,\text{m}$. This example shows that, even though a prediction time δ_t of one second before crossing the lane markings (hereinafter referred to as *lane change event*) seems to be short, the overall safety of the traffic can be improved considerably, since the relative braking distance can be up to about 23% reduced.

Motion prediction in dynamic environments requires an on-line capable algorithm which necessarily captures the interaction between different agents. The proposed framework in this thesis meets these requirements. The idea of this novel approach is to combine complementary methods of prediction to provide an accurate estimation of long-term motion in order to increase the robustness and, as a consequence, the safety and comfort of the tacti-

[2]Here, the relative distance between vehicles is considered from bumper to bumper assuming constant acceleration. In addition, reaction time is neglected.

cal decision-making. At first it estimates the motion intention of each driver regarding the modelled interaction with his/her surrounding road users in a traffic scene. Combining this initial estimate with a classifier based on supervised learning, different future maneuvers of each traffic participant with their probabilities are determined.

Thanks to the suggested combination of model-based and learning-based approaches, the best of two worlds is offered: Firstly, expert knowledge about driving behavior and traffic rules is integrated in the framework, which simplifies modelling of the interaction. Secondly, the amount of required labeled training data is minimized, since there is no need anymore to recognize different patterns of interaction between road users within the classifier. Consequently, the costs associated with acquiring, labeling and storing the training data can be reduced.

In the following, an overview of the related publications is given, the problem of interaction-aware prediction is defined and a solution is proposed fulfilling the above requirements. The developed approach is evaluated in real traffic scenarios on highways, demonstrating the benefits. Additionally, a quantitative analysis based on a test set from several hours of real traffic is given.

As pointed out above, motion prediction is one of the key elements of today's robotics and autonomous driving research. Not surprisingly, various approaches have been suggested over the recent years, each of which has different characteristics regarding the degree of abstraction. The survey of [95] classifies the existing methods of motion prediction in three different approaches: *Physics-based*, *Maneuver-based* and *Interaction-aware* models. Simply put, physics-based models have the lowest degree of abstraction and are limited to non-reliable short-term prediction, while interaction-aware models works on a symbolic level (i.e. different model assumptions) providing a more reliable long-term prediction. The maneuver-based approaches are in-between.

Physics-based Motion Prediction

The physics-based approaches are the most simplest motion prediction methods, since they only consider the current observations without any situation interpretation. Here, the maneuvers are predicted by simple kinematic models such as constant velocity, constant acceleration or constant turn rate [16, 80, 139] thanks to the simplicity and computational efficiency. Compared to this single trajectory simulation approaches, the Gaussian noise simulation can be used to represent the uncertainty on the predicted trajectory [9]. A further example is the use of Monte Carlo simulation [8, 28]. Hereby, the input vector is randomly sampled with respect to certain dynamic constraints (approximating the reachable set of states). Subsequently, the different future trajectories are evaluated by their risk, driving comfort and other predefined criteria, allowing a quasi stochastic prediction. The physics-based approaches are limited to short-term motion prediction (less than one second [95]). Besides, the unobservable drivers' intent and the semantic interpretation of the surrounding situations are completely neglected, limiting their reliability.

Maneuver-based Motion Prediction

The maneuver-based motion models eliminate this drawback. Here, each driver is represented as a maneuvering entity which executes its intended maneuvers independently from other traffic. The term "maneuver" is defined in [44] as "a physical movement or series of moves requiring skill and care". The most common way is thus to define a finite set of prototype discrete maneuvers (e.g. lane keeping, lane change or turning) and classify the future continuous motion of each vehicle to one of these maneuvers based on measured features. Different machine learning methods such as generative classifier [137, 195], artificial neural networks [45], support vector machines [7, 45, 90], Bayesian Networks [38, 83, 130] and Hidden Markov Models [10, 109] can be found in the literature.

The prediction based on the maneuver-based approaches is in general more reliable in the long term. As an example, the approach in [83] detects a lane change maneuver about 0.6 s earlier than a standard active cruise control system. The approach in [195] is able to predict driver intention to change lanes of other traffic on average about 1.1 s in advance (i.e. 1.1 s earlier than a lane change event). The approach in [90] predicts the lane change maneuver of the host vehicle about 1.3 s in advance. However, if the dimensionality of the feature space increases, the classification problem becomes significantly more difficult due to the *curse of dimensionality* [134, 166]. Furthermore, the amount of available high-quality labeled training data is usually very limited and does not cover all possible situation, which refers to as the problem of *data sparsity* [134].

Interaction-aware Motion Prediction

The interaction-aware prediction models are the most comprehensive approaches. Here, the future motion of each vehicle is assumed to be influenced by other traffic. The consideration of interaction reflects the reality better in comparison with the previous two motion models. One idea is to consider the interaction between the road users by finding an optimal predicted scene in terms of minimizing the risk for all the traffic participants [93]. Other solutions are based on Dynamic Bayesian Networks [6, 60]. Another idea is a game theoretic approach to replanning-aware interactive scene prediction as presented in [193]. The interaction-aware models allow longer-term reliable prediction compared to the two previous approaches since they consider the mutual dependencies between the drivers' motions decisions. However, the quality strongly depends on the correctness of the model assumptions. For example due to the risk minimizing assumption, real dangerous traffic situations might not be predicted properly. A further problem is the computational complexity which usually grows exponentially with the number of vehicles in a group that interact with each other. Thus, it becomes difficult to meet the on-line requirement. Furthermore, as these models often have problems with modeling mutual dependencies, they are often implemented asymmetric with the assumption that the dependency is only one directional [120].

While inter-vehicle communication unarguably does bring benefits to maneuver prediction, since certain information will be available as a priori knowledge [98], there is also "need for significant penetration before [inter-vehicle communication systems] can become effective" [143]. However, the disadvantages due to the high cost of the needed infras-

tructure, the scalability problem of the networks and the related security issues make its industrialization very difficult [125]. Therefore, a framework is required which enables a reliable long-term maneuver prediction without a specific need of inter-vehicle communication.

Discussion

As mentioned before, the novel idea of the maneuver prediction framework presented in this thesis is to divide the prediction task into two main groups of interaction-aware model-based and interaction-unaware supervised learning-based subtasks. The interaction-aware prediction model is based on the game theoretic idea of stochastic multi-agent simulation using cost functions [134, 142, 183]. Here, spatio-temporal cost maps are applied for predicting other drivers' intention taking into account the interaction between vehicles in a traffic scene. This initial estimate is further used in an Bayesian network which classifies the possible future maneuvers of each vehicle based on its most discriminant interaction-unaware features. Subsequently, the results of these two complementary methods are combined. This provides an accurate estimation of long-term motion.

The contributions of the proposed algorithm are thus twofold. On the one hand, an online capable interaction-aware intention estimation model is implemented which considers the road geometry, traffic rules as well as the manner of interaction between the vehicles in a traffic scene. The expert knowledge is integrated and can be extended easily in this model in the form of further cost functions. On the other hand, a maneuver-based classifier is combined to learn different maneuver patterns and make the prediction even more robust against possibly improper model assumptions in the case of unusual style of driving. Here, a compact set of relevant interaction-unaware features is selected and the parameters are learned based on a limited amount of labeled real traffic data. Hence, the difficulties arising from the previously mentioned curse of dimensionality and data sparsity are overcome.

3.2 Problem Formulation

Making use of the fact that highways can be seen as a structured environment, the infinite number of possible movements a driver is able to perform can be approximated using a *finite set of basic maneuvers* $\mathcal{M}$. In the following, each j-th basic maneuver of the v-th vehicle at the discrete time step t belongs to a different set as, $m_{j,v}^t \in \mathcal{M}_v^t$.[3] Prediction over multiple time steps are represented as maneuver sequences. The *set of maneuver sequences* of the v-th vehicle $\mathbf{\Pi}_v$ is defined as the Cartesian product of its predicted basic maneuver sets for all time steps up to the predefined *prediction horizon* T as

$$\mathbf{\Pi}_v := \prod_{t=1}^{T} \mathcal{M}_v^t. \tag{3.3}$$

[3] To simplify the notation, it is ignored that the set of basic maneuvers of each vehicle is dependent on its current state. However, this fact is taken into account in the implementation.

A predicted maneuver sequence is thus defined as a T-tuple of basic maneuvers

$$\boldsymbol{\pi}_v \in \boldsymbol{\Pi}_v := (m^1_{j,v}, m^2_{k,v}, \ldots, m^T_{n,v}). \tag{3.4}$$

Put simply, this assumption simplifies modelling of the possible continuous trajectories of each vehicle by the ordered set of its basic maneuvers defined through the Cartesian product. The Cartesian product thus describes the temporal concatenation of the basic maneuvers.

In the following, each predicted basic maneuver $m^t_{j,v}$ is modeled as a set of pairs of a *lateral motion*, $m_{\text{lat},v}$ and a *longitudinal motion*, $m_{\text{long},v}$

$$m^t_{j,v} = \{m_{\text{lat},v}, m_{\text{long},v}\}. \tag{3.5}$$

The lateral motion in this work is an element from the discrete set of feasible lateral movements on highways, $\mathcal{M}_{\text{lat}}$, given by

$$m_{\text{lat},v} \in \mathcal{M}_{\text{lat}} := \{-1, 0, +1\} \mathrel{\widehat{=}} \{\text{LCL, LK, LCR}\}, \tag{3.6}$$

corresponding to a lane change to left, keeping the lane or a lane change to right. The maximal number of predicted lane changes up to the prediction horizon is hereinafter limited to one. In other words, each maneuver sequence represents a maximum of one change in the lateral direction

$$\forall \boldsymbol{\pi}_v \in \boldsymbol{\Pi}_v : \sum_{t=1}^{T} |\dot{m}^t_{\text{lat},v}| \leq 1 \tag{3.7}$$

The longitudinal motion is, however, continuous. It is an element from the set of feasible longitudinal accelerations (resp. decelerations) $\mathcal{M}_{\text{long}}$ given by

$$m_{\text{long},v} \in \mathcal{M}_{\text{long}} := \{m_{\text{long},v} | a_{\min} \leq m_{\text{long},v} \leq a_{\max}\}. \tag{3.8}$$

Given the set of the last n measured dynamic states

$$\mathcal{X}^{t-n:t} := (\mathbf{X}^{t-n:t}_{v=1}, \mathbf{X}^{t-n:t}_{v=2}, \ldots)$$

of all vehicles up to the current time t, the task of prediction is to determine the set of future maneuver sequences $\boldsymbol{\Pi}_v$ of every vehicle with the corresponding probabilities. The probabilistic nature of the prediction arises from the non-observable future driver intention $\mathcal{I}^{t:t+T}_v$ considering the interaction to surrounding traffic and other information like as traffic rules and structure of the road network. Thus, a probability will be assigned to each maneuver sequence,

$$P(\boldsymbol{\pi}_v | \mathcal{X}^{t-n:t}, \mathcal{I}^{t:t+T}_v) \in [0, 1]\,. \tag{3.9}$$

In this thesis, the future driver intention is defined as $\mathcal{I}^{t:t+T}_v \in \{\text{LCL, LK, LCR}\}$.

In the next section, the novel intention and maneuver prediction framework is discussed

in detail.

3.3 Approach

One of the key elements in the development of learning algorithms is to have enough data for learning so that they fill the space where the model must be valid. It is easy to prove that the number of learning data should grow exponentially with the dimension of feature space [166]. The novel idea in this work is to overcome this problem through a sophisticated combination of model-based and learning-based approaches.

Figure 3.2 visualizes the information flow of the proposed framework. The goal is to predict the future maneuver sequence of each traffic participant based on the actual and previous data. Expert knowledge is easily integrated in the model, since certain assumptions like following the traffic rules, overtaking a slow leading vehicle, merging on the highway and risk-aware driving can be modeled very well. Consequently, the amount of required labeled training data and its associated high computational cost and memory usage can be minimized. All this leads to a comprehensible maneuver prediction framework. In the current setting (see Section 2.2), the set of predicted traffic scenes will be passed subsequently to the Arbitration and behavioral strategies to plan the most comfortable and safe trajectory for the host (cognitive) vehicle.

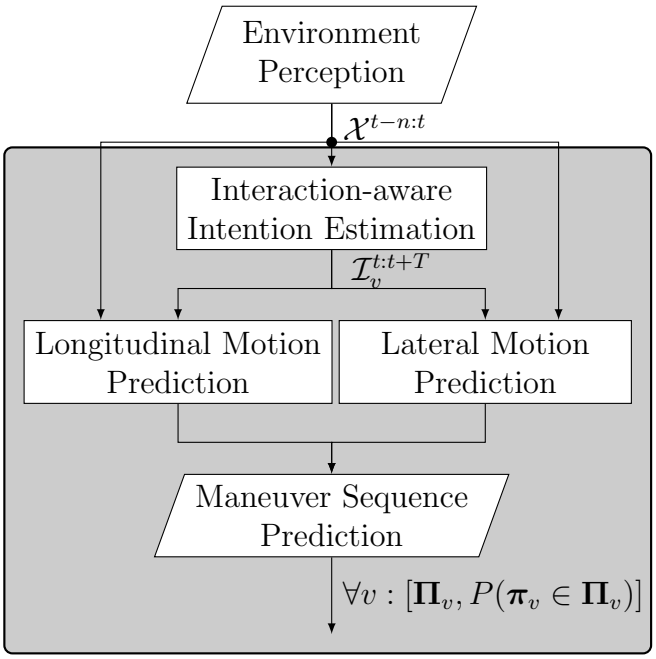

Fig. 3.2: Overview of the maneuver prediction framework. First, the interaction-aware motion intention of each driver is predicted iteratively based on the idea of multi-agent-simulation using model-based cost functions. This provides a reliable first estimate for the subsequent lateral and longitudinal motion predictions.

In the first step, the motion intention of each driver $\mathcal{I}_v^{t:t+T}$ from his/her perspective is predicted. This approach is based on the game-theoretic idea of multi-agent simulation.

Thus, the future motion planning (i.e. decision making) of each driver is simulated, taking into account the interaction with its surrounding traffic. The interaction is considered iteratively by means of various model-based *cost functions*. They are formulated in this work using a heuristic approach based on expert knowledge and certain traffic regulations. The output of this *interaction-aware intention estimation* model builds up the foundation on which the subsequent lateral and longitudinal motion predictions are based on. This model is on-line capable and adaptable in terms of prediction horizon T and step size. Furthermore, the hierarchy between the road users in a traffic scene has not to be considered explicitly.

The *lateral motion prediction* determines the probability of the different lateral motions from (3.6) for each vehicle. In this work, the generative approach of the Bayesian network classifier [134] is applied. The already estimated interaction-aware motion intention of each vehicle is considered here as a further evidence. Therefore, the required feature space for the classification is considerably reduced to the lower dimensional space of interaction-unaware lane-relative features.

The *longitudinal motion prediction* corresponds in this work to the sequence of longitudinal accelerations determined directly by the intention estimation model. Thus, the motion prediction in this direction is interaction-aware as well. However, no further learning-based approach is used here explicitly for the longitudinal motion prediction, since the focus is on the (more critical) lateral motion prediction.

3.3.1 The Interaction-aware Intention Estimation Model

The following assumption describes the idea of the developed interaction-aware intention estimation model

Assumption 3.1 *The most likely intended maneuver of each rational driver corresponds to his/her risk-aware motion planning. Therefore, it is assumed that each traffic participant tries to follow the traffic rules and drives preferably at its desired speed. Any deviation from this assumption is because of certain interactions with the surrounding traffic which results in additional acceleration (resp. deceleration). In other words, the interaction-aware planning of each agent in this multi-agent system is equivalent to its prediction from subjective view of other traffic participants.*

The interaction-aware maneuver planning of the v-th vehicle is determined in this work using a spatio-temporal cost map $\mathbf{U}_v^t(x, y)$ in the two-dimensional Cartesian space (spatio) at the predicted time step t (temporal). Its value given by

$$\mathbf{U}_v^t(x,y) := \frac{\sum_i \lambda_i u_i(\mathbf{x}_v^t, \bigcup_{v'} \mathbf{x}_{v'}^t, \mathbf{c}_v^t)}{\sum_i \lambda_i} \in [0,1] \tag{3.10}$$

with

$$\mathbf{x}_v^t \in \mathbb{R}^4 \sim \mathcal{N}_4\left(\boldsymbol{\mu}_{\boldsymbol{x_v}}^t, \boldsymbol{\Sigma}_{\boldsymbol{x_v}}^t\right) := \begin{pmatrix} x_v^t \\ y_v^t \\ \dot{x}_v^t \\ \dot{y}_v^t \end{pmatrix} \mathrel{\widehat{=}} \begin{pmatrix} \text{long. position} \\ \text{lat. position} \\ \text{long. velocity} \\ \text{lat. velocity} \end{pmatrix},$$

the multivariate normally distributed state vector of each vehicle at the time step t and

$$\mathbf{c}_v^t := \begin{pmatrix} \text{distance to the next highway junction} \\ \text{type of lane marking (left/right)} \\ \text{distance to lane end (current/left/right)} \\ \text{current speed limit} \end{pmatrix} \in \mathbb{R}^7,$$

the *contextual* state vector from perspective of the evaluated vehicle v. The state vector is directly provided by the object detection and fusion algorithm [189]. It applies a traditional Kalman filter tracking algorithm which assumes normally distributed state vector. The information about the contextual state vector is provided by the already generated digital maps [189].

The spatio-temporal cost map is thus a linear combination of different, partially competitive cost functions $u_i : \mathbb{R}^{4(1+|v'|)} \times \mathbb{R}^7 \rightarrow [0,1]^2$ with the respective weighting factors $\lambda_i \in [0,1]$.[4] The cost functions on the one hand take into account the state of the evaluated vehicle $\mathbf{x}_v^t$ as well as the set of state vectors of its *relevant traffic* $\mathbf{x}_{v'}^t$ ($|v'|$ is the number of relevant vehicles). This is more realistic as most of the drivers only consider vehicles in their immediate surroundings. On the other hand, the contextual state vector of the evaluated vehicle is considered.

The cost functions model heuristics about various driving behaviors such as staying on the road with respect to the hard barriers on roadway edges, driving towards the (estimated) desired speed with a preference to travel in a lane center, velocity-dependent distance control to the vehicle ahead, safe overtaking maneuvers considering the traffic on the desired lane and obeying traffic rules. Any collision with the surrounding traffic is represented as infinite costs in this map. Particularly, the shape and dimensions of the cost map around each obstacle vehicle from perspective of the evaluated vehicle can appropriately encourage control vehicle slowing or overtaking on the left, depending on relative speeds and surrounding traffic. The appropriate implementation of the different cost functions and the parameters in this thesis is based on the approach presented in [182].

In Figure 3.3 the cost map from perspective of the rear vehicle for one single time step is exemplarily illustrated. It shows a situation where the rear vehicle is approaching at a higher relative speed and does not maintain a safe distance to the vehicle ahead. A further cost map (not shown here) is determined simultaneously from the driver's view of the front vehicle which models its interaction with the rear traffic. Thus, each vehicle perceives its surrounding environment in an individual way.

According to Assumption 3.1, it is expected that each vehicle plans its future intended maneuver along the negative gradient of its cost map as

$$\mathbf{f}_v^t := -\mathbf{k} \circ \left[\frac{\partial \mathbf{U}_v^t(x,y)}{\partial x}, \frac{\partial \mathbf{U}_v^t(x,y)}{\partial y} \right]^{\mathrm{T}} \in \mathbb{R}^2. \tag{3.11}$$

The resulting *force vector* $\mathbf{f}_v^t$ minimizes the local planning cost of the v-th vehicle at the time step t based on the modelled interaction with its surrounding traffic (gradient descent).

[4] In the implementation, the cost map for each vehicle is filtered using weighted moving average in order to create situational memory from perspective of the corresponding vehicle.

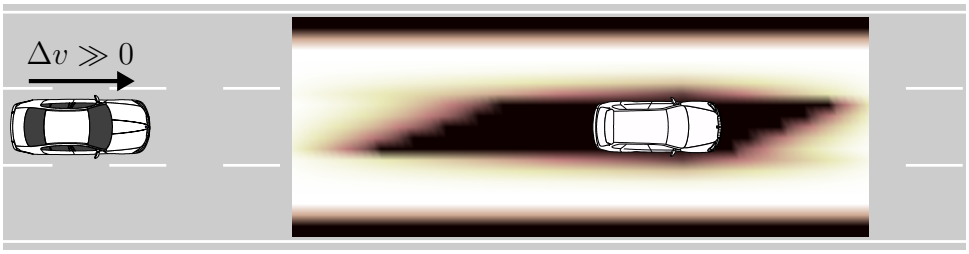

Fig. 3.3: The cost map as calculated by the rear vehicle for a single prediction time step. It is determined for the situation where the rear vehicle is approaching at higher velocity and does not respect the safety distance. The darker color corresponds to a higher cost for its future intended maneuver. The designed cost functions enable a transition between maintaining a safe distance versus forcing a lane change (pushing to the left side).

It is scaled by the vector $\mathbf{k}$ to respect dynamic constraints in the lateral and longitudinal directions (element-wise product). Thus, it is assumed that each traffic participant plans in the direction of its calculated gradient vector which is in the following referred to as *interaction-aware acceleration (resp. deceleration)*.

In an iterative manner, the cost map of each vehicle is updated based on the latest predicted states of its own and relevant traffic and the gradient vector is calculated again. In the following, the multivariate normally distributed state vector of each vehicle at the time step t is given by

$$\mathbf{x}_v^t \in \mathbb{R}^4 \sim \mathcal{N}_4\left(\boldsymbol{\mu}_{\boldsymbol{x_v}}^t, \boldsymbol{\Sigma}_{\boldsymbol{x_v}}^t\right) := \begin{pmatrix} x_v^t \\ y_v^t \\ \dot{x}_v^t \\ \dot{y}_v^t \end{pmatrix} \mathrel{\widehat{=}} \begin{pmatrix} \text{longitudinal position} \\ \text{lateral position} \\ \text{longitudinal velocity} \\ \text{lateral velocity} \end{pmatrix}. \tag{3.12}$$

To simplify the representation of vehicle dynamics, the interaction-aware intention estimation is implemented through a double integrator system in the following steps

1. Starting from the latest predicted states (resp. the latest measurements) of all traffic participants, the spatio-temporal cost map of each vehicle is updated and the force vector is calculated with (3.11). As described before, this term is equivalent to its longitudinal and lateral interaction-aware acceleration

   $$\left[\ddot{x}_v^t, \ddot{y}_v^t\right]^{\mathrm{T}} = \mathbf{f}_v^t \tag{3.13}$$

   with

   $$\mathbf{f}_v^t \sim \mathcal{N}_2\left(\boldsymbol{\mu}_{\boldsymbol{f_v}}^t, \boldsymbol{\Sigma}_{\boldsymbol{f_v}}^t\right).$$

   The assumption of normal distribution here is inspired by the state vector and enables the following linear superposition of state variables.

2. With a uniform acceleration assumption, the next mean vector of each vehicle's state

is predicted with[5]

$$\boldsymbol{\mu}_{\boldsymbol{x_v}}^{t} = A\boldsymbol{\mu}_{\boldsymbol{x_v}}^{t-1} + B\boldsymbol{\mu}_{\boldsymbol{f_v}}^{t-1}. \tag{3.14}$$

with

$$A = \begin{pmatrix} 1 & 0 & \Delta t & 0 \\ 0 & 1 & 0 & \Delta t \\ 0 & 0 & 1 & 0 \\ 0 & 0 & 0 & 1 \end{pmatrix} \text{ and } B = \begin{pmatrix} \frac{\Delta t^2}{2} & 0 \\ 0 & \frac{\Delta t^2}{2} \\ \Delta t & 0 \\ 0 & \Delta t \end{pmatrix}.$$

The uncertainties of the initial measured state variables are taken in the entire intention estimation process by

$$\boldsymbol{\Sigma}_{\boldsymbol{x_v}}^{t} = \hat{A}\boldsymbol{\Sigma}_{\boldsymbol{x_v}}^{t-1} + \hat{B}\boldsymbol{\Sigma}_{\boldsymbol{f_v}}^{t-1} \tag{3.15}$$

with

$$\hat{A} = \begin{pmatrix} 1 & 0 & \Delta t^2 & 0 \\ 0 & 1 & 0 & \Delta t^2 \\ 0 & 0 & 1 & 0 \\ 0 & 0 & 0 & 1 \end{pmatrix} \text{ and } \hat{B} = \begin{pmatrix} \frac{\Delta t^4}{4} & 0 \\ 0 & \frac{\Delta t^4}{4} \\ \Delta t^2 & 0 \\ 0 & \Delta t^2 \end{pmatrix}.$$

As the initial state variances are given to the prediction framework by the object detection and fusion algorithm [189], the variance of the calculated interaction-aware accelerations $\boldsymbol{\Sigma}_{\boldsymbol{f_v}}^{t}$ represents the uncertainty of the intention estimation model. Its initial value is given as a parameter. The value increases linearly with the prediction time steps. The variable Δt corresponds to the predefined discrete time step resp. replanning period. Its value is set to $\Delta t = 0.5\,\mathrm{s}$.

3. The steps 1-2 are repeated for all the prediction steps $t = 1, 2, \ldots T$ up to the prediction horizon. The intention estimation is calculated in this work for a prediction horizon of $T = 5\,\mathrm{s}$.

Figure 3.4 exemplarily shows the iterative process of interaction-aware intention estimation for the initial scenario given in Figure 3.3. The driver of the rear vehicle intends an overtaking maneuver to continue at its higher (desired) speed. At the same time, the slower front vehicle plans a maneuver towards its gradient vector making a lane change to right in order to obey the traffic rule (driving on the right most free lane). In addition, it accelerates slightly to minimize the overall risk.

The determined intention of each vehicle $\mathcal{I}_v^{t:t+T}$ (in the following as $\mathcal{I}_v$), in the form of its interaction-aware planning up to the predefined horizon T, provides a decent guess about its future motion. Although this model can be used directly to predict the future maneuvers of traffic, the predicted intentions will be used for the subsequent lateral and longitudinal motion predictions. The integration of this information in a learning-based approach will be discussed for the lateral motion prediction. This approach has two main benefits. First, a correct prediction is still possible even if model assumptions do not apply

[5]The state variables are assumed to be independent, since e.g. the longitudinal position of a vehicle does not carry any information about its other state variables. The mean and variance vectors at each time step are determined with the rule of linear combination of random variables [84, 153].

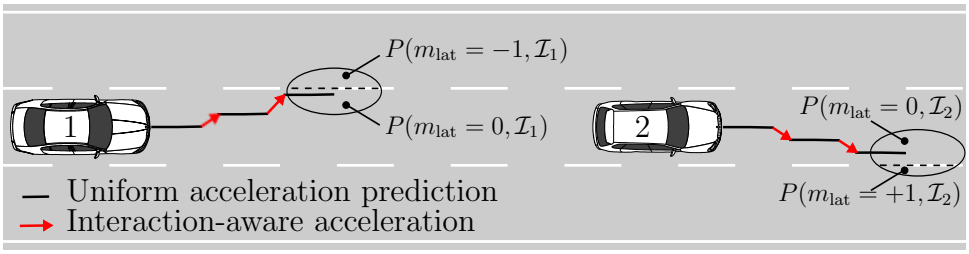

Fig. 3.4: The iterative process of interaction-aware intention estimation for each vehicle in the described traffic scene from Figure 3.3. Δt is the discrete time step in which the intention estimation model replans.

for a driver. In addition, as mentioned above, the required feature space of the classifier can be reduced to the most relevant interaction-unaware ones.

3.3.2 Lateral Motion Prediction

According to definition (3.6), the lateral motion prediction determines the joint probability distribution $P_v(m_{\text{lat}}, \mathcal{F}_v, \mathcal{I}_v)$ depending on the measured multidimensional feature vector $\mathcal{F}_v \in \mathbb{R}^n$ of the v-th vehicle and its estimated intention $\mathcal{I}_v$ as a further clue. The Bayesian network given in Figure 3.5 shows the conditional dependencies between the different variables. With the chain rule of probability theory, the joint probability distribution is given as

$$P_v(m_{\text{lat}}, \mathcal{F}_v, \mathcal{I}_v) \propto P(\mathcal{F}_v | m_{\text{lat}}) P(m_{\text{lat}}, \mathcal{I}_v), \tag{3.16}$$

where

$$\sum_{m_{\text{lat}} \in \mathcal{M}_{\text{lat}}} P_v(m_{\text{lat}}, \mathcal{F}_v, \mathcal{I}_v) = 1.$$

Additional conditionally independent features $\hat{\mathcal{F}}_v \in \mathbb{R}^n$ can be easily integrated in the model with the assumption of naïve Bayes as

$$P_v(m_{\text{lat}}, \mathcal{F}_v, \mathcal{I}_v) \propto P(\mathcal{F}_v | m_{\text{lat}}) P(\hat{\mathcal{F}}_v | m_{\text{lat}}) P(m_{\text{lat}}, \mathcal{I}_v). \tag{3.17}$$

The reason for applying the naïve Bayes approach is that its competitive classification performance on real world applications is surprising [184]. Moreover, it fulfills the requirement of on-line capability. An overview about the features used in this work and the estimation process of the conditional probability distribution of $P(\mathcal{F}_v | m_{\text{lat}})$ is given below. As mentioned earlier, the joint probability $P(m_{\text{lat}}, \mathcal{I}_v)$ of each single lateral motion is interaction-aware and situation-dependent from the individual view for each vehicle. For this purpose, the predicted normally distributed lateral position of each vehicle from (3.14) is integrated at the prediction horizon T over its current and neighboring lanes (see Figure 3.4)

$$P(m_{\text{lat}}, \mathcal{I}_v) = \begin{cases} \int_{\text{left lane}} \mathcal{N}(\mu_{y_v}^T, \sigma_{y_v}^T) & \text{for } m_{\text{lat}} = -1 \\ \int_{\text{current lane}} \mathcal{N}(\mu_{y_v}^T, \sigma_{y_v}^T) & \text{for } m_{\text{lat}} = 0 \\ \int_{\text{right lane}} \mathcal{N}(\mu_{y_v}^T, \sigma_{y_v}^T) & \text{for } m_{\text{lat}} = +1. \end{cases} \tag{3.18}$$

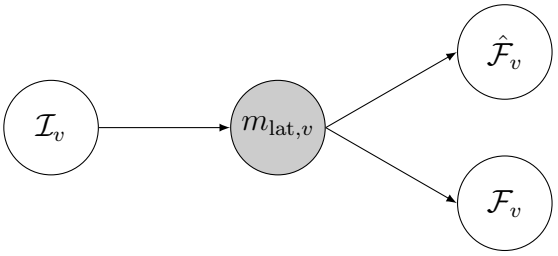

Fig. 3.5: Causal chain of the proposed Bayesian network classifier for the lateral motion prediction.

The joint probabilities for the lane change maneuvers are limited within certain minimum and maximum values by

$$P_{\pm 1,\min} \leq P(m_{\mathrm{lat}} = \pm 1, \mathcal{I}_v) \leq P_{\pm 1,\max}. \tag{3.19}$$

3.3.3 Longitudinal Motion Prediction

The longitudinal motion prediction in this work makes directly use of the predicted intention. According to (3.8), the continuous longitudinal motion m_{long} of each vehicle at a prediction time step is equivalent to its interaction-aware longitudinal acceleration from (3.13). The intermediate values are obtained by a cubic smoothing spline with a predefined smoothing parameter. Consequently, a comfortable and risk-aware way of driving is predicted for each vehicle.

For $m_{\mathrm{lat}} = \pm 1$, the maneuver prediction framework generates a continuous trajectory from the actual state of the evaluated vehicle to the middle of its respective target lanes. The calculation of these trajectories has been adopted from [178], however, the length of the trajectories depends on the predicted longitudinal motion of the vehicle. The endpoint of the lane keeping trajectory ($m_{\mathrm{lat}} = 0$) remains the center of its current lane. A more detailed description about the trajectory generation is provided in Appendix A.1.

Recalling the problem formulation from Section 3.2, the Cartesian product of the lateral motions with the T-tuple of interaction-aware longitudinal motions determines the set of predicted maneuver sequences $\mathbf{\Pi}_v$. The probability of each maneuver sequence $P(\boldsymbol{\pi}_v | \mathcal{X}^{t-n:t}, \mathcal{I}_v^{t:t+T})$ is equal to the calculated probabilities from (3.16). The pseudo-code of the presented maneuver prediction framework is given in Algorithm 1. In the following an exemplary implementation of the presented approach in this thesis will be outlined.

The Interaction-aware Intention Estimation Model

The accuracy of this model depends on the appropriate design of the cost functions. In this thesis, two different types of cost functions are implemented.

The first type is the *environment-based cost function*,

$$u_1(\mathbf{x}_v^t, \mathbf{c}_v^t) : \mathbb{R}^4 \times \mathbb{R}^7 \rightarrow [0, 1]^2, \tag{3.20}$$

which depends only on the state of the evaluated vehicle as well as certain contextual

Algorithm 1 Interaction-aware Prediction Framework

for all v **do**
  procedure PredictionFramework
    function IntentionPrediction($\mathcal{X}^{t-n:t}$)
      # Sec. 3.3.1
      for $t = 1$ to T **do**
        UpdateStatesOfOthers ()
        # Interaction-aware
        Calculate $\mathbf{U}[t]$ # wrt. relevant traffic
        $\mathbf{f}[t] \leftarrow -\mathbf{k} \circ \nabla \mathbf{U}[t]$
        $\boldsymbol{\mu}[t] \leftarrow A\boldsymbol{\mu}[t-1] + B\boldsymbol{\mu}_{\mathbf{f}}[t-1]$
        $\boldsymbol{\Sigma}[t] \leftarrow \hat{A}\boldsymbol{\Sigma}[t-1] + \hat{B}\boldsymbol{\Sigma}_{\mathbf{f}}[t-1]$
      end for
      return $[\mathbf{f}, \boldsymbol{\mu}, \boldsymbol{\Sigma}]$
    end function
    function LongPrediction($\mathbf{f}$)
      # Sec. 3.3.3
      for $t = 1$ to T **do**
        $\mathbf{m}_{\text{long}}[t] \leftarrow \mathbf{f}_1[t]$
      end for
      return $[\mathbf{m}_{\text{long}}]$
    end function
    function LatPrediction($\mathbf{X}_v^{t-n:t}\boldsymbol{\mu}, \boldsymbol{\Sigma}, \mathbf{m}_{\text{long}}$)
      # Sec. 3.3.2
      $\mathcal{F} =$ CalculateFeatures($\mathbf{X}_v^{t-n:t}$)
      for $i = 1$ to 3 **do** # 3 Different lateral motions
        $p \leftarrow \int_{\text{corresponding lane}}(\boldsymbol{\mu}, \boldsymbol{\Sigma})$
        $\mathbf{P}[i] \leftarrow$ BayesClassifier($\mathcal{F}, p$)
        $\mathbf{m}_{\text{lat}}[i] \leftarrow$ CalcTrajectory($\mathbf{m}_{\text{long}}$)
      end for
      return $[\mathbf{P}, \mathbf{m}_{\text{lat}}]$
    end function
    $\boldsymbol{\Pi} \leftarrow \mathbf{m}_{\text{long}} \times \mathbf{m}_{\text{lat}}$
    return $[\boldsymbol{\Pi}, \mathbf{P}]$
  end procedure
end for

information at the time step t. It takes into account whether from the perspective of the evaluated vehicle a lane change is possible (it means if the respective lane exists). It is realized through a repulsive potential with a maximum in the near of roadway barriers (similar to [182]). Additionally, the German *Rechtsfahrgebot* regulation, which states that one must generally drive on the right-most lane unless overtaking, is modelled by a linear function with a positive slope of cost in the direction of the left-most lane. The latter cost map is enabled only if the corresponding right lane from perspective of the evaluated vehicle provides a suitable gap for changing the lane. Near to highway junctions, another linear function generates costs depending on the distance to the end of ramp for a merging

vehicle (information provided by the digital map [189]), to simulate its merging intention. Further information like the lane marking types (dashed or solid) represent additional constant costs. Lastly, a Gaussian-like function is applied to model preferred driving on a lane center (similar to [182]).

The second cost function is the *interaction-based cost function*,

$$u_2(\mathbf{x}_v^t, \bigcup_{v'} \mathbf{x}_{v'}^t, \mathbf{c}_v^t) : \mathbb{R}^{4(1+|v'|)} \times \mathbb{R}^7 \rightarrow [0,1]^2, \tag{3.21}$$

which additionally considers the states of the relevant traffic from perspective of the evaluated vehicle at time step t. Using various information such as desired velocity of the v-th vehicle (estimated as the highest velocity since the first observation considering current speed limit), current speed limit, the remaining distance to the end of acceleration lane and the relative distance and velocity to traffic ahead, the lane change intention of the evaluated vehicle is estimated. The higher this intention, the higher the force in the direction of the respective lane. Moreover, the collision risks to its surrounding vehicles on the current and adjacent lanes are assessed.

As proposed in [62, 196], the collision risk in this work is a heuristic of time to collision (TTC) and intervehicular time (TIV) values. TTC is the time it takes two vehicles to collide under a constant velocity assumption. TIV is the time it takes a following vehicle to travel the current distance to a leading vehicle. The higher the risk, the higher the force in the opposite direction in order to minimize the collision risk. A further function creates a linear feedback law in the longitudinal direction in order to guide the evaluated vehicle towards its (estimated) desired speed taking into account the risk to its preceding vehicle. The resulting second cost function is implemented in a similar manner as the introduced "car and velocity" potentials in [182].

Finally, the overall cost map from perspective of the evaluated vehicle is calculated as

$$U_v^t(x,y) = \frac{u_1(\mathbf{x}_v^t, \mathbf{c}_v^t)\lambda_1 + u_2(\mathbf{x}_v^t, \bigcup_{v'} \mathbf{x}_{v'}^t, \mathbf{c}_v^t)\lambda_2}{\lambda_1 + \lambda_2}. \tag{3.22}$$

In this work, the parameters of the cost functions are determined by expert knowledge. Some sophisticated learning methods such as genetic algorithm can be used to further tune these parameters [163]. However, they require large amounts of learning data. The intention estimation is calculated in this work for a prediction horizon of $T = 5\,\mathrm{s}$. The prediction interval is set to $\Delta t = 0.5\,\mathrm{s}$.

The Lateral Motion Prediction

In this Implementation a three dimensional feature vector is considered. The first feature $f_{1,v} \in \mathcal{F}_v$ represents the lateral position of each vehicle within its lane. It is given by (see Figure 3.6a)

$$f_{1,v} := d_{\mathrm{left},v} - d_{\mathrm{right},v}. \tag{3.23}$$

This way, the widths of the lane and the vehicle are inherently taken into account. Therefore, on broader lanes a higher lateral offset is tolerated before a lane change maneuver will be predicted. Compared to the lateral offset to the lane center which was used as a feature

in [195], $f_{1,v}$ shows about 15% higher variable ranking in terms of Fisher's criterion[6] [65]. Thus, this feature enables a better classification.

The second feature

$$f_{2,v} := \dot{d}_v \tag{3.24}$$

represents the lateral velocity of the v-th vehicle in a road aligned (Frenet) coordinate system, where the origin is the center of its lane, guaranteeing a correct prediction especially in curves.

These two features have been shown to be the most discriminant interaction-unaware ones for the lateral motion prediction [130]. Additionally, in contrast to the approaches presented in [130] and [137], not only the current but also the previous measurements are taken into account by the third feature $f_{3,v}$ to create a memory in the classifier. The idea is to recognize if a vehicle drives over multiple time steps in a way which resembles the beginning of a lane change maneuver. The similarity of the latest n measurements are compared to a set of prototype lane change trajectories to left and right. These trajectories (Appendix A.2) are extracted from real traffic data on highways. The similarity can be used as a further clue to predict the future lateral movement of vehicles. The feature $f_{3,v}$ is given by

$$f_{3,v} := e_{\text{left},v} + \dot{e}_{\text{left},v} - (e_{\text{right},v} + \dot{e}_{\text{right},v}), \tag{3.25}$$

with

$$e_{\text{left/right},v} = \sum_{i=0}^{n} ||f^{t-i}_{\text{proto,left/right}} - f^{t-i}_{1,v}||_2$$

and

$$\dot{e}_{\text{left/right},v} = \sum_{i=0}^{n} ||\dot{f}^{t-i}_{\text{proto,left/right}} - \dot{f}^{t-i}_{1,v}||_2$$

for the errors in distance and velocity to the prototype maneuver of the lane change to left, or to right resp. This feature is exemplary shown in Figure 3.6b.

The introduced features are assumed to be normally distributed within each class. The lateral acceleration as a further feature is neglected in favor of robustness in real world, since it is usually noisy. The training process of the presented classifier is performed on a database from several hours of real traffic data from German highways. With a cycle-time of 100 ms, the feature vector for every observed vehicle within a radius of about 80 m was written to the database. The data was recorded by an especially equipped test vehicle containing 12 sensors for environment perception. The sensor configuration is shown in Figure 3.7. With the exception of the laser scanner sensors, all of the sensors are series production sensors currently integrated into the BMW 5 series for various driver assistance applications. Additionally, a Differential GPS combined with high-precision digital maps deliver relevant data regarding the road geometry. A detailed overview of the test vehicle and the algorithms for the environment perception are given in [189].

One of the main challenges is the automatic labeling of the training data. In this

[6] This criterion describes the the ratio of the between class variance to the within-class variance.

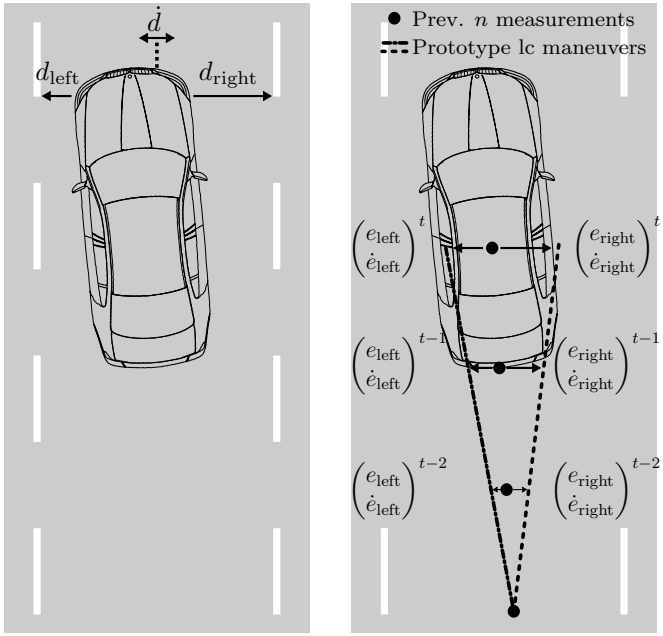

Fig. 3.6: The representation of different features used for the learning-based approach of the lateral motion prediction.

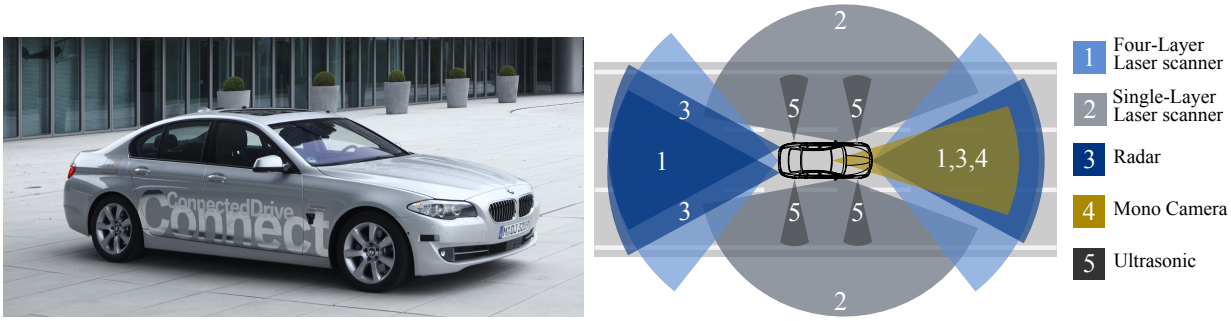

Fig. 3.7: Sensor configuration for the environment perception used in the test vehicle [189].

work, all the samples within a time interval of t_{lc} seconds before a lane change event are labeled as the ground-truth data-points representing the corresponding lane change. In this work, a lane change event is referred to the moment when the center of front bumper of a vehicle crosses the lane markings, i.e. it is on the other lane than in the time step before. Subsequently, the remaining samples are labeled as lane keeping maneuvers.

Based on this labeled data, the parameters of the three multivariate normal distributions $P(\mathcal{F}_v|m_{\text{lat}})$ of the respective lateral motions (3.6) were estimated using the MATLAB® library LIBRA [165] (Appendix A.3). The method is resistant to outliers in the training data. The predictors are conditionally dependent given the classes, because the correlation between the features in the training data set is significant. As mentioned before, the joint probabilities $P(m_{\text{lat}}, \mathcal{I}_v)$ were not learned, but they are provided dynamically by the interaction-aware intention estimation model.

With this setup, the potential of the developed interaction-aware prediction framework is evaluated.

3.4 Evaluation

The presented maneuver prediction framework runs at 10 Hz for typical highway scenarios in a multithreaded C++ framework, where other software modules such as object detection and fusion are implemented simultaneously. The evaluation is automatically performed on a separate test set recorded by the test vehicle. In the following, the performance of the lateral motion prediction is evaluated in detail, since, according to the example from Section 3.1, an accurate prediction in this direction has great impact on the overall safety and comfort. The longitudinal motion prediction is evaluated only qualitatively.

Within the first part of the evaluation, the advantages of the interaction-aware intention estimation module is demonstrated in two different traffic scenarios. In the second part, a quantitative evaluation is provided for an independent test set consisting of about 2 hours of real traffic on the German highway A9 from Munich to Ingolstadt with about 60 lane changes to left and right of other traffic participants. Hereby, the performance of the interaction-aware lateral motion prediction is compared to a interaction-unaware state-of-the-art approach in terms of average prediction time before a lane change event and different statistical measures. Furthermore, the benefits of the interaction-aware intention estimation are examined.

Prototype Scenarios

Two different traffic scenarios are shown in Figure 3.8 and Figure 3.10. The bars below the relevant vehicles represent the interaction-aware joint probabilities $P(m_{\text{lat}}, \mathcal{I}_v)$ for a lane change to left (red), lane keeping (blue) and lane change to right (green). Once the calculated lane change probability $P_v(m_{\text{lat}} = \pm 1, \mathcal{F}_v, \mathcal{I}_v)$ exceeds the threshold of 50%, the corresponding vehicle is drawn in red. The most likely trajectories of the host and relevant vehicles for the next five seconds are determined and shown as well.

Non-Critical Overtaking because of Different Speeds

Figure 3.8 shows a typical traffic scene on highways. The initial state of the situation shown in frame (a) is that vehicle 1 approaches vehicle 2 on the right-most lane with a relative velocity of about $+30\,\frac{\text{km}}{\text{h}}$. The respective interaction-based cost function of vehicle 1, thus, models an overtaking maneuver because of its estimated desired speed. The lane change to left joint probability of vehicle 1 is estimated about $P(m_{\text{lat}} = -1, \mathcal{I}_1) = 24\%$. It increased continuously up to $P(m_{\text{lat}} = -1, \mathcal{I}_1) = 30\%$ in frame (b). Finally, the lane change maneuver is predicted about 1.8 s in advance. This is about three times higher compared to the similar scenario presented in [83]. The framework predicts a further acceleration of vehicle 1 during its lane change. The lane change maneuver of vehicle 1 is finished in frame (d). However, its joint probability of the lane change to left remains still relatively high with $P(m_{\text{lat}} = -1, \mathcal{I}_1) = 18\%$. This is because vehicle 1 now drives behind

the slower vehicle 3 and again has a relative velocity of about $+18\,\frac{\text{km}}{\text{h}}$ and its left adjacent lane is free. The interaction-aware longitudinal motion prediction is evaluated here for the vehicle 1, which was tracked more than one minute by the test vehicle. Fig. 3.9 shows its overall prediction performance against different prediction times in the form of boxplots. Even for a long prediction time of $\delta_t = 5\,\text{s}$, the absolute error in longitudinal position and velocity remains quite small.

However, it is obvious that the spread of the error is increasing for prediction times. The results show that the interaction-aware longitudinal motion prediction combines the precision of a physics-based model for short prediction times with the situation knowledge and interaction modelling for a reliable long-term prediction.

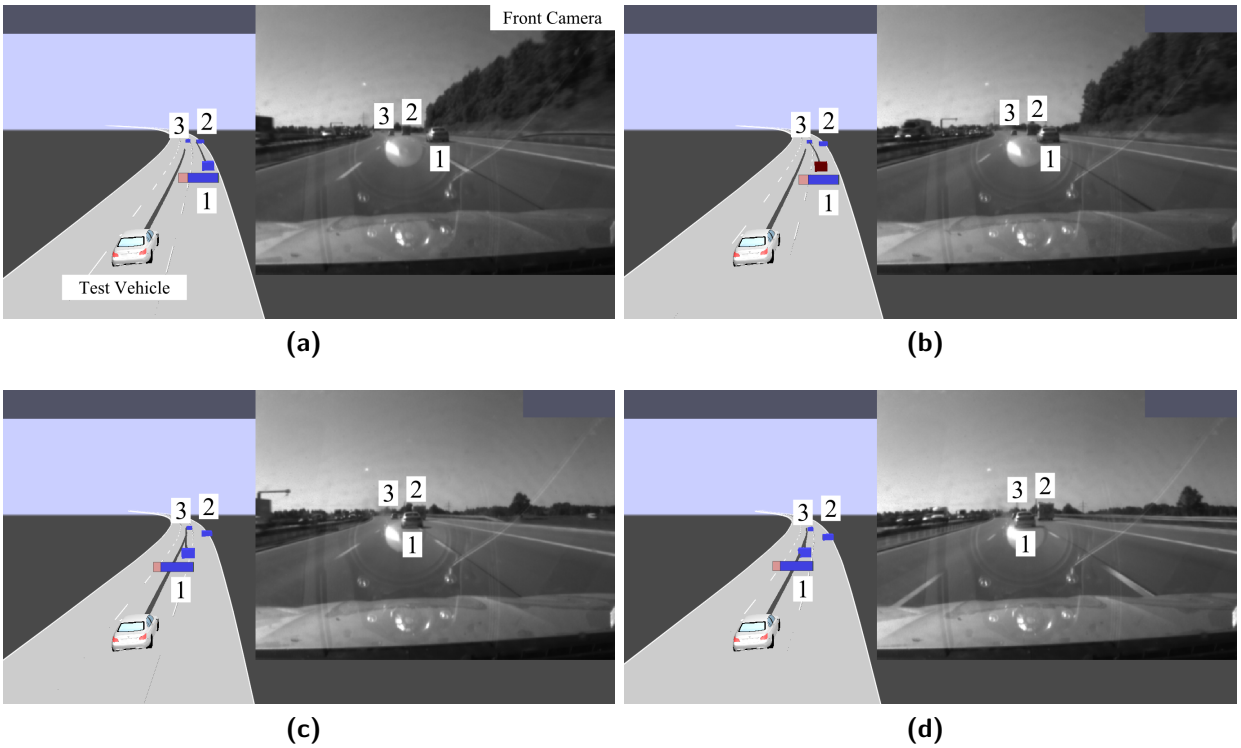

Fig. 3.8: Evaluation scene 1: non-critical overtaking because of different speeds.

Lane Change Feasibility and Rechtsfahrgebot

The traffic situation in Figure 3.10 demonstrates other aspects of the interaction-aware intention estimation model. Here, vehicle 1 overtakes slower traffic on the left-most lane. The joint probability of the lane change to right $P(m_{\text{lat}} = +1, \mathcal{I}_1) = 9\%$ is relatively low. The reason is the collision risk to the adjacent vehicles from perspective of the vehicle 1 in frames (a) and (b). Frame (c) shows the scene 15 s later, where vehicle 1 has already overtaken other traffic on the middle lane. The joint probability of the lane change to right is increasing now from $P(m_{\text{lat}} = +1, \mathcal{I}_1) = 21\%$ up to $P(m_{\text{lat}} = +1, \mathcal{I}_1) = 35\%$ in frame (d), as the middle lane is completely free. Nevertheless, it can be seen that vehicle 1 does not respect the previously described *Rechtsfahrgebot* (see Section 3.3) and drives steadily on the left-most lane. However, despite the high modelled intention probability, the lateral

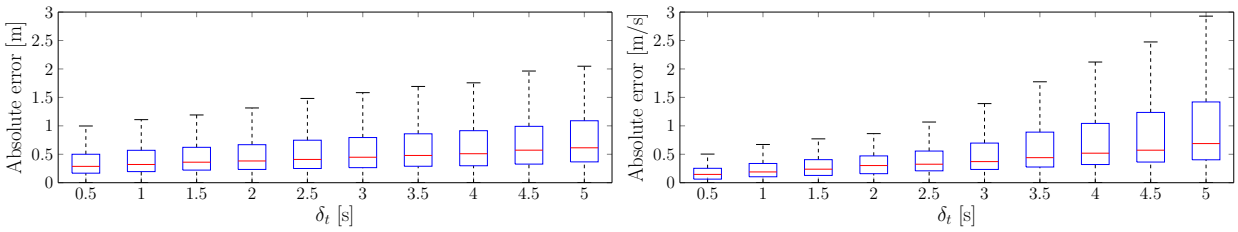

(a) Absolute error in the predicted longitudinal position vs. prediction time δ_t.

(b) Absolute error in the predicted longitudinal velocity vs. prediction time δ_t.

Fig. 3.9: The statistical properties of the absolute error in the interaction-aware longitudinal motion prediction against the prediction time for the entire time period, in which vehicle 1 was tracked in the first traffic scene (partly shown in Fig. 3.8). The whisker visualize 99.3% coverage of the absolute errors, the red line the median and the boxsize the 50% coverage of the absolute errors. One can see in Fig. 3.9a, that the absolute error in the predicted longitudinal position relative to the ground truth increases almost linearly with the prediction time. Even for a long prediction time of $5\,\mathrm{s}$ the prediction outcome remains reliable and has a maximum absolute error of about $2\,\mathrm{m}$. In case of predicted longitudinal velocity as in Fig. 3.9b, the maximum of absolute error grows stronger with the prediction time. However, the median of the absolute error remains with a maximum of about $0.68\,\frac{\mathrm{m}}{\mathrm{s}}$ low. The overall error increases with the relative distance to vehicle 1, since the sensor data will be inaccurate as well.

motion classifier correctly predicted that no lane change maneuver in the entire traffic scene occurs.

The first example demonstrates that the developed interaction-aware intention estimation enables a long-term prediction thanks to the correct recognized driver intention regarding its interaction with surrounding traffic. The second scene shows the robustness of the entire maneuver prediction framework in the case of incorrect predicted intents due to differing model assumptions (e.g. assumption of driving on the next free right lane). It is obvious that there is always a trade-off between the length of prediction horizon and the false prediction rate. This trade-off is increased by measurement noise as well as ambiguous driving styles (e.g. driving snaky line) and inconsistent model assumptions.

Quantitative Evaluation

The following section evaluates quantitatively the performance of the presented lateral motion prediction. First, the significance of the interaction-aware intention estimation model is verified. Finally, the lateral motion prediction performance is compared to the interaction-unaware approach presented in [195] based on different statistical measures.

Benefits of the Interaction-aware intention estimation

The idea behind the interaction-aware intention estimation is, among others, to provide interaction-aware joint probabilities $P(m_{\mathrm{lat}}, \mathcal{I}_v)$ which are dynamically adapted to the cur-

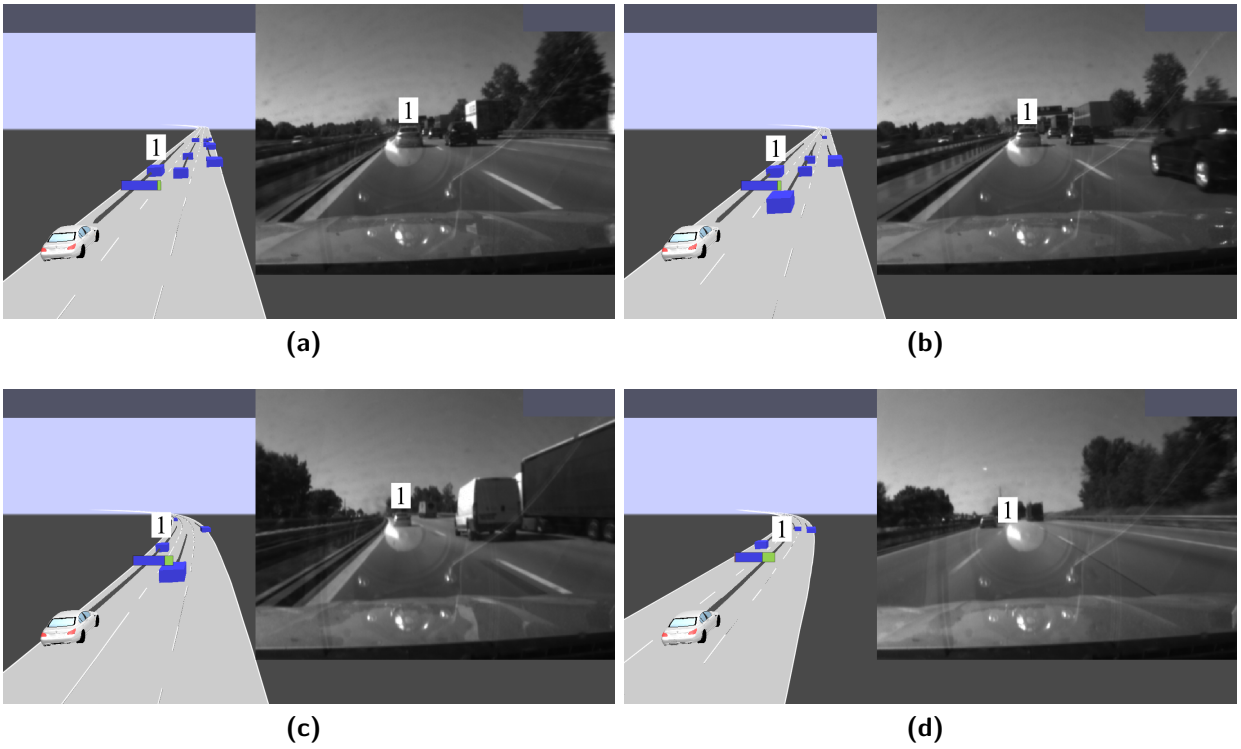

Fig. 3.10: Evaluation scene 2: lane change feasibility and *Rechtsfahrgebot*.

rent situation. As discussed in Section 3.3, the calculation is based on various model assumptions about the traffic behavior. The following evaluation is performed to verify whether these assumptions are in general true.

The average of interaction-aware lane change joint probabilities over all the test samples $\bar{P}_{\mathrm{LC}}$ is compared with the average of joint probabilities for the lane change to left $\bar{P}_{\mathrm{LCL}}$ and to right $\bar{P}_{\mathrm{LCR}}$ one second before the labeled lane change events. If the model assumptions would be completely incorrect, these three values must be almost the same. The result is shown in Figure 3.11 for different minimum lane change joint probabilities and the maximum value of $P_{\pm 1,\max} = 0.45$.

While the drivers' intention for the lane changes to the left can be predicted distinctly by the model, only about half of the significance can be achieved for the other direction. The reason is that the intention for a lane change to left is usually easier to predict, because in most of the cases the driver intends to overtake a slower vehicle ahead to reach its desired velocity or to merge on the highway. However, it is not the case for the other direction, as some of the reasons for a lane change to right, like as leaving the highway, cannot be predicted only with on-board sensors.

Classification Performance

In the second experiment, the predictive power of the lateral motion prediction is evaluated using the Receiver Operating Characteristic (ROC curve) [51]. The curve is created by plotting the *true positive rate* (TPR, also known as *recall*) against the *false positive rate* (FPR, also known as *fall-out*) at various threshold settings. In the case of a multiclass

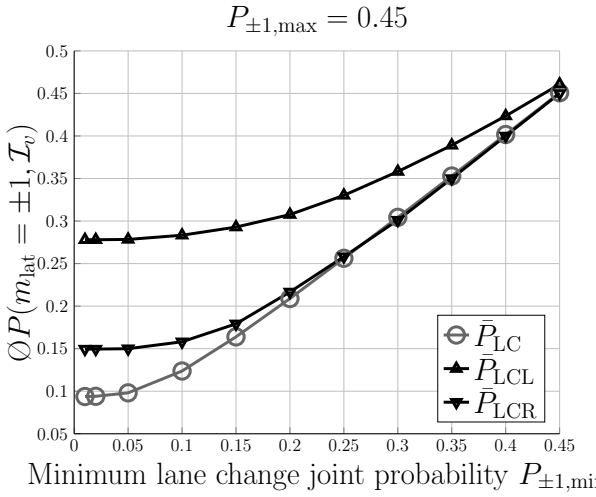

Fig. 3.11: The average of the interaction-aware lane change probabilities one second before the respective lane change events compared to the average of interaction-aware lane change probabilities over all the test data.

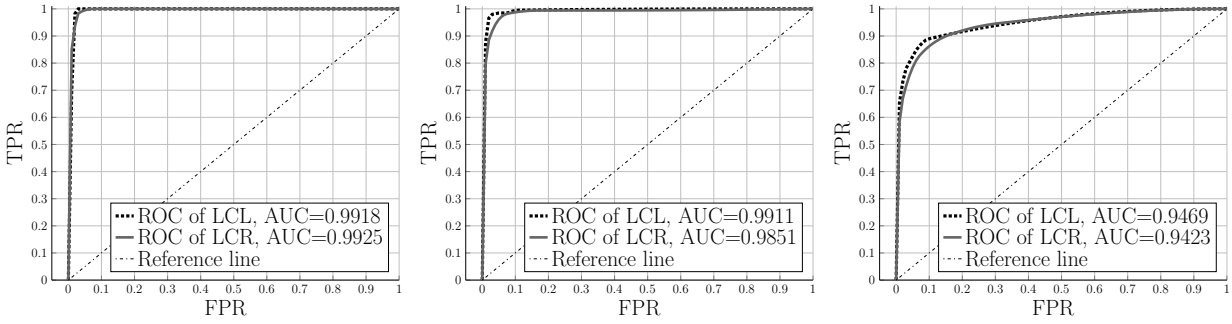

(a) $t_{\text{lc}} = 0.5\,\text{s}$ **(b)** $t_{\text{lc}} = 1.5\,\text{s}$ **(c)** $t_{\text{lc}} = 2.5\,\text{s}$

Fig. 3.12: ROC showing the predictive power of the proposed lateral motion prediction for different time intervals t_{lc} before a lane-change event.

classification, a ROC curve is generated for every class against the remaining ones. A greater area under the ROC curve (AUC) means a better average performance [51]. In this work, the minimum interaction-aware lane change joint probability $P_{\pm1,\min}$ of the interaction-aware intention estimation model is chosen as the threshold parameter which is varied between 0.01 and 0.5. Figure 3.12 shows the ROC curves for three different time intervals t_{lc} before lane change events. As discussed before, it is not surprising that an increase of the required prediction time has a negative effect on the performance of the prediction.

In the last experiment, the performance of the proposed interaction-aware lateral motion prediction (in the following referred to as approach A) is compared to the interaction-unaware state-of-the-art approach presented in [195] (Approach B) by means of different statistical measures. The latter consists of a naïve Bayes classifier with estimated static priors using two independent features of the lateral distance to the center of the lane and lateral velocity. Here, the interaction between the traffic participants is not considered.

Due to the imbalanced test set, as more than 99% of samples belong to the lane keeping maneuver, the performance of the both approaches is compared in the following using *balanced measures*. According to the definition of balanced accuracy in [30], the balanced precision prc and F_1 score [77] are defined as

$$\begin{aligned} prc &= \frac{TPR}{TPR + FPR} \\ F_1 &= 2\frac{prc \cdot TPR}{prc + TPR}. \end{aligned} \tag{3.26}$$

In simple terms, precision here means how likely a predicted lane change will happen, while TPR means how likely a lane change will be predicted by the respective approach. The F_1 score can be interpreted as the harmonic mean of the precision and recall. Based on these two measures, the minimum lane change joint probability for the interaction-aware intention estimation model is set to $P_{\pm 1,\min} = 5\%$. Table 3.1 summarizes the performance of both approaches, where a static prior of 18.5% for the lane change classes is used, as given in the previous work.

Tab. 3.1: Classification Performance of the two approaches using the balanced measures for the time interval of $t_{\mathsf{lc}} = 1.5\,\mathrm{s}$ before a lane change event.

Approach		TPR	prc	F_1	Ø prediction time [s] before a lane change event
A	LCL	0.98	0.97	0.9750	1.78
	LCR	0.9	0.98	0.9383	
B	LCL	0.98	0.9	0.9383	1.1
	LCR	0.93	0.88	0.9043	

It is important to note that all the measures above refer to the test samples (cycle-time of 100 ms). Both approaches were able to predict all the lane change maneuvers in the test set. The proposed approach in this work shows a distinct improvement in terms of the precision, F_1 score and average prediction time before a lane change event.

Discussion of the Results

The previous evaluations show the most important benefits of the presented maneuver prediction framework. First, the intention of each traffic participant is predicted by a novel approach which models the future planing of each vehicle with respect to the interaction with its surrounding traffic up to the predefined prediction horizon of 5 s. This information is reformulated in a joint probability which enables a precise lateral motion prediction up to a maximum of 2.3 s in advance in the given test set. Compared to the interaction-unaware case, the average prediction time before a lane change event is extended by more than 60%. Furthermore in contrast to the approaches presented in [83, 90, 137], the framework in this work also predicts the future interaction-aware longitudinal motion of each vehicle. Recalling the example of the cut-in situation on highway from Section 3.1, the presented

maneuver prediction framework can improve greatly the driving safety of the overall traffic in such critical situations.

Beside the improvement in the prediction time, the overall precision of the maneuver prediction could be improved by about 10%. Since compared to [195], the number of false detections on the test data is decreased by about 42%. This has a positive effect on the acceptance of tactical decision-making based on this prediction module by the passengers. The precision of the overall maneuver prediction can be certainly improved if relevant information such as desired velocities of other traffic participants are a priori known to the framework. This can be achieved in the future through the inter-vehicle communication.

3.5 Conclusion and Discussion

This chapter presented a novel on-line capable approach to maneuver prediction of highway traffic. The introduced intention estimation model, based on the idea of multi-agent simulation, models the interaction between the future planned maneuvers of all traffic participants over multiple time steps. The predicted intention is independent of the subsequent maneuver-based prediction model and can thus be combined with any other approach. This may be done by using the prior probabilities directly in the classifier or as additional features if the applied classifier is not based on prior knowledge (e.g. in the case of support vector machines or artificial neural networks [134]). It was shown that the sophisticated combination of the model-based intention estimation with the learning-based motion prediction has benefits in terms of native extensibility by expert knowledge and reduction of difficulties associated with the curse of dimensionality. Furthermore, the achieved precision and average prediction horizon can be greatly improved.

The possible inconsistent model assumptions will be compensated by the subsequent learning-based maneuver prediction up to a certain limit. However if the driving style of the traffic greatly differs from the model assumptions (such as in the case of *Rechtsfahrgebot*), the maneuvers will be predicted even too late. This has a negative impact on the recall as well.

To improve the interaction-aware intention estimation model, the parameters of the cost functions can be adapted to different driving styles by learning directly from different sets of training data. Another approach to improve the interaction-aware intention estimation model is to consider the mutual dependence between maneuver choices of relevant traffic participants over multiple time steps in some specific traffic situations. This novel idea will be discussed in Chapter 5. A major challenge here is to meet the requirement of on-line capability.

The proposed traffic scene prediction module provides the subsequent behavioral strategies with the required information about the future state of the environment. Thus, a forward-looking maneuver planning is enabled. In the following three chapters, the introduced behavioral strategies from the Chapter 2.2.4 will be discussed in detail and evaluated. It will be shown that each of the behavioral strategies makes use of the prediction module's results in a different manner depending on its overall objective and requirements.

4 Basic Behavioral Strategy

As described in Section 2.2, the tactical decision-making process consists of different behavioral strategies. Each of them implements an appropriate model predictive maneuver planning which is responsible for achieving a specific medium-term behavioral goal. In order to enable a mode predictive maneuver planning, the future movement of other traffic participants should be predicted. Hence, in the previous chapter the novel framework for interaction-aware traffic scene prediction was discussed in detail. It constitutes the basis on which the model predictive maneuver planning within the basic behavioral strategy, discussed in this chapter, is based. The basic behavioral strategy ensures a comfortable and safe driving with respect to the surrounding traffic. It does not consider specific medium term goals like as explicit cooperative driving[1].

4.1 Introduction and State of the Art

In [174] and [175] a prediction- and cost function-based algorithm for autonomous highway driving was presented. Figure 4.1a shows the three primary steps in this algorithm: candidate parameters, prediction engine and cost function based evaluation. The candidate parameter generation outputs an appropriate set of parameters. A set contains the possible accelerations, produced e.g. by the distance keeper module and the current vehicle states. The subsequent prediction engine generates a series of simulated traffic scenarios. Finally, the cost function based evaluation algorithm determines the cost of each scenario. The

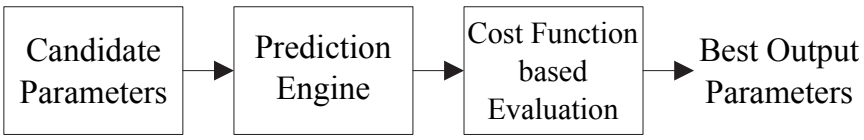

(a) Diagram of the prediction and cost function based algorithm. Image source: [174]

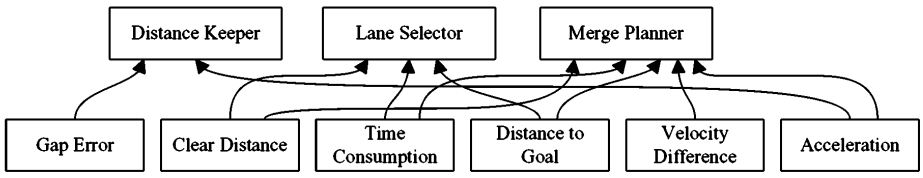

(b) Cost function library. Image source: [174]

prediction engine relies on an 8-vehicle micro traffic environment. Furthermore, two different basic prediction models were implemented: constant velocity assumption and ACC

[1]Parts of the results in this chapter have been pre-published in [196].

behavior. In the first method, the velocities of other traffic participants are assumed to be constant. Whereas in the latter the velocity is predicted dependent on the distance to the vehicle in front. The scenario evaluation consists of seven kinds of base cost functions, which can be seen in Figure 4.1b. A disadvantage of this approach is that it tries to solve the whole driving task without subdivision in various behavioral contexts. For a real-world application it might get hard to achieve all intended driving behaviors through only one decision-making algorithm.

The decision-making process is realized in other state-of-the-art approaches either with rule-based [16] or utility-based [12, 56, 117] algorithms. The advantages of the rule-based approach are simple implementation and traceability. However, the decision-making in complex traffic situations can not be modeled accurately enough. The approach based on the utility functions considers several criteria due to their weights. It can be extended relatively simple to complex scenarios. The disadvantage of this approach is, however, the large number of weighting parameters that are usually determined by trial and error tuning.

The main advances of the current work are on the one hand a well-organized tactical decision-making architecture. Compared to [11], it meets a higher requirement of modular expandability. On the other hand, the decision-making process within each behavioral strategy is based on the model predictive maneuver planning which enables the driving strategy to be reactive and to simultaneously consider the future evolution of the environment. In comparison to [12, 48, 119, 175], a dynamic model is derived which predicts both the interaction-aware longitudinal and lateral maneuvers of all traffic participants.

The mathematical formulation of the proposed model predictive maneuver planning within the basic behavioral strategy is based on the approach of *constrained optimization of hybrid systems*. It is solved by the two different formulations of *mixed-integer quadratic program* and *combinatorial optimization*. Both methods in the current implementation always guarantees a solution. Consequently, the system robustness is given. Although the first method determines a "globally optimal driving behavior", it has disadvantages in terms of computation time and freedom in problem formulation. These drawbacks are thus eliminated by the second method. One of the main challenges here is to achieve the same "optimal driving behavior" as the mixed-integer linear formulation. The success of which is shown by various qualitative and quantitative evaluations of these both approaches.

4.2 Mathematical Backgrounds

This section reviews some of the most important mathematical foundations of the dynamical systems, optimization problems and model predictive control which will be used throughout this chapter. For more detailed explanations as well as proof of the theorems, reference is made to appropriate literature.

Dynamical Systems

Linear Systems[2]

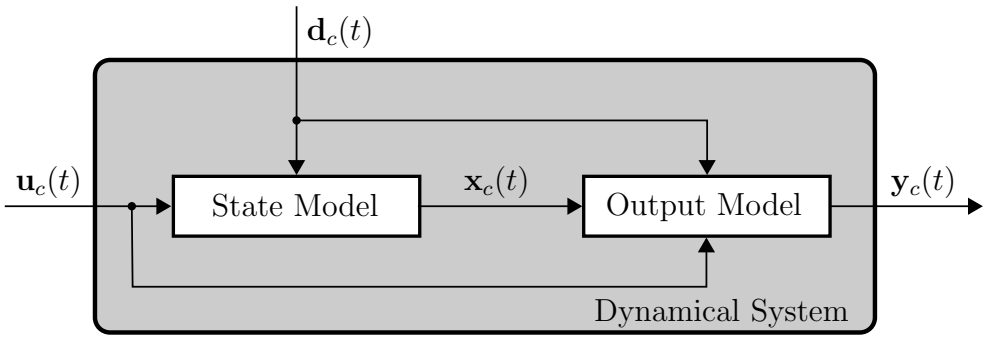

Fig. 4.1: Block diagram of a dynamical system.

The *dynamical systems* (Figure 4.1) can be mathematically described with the state differential equation (4.1a) and the output differential equation (4.1b)

$$\dot{\mathbf{x}}_c(t) = f\left(\mathbf{x}_c(t), \mathbf{u}_c(t), \mathbf{d}(t), t\right) \tag{4.1a}$$
$$\mathbf{y}_c(t) = g\left(\mathbf{x}_c(t), \mathbf{u}_c(t), \mathbf{d}(t), t\right), \tag{4.1b}$$

where $\mathbf{x}_c \in \mathbb{R}^{n_c}$ is the continuous state vector, $\mathbf{u}_c \in \mathbb{R}^{p_c}$ is the continuous input vector, $\mathbf{y}_c \in \mathbb{R}^{q_c}$ is the continuous output vector and $\mathbf{d} \in \mathbb{R}^{k_c}$ is the continuous disturbance vector. An important special case of dynamical systems is the *discrete-time dynamical systems*. In this case, the evolution of the system can be written in the form of the state difference equation (4.2a) and the output difference equation (4.2b)

$$\mathbf{x}_c(k+1) = f\left(\mathbf{x}_c(k), \mathbf{u}_c(k), \mathbf{d}(k), k\right) \tag{4.2a}$$
$$\mathbf{y}_c(k+1) = g\left(\mathbf{x}_c(k), \mathbf{u}_c(k), \mathbf{d}(k), k\right), \tag{4.2b}$$

where k is the discrete time index. The system variables are assumed to be constant between two consecutive samples. A system is called linear if the functions f and g are linear in $\mathbf{x}_c$ and $\mathbf{u}_c$. The linear state space system can thus be represented by

$$\dot{\mathbf{x}}_c = \mathbf{A}\mathbf{x}_c + \mathbf{B}\mathbf{u}_c \tag{4.3a}$$
$$\mathbf{y}_c = \mathbf{C}\mathbf{x}_c + \mathbf{D}\mathbf{u}_c, \tag{4.3b}$$

where $\mathbf{A} \in \mathbb{R}^{n_c \times n_c}$ is the dynamics matrix, $\mathbf{B} \in \mathbb{R}^{n_c \times p_c}$ is the control matrix, $\mathbf{C} \in \mathbb{R}^{q_c \times n_c}$ is the output matrix and $\mathbf{D} \in \mathbb{R}^{q_c \times p_c}$ is the feed-through matrix. Such a dynamical system is referred to as *linear and time-invariant system* (LTI).

Piecewise Affine System The main idea of the *piecewise affine systems* (PWA) is to split the space of states and inputs in a finite number of polyhedral regions. In each polyhedral

[2]Many parts in this section are based on [25, 26] and are not mentioned each time separately.

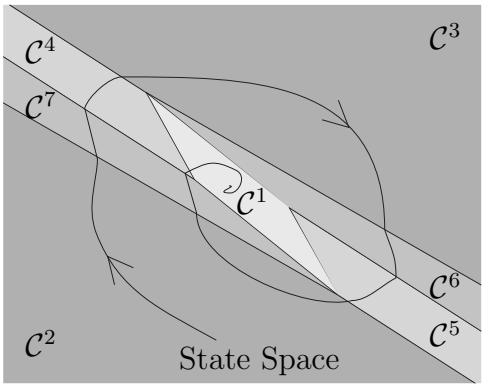

Fig. 4.2: Piecewise affine systems. Mode switches are triggered by linear threshold events. Image source: [26]

region different affine state-update and output equations will be then valid

$$\mathbf{x}(k+1) = \mathbf{A}^{i(k)}\mathbf{x}(k) + \mathbf{B}^{i(k)}\mathbf{u}(k) + \mathbf{f}^{i(k)} \tag{4.4a}$$

$$\mathbf{y}(k) = \mathbf{C}^{i(k)}\mathbf{x}(k) + \mathbf{D}^{i(k)}\mathbf{u}(k) + \mathbf{g}^{i(k)} \tag{4.4b}$$

$$\mathbf{H}^{i(k)}\mathbf{x}(k) + \mathbf{J}^{i(k)}\mathbf{u}(k) \leq \mathbf{K}^{i(k)}, \tag{4.4c}$$

where $i(k)$ is the current mode of the system. Each vector inequality (4.4c) defines a different polyhedron $\mathcal{C}^i$ in the state of states and inputs which is referred to as a *cell* (Figure 4.2). The union of such polyhedral cells is called *partition*. In the following, the cells are considered as closed sets, because numerical solvers can not handle open sets. A PWA system is called *well-posed* if it satisfies the following property [20]:

Theorem 4.1 *Let P be a PWA system of the form (4.4a)-(4.4c) and let $\mathcal{C} := \bigcup_{i=1}^{s} \mathcal{C}^i$ be the polyhedral partition associated with it. System P is called well-posed if for all pairs $(x(k), u(k)) \in \mathcal{C}$ there exists only one index $i(k)$ satisfying (4.4a)-(4.4c).*

Theorem 4.1 implies that $\mathbf{x}(k+1)$, $\mathbf{y}(k)$ are single-valued functions of $\mathbf{x}(k)$ and $\mathbf{u}(k)$ and thus the state and output trajectories are uniquely determined by the initial state and input trajectory. Outside the state and input boundaries, the system becomes undefined.

Hybrid Systems

In contrast to the above-mentioned dynamical systems, there are problems which can not only be formulated with differential or difference equations. In many real-world applications, however, the system also contains discrete-valued signals or if-then-else statements. Therefore, the class of *hybrid systems* describes in a common framework the dynamics of continuous and discrete variables and their interaction, as shown in Figure 4.3.

The state space model of the *discrete-time hybrid system* is generally defined as

$$\mathbf{x}_c(k+1) = f\left(\mathbf{x}_c(k), \mathbf{x}_l(k), \mathbf{u}(k), k\right) \tag{4.5a}$$

$$\mathbf{x}_l(k+1) = \Psi\left(\mathbf{x}_l(k), \mathbf{u}(k), k\right), \tag{4.5b}$$

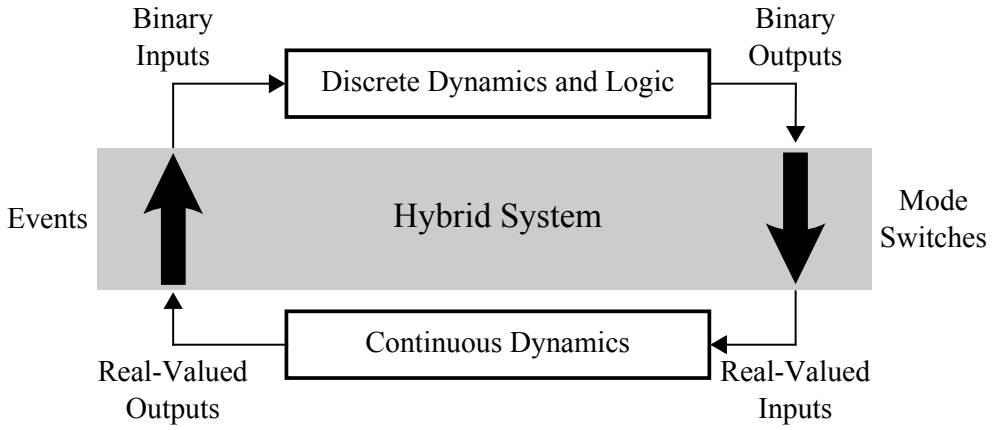

Fig. 4.3: The overall structure of hybrid systems. Continuous dynamics and logic-based discrete dynamics interact through events and mode switches. Image source: [26]

where $\mathbf{x} \in \mathbb{R}^{n_c} \times \{0,1\}^{n_l}$ is the hybrid state vector consisting of $\mathbf{x}_c \in \mathbb{R}^{n_c}$ and the logical state vector $\mathbf{x}_l \in \{0,1\}^{n_l}$. Similarly, $\mathbf{u} \in \mathbb{R}^{p_c} \times \{0,1\}^{p_l}$ is the hybrid input vector consisting of $\mathbf{u}_c \in \mathbb{R}^{p_c}$ and the logical input vector $\mathbf{u}_l \in \{0,1\}^{p_l}$. Finally, $\mathbf{y} \in \mathbb{R}^{q_c} \times \{0,1\}^{q_l}$ is the hybrid output vector consisting of $\mathbf{y}_c \in \mathbb{R}^{q_c}$ and the logical output vector $\mathbf{y}_l \in \{0,1\}^{q_l}$. In the following, three important classes of hybrid systems are presented which are of great interest for *model predictive control* (MPC) with hybrid characteristic.

Discrete Hybrid Automaton As depicted in Figure 4.4, the *discrete hybrid automaton* (DHA) is formed by generating the mode $i(k)$ of a switched affine system through a mode selector function that depends on the discrete state of a finite state machine, discrete events generated by the continuous variables of the switched affine system exceeding given linear thresholds and exogenous discrete inputs. Finally, the dynamics of the system are chosen respectively to the current mode $i(k)$.

The *event generator* is an object which generates a binary condition vector $\boldsymbol{\delta}_e(k) \in \{0,1\}^{b_l}$ according to the satisfaction of linear conditions. A single event is given by

$$\boldsymbol{\delta}_e(k) = \mathbf{h}\left(\mathbf{x}_c(k), \mathbf{u}_c(k), k\right), \tag{4.6}$$

with the vector function $\mathbf{h} : \mathbb{R}^{n_c} \times \mathbb{R}^{p_c} \to \{0,1\}^{b_l}$ defined as

$$\mathbf{h}\left(\mathbf{x}_c(k), \mathbf{u}_c(k)\right) = \begin{cases} 1 & \text{if } \mathbf{H}^{i(k)}\mathbf{x}_c(k) + \mathbf{J}^{i(k)}\mathbf{u}_c(k) + \mathbf{K}^{i(k)} \leq 0 \\ 0 & \text{if } \mathbf{H}^{i(k)}\mathbf{x}_c(k) + \mathbf{J}^{i(k)}\mathbf{u}_c(k) + \mathbf{K}^{i(k)} > 0 \end{cases} \tag{4.7}$$

The *finite state machine* evolves the discrete states of the system and gives thus the possibility to enable, e.g., different dynamics or constraints dependent on the current state.

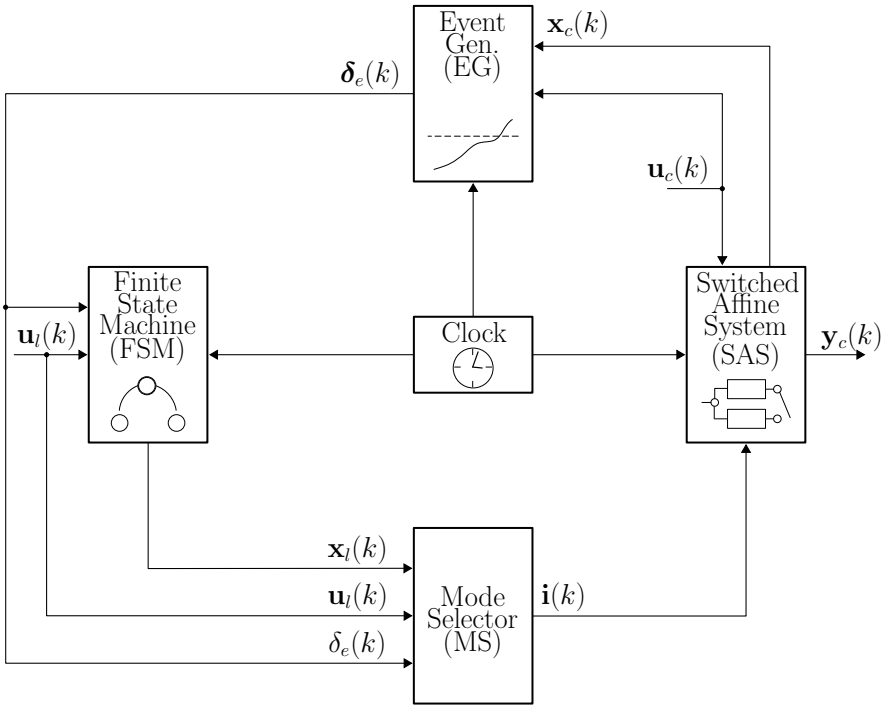

Fig. 4.4: A discrete hybrid automaton (DHA) is the connection of a finite state machine (FSM) and a switched affine system (SAS), through a mode selector (MS) and an event generator (EG). Image source: [26]

It can be expressed mathematically as logical state and output functions

$$\mathbf{x}_l(k+1) = \mathbf{f}_l\left(\mathbf{x}_l(k), \mathbf{u}_l(k), \boldsymbol{\delta}_e(k)\right) \tag{4.8a}$$

$$\mathbf{y}_l(k) = \mathbf{g}_l\left(\mathbf{x}_l(k), \mathbf{u}_l(k), \boldsymbol{\delta}_e(k)\right), \tag{4.8b}$$

where $\mathbf{f}_l : \{0,1\}^{n_l} \times \{0,1\}^{p_l} \times \{0,1\}^{b_l} \to \{0,1\}^{n_l}$ and $\mathbf{g}_l : \{0,1\}^{n_l} \times \{0,1\}^{p_l} \times \{0,1\}^{b_l} \to \{0,1\}^{q_l}$ are deterministic logical functions. The *mode selector* (MS) determines the dynamic mode of the DHA. The *active mode* of the DHA is indicated through its binary encoding $\mathbf{i}(k) \in \{0,1\}^{n_s}$

$$\mathbf{i}(k) = \mathbf{f}_m\left(\mathbf{x}_l(k), \mathbf{u}_l(k), \boldsymbol{\delta}_e(k)\right), \tag{4.9}$$

where $\mathbf{f}_m : \{0,1\}^{n_l} \times \{0,1\}^{p_l} \times \{0,1\}^{b_l} \to \{0,1\}^{s_l}$ is a further logical function. A *mode switch* can only occur at discrete sampling instants. The *switched affine system* (SAS) can be compared to PWA, where the mode $i(k)$ is here an exogenous variable and therefore the conditions in equation (4.4c) disappear

$$\mathbf{x}_c(k+1) = \mathbf{A}^{i(k)}\mathbf{x}_c(k) + \mathbf{B}^{i(k)}u_c(k) + \mathbf{f}^{i(k)} \tag{4.10a}$$

$$\mathbf{y}_c(k) = \mathbf{C}^{i(k)}\mathbf{x}_c(k) + \mathbf{D}^{i(k)}\mathbf{u}_c(k) + \mathbf{g}^{i(k)}. \tag{4.10b}$$

Depending on the active mode in the MS, the SAS enables the dynamics in form of difference equations of the DHA. For a given initial condition and inputs, the state $x(k)$ of the system is now computed by recursively iterating through the following steps:

1. Calculate the binary events (4.6).
2. Activate the appropriate Modes (4.9).
3. Calculate the logical and continuous system outputs (4.8b), (4.10b).
4. Update the logical and continuous system states (4.8a), (4.10a).

"Despite the fact that DHA are rich in their expressiveness and are therefore quite suitable for modeling and simulating a wide class of hybrid dynamical systems, they are not directly suitable for solving optimal control problems, because of their heterogeneous discrete and continuous nature." [26, p.353]. Therefore, a further hybrid system formulation which is more suitable for solving open-loop finite time optimal control problems is introduced below.

Mixed Logical Dynamical Systems PWA and DHA systems can be translated into a form, denoted as *mixed logical dynamical system* (MLD), which is more suitable for solving optimization problems. In particular, complex finite-time hybrid dynamical optimization problems can be recast into mixed-integer linear or quadratic programs. In other words, the main idea of MLD systems is to link logic and dynamics of a system through mixed-integer inequalities, i.e. linear inequalities involving both real and binary variables. To transform a DHA into a MLD system, the binary expressions have to be transformed into linear mixed-integer Relations. For instance, $\delta_1 \vee \delta_2$ is equivalent to $\delta_1 + \delta_2 \geq 1$.

Theorem 4.2 *For every binary formula $F(\delta_1, \delta_2, ..., \delta_n)$ there exists a polyhedral set P such that a set of binary values $\{\delta_1, \delta_2, ..., \delta_n\}$ satisfies the binary formula F if and only if $\delta = [\delta_1, \delta_2, ..., \delta_n] \in P$.*

According to the Theorem 4.2, the event generator from (4.6) can be formulated equivalently as

$$h^i(\mathbf{x}_c(k), \mathbf{u}_c(k), k) \leq M^i(1 - \delta_e^i) \tag{4.11a}$$
$$h^i(\mathbf{x}_c(k), \mathbf{u}_c(k), k) \geq m^i \delta_e^i, \tag{4.11b}$$

where M^i, m^i are upper and lower bounds, respectively, on h^i. The other parts of the DHA can be translated into linear mixed-integer relations as well [21, 26]. There are some tools which automatically transform DHA to MLD formulation. In this thesis, the two toolboxes of HYbrid System DEscription Language (HYSDEL) [26] and the Multi-Parametric Toolbox (MPT3) [70] will be used.

The equivalent representation of the DHA as a mixed logical dynamical system can be obtained as

$$\mathbf{x}(k+1) = \mathbf{A}\mathbf{x}(k) + \mathbf{B}_1\mathbf{u}(k) + \mathbf{B}_2\mathbf{z}_l(k) + \mathbf{B}_3\mathbf{z}_c(k) + \mathbf{B}_4 \tag{4.12a}$$
$$\mathbf{y}(k) = \mathbf{C}\mathbf{x}(k) + \mathbf{D}_1\mathbf{u}(k) + \mathbf{D}_2\mathbf{z}_l(k) + \mathbf{D}_3\mathbf{z}_c(k) + \mathbf{D}_4 \tag{4.12b}$$
$$\mathbf{E}_2\mathbf{z}_l(k) + \mathbf{E}_3\mathbf{z}_c(k) \leq \mathbf{E}_1\mathbf{u}(k) + \mathbf{E}_4\mathbf{x}(k) + \mathbf{E}_5, \tag{4.12c}$$

where $\mathbf{z} \in \mathbb{R}^{r_c} \times \{1,0\}^{r_l}$ is the vector of continuous and logical auxiliary variables which arise in the transformation and $\mathbf{A}, \mathbf{B_1} \dots \mathbf{B_4}, \mathbf{C}, \mathbf{D_1} \dots \mathbf{D_4}, \mathbf{E_1} \dots \mathbf{E_5}$ are matrices of suitable dimensions. Given the current state $\mathbf{x}(k)$ and input $\mathbf{u}(k)$, the time evolution of (4.12) is determined by finding feasible values for auxiliary variables satisfying (4.12c) and then by computing $\mathbf{x}(k+1)$ and $\mathbf{y}(k)$ from (4.12a) and (4.12b).

"The ability to include constraints, constraint prioritization, and heuristics adds to the expressiveness and generality of the MLD framework. Note also that despite the fact that the description (4.12) seems to be linear, clearly the non-linearity is concentrated in the integrality constraints over binary variables." [26, p.356].

Optimization Problems

General Constrained Problems[3]

The general definition of an optimization problem is

$$\min_{\mathbf{x} \in X} f(\mathbf{x}), \quad \text{with} \quad X = \{\mathbf{x} | \mathbf{c}(\mathbf{x}) = \mathbf{0}; \mathbf{h}(\mathbf{x}) \leq \mathbf{0}\}, \tag{4.13}$$

where f is the *objective function*, $\mathbf{x} \in \mathbb{R}^n$ is here the vector of the decision variables, $\mathbf{c}$ is the vector function of the equality constraints, and $\mathbf{h}$ is the vector function of the inequality constraints. The *decision set* $X \subset \mathbb{R}^n$ is the set of all feasible solutions $\mathbf{x} \in X$ which fulfill the constraints. The goal is to find the solution with the minimum (resp. maximum) value of the objective function.

Theorem 4.3 *The objective function $f(\mathbf{x})$ has a local minimum at $\mathbf{x}^*$, if there exists some $\epsilon > 0$ such that $f(\mathbf{x}^*) \leq f(\mathbf{x}) \quad \forall \mathbf{x} \in \{\mathbf{x} \in X \mid |\mathbf{x} - \mathbf{x}^*| \leq \epsilon\}$. If $f(\mathbf{x}^*) < f(\mathbf{x})$ holds, then it is called a strict local minimum.*

Theorem 4.4 *The objective function $f(\mathbf{x})$ has a global minimum at $\mathbf{x}^*$, if $f(\mathbf{x}^*) \leq f(\mathbf{x}) \quad \forall \mathbf{x} \in X$. If $f(\mathbf{x}^*) < f(\mathbf{x})$ holds, then it is called the strict global minimum.*

The property of *convexity* plays an important role in the optimization problems. A fundamental benefit of convex optimization problems is that the local optimizers are at the same time the global optimizers. In general, optimization problems are solved numerically going downhill until one reaches a minimum. The problem is that usually there are many local minima and the algorithm can get stuck in one of them. In a convex optimization problem this can not occur. "The convexity guarantees that there is only one minimum or a connected set of equally good minima" [105, p.84]. The general optimization problem (4.13) is convex if the feasible solution set X is a convex set and $f(x)$ is a convex function.

Theorem 4.5 *A set $\mathcal{C} \subset \mathbb{R}^n$ is convex, if*

$$\mathbf{x}_1, \mathbf{x}_2 \in \mathcal{C} \Rightarrow \mathbf{x}(\sigma) \in \mathcal{C} \quad \forall \sigma \in [0,1]$$

[3]Many parts in this section are based on [110, 124] and are not mentioned each time separately.

with

$$\mathbf{x}(\sigma) = \sigma\mathbf{x}_1 + (1-\sigma)\mathbf{x}_2$$

Theorem 4.6 *A function $f(\mathbf{x})$ with the convex set $\mathcal{C}$ and $\mathbf{x}_1, \mathbf{x}_2, \mathbf{x} \in \mathcal{C}$ is convex, if*

$$f(\mathbf{x}(\sigma)) \leq \sigma f(\mathbf{x}_1) + (1-\sigma) f(\mathbf{x}_2) \quad \forall \sigma \in [0,1]$$

Based on the previous theorems, a linear and quadratic functions are convex for any real number.

Linear and Quadratic Programming

When the objective and the constraints of the continuous optimization problem (4.13) are affine, then the problem is called a *linear program* (LP). This is the most commonly used case in practical applications, even though many of the real-world problems are non-linear. Therefore, the problems are linearized at an operating point and LP solvers will be applied. The general formulation of a linear program is

$$\min_{\mathbf{x} \in X} f(\mathbf{x}) = \mathbf{c}^T\mathbf{x} \quad \text{with} \quad X = \{\mathbf{x} | \mathbf{A}\mathbf{x} = \mathbf{0}; \mathbf{b}\mathbf{x} \geq \mathbf{0}\}, \tag{4.14}$$

where $\mathbf{A}$ is in this case the matrix of equality constraints and $\mathbf{b}$ is the vector of inequality constraints. Regarding the previous theorems, linear programs are convex optimization problems. Figure 4.5 illustrates a two-dimensional LP problem. It can be easily shown

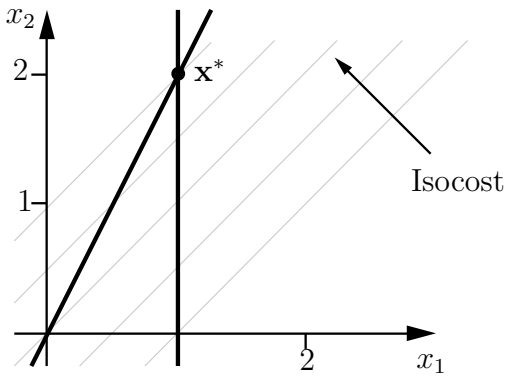

Fig. 4.5: Visualization of a two-dimensional linear program. Image source: [124].

that there is either an unique solution on a corner of the feasible region (extreme point) or there are multiple solutions along an edge of the region. To find the global optimal solution of a LP, various numerical algorithms like the *simplex algorithm* can be applied.

In the case of quadratic programming (QP) the objective function is quadratic convex. It can be expressed as

$$f(\mathbf{x}) = \mathbf{x}^T\mathbf{Q}\mathbf{x} + \mathbf{c}^T\mathbf{x}, \tag{4.15}$$

where $\mathbf{Q}$ is a positive-semidefinite matrix. LPs are special cases of QPs, in which the matrix $\mathbf{Q}$ is zero.

Mixed-Integer Optimization

If the decision set X in the optimization problem (4.13) is a subset of the Cartesian product of an integer set and a real Euclidean space, then the problem is said to be *mixed-integer*. Optimization in hybrid systems is one of the important application of mixed-integer program. With the exception of trivial cases, integer and mixed-integer optimization problems are always non-convex problems because $\{0, 1\}$ is not a convex set. Basically solving a mixed-integer problem includes the following steps [2]:

- *Branch and Bound*: Dividing the problem in various subproblems.
- *LP Relaxation*: Replacing the integer constraints with linear constraints on continuous variables.
- *Cutting Plane Separation*: Formulating a new LP problem with additional constraints.
- *Domain Propagation*: Reducing the domains of the variables.
- *Conflict Analysis*: Infeasible subproblems are analyzed to extract additional valid constraints.

The algorithm ends when the optimal solution of a subproblem is found, when it is infeasible, or when no better solution can be contained in the subproblem.

Combinatorial Optimization

If the decision set X in the optimization problem (4.13) is finite, then the optimization problem is called *combinatorial optimization* (CO). There are two classes of problems where combinatorial optimization has to be applied. In the first case, the real-world problem is of a combinatorial fashion itself. The *traveling salesman* is a prominent example of such a combinatorial problem. The objective here is to visit a finite number of cities exactly once and finally return to the starting point with the minimum traveled distance. The other case is that real-world problems with a continuous solution space are approximated by a model with a discrete solution space and finally applies the combinatorial optimization to find the optimal solution.

Like other optimization algorithms, it can also be distinguished here between methods which guarantee to find the global optimal solution (e.g. *exhaustive search* and *backtracking*) and other methods which do not guarantee this, but reduce the computational effort (e.g. *local search*).

Model Predictive Control

"Model predictive control (MPC) (also called receding horizon control) is the only advanced control technique - that is, more advanced than standard PID control - to have had a significant and widespread impact on industrial process control." [105]. One important reason for this success is that MPC is the only generic controller which considers the

future evolution of the system and deals implicitly with constraints on the system states and inputs.[4]

Figure 4.6 shows the basic model of the MPC. At each discrete time instant, the model

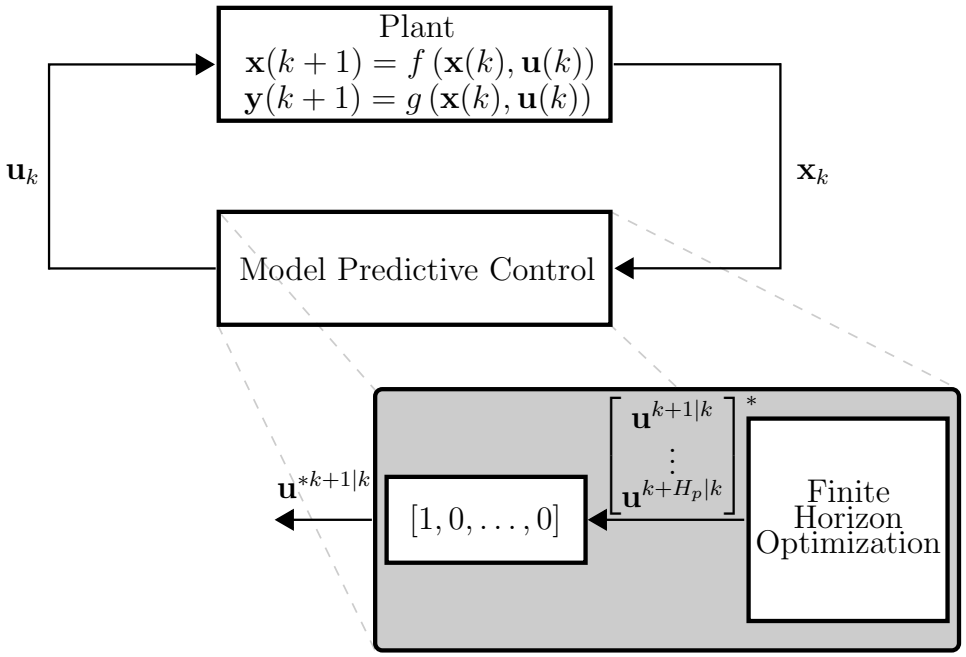

Fig. 4.6: Basic model of the model predictive control (MPC).

predictive controller performs the following three tasks:

1. Takes the latest measurements of the system states and outputs.
2. Computes a finite horizon control sequence which
   - based on an internal model to predict system behavior,
   - minimizes (resp. maximizes) some defined objective function and
   - does not violate any constraints on states and inputs.
3. Implements the first part of the optimal sequence $\mathbf{u}^*(k)$.

This sequence is repeated every *replanning time*. In this thesis, only LTI systems will be considered. Though the model is linear, the MPC might behave non-linearly, especially when constraints are approached too closely. Another important point is that the linear model is used not only off-line but directly as part of the control algorithm itself. It means that there is always difference in the behavior of the model and the real plant. This must be taken into account while formulating the MPC.

The objective function up to the *prediction horizon* H_p is generally defined as

$$\sum_{j=1}^{H_p} \Phi(\mathbf{x}^{k+j|k}, \mathbf{u}^{k+j|k}, \Delta\mathbf{u}^{k+j|k}), \tag{4.16}$$

[4]Many parts in this section are based on [105] and are not mentioned each time separately

where it is based on the estimated system variables regarding measurements up to the current sampling time instance $k + j$. The general form of the constraints is

$$\Delta \mathbf{u}_{\min} \leq \left[\Delta \mathbf{u}^{k+1|k}, \ldots, \Delta \mathbf{u}^{k+H_p|k}\right]^{\mathrm{T}} \leq \Delta \mathbf{u}_{\max} \tag{4.17a}$$

$$\mathbf{u}_{\min} \leq \left[\mathbf{u}^{k+1|k}, \ldots, \mathbf{u}^{k+H_p|k}\right]^{\mathrm{T}} \leq \mathbf{u}_{\max} \tag{4.17b}$$

$$\mathbf{x}_{\min} \leq \left[\mathbf{x}^{k+1|k}, \ldots, \mathbf{x}^{k+H_p|k}\right]^{\mathrm{T}} \leq \mathbf{x}_{\max} \tag{4.17c}$$

(4.17a) represents possible input slew rates, (4.17b) input ranges and (4.17c) constraints on the state variables. By re-evaluating and resolving the problem at each replanning time, changes in the environment will be taken in to account for the subsequent decision-making. Thus, the decision-making process based on the model predictive approach satisfies the two important requirements for reactivity and anticipatory.

Discussion

The following three basic concepts are common to every algorithmic approach for problem solving [110]. The *representation* (1) defines the solution space, the *objectives* (2) describe the goal(s) of the optimization problem and finally the *evaluation function* (3) provides mapping of a real-valued number to each solution, representing its overall "quality". Most often, the evaluation function can be derived directly from the objectives, especially in the case of LP problems. The structure of the following chapters, discussing the different behavioral strategies, represents thus the above idea. First, an appropriate model representation of the corresponding behavioral strategy will be determined. As discussed in Section 2.2.4, modified approaches of the model predictive maneuver planning algorithms are implemented in each behavioral strategy which individually are responsible for achieving a specific medium-term behavioral goal. Therefore, the respective high-level objectives will be separately described in detail in each chapter. Finally, suitable algorithms are provided which solve these different finite horizon optimization problems.

In the following case of the basic behavioral strategy, the two different approaches of the mixed-integer and combinatorial optimization will be described. Finally, both approaches are evaluated in a simulated environment and the results are discussed in detail.

4.3 Problem Formulation

Given the current sensor measurements, optimal decisions for further driving has to be determined. For this reason, a model predictive maneuver planning approach is derived which satisfies the two important requirements for reactivity and anticipatory. It relies on a suitable dynamic model of the process. Therefore, at the k-th replanning time instance the state vector of the v-th vehicle $\mathbf{x}_v^{k+j|k}$ is predicted for the next p instances up to the prediction horizon H_p. Subsequently, a cost minimizing control strategy is computed for the fixed *control horizon* in the future $H_c \leq H_p$, taking into account the input and state constraints. As long as basic behavioral strategy is active, the *optimal policy sequence* $\mathbf{\Pi}^{*k}$ is implemented as the driving goals until the next replanning time instance $k+1$. It defines

the solution space of the subsequent trajectory planning (operational level)

$$\mathbf{\Pi}^{*k} \in \mathbb{R}^{2\times p} = \bigcup_{j=1}^{p} \boldsymbol{\pi}^{*k+j|k} \tag{4.18}$$

with its j-th elements

$$\begin{aligned} \pi_1^{*k+j|k} &\in \mathbb{Z} = \{\pi_1^{*k+j|k} | -1 \leq \pi_1^{*k+j|k} \leq +1\} \\ \pi_2^{*k+j|k} &\in \mathbb{R} = \{\pi_2^{*k+j|k} | 0 \leq \pi_2^{*k+j|k} \leq v_{\text{long,max}}\} \end{aligned} \tag{4.19}$$

where $\pi_1^{*k+j|k}$ specifies the optimal maneuver at the corresponding prediction instance. $\pi_1^{*k+j|k} = 0$ represents the lane keeping (LK) maneuver, whereas $\pi_1^{*k+j|k} = \pm 1$ corresponds to the lane change left (LCL) resp. right (LCR) maneuvers. The optimal longitudinal target velocity $\pi_2^{*k+j|k}$ is bounded to the upper limit of $v_{\text{long,max}}$. This itself is determined by the minimum of the driver's desired speed, road speed limits and comfortable speed in curves.

At the next consecutive sampling time instance, the p-step policy is recalculated using the latest measurements. This procedure is repeated for an infinite sampling time instances (receding horizon approach). The main advantage of the model predictive maneuver planning is the fact that it allows the current time slot to be optimized, while keeping account of future time slots. Additionally, it has the ability to anticipate future events and react accordingly. Through sufficiently rapid replanning, it is guaranteed that the cognitive vehicle responds to unforeseen events as well and, when necessary, abort the planned action.

For the model predictive decision-making a robust and computationally efficient maneuver prediction of all the traffic participants is required. For this reason, the results of the interaction-aware maneuver prediction model from Chapter 3 are applied and a suitable dynamic model is derived in the next section.

Maneuver Prediction and Dynamic Model

The developed maneuver prediction framework in Chapter 3 provides the most probable interaction-aware lateral and longitudinal future motion of the surrounding traffic. The output of the model is exemplary shown in Figure 4.7 for the front vehicle at a distance of about 80 m in a real highway traffic situation. The bottom plots show its measured interaction-unaware features (lateral deviation d and lateral velocity $\dot{d}$) and the lane change probability. In order to assign objects to the lanes of the highway, matching algorithms are required. Therefore, a road coordinate system (RCS, also called Frenet coordinate) is defined and the state vector of each vehicle is transformed into it (Figure 4.8). In this system x represents the driven distance from the starting point of the road section and y the lateral distance from the leftmost lane marking. Thanks to this coordinate system, there is no difference made between straight and curve segments. In other words, only straight highways can be simulated without loss of generality [178].

The time-invariant nonlinear dynamic model of the traffic $g_{\text{TFC}} : \mathbb{R}^3 \times \mathbb{R}^2 \to \mathbb{R}^3$ deter-

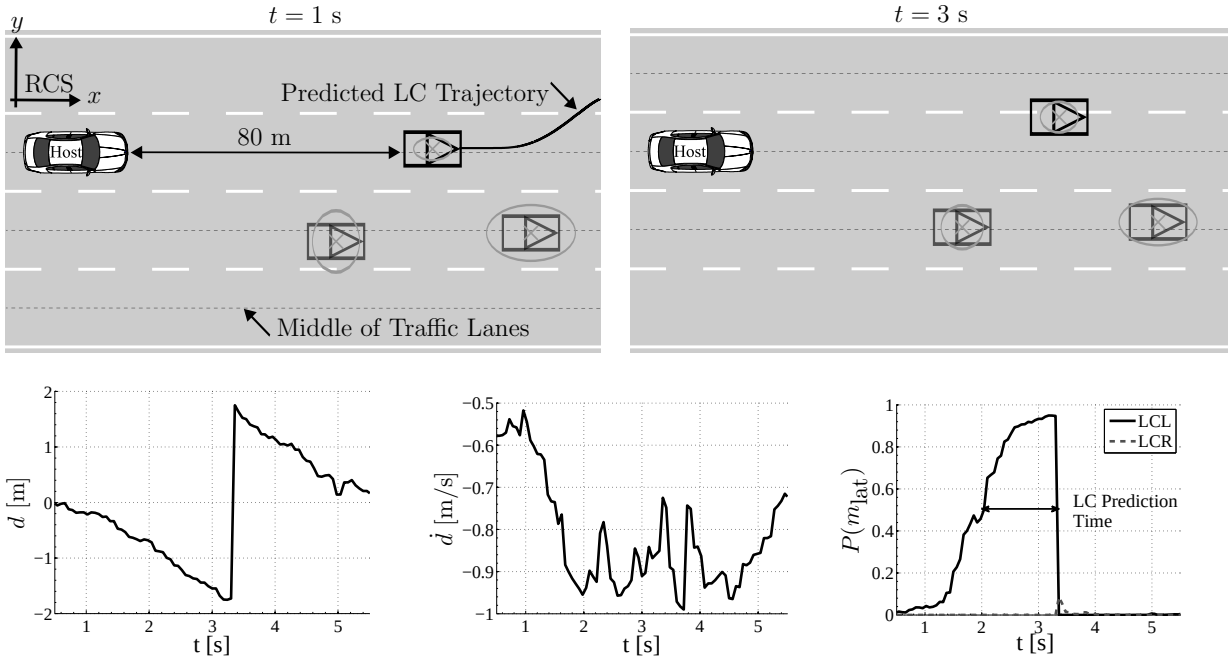

Fig. 4.7: Lane change prediction of the front vehicle (bold marked). Despite the relative high level of uncertainty (grey ellipses), the prediction is robust and reliable.

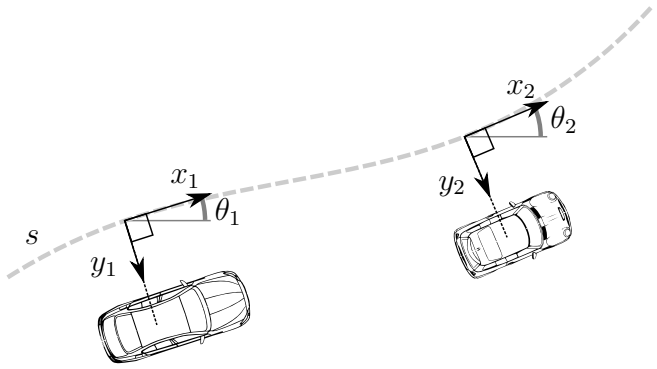

Fig. 4.8: Two vehicles represented in the road coordinate system $x_i(t)$ and $y_i(t)$. Image source: [92, 93]

mines the state vector $\mathbf{x}_v^{k+j|k}$ of the v-th vehicle for the next p prediction instances based on the Markov assumption

$$\mathbf{x}_v^{k+j|k} = g_{\mathrm{TFC}}\left(\mathbf{x}_v^{k+j-1|k}, \mathbf{u}_v^k\right) \tag{4.20}$$

with the v-th vehicle's state vector in the RCS

$$\mathbf{x}_v^{k+j|k} \in \mathbb{R}^3 = \begin{pmatrix} x_v^{k+j|k} \\ y_v^{k+j|k} \\ v_{\mathrm{long},v}^{k+j|k} \end{pmatrix} = \begin{pmatrix} \text{longitudinal position} \\ \text{lateral position} \\ \text{longitudinal velocity} \end{pmatrix} \tag{4.21}$$

and its measured (resp. predicted) control input vector at the corresponding sampling time instance

$$\mathbf{u}_v^{k+j|k} \in \mathbb{R}^2 = \begin{pmatrix} \mathcal{I}_v^{k+j|k} \\ a_{\text{long},v}^{k+j|k} \end{pmatrix} = \begin{pmatrix} \text{Interaction-aware lateral maneuver intention} \\ \text{Interaction-aware longitudinal acceleration} \end{pmatrix}. \tag{4.22}$$

g_{TFC} can be described by the following system of equations (assumption of constant acceleration)

$$\begin{aligned} x_v^{k+j|k} &= x_v^{k+j-1|k} + v_{\text{long},v}^{k+j-1|k}\Delta t_{p_j} + \frac{a_{\text{long},v}^{k+j-1|k}\Delta t_{p_j}^2}{2} \\ y_v^{k+j|k} &= y_v^{k+j-1|k} + \Delta y_v^{k+j|k}\left(\mathcal{I}_v^{k+j|k}\right) \\ v_{\text{long},v}^{k+j|k} &= v_{\text{long},v}^{k+j-1|k} + a_{\text{long},v}^{k+j-1|k}\Delta t_{p_j}, \end{aligned} \tag{4.23}$$

Where Δt_{p_j} represents the intervals in seconds between the prediction instances. Based on the predicted maneuver intention, an appropriate fifth-order polynomial trajectory for the v-th vehicle is generated and its lateral position along this trajectory at each prediction instance j is determined by $\Delta y_v^{k+j|k}\left(\mathcal{I}_v^{k+j|k}\right)$ (see Appendix A.1).

There is a reasonable simplification made by the traffic dynamic model: The predicted sates of the v-th vehicle is decoupled from the policy of the host (cognitive) vehicle at the specific prediction instance. It reduces the computational complexity of the subsequent optimization problem. This simplification is feasible, since the mutual interaction between different traffic participants has not always be considered in every situation. However, in traffic situations where cooperation is desired (Chapter 5), the mutual dependency will be explicitly taken in to account.

Because of the known host policy at each prediction time instance, the control input vector of the host vehicle is defined as

$$\mathbf{u}_{\text{Host}}^{k+j|k} \in \boldsymbol{\mathcal{U}}_{\text{Host}}^{k+j|k} \in \mathbb{Z} \times \mathbb{R} = \begin{pmatrix} \pi_1^{k+j|k} \\ \dot{\pi}_2^{k+j|k} \end{pmatrix} \tag{4.24}$$

$\boldsymbol{\mathcal{U}}_{\text{Host}}^{k+j|k}\left(\mathbf{x}_{\text{Host}}^{k+j-1|k}\right)$ determines the feasible solution space of the host control input dependent on its previous state. The host vehicle dynamics and other constrains are considered here. The motion of the host vehicle is also predicted based on the constant acceleration assumption. Therefore, a similar dynamic model $g_{\text{Host}} : \mathbb{R}^3 \times \mathbb{R}^2 \to \mathbb{R}^3$ is derived which is described by the following system of equations

$$\begin{aligned} x_{\text{Host}}^{k+j|k} &= x_{\text{Host}}^{k+j-1|k} + v_{\text{long,Host}}^{k+j-1|k}\Delta t_{p_j} + \frac{\dot{\pi}_2^{k+j-1|k}\Delta t_{p_j}^2}{2} \\ y_{\text{Host}}^{k+j|k} &= y_{\text{Host}}^{k+j-1|k} + \Delta y_{\text{Host}}^{k+j|k}\left(\pi_1^{k+j|k}\right) \\ v_{\text{long,Host}}^{k+j|k} &= v_{\text{long,Host}}^{k+j-1|k} + \dot{\pi}_2^{k+j-1|k}\Delta t_{p_j} \end{aligned} \tag{4.25}$$

where $\Delta y_{\text{Host}}^{k+j|k}\left(\pi_1^{k+j|k}\right)$ specifies the lateral position of the host vehicle along the fifth-order polynomial trajectory dependent on its planned maneuver.

Based on the derived dynamic models, the evolution of the environment can be predicted. This is the precondition for the subsequent online finite horizon optimization. The optimal policy sequence $\mathbf{\Pi}^{*k}$ is computed by solving the following discrete-time constrained optimization problem

$$\min_{\boldsymbol{\pi}^{k+j|k}} \left[\sum_{j=1}^{p} \Phi \left(\bigcup_{v} \mathbf{x}_v^{k+j|k}, \mathbf{x}_{\text{Host}}^{k+j|k}, \boldsymbol{\pi}^{k+j|k} \right) \lambda^j \right] \tag{4.26}$$

with respect to the general constraints

$$\sum_{j=1}^{p} |\dot{\pi}_1^{k+j|k}| \leq 1 \tag{4.27}$$

$$a_{\text{decel,max}} \leq \dot{\pi}_2^{k+j|k} \leq a_{\text{accel,max}} \tag{4.28}$$

It is a cost-minimizing problem (with respect to the objective function $\Phi(.)$) taking into account the derived dynamic models from (4.23) and (4.25) and the hard inequality constrains. The discount factor $\lambda^j \in]0,1]$, $\lambda^{j+1} < \lambda^j$ considers the predicted costs with continuously falling weights in the overall optimization due to the increase of uncertainty in the prediction. In the lateral direction, the maximal number of lane changes is limited to one (4.27). The longitudinal vehicle dynamics with respect to the maximum acceleration and deceleration is limited by (4.28). In order to guarantee a reactive behavior, the decision-making process has to be performed with a replanning period of at least $\Delta T = 0.2$ seconds [11].

Regarding the discrete control input of the host vehicle in the lateral direction (i.e. doing a lane change or not) and possible nonlinearities in the objective function, a mixed-integer nonlinear optimization problem has to be solved, which is in general computationally expensive [107]. Hence, the nonlinear system has to be approximated with a linear model. The approach chosen in this thesis is to implement the nonlinear plant using the hybrid system formulation, which was already introduced in Section 4.2. The optimal solution of the model predictive maneuver planning can be finally determined through by mixed-integer linear optimization.

The second approach, presented in this thesis, formulates the problem of model predictive maneuver planning in a combinatorial manner. It ensures the requirement of on-line capability and guarantees finding a solution (even though not globally optimal). In the next sections, these both approaches will be discussed and evaluated in detail.

4.4 Approach

In this section, the model predictive maneuver planning within the basic behavioral strategy will be discussed in detail by means of the two different approaches of constrained optimization of hybrid systems and combinatorial optimization.

4.4.1 Constrained Optimization of Hybrid Systems

Environment Model

In the classic maneuver planning approaches of autonomous driving, only the current state of the interesting traffic (in most cases the leading vehicle) is considered to avoid collisions. In the model predictive maneuver planning, however, the states of other traffic participants have to be a part of the model, in order to consider the predicted traffic scenes in the optimization problem. To reduce the overall complexity, an *environment model* is developed which considers the six neighboring vehicles from perspective of the host vehicle on its current and adjacent lanes. The state vectors are provided in the above-mentioned road coordinate system. Figure 4.9 illustrates exemplarily the environment model, when the host vehicle is driving on a middle lane.

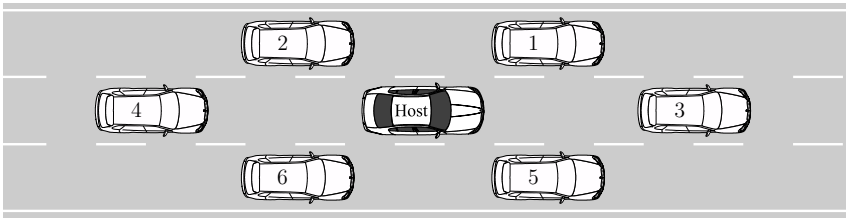

Fig. 4.9: The environment model, when the host vehicle is driving on a middle lane.

The continuous state vector of the complete system $\mathbf{x}_c^{k+j|k}$ thus includes the state vectors of the host and the relevant vehicles at the j-th prediction instance

$$\mathbf{x}_c^{k+j|k} \in \mathbb{R}^{21} = \begin{pmatrix} \mathbf{x}_{c,\text{Host}}^{k+j|k} \\ \mathbf{x}_{c,1}^{k+j|k} \\ \mathbf{x}_{c,2}^{k+j|k} \\ \mathbf{x}_{c,3}^{k+j|k} \\ \mathbf{x}_{c,4}^{k+j|k} \\ \mathbf{x}_{c,5}^{k+j|k} \\ \mathbf{x}_{c,6}^{k+j|k} \end{pmatrix} = \begin{pmatrix} x_{\text{Host}}^{k+j|k} \\ y_{\text{Host}}^{k+j|k} \\ v_{\text{long,Host}}^{k+j|k} \\ \vdots \\ y_6^{k+j|k} \\ v_{\text{long,6}}^{k+j|k} \end{pmatrix}. \tag{4.29}$$

In situations where the corresponding vehicles do not exist (e.g. the host vehicle drives on the leftmost (resp. rightmost) lane or some vehicles are out of the sensor range), the continuous sate vector will be adapted accordingly.

Hybrid System Formulation

As previously discussed in Section 4.2, the model predictive maneuver planning is first formulated as a DHA using the modeling language HYSDEL. Finally, the HYSDEL compiler translates the developed DHA into the equivalent MLD system, which is more suitable for the mixed-integer quadratic program. In the following, the most important parts of the DHA will be discussed. A more detailed description of the algorithm can be found in [201].

Event Generator The event generator determines binary variables according to the satisfaction of linear constraints. Two different types of events are taken into account in the current implementation:

1. End of a lane change maneuver: Whenever the host vehicle has reached its desired lane after a lane change maneuver, the appropriate event will be triggered

$$\delta_{lm} = 1 \quad \Leftrightarrow \quad y_m - y_{\text{Host}}^{k+j|k} \leq 0 \tag{4.30a}$$
$$\delta_{mr} = 1 \quad \Leftrightarrow \quad y_r - y_{\text{Host}}^{k+j|k} \leq 0 \tag{4.30b}$$
$$\delta_{ml} = 1 \quad \Leftrightarrow \quad y_{\text{Host}}^{k+j|k} - y_l \leq 0 \tag{4.30c}$$
$$\delta_{lm} = 1 \quad \Leftrightarrow \quad y_{\text{Host}}^{k+j|k} - y_m \leq 0, \tag{4.30d}$$

   where $y_\square$ represents the lateral position of the corresponding lane. The indices m, l and r mean the current (middle) lane, the adjacent lane on the left side and the adjacent lane on the right side, respectively. For example, the event δ_{lm} is true, when the host vehicle has reached its desired lane after a lane change maneuver form the left adjacent lane to the middle lane.

2. Overtaking maneuver: If the vehicle i overtakes the vehicle j then the event δ_{ji} will be triggered

$$\delta_{Host2} = 1 \quad \Leftrightarrow \quad x_{\text{Host}}^{k+j|k} - x_2^{k+j|k} \leq 0 \tag{4.31a}$$
$$\delta_{Host4} = 1 \quad \Leftrightarrow \quad x_{\text{Host}}^{k+j|k} - x_4^{k+j|k} \leq 0 \tag{4.31b}$$
$$\delta_{Host6} = 1 \quad \Leftrightarrow \quad x_{\text{Host}}^{k+j|k} - x_6^{k+j|k} \leq 0 \tag{4.31c}$$
$$\delta_{5Host} = 1 \quad \Leftrightarrow \quad x_5^{k+j|k} - x_{\text{Host}}^{k+j|k} \leq 0. \tag{4.31d}$$

   This binary event is necessary because after the above-mentioned overtaking maneuvers the environment model has to be re-evaluated.

Finite State Machine The FSM is applied to consider the discrete states of the hybrid system. On the one hand, it enables different dynamics of the system since the difference equations differs based on the lateral policy $\pi_1^{k+j|k}$ of the host vehicle. On the other hand, certain constraints should be enabled dependent on the discrete state of the system. For instance, the currently active state determines which vehicles are of interest for collision avoidance.

The transition conditions are the binary events of (4.30), (4.31) and the lateral policy $\pi_1^{k+j|k}$ of the host vehicle. The nodes represent different possible traffic situations. For example, if the host vehicle takes over the vehicle $v = 5$, the environment and also the constraints will be changed. One problem is that the number of transitions within the FSM is increasing exponentially with the discontinuities. Thus, the general problem of finding the optimal policy sequence is separated into the three less complex optimization problems:

- Finding the optimal policy sequence if the desired lane is the rightmost lane.

- Finding the optimal policy sequence if the desired lane is the leftmost lane.
- Finding the optimal policy sequence if the desired lane is a middle lane.

This approach reduces the complexity of the single optimization problem enormously without any lost of generality.

Figure 4.10 shows the developed FSM used for the optimization problem when the desired lane is the rightmost lane. The first letter gives the current and the last gives the

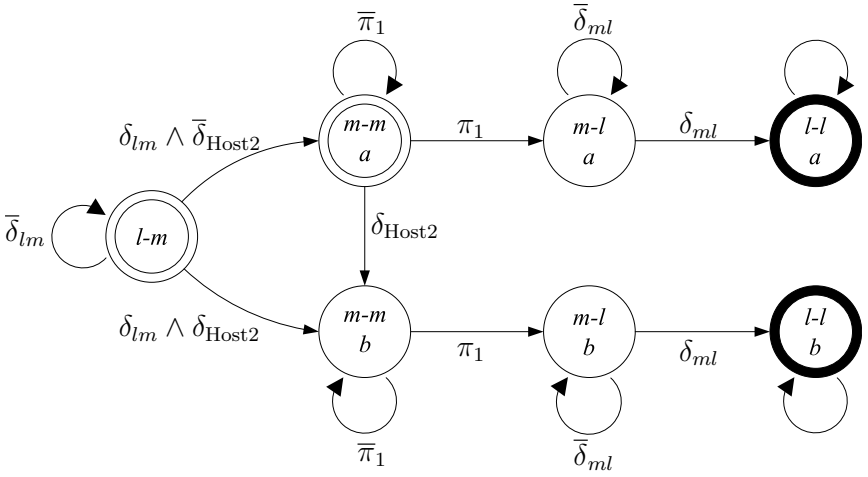

Fig. 4.10: FSM for the optimization problem on the rightmost lane.

desired lane. For example, *l-l* means "keep driving on the left adjacent lane" or *m-l* means "lane change maneuver from the current lane (here the rightmost lane) to the left adjacent lane". The initial situation (entry point) is either *m-m_a* "keep driving on the rightmost lane" or *l-m* "change lane to the rightmost lane". Depending on the event δ_{Host2} (vehicle 2 overtakes the host vehicle), the FSM follows either trace (a) or (b). The final state (shown in bold) is at the same time the initial state of the corresponding FSM of the other optimization problem. The FSMs of the two other optimization problems are significantly more complex. In the current implementation, besides the continuous state vector, the logical state vector of the overall hybrid system has the dimension of $\mathbf{x}_l^{k+j|k} \in \{0,1\}^{35}$.

Mode Selector and Switched Affine System The mode selector determines the dynamic model of the subsequent switched affine system. The respective mode $i^{k+j|j}$ at the j-th prediction instance is selected based on the currently active states of the three FSMs and the binary events. Finally, the switched affine system determines which difference equations from (4.23) and (4.25) must be enabled depending on the current mode $i^{k+j|j}$.

Mixed-Integer Quadratic Program (MIQP)

In the previous sections the environment model and the hybrid system based on DHA were discussed. In the following, the optimization problem will be formulated in detail. The task now is to find the optimal policy sequence (resp. driving goals) $\mathbf{\Pi}^{*k}$. Thus, the objective function and the constraints should be defined in the next step.

Objectives The high-level objectives of the proposed model predictive maneuver planning are:

1. If possible drive on the "optimal" lane: The definition of the optimal lane is in most of the time motivated by the traffic rules rather than an objective. In Germany (generally right-hand traffic), for instance, the optimal lane is the rightmost lane due to the traffic regulations (*Rechtsfahrgebot*, Art. 2 Sec.2, *StVO*). However, other motivations are possible as well. For example, if the average traffic velocity on the rightmost lane is much lower than the desired speed, the optimal lane could be chosen as a middle lane.

2. If possible drive with the "desired speed": The goal is to retain a desired speed which is set by the driver itself.

3. Minimize the longitudinal jerk: Longitudinal jerk has to be minimized in order to enable a comfortable driving.

4. Minimize the number of lane changes: Number of lane changes (resp. lateral jerk) has to be minimized in order to enable a comfortable driving.

The formulated objectives considers thus not only the comfort aspects but also the traffic rules. The objective function of the mixed-integer quadratic program is formulated as

$$\Phi^{k+j|k}(\mathbf{x}_{\text{Host}}^{k+j|k}, \boldsymbol{\pi}^{k+j|k}) = \sum_{j=1}^{p} \underbrace{\|\mathbf{x}_{\text{Host}}^{k+j|k} - \mathbf{r}^{k}\|_{\mathbf{Q}}}_{1,2} + \sum_{j=1}^{p} \underbrace{\|\Delta\boldsymbol{\pi}^{k+j|k}\|_{\mathbf{R}}}_{3,4}, \tag{4.32}$$

where $\mathbf{r}^k$ is the *reference trajectory* and $\mathbf{Q}$ is the *weighting matrix reflecting the relative importance of each individual state*. Accordingly, $\mathbf{R}$ is the *weighting matrix penalizing relative big changes in the policy*. The first and second objectives are considered with the help of the reference trajectory:

$$\mathbf{r}^k = \begin{pmatrix} 0 \\ y_{\text{des}}^k \\ v_{\text{des}}^k \end{pmatrix},$$

where y_{des}^k represents the lateral position of the desired lane and v_{des}^k is the desired speed of the host vehicle.

Constraints The constraints are limiting the solution space of the optimization problem. For the mixed-integer quadratic program, it is necessary to formulate a convex set. Thus, only linear constraints are applied to bound the solution set. This guarantees that the resulting optimization problem is convex and thus the found policy is global optimal. The constraints of the proposed model predictive maneuver planning are given by the following two traffic rules:

1. The distance to the leading vehicle must be sufficiently large to be able to stop the host vehicle behind the leading traffic $v = dl$, even if it brakes instantaneously (Art. 4 Sec.1, *StVO*).

   This is achieved by the following two constraints:

- Time to Collision (TTC)

$$t_{\text{ttc,min}} \leq t_{\text{ttc},v=dl}^{k+j|k} := \frac{x_{v=dl}^{k+j|k} - x_{\text{Host}}^{k+j|k}}{\pi_2^{k+j|k} - v_{\text{long},v=dl}^{k+j|k}} \tag{4.33}$$

- Intervehicular Time (TIV)

$$t_{\text{tiv,min}} \leq t_{\text{tiv},v=dl}^{k+j|k} := \frac{x_{v=dl}^{k+j|k} - x_{\text{Host}}^{k+j|k}}{\pi_2^{k+j|k}} \tag{4.34}$$

2. Vehicles must be overtaken on the left side (Art. 5 Sec.1, *StVO*). This is achieved by projecting the vehicles, which drive in front and on the left side of the host vehicle, onto its current lane. Subsequently, the TTC and TIV constraints to the projected vehicles has to be achieved as well. The limits are further reduced due to the fact that the risk of colliding is smaller if the vehicle is not on the same lane. During a lane change maneuver, however, the leading vehicle and the vehicles in front and back sides on the desired lane has to be taken into account.

Together with the previously formulated restrictions on the states and inputs, the overall constraints of the optimization problem is determined.

Mixed Logical Dynamical Formulation As discussed before, the DHA formulation is not suitable for the mixed-integer linear optimization problem. Thus, the proposed DHA will be translated in the equivalent mixed logical dynamical system. By considering the presented problem as a MLD system, collision avoidance constraints and conditions on states and inputs can be expressed as logic constraints which can be transformed into linear inequalities through propositional calculus.

One of the main challenges in maneuver planning based on mixed-integer optimization is dealing with infeasibilities due to model inaccuracies or unforeseen plant disturbances. For example, if the leading vehicle suddenly breaks without any reason, future maneuver planning of the host vehicle becomes infeasible since due to the limited maximum deceleration, collision can not be avoided. The approach which overcomes the infeasibilities is the *constraint softening* [85]. It is used in this thesis to make the maneuver planning even more robust against disturbances. The idea is to allow slight violation of certain constraints. This violation will be penalized in the objective function. As a result, the model predictive maneuver planning should try to bring the system back into the feasible area.

Comparing the performance of different mixed-integer optimizers shows that SCIP together with SoPlex [2] is currently the fastest non-commercial solver. It is in average two times faster and solved about 30% more problems than the second best non-commercial solver [88]. Particularly the latter fact motivated the decision to use SCIP+SoPlex as the solver for the mixed-integer linear problem in this thesis.

4.4.2 Combinatorial Optimization

Regarding the developed environment model in the last section, the second approach of model predictive maneuver planning based on combinatorial optimization will be discussed in this section. The feasible solution space of the host's policy (i.e. control input) $\boldsymbol{\mathcal{U}}_{\text{Host}}^{k+j|k}$ will be sufficiently fine discretized at each prediction instance. The problem can thus be viewed as a combinatorial optimization, searching for the best policy out of the discretized feasible solution space [124]. Depending on the discretization step size, the solution found is "sufficiently close" to the optimum. Subsequently, the underlying trajectory planning (operational level) guarantees a minimum jerk implementation of the driving goals.

For this reason, at each replanning instance a weighted tree $T\,(V, E)$ is considered which is described by the two sets of vertices (nodes) V and edges E. The depth of each node corresponds to the specific prediction instance j. The edge weights represent their calculated costs. The problem is now reformulated in the well-known "single-source shortest path problem". In the following, the control horizon is limited to the prediction horizon (i.e. $H_c = H_p = 5\,\text{s}$) and is divided into three instances (i.e. $p = 3$). The feasible solution space of the host's control input $\boldsymbol{\mathcal{U}}_{\text{Host}}^{k+j|k}$ for each of the three prediction instances $j = 1, 2, 3$ is discretized as follows: in the lateral direction the ego lane as well as lane change requests to the directly adjacent lanes (if they exist) is considered, taking into account the constrain from (4.27). In the longitudinal direction the velocity is discretized by a linearly spaced vector with respect to (4.28)

$$\boldsymbol{\pi}_2^{k+j|k} = \boldsymbol{\pi}_2^{k+j-1|k} + [a_{\text{decel,max}} : a_{\text{accel,max}}]\,\Delta t_{p_j}. \tag{4.35}$$

This results in a rooted search tree where each node has no more than $N = \min(3, l_{\text{max}}) \cdot |\boldsymbol{\pi}_2^{k+j|k}|$ children (with l_{max} = number of lanes). The variable N determines how accurate the discretization of the solution space is. However, the computational complexity rises polynomial with the discretization of the solution space N but exponential with the prediction instances p (i.e. $\mathcal{O}(N^p)$). Thus, these two variables must be chosen carefully.

Figure. 4.11 shows the introduced search tree for the replanning time instance k. The circles represent the set of all nodes at the j-th prediction instance. A distinction is made between the solid (continue on the same lane) and dashed nodes (with lane change request). The arrows illustrate the discretized velocities. The root node ($j = 0$) corresponds to the current measured state of the host vehicle and the measured states and control inputs of surrounding traffic. Each other node represents a policy combination from the feasible solution space. In addition, it represents a separate data structure which stores, among others, the predicted state vectors and the accumulated cost from the root node along exactly one elementary path (because of the arborescence property of the tree). Finally the tree will be searched for the shortest path, i.e. the path with the lowest cost, by using the exhaustive search [37]. When the host vehicle is forced to merge into another lane as soon as possible (e.g. in highway entrance), the best solution for the requested lane change direction can be also passed as a further driving goal to the trajectory planning. This shows thus the flexibility of the presented approach.

The definition of suitable objective functions has a great influence on the safety and comfort of the maneuver planning. For this reason, a priority-based approach is discussed

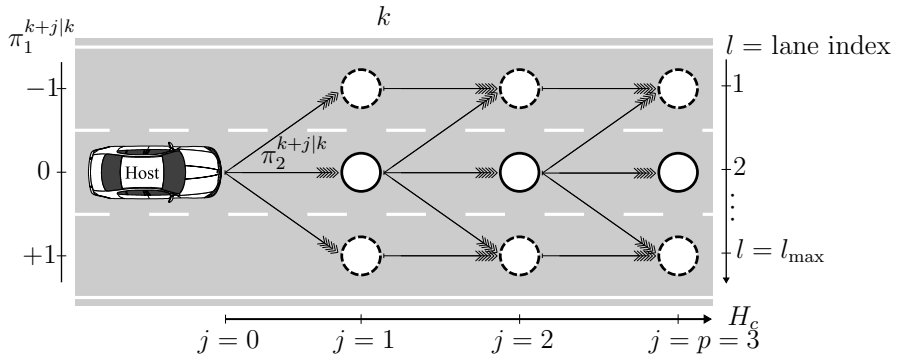

Fig. 4.11: Visualization of the search tree for the model predictive maneuver planning based on combinatorial optimization.

in detail in the next section. The goal is to define a set of representative functions with a minimal number of parameters. The mathematical formulation of the objective functions is based on the high-level objectives, introduced in the last section.

Objective and Constraints A main issue in constrained problems is that they may get infeasible when disturbances occur (as discussed in the case of mixed-integer program). The idea to overcome this in the combinatorial optimization is to introduce a *level-based objective function*. The cost resulting from the objective function is sub-divided here in 3 levels. The priority is ascending with the level number. This type of constraint softening approach guarantees, that the problem remains always feasible.

The level-3 cost takes account of the host vehicle's safety (including surrounding safety). For this purpose, a risk factor to the vehicles ahead is calculated based on time to collision (TTC) and intervehicular time (TIV). The maximum risk is determined by the minimum time. Thus, the risk r for both the TTC and TIV times is given by

$$r_{\text{ttc/tiv}}^{k+j|k} = \begin{cases} 1, & \text{if } t_{\text{ttc/tiv}}^{k+j|k} \leq t_{\text{ttc/tiv,min}} \\ 0, & \text{if } t_{\text{ttc/tiv}}^{k+j|k} \geq t_{\text{ttc/tiv,max}} \\ 1 - \frac{t_{\text{ttc/tiv}}^{k+j|k} - t_{\text{ttc/tiv,min}}}{t_{\text{ttc/tiv,max}} - t_{\text{ttc/tiv,min}}} \end{cases} \tag{4.36}$$

The accumulated level-3 cost along each n-th elementary path is

$$\begin{aligned} &\Phi_{\text{L3}_n}^k \in [p+1, p+2] \\ &= p + 2 - \prod_{j=1}^{p} \left[\left(1 - r_{\text{ttc}_n}^{k+j|k}\right) \left(1 - r_{\text{tiv}_n}^{k+j|k}\right) \right]. \end{aligned} \tag{4.37}$$

The level-2 cost considers the traffic laws. Initially only one of the key regulations for driving on Germany's highway, not overtaking on the right side, is implemented. For this reason, the front vehicle on the left adjacent lane $v = fl$ is taken into account. Similar to the approach from the last section, the idea is also here to project this vehicle on all lanes on its right side. Then the risk to collide with the projected vehicle based on TIV and TTC is calculated in the same way as for the level-3 cost. The accumulated level-2 cost

along each n-th elementary path is

$$\begin{aligned}&\Phi^k_{\mathrm{L2}_n} \in [p, p+1]\\ &= p + 1 - \prod_{j=1}^{p} \left[\left(1 - r^{k+j|k}_{\mathrm{ttc}_{n,v=fl}}\right) \left(1 - r^{k+j|k}_{\mathrm{tiv}_{n,v=fl}}\right) \right].\end{aligned} \tag{4.38}$$

The level-1 cost represents the comfort. The accumulated level-1 cost along each n-th elementary path is

$$\begin{aligned}&\Phi^k_{\mathrm{L1}_n} \in [0, p]\\ &= \sum_{j=1}^{p} \left[\frac{\left(w_1 \phi^{k+j|k}_{1_n} + w_2 \phi^{k+j|k}_{2_n} + w_3 \phi^{k+j|k}_{3_n} + w_4 \phi^{k+j|k}_{4_n}\right)}{w_1 + w_2 + w_3 + w_4} \right].\end{aligned} \tag{4.39}$$

The ϕ_1 cost is dependent on the difference to the bounded desired speed v_{des}

$$\phi^{k+j|k}_{1_n} = 1 - sech\left(v_{\mathrm{des}} - \pi^{k+j|k}_{2_n}\right). \tag{4.40}$$

The ϕ_2 cost prefers free lanes. The cost of the desired lane is dependent on the distance to the leading car $d^{k+j|k}_{n,v=dl} = |x^{k+j|k}_{n,v=dl} - x^{k+j|k}_{n,\mathrm{Host}}|$ and the distances to the leading cars on all reachable lanes $v \in F_v$

$$\phi^{k+j|k}_{2_n} = \frac{\frac{1}{d^{k+j|k}_{n,v=dl}}}{\sum\limits_{v \in F_v} \frac{1}{d^{k+j|k}_{n,v}}}. \tag{4.41}$$

The ϕ_3 cost rewards driving on the rightmost lane $l^k_{\max}$

$$\phi^{k+j|k}_{3_n} = \frac{l^k_{\max} - l^{k+j|k}_{n,\mathrm{Host}}\left(y^{k+j|k}_{n,\mathrm{Host}}\right)}{l^k_{\max} - 1}. \tag{4.42}$$

The ϕ_4 cost is introduced in order to minimizes the longitudinal jerk.

Furthermore, it must be guaranteed that paths with level-3 or level-2 cost are only taken, if there are no paths with level-1 cost:

$$\begin{aligned}&\text{If} \quad \Phi^k_{\mathrm{L3}_n} \geq p+1 \qquad \text{then} \quad \Phi^k_{\mathrm{L2}_n} = \Phi^k_{\mathrm{L1}_n} = \infty\\ &\text{If} \quad \Phi^k_{\mathrm{L2}_n} \geq p \qquad\qquad\quad \text{then} \quad \Phi^k_{\mathrm{L1}_n} = \infty\end{aligned} \tag{4.43}$$

Finally, the path with the minimum cost is taken

$$\Phi^{*k} = \min_n \left[\min\left[\Phi^k_{\mathrm{L1}_n}, \Phi^k_{\mathrm{L2}_n}, \Phi^k_{\mathrm{L3}_n}\right]\right] \tag{4.44}$$

This formulation guarantees that the problem is always feasible. Moreover, the host vehicle would always prefer to take over a car on the left side. However, when it is not possible, it would rather take over another car on the right side, than daring to collide with it. In other words, by the separation in levels it is guaranteed that no unsafe policy is chosen and a policy which violates traffic laws is only chosen if a risky situation can be avoided.

During a planned lane change maneuver, the traffic on the desired lane is permanently monitored. If the risk exceeds a threshold, the lane change maneuver will be aborted accordingly. After abortion, the whole tree is expanded again for the opposite direction and the new optimal policy will be determined.

The weights w_1, w_2, w_3, w_4 were trained here using a genetic algorithm based on natural selection [49]. An individual is defined by a set of weights $\mathbf{w}$

$$\mathbf{w} \in \mathbb{R}^4 = \{w_i | 0 < w_i \leq 1\} \tag{4.45}$$

The idea is to take a set of highway traffic scenes, which represents the situation space as good as possible. The fitness function evaluates how well the host vehicle drives with a set of $\mathbf{w}$ in these scenes. The evaluation is inspired by human driving behavior. The criteria are the number of crashes, the reached percentage of the desired velocity and the lateral and longitudinal jerk. This multi-objective optimization problem is solved using the ϵ-constrained method. The host vehicle must not crash ($\epsilon = 0$) and the average velocity must be at least 95% of the desired velocity ($\epsilon = 0.95$). Finally, the genetic algorithm evolves the individual solution $\mathbf{w}^*$ with minimum lateral and longitudinal jerk.

The entire process flow of the model predictive maneuver planning based on combinatorial optimization is given in Algorithm 4.4.2.

Algorithm 2 Model predictive maneuver planning based on combinatorial optimization.

for $k = 0$ to ∞ **do** # in each replanning instance
  DATA-PREPROCESSING(.)
  for $j = 1$ to p **do**
    for $v = 1$ to N_{CARS} **do**
      $\mathbf{u}_{\text{TFC}}[v] \leftarrow Measurements$
      $\mathbf{x}_{\text{TFC}}[v][j] \leftarrow g_{\text{TFC}}\left(\mathbf{x}_{\text{TFC}}[v][j-1], \mathbf{u}_{\text{TFC}}[v]\right)$ # interaction-aware prediction
    end for
  end for
  $tree \leftarrow$ EXPAND-TREE(.) # wrt. constraints
  for $n = 1$ to N_{NODES} **do**
    $f \leftarrow$ FATHER-NODE(n)
    $\boldsymbol{\pi} \leftarrow$ POLICY-VECTOR(n)
    $\mathbf{x}_{\text{Host}}[n] \leftarrow g_{\text{Host}}\left(\mathbf{x}_{\text{Host}}[f], \boldsymbol{\pi}\right)$
    $\Phi[n] \leftarrow \Phi\left(\mathbf{x}_{\text{TFC}}[n], \mathbf{x}_{\text{Host}}[n], \boldsymbol{\pi}\right)$
  end for
  $\boldsymbol{\Pi}^{*k} \leftarrow$ EXHAUSTIVE-SEARCH ($tree$)
end for

4.5 Evaluation

In this section the functionality of the presented basic behavioral strategy will be evaluated. For this purpose, a simulated environment is developed for common and extreme highway situations. Multiple parameters such as the number of lanes, the number of vehicles or

the duration of the simulation are adjustable. Different intelligent vehicles can be chosen. Vehicles without the possibility to change the lane (only longitudinal controller) are available as well as vehicles which have a longitudinal and lateral controller, but only with a reactive driving strategy very similar to the previous implementation of driving strategy in the prototype vehicles at BMW Group Research and Technology [11, 12]. Lastly, vehicles with the basic behavioral strategies described in Section 4.4 can be chosen, e.g. the host vehicles in the following examples. The simulation environment is deterministic and the simulations are reproducible. These are important characteristics when the simulation environment is used as a part of the development process.

One the one hand, the focus of the evaluation is on the benefits from the model predictive maneuver planning in general. On the other hand, the model predictive maneuver planning based on the two different approaches of mixed-integer quadratic program (MIQP) and combinatorial optimization (CO) will be compared and the advantages and disadvantages will be discussed.

Qualitative Evaluation of the Length of the Prediction Horizon

The focus of this evaluation part is to demonstrate the advantages of the model predictive maneuver planning with a longer prediction horizon. Thus, a common highway situation is simulated. In Figure 4.12 the host vehicle is approaching the slower leading vehicle 3 on a single-lane road. The desired velocity is $v_{\text{des}} = 40\,\text{m/s}$. The leading vehicle keeps its velocity constant at $v_3 = 30\,\text{m/s}$. The host vehicle has thus to decelerate in order reach the desired safety distance to its leading vehicle.

This situation is simulated two times with the proposed model predictive maneuver planning based on the mixed-integer quadratic program. The prediction horizon in the first run is $H_p = 2\,\text{s}$, whereas in the second simulation the prediction horizon is extended to $H_p = 5\,\text{s}$. At the top of Figure 4.12 (a) the initial states of the vehicles at time $t = 0\,\text{s}$ and the predicted states at time $t = 0.5\,\text{s}$ for the system with prediction horizon of $H_p = 2\,\text{s}$ are visualized. The diagrams below show the respective costs of the host's optimal policy at this replanning time instance. Figure 4.12 (b) shows basically the same diagrams for the system with the prediction horizon of $H_p = 5\,\text{s}$. Here, the initial state and the predicted states at time $t = 2\,\text{s}$ and $t = 3.5\,\text{s}$ are visualized. The maneuver planning with $H_p = 5\,\text{s}$ predicts the threatening violation of the TTC and TIV constraints to the leading vehicle already from the initial state on. It plans to reduce its velocity step by step starting at $t = 2\,\text{s}$. Whereas the system with $H_p = 2\,\text{s}$ does not detect the threat of the decreasing distance to vehicle 3 until the time $t = 4.5\,\text{s}$.

Figure 4.13 shows a comparison of the acceleration and the jerk resulting of both determined optimal policies. Due to the fact that the controller of the simulation (plant) is different to the internal prediction model, the behavior is slightly different to the planned behavior. The behavioral strategy with the longer prediction horizon starts to decelerate at $t = 2\,\text{s}$. Whereas the more reactive one does not decelerate until the time $t = 4.5\,\text{s}$. But then it has to brake very fast and strongly. While the longitudinal jerk for the model predictive maneuver planning with $H_p = 5\,\text{s}$ is never greater than $1.5\,\text{m/s}^3$, the jerk for the system with $H_p = 2\,\text{s}$ reaches $4\,\text{m/s}^3$ at its maximum. Such a high longitudinal jerk affects the driving comfort negatively. Therefore, the first benefit from model predictive

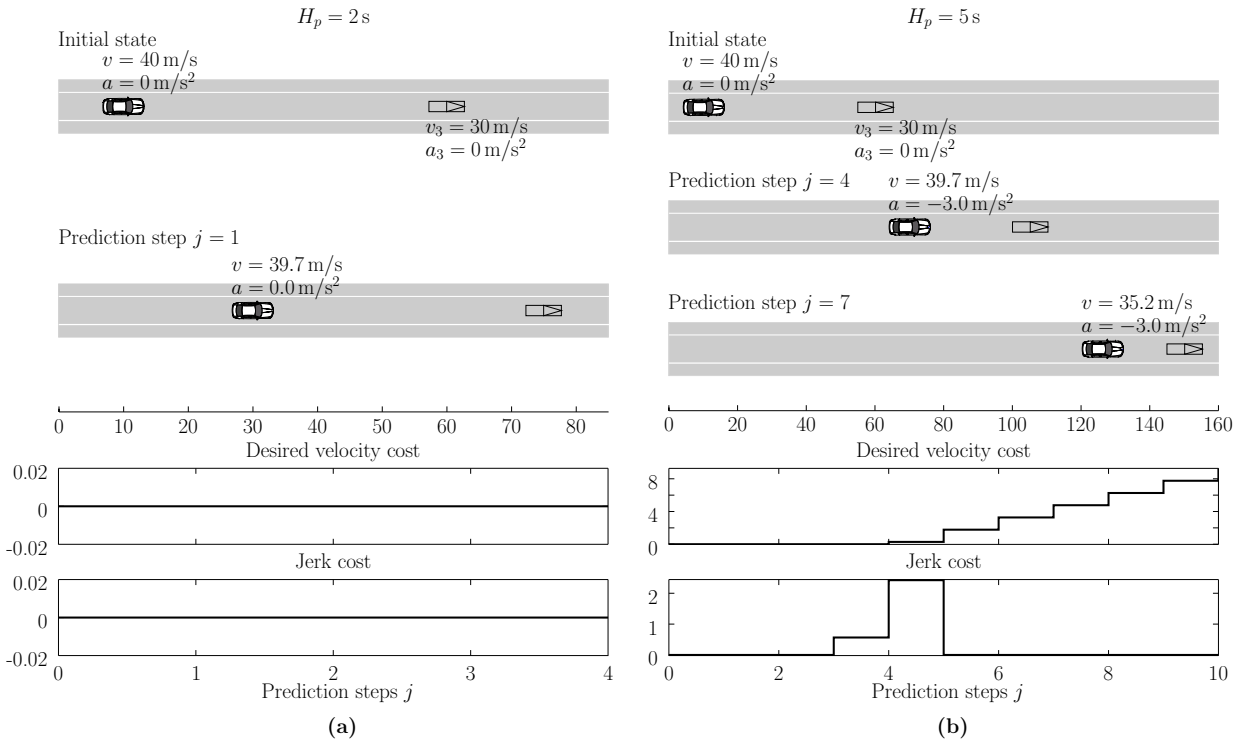

Fig. 4.12: Model predictive planning with (a) $H_p = 2\,\mathrm{s}$ and (b) $H_p = 5\,\mathrm{s}$.

maneuver planning with higher prediction horizon is its improvements in terms of driving comfort.

The acceleration course of the first system with $H_p = 2\,\mathrm{s}$ gets at about $t = 8.5\,\mathrm{s}$ positive values. Later the host vehicle decelerates again, which is not shown on the diagram anymore. This overshoot of the desired value is also a direct result of the shortsighted planning. Thus, a further advantage of the maneuver planning with longer prediction horizon is its ability to avoid oscillating in the determined policy. To sum it up, model predictive maneuver planning provides compared to a more reactive one various advantages in terms of driving comfort, prevention of oscillating and contribution to early collision avoidance.

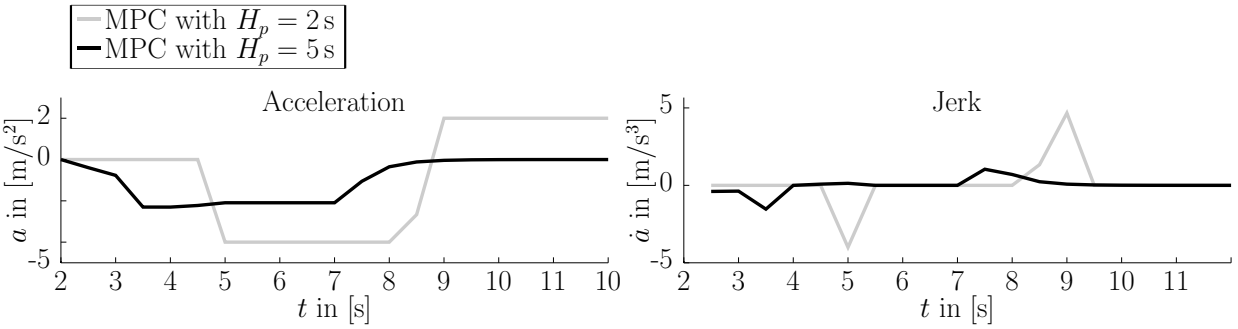

Fig. 4.13: Comparison of model predictive planning with $H_p = 2\,\mathrm{s}$ and $H_p = 5\,\mathrm{s}$.

Qualitative Comparison of MIQP and CO approaches based on Prototype Scenarios

In Section 4.4 the model predictive maneuver planning based on the two different approaches of MIQP and CO and in particular their differences in dealing with infeasibilities were discussed in detail. As described above, the approach based on the CO does not find the global optimum exactly, but can only guarantee to miss it not further than the discretization interval. The motivation in this section is to evaluate if the solution provided by the CO approach is comparable with the provided global optimal solution from the MIQP approach. Furthermore, it will be shown that the achieved driving behavior is reasonable and rational from a human point of view. Hence, various highway situations will be simulated in the following.

Critical Cut-in Maneuver

The following highway situation is illustrated in Figure 4.14. The host vehicle is driving autonomously on a multi-lane highway and is approaching the slower vehicle 5 on its right side. The host is accelerating to reach its desired velocity, whereas the other vehicle drives already at its desired velocity. Right before the host vehicle is next to it, vehicle 5 changes to the lane of the host vehicle. A rational human driver would instantly brake and change to the left adjacent lane to avoid a collision.

The simulations are performed with the already described approaches of MIQP and CO. The prediction horizon of the CO approach is set to 5 s (only the first three seconds are shown in the diagrams). Due to the increase in uncertainty with a longer prediction time, the prediction intervals are increased linearly. The prediction horizon of the MIQP approach is set to 6 s, which is slightly higher. The reason is that in case of the hybrid system formulation the entire lane change maneuver should be predicted in order to enable the appropriate binary events. Two instants of the simulations are visualized in Figure 4.14 at time $t = 0\,\mathrm{s}$ and in Figure 4.15 at time $t = 6.5\,\mathrm{s}$. The crosses illustrate the predicted positions of the host vehicle with both approaches and the predicted position of the vehicle 5, respectively. The diagrams below show the course of different costs of each approach at the given replanning time instance for different prediction steps. For reasons of clarity the values are neglected, but the progress is sufficient.

In the initial state none of the systems expects the lane change maneuver. In this situation a larger prediction horizon does not provide any advantage because it can not predict disturbances to the model. Thus, the host vehicle accelerates to reach its desired velocity which can be seen in the reducing cost of the desired velocity. All other costs are constant, except the jerk cost, which penalizes the changes in the longitudinal acceleration. In the time $t = 6.5\,\mathrm{s}$ both systems have recognized the lane change maneuver of the vehicle 5. The methods how both optimization approaches handle this "disturbance" are different. In the CO approach suddenly every node in the search tree has level-3 cost. Therefore, it takes the node with the lowest level-3 cost independently of the level-1 objectives. Whereas the MIQP penalizes this violation with the help of constraint softening. Although the methods are different, the calculated policies are comparable.

The similarity of both solutions is even more obvious in Figure 4.16 which shows the

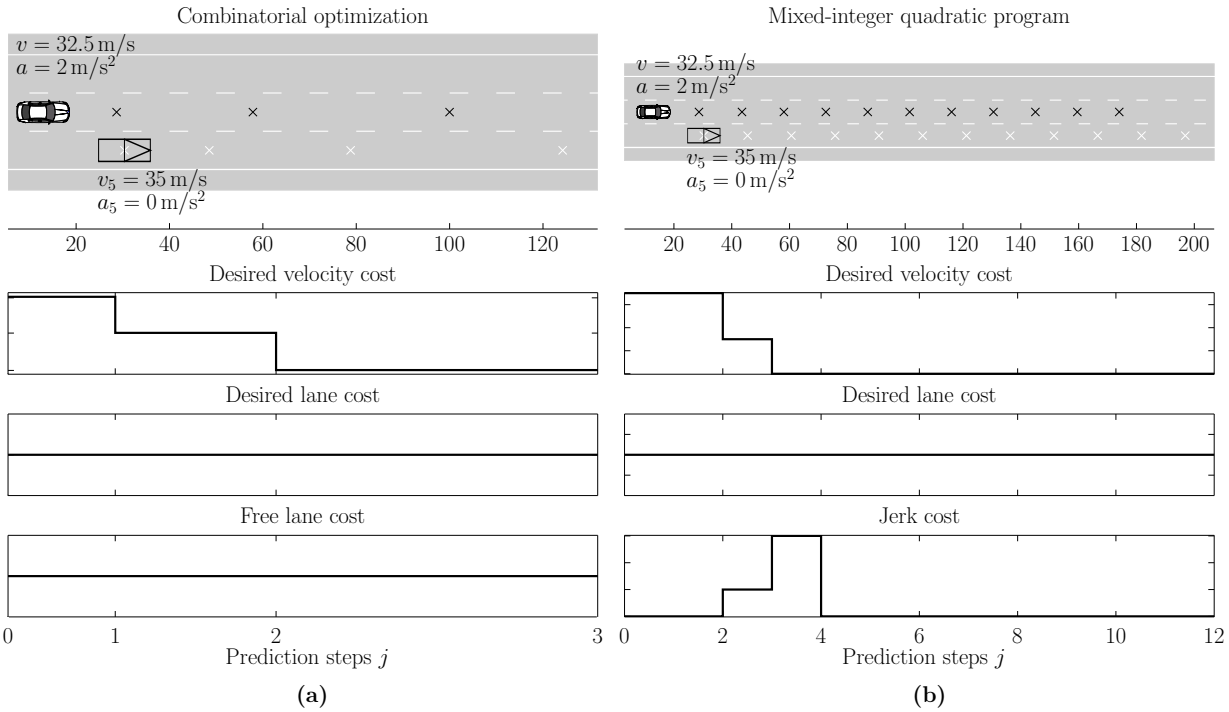

Fig. 4.14: Model predictive planning in the case of "critical cut-in maneuver" at time $t = 0\,\mathrm{s}$ with (a) CO and (b) MIQP.

driven paths for the host vehicle with CO and MIQP and for the vehicle 5. The paths nearly match each other. Besides the fact, that the CO begins the lane change maneuver already at $x \approx 190\,\mathrm{m}$, whereas the MIQP begins it not before $x \approx 210\,\mathrm{m}$. One reason for this delay is that in the level-based disturbance handling of the CO the decision is made independently of the lower levels. Whereas by the constraint softening method of the MIQP the comfort objectives are still considered in the overall cost. Consequently, an uncomfortable braking and lane changing might be avoided in the first instance. The global optimal policy depends highly on the weighting matrix of the penalty for the constraint softening.

In summary, the driving behavior based on the CO approach is in the simulated traffic situation mostly equal to the "optimal driving behavior" of the MIQP approach and it corresponds to the driving behavior of a rational human driver. Furthermore, it demonstrates that the level-based objective function of the CO approach provides similar possibilities in terms of handling of infeasibility as the MIQP's constraint softening method.

Overtaking on the Right Side to Avoid Collision

One novel idea of the developed CO approach is the prioritization of the objectives thanks to the level-based formulation. As discussed in Section 4.4, three levels were introduced in this thesis: level-1 cost represents the comfort costs, level-2 cost represents the traffic rule "not overtake on the right side" and the level-3 cost considers the risk of colliding with surrounding traffic. This formulation guarantees that when the constraints for level-1 and level-2 are not met anymore, e.g. due to model disturbances, the policy with the

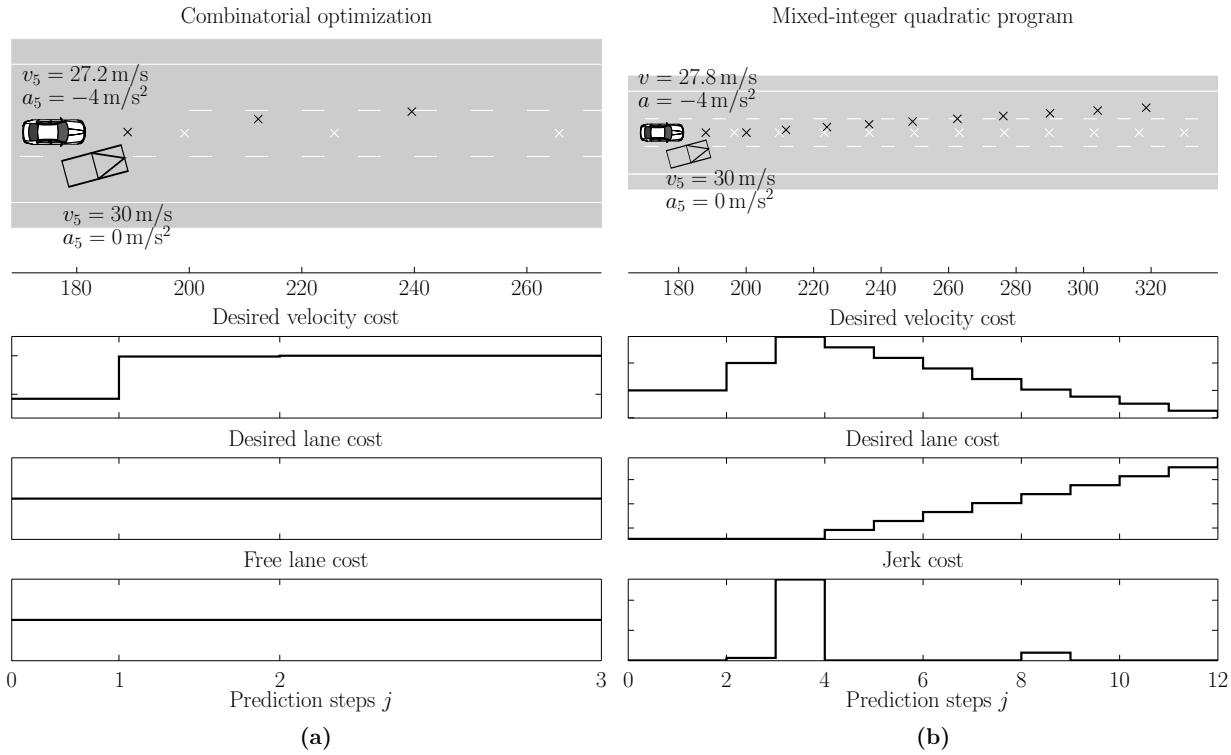

Fig. 4.15: Model predictive planning in the case of "critical cut-in maneuver" at time $t = 6.5\,\mathrm{s}$ with (a) CO and (b) MIQP.

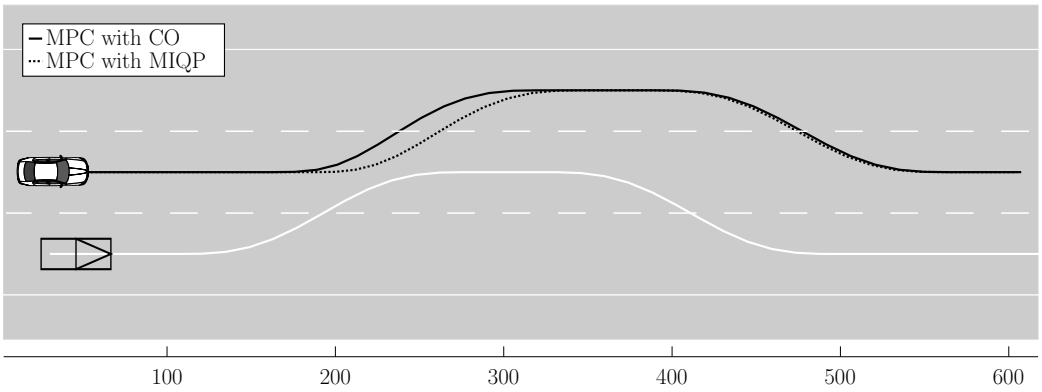

Fig. 4.16: Model predictive planning in the case of "critical cut-in maneuver". Comparison of different driven paths by the both provided approaches.

lowest level-3 cost, which is the one with the lowest collision risk, will be chosen. In contrast, the MIQP formulation provides the method of constraint softening to achieve a comparable behavior. The focus of the following evaluation is to proof the functionality of both methods in a further extreme traffic situation and to show that the resulting driving behavior is rational as well.

As shown in Figure 4.17, the host vehicle is now driving autonomously on its desired lane (here the leftmost lane). Due to "faulty sensor measurements", the much slower leading vehicle 3 is not recognized until the distance and velocity difference between both

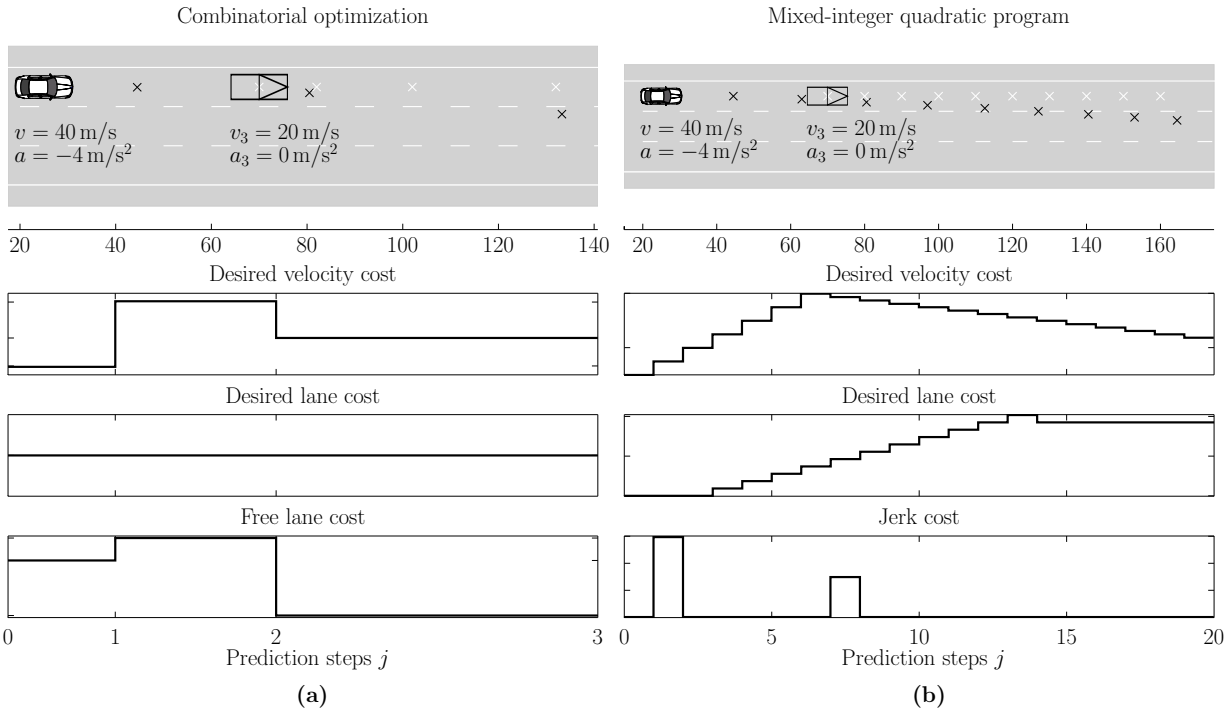

Fig. 4.17: Model predictive planning in the case of "overtaking on the right side to avoid collision" at time $t = 0\,\mathrm{s}$ with (a) CO and (b) MIQP.

vehicles makes a braking maneuver without lane change impossible. In this situation, a rational human driver would also brake and take over vehicle 3 on the right side rather than collide with it. Thus, both optimization approaches start now to brake, which can be seen in increasing of the desired velocity cost. At the same time both systems plan a lane change maneuver to the right adjacent lane, which is illustrated in the predicted positions and in the increasing of the desired lane cost. After the host vehicle has passed vehicle 3, it accelerates again to reach its desired velocity. This can be seen in the decreasing desired velocity cost in both approaches. After the vehicle 3 has been overtaken, the host vehicle changes back to the leftmost lane, which is in this simulation per definition its desired lane (see Figure 4.18). Finally, the host vehicle accelerates further to reach its desired velocity.

The similarity of both maneuver planning approaches is demonstrated even better in Figure 4.19, which shows the driven paths during the simulation. It is easy to see that the resulting policies of both systems are nearly identical in this simulated traffic situation.

Discussion

Besides the above prototype scenarios, an extensive quantitative comparison of both approaches proves that both approaches determines almost the same driving goals in most of the simulated traffic situations [201]. The implemented model predictive maneuver planning based on the MIQP shows however a slightly more comfortable driving behavior in general (i.e. less longitudinal jerk). However, the very high computation time (in average about 6 s for each replanning time instance on an Intel® Core i5-2540M@2.6 GHz. despite the efficient implementation of the solver in C) and the fact that the solution finding is

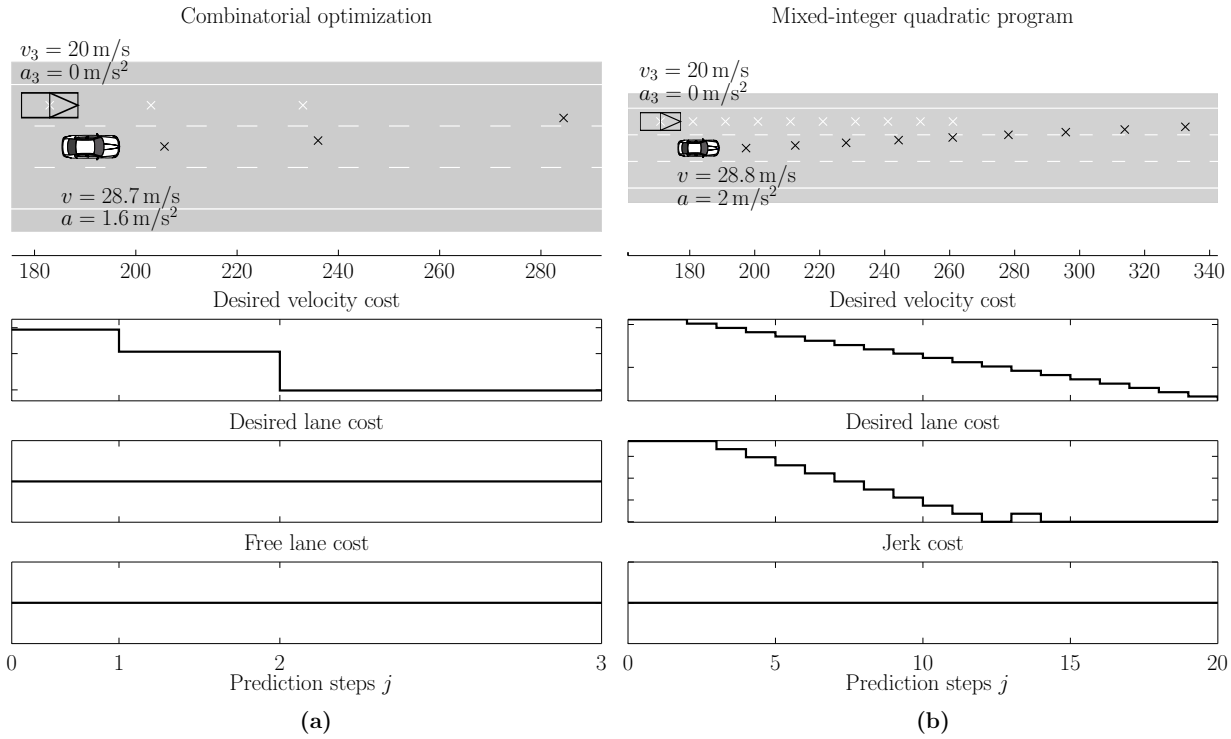

Fig. 4.18: Model predictive planning in the case of "overtaking on the right side to avoid collision" at time $t = 6\,\mathrm{s}$ with (a) CO and (b) MIQP.

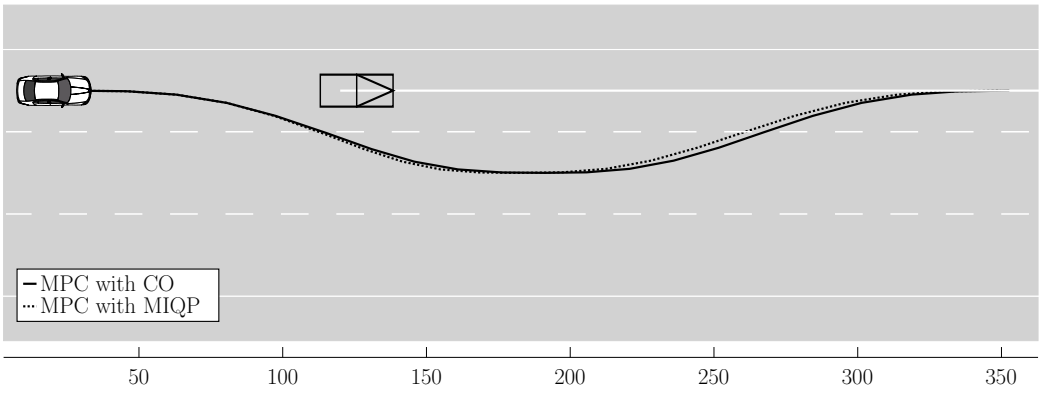

Fig. 4.19: Model predictive planning in the case of "overtaking on the right side to avoid collision". Comparison of different driven paths by the both provided approaches.

highly dependent on the chosen solver, make an on-line implementation in highway scenarios currently impossible. Furthermore, the approach of constrained optimal control of hybrid systems does not provide the necessary freedom in the problem formulation. Thus, the CO approach is chosen as the appropriate method which meets the requirements of on-line capability and robustness. The following evaluations focus thus more detailed on the CO approach.

Detailed Evaluation of the CO Approach

To further prove the functionality of the basic behavioral strategy based on the combinatorial optimization approach, two other highway scenes are chosen. Figure 4.20 and Figure 4.21 provides two plots of moments of the scenes. Each plot visualizes the vehicles their current state. The diagrams below display the single costs of the path with the global minimum cumulated cost along the predicted steps. The first three charts illustrate the single level-1 criteria (4.40), (4.41) and (4.42). The last chart shows the cumulated cost (4.44). The optimal policy (i.e. the best path in the search tree) is also shown. Additional to the states of the surrounding vehicles at time t the state of the host vehicle at time $t + \Delta t_{p_1}$ is visualized as a transparent car. Due to the time shift, the visualization of the positions of the other vehicles and the host vehicle prediction have to be regarded with caution. I.e. the transparent car and the vehicles are not colliding.

In Figure 4.20 the host vehicle has a desired velocity of 35 m/s. But vehicle 2 only driving at 31 m/s with a constant acceleration of $0\,\mathrm{m/s^2}$. At the same time vehicle 3 is nearly at the same longitudinal position on the adjacent lane of the host vehicle and is driving faster. A rational human driver would wait until the faster vehicle 3 passed and would then take over vehicle 2. In the first plot all policies which change the lane in the first prediction step have level-3 cost, because the host vehicle would collide with vehicle 3. Therefore, a policy is chosen which makes the host vehicle stay behind in the first prediction step and then begins the overtaking maneuver in the second prediction step after vehicle 3 has passed. This is reflected in the increasing ϕ_3 cost (host vehicle is not on the rightmost lane anymore) and the decreasing ϕ_2 cost (there is no slower car on the middle lane). A few seconds later (see lower plot in Figure 4.20) the ϕ_1 cost for driving the desired velocity decreases rapidly because the host vehicle can drive faster on the free lane.

The initial state of the situation shown in Figure 4.21 is that the host vehicle approaches two vehicles on the right lane with a desired velocity of 30 m/s. Suddenly vehicle 4 changes to the middle lane just in front of the host vehicle. If the host vehicle keeps its velocity and lane, it would collide with vehicle 4. The upper plot shows that the maneuver prediction already recognized the lane change intention (see vehicle 104 with dashed line) even before vehicle 4 has reached the middle lane. The basic behavioral strategy chooses a policy with safety cost at the third prediction step, because at this moment each policy has safety cost due to the inevitable small distance to vehicle 4. The chosen policy reduces the velocity of the host vehicle (see increasing ϕ_1 cost) and initiates a lane change. The lower plot shows that the optimal policy is now not risky anymore because vehicle 4 is already driving faster than the host vehicle.

The first scene demonstrates that the model predictive maneuver planning based on the combinatorial optimization chooses the most comfortable policy by consideration of the current situation (reactive). Moreover, the maneuver planning based on the level-1 cost is coherent by taking a look at the single objectives (transparent and deterministic). The second scene proves that the maneuver planning takes the future evolution of the environment into account (anticipating). Last it shows that in critical situations safe policies are favored over comfortable policies.

The current approach of exhaustive search is an NP-hard problem since the number

of nodes and thus the computing time is increasing exponentially with the number of prediction steps. Therefore, two further approaches of *graph search* and *greedy search* are applied [37] which do not guarantee to find the "global optimal" solution but reduces the computing time dramatically. The idea of the graph search is to combine similar states into the one based on their longitudinal and lateral positions after each prediction instance. The graph search performs much faster than the exhaustive search with increasing number of prediction steps. Another time-saving solution is the greedy search. Instead of expanding the whole tree, a greedy search is done along the best policy (i.e. the solution with the minimum cost) after each prediction time step. A comparison between these search methods for a model predictive maneuver planning with 3 prediction steps is given in Table 4.1. The values are averaged over 100 random traffic scenes with 60 second simulation time for each scene.

Method	Exhaustive	Graph	Greedy	Unit
# of collisions	0	0	0	–
# of lane changes	88	81	90	–
# of lane change aborts	0.02	0.02	0.02	–
∅ Longitudinal jerk	0.5013	0.747	0.84	s^3
∅ Cost value	0.141	0.203	0.366	–
∅ Computing time (MATLAB® MEX-function implementation)	0.15	0.06	0.005	s

Tab. 4.1: Comparison of the different search methods for the combinatorial optimization approach.

4.6 Conclusion and Discussion

In this chapter, a novel model predictive maneuver planning for the basic behavioral strategy was presented. The motivation was to develop a maneuver planning which determines the "global optimum" in terms of the above-mentioned definitions and which satisfies the requirements for reactivity and anticipatory. It allows comfortable and safe driving for all the traffic participants. Additionally, the traffic rules are also considered. The non-linear model was first approximated with a hybrid system formulation. To determine the optimal driving goals, two different approaches were developed: A mixed-integer quadratic program with an approximated linear objective function and a combinatorial optimization with partly non-linear objective functions.

The combinatorial formulation of the problem achieves the on-line requirement and the freedom in problem formulation to get the "optimal driving behavior", but holds the risk of getting stuck in a local optimum. Thanks to the separation in levels with different priorities, the approach allows a straightforward extension to additional costs. Solving the problem by the mixed-integer quadratic program provides in most cases the same or at least a similar driving behavior, but guarantees to find the global optimum. It could be used to ensure the functionality of the driving behavior and the solution exactness of the combinatorial optimization.

The results of the evaluation confirmed the motivation and the selected methods. The Analysis showed that both driving behaviors were similar. In other words, the "optimal driving behavior" of the mixed-integer quadratic program could be achieved via combinatorial formulation. Furthermore, the results have been shown that the computational performance of the MIQP is most certainly insufficient for an application in real highway application. Consequently, further works has to be done especially in order to reduce the required computing time. One idea here is to use the solution provided by the CO as the initial solution for the MIQP solver. This "warm start" enables a further acceleration of finding the optimal driving goals. Additional research must be also applied to determine the best value of penalty for constraint softening by MIQP formulation. For example, the authors in [85] introduced a method to calculate a feasible initial set and penalty weights, which guarantees the same solution of the soft-constrained and the hard-constrained cases if no constraint is violated.

In the next chapter, the cooperative behavioral strategy will be discussed in detail. In some specific situations, such as late merging or highway entry ramp merging, a higher level of cooperation between the cognitive vehicle and the relevant traffic participants is needed. The novel planning and prediction framework within this behavioral strategy is based on the methods of game theory which models the replanning capabilities of surrounding traffic. With that, the driving strategy is able to capture complex mutual interaction between vehicles, planning maneuver sequences over longer time horizons.

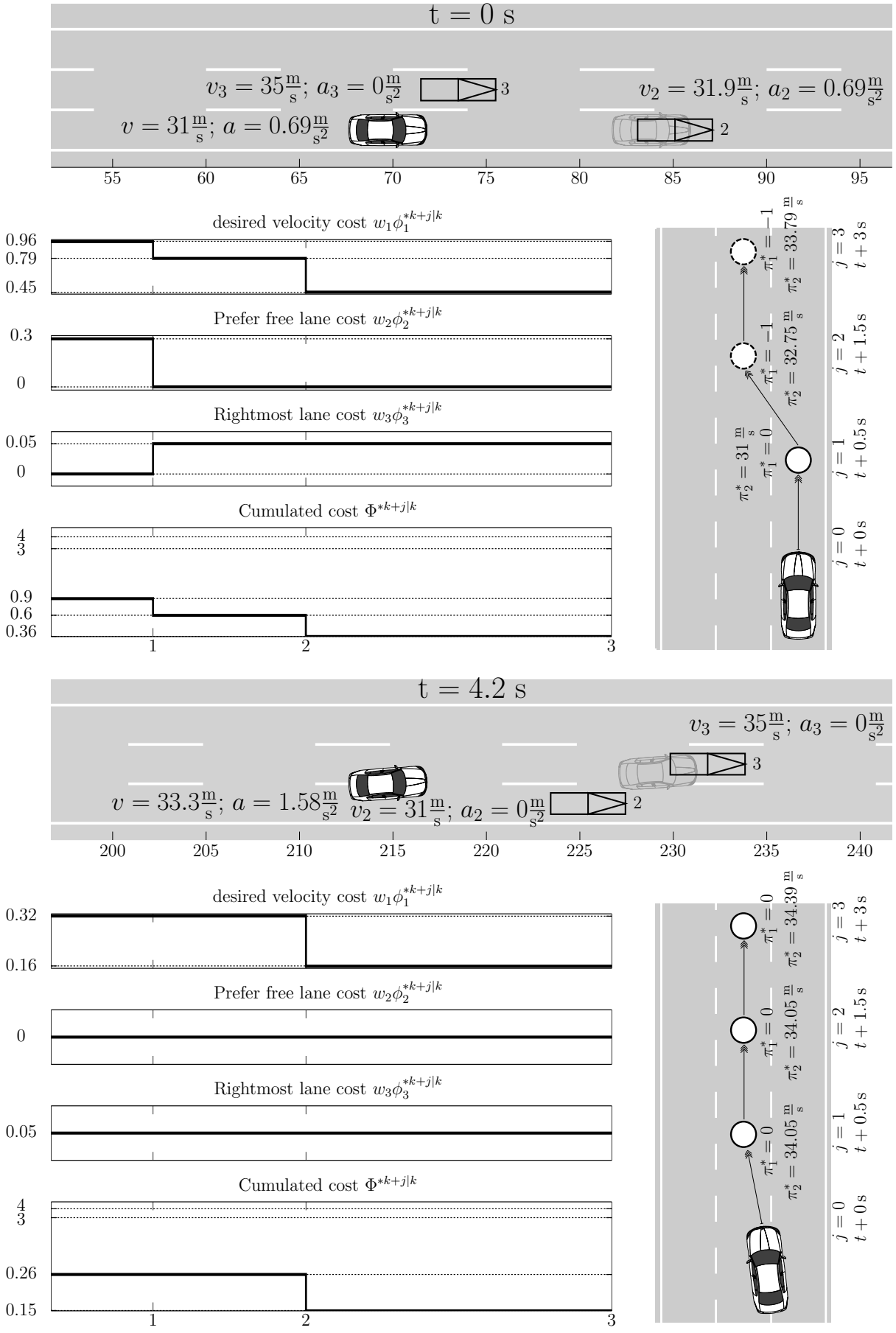

Fig. 4.20: Highway situation 1: The host vehicle overtakes vehicle 2 after faster vehicle 3 passed.

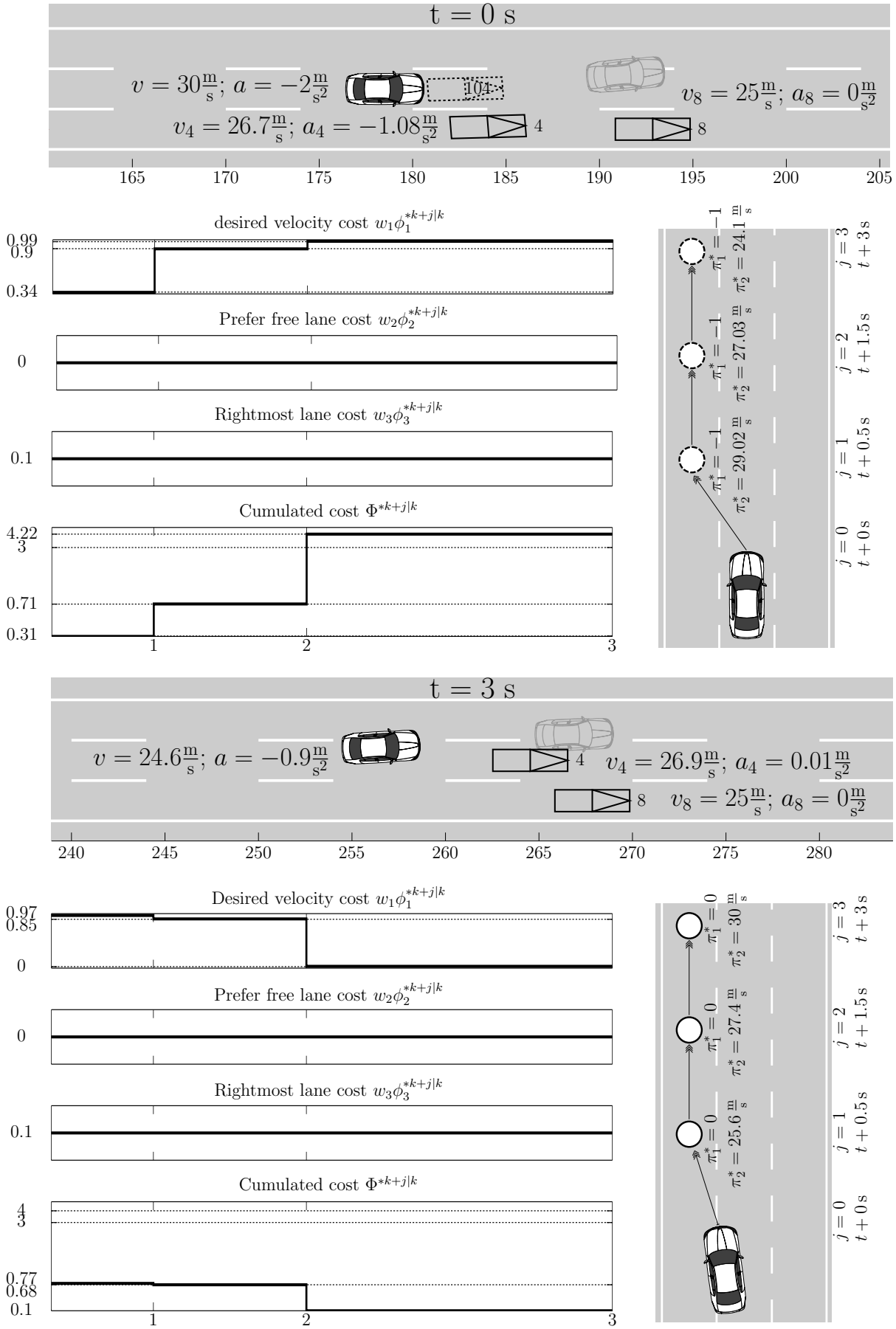

Fig. 4.21: Highway situation 2: vehicle 4 cuts in close in front of the host vehicle.

5 Cooperative Behavioral Strategy

This chapter presents a novel cooperative-driving prediction and planning framework for dynamic environments based on the methods of game theory[1]. The proposed algorithm can be used for highly automated driving or as a sophisticated prediction module for advanced driver assistance systems without the need of inter-vehicle communication. The main contribution here is a model-based, interaction-aware motion prediction of all vehicles in a scene. In contrast to other state-of-the-art approaches and the one presented in Chapter 3, the system also models the replanning capabilities of all drivers. With that, the cooperative behavioral strategy is able to capture complex interaction between vehicles, planning maneuver sequences over longer time horizons. It also enables an accurate prediction of the traffic for the next immediate time step. The initial motion prediction of other traffic participants is supported by the framework presented in Chapter 3. As part of the prediction loop, the proposed planning strategy incorporates the expected reactions of all traffic participants, offering cooperative and robust driving decisions. By means of experimental results in simulated highway scenarios, the validity of the proposed concept and its on-line capability is demonstrated.

5.1 Introduction and State of the Art

In the intuitive structure of independent prediction and planning phases discussed in the previous chapter, the planning of the future trajectory is performed on the predicted motion of other traffic. This does not take into account the mutual influence on each other's motion, decreasing the reliability of the safety assessment and, as a consequence, the safety and comfort of the system in certain traffic situations like as late merging or highway entry ramp merging. Driving decisions influence the motion plans of the surrounding vehicles and vice versa. Of course, this interaction takes place between all traffic participants in the scene. It implies that prediction of *scenes* has to be performed instead of prediction of each individual vehicle in the above-described traffic situations.

Put differently, there is always a feedback loop between own driving decisions and the evolution of the environment, however, in some situations this feedback should be explicitly taken into account. It is shown in [156] that performance is limited if prediction and planning are treated independently. It means that accurate prediction and planning algorithms have to be aware of this interaction or suffer from low accuracy over expected time horizons, hence, risking safety.

The explained consideration can be compared to chess, where each player plans his strategy for several moves into the future. He also assumes that his next move is noticed by the other player, who in turns adapts his strategy. Therefore, the problem formulation

[1] Parts of the results in this chapter have been pre-published in [193].

of the planing process within the cooperative behavioral strategy and its solution with *game theoretic* approaches is conclusive. Game theory can be defined as "the study of mathematical models of conflict and cooperation between intelligent rational decision-makers" [115]. It is mainly used in economics, political science, as well as logic and computer science.

The maneuver planning within the cooperative behavioral strategy explicitly respects this mutual influence. First, an overview of related publications is given, the mathematical backgrounds about the applied methods from game theory is introduced, the problem of prediction and planning under mutual influence is defined and a solution is proposed. In contrast to the basic behavioral strategy, this approach fully exploits the implications of the interaction loop, respecting an ongoing mutual influence of the driving decisions. The approach is evaluated in simulated scenarios, pointing out the benefits. Finally, a complexity analysis of the approach is given and the on-line capability is shown.

As pointed out before, motion prediction and prediction-based planning are key elements of today's robotics and autonomous driving research. It is therefore not surprising that various approaches have been suggested over the recent years. But, in many architectures navigation consists of separate modules for prediction and for planning, e.g. in [12, 48, 117, 119, 141, 175, 176, 196]. Although this strategy clearly reduces computational demand, specific situations (e.g. highway entrance or late merging at end of a lane), where a strong coupling of own driving decisions with others' behavior exist, leading to inaccuracies in prediction and inconsistent planning.

Different approaches have been developed which take this interactive coupling explicitly into account. In [158], the interactive human navigation is analyzed from a game theoretic perspective. The agents are assumed to make their decisions once and simultaneously. Hence, this approach does not model the replanning capability of the humans.

In [14], the authors investigated the collision free control strategy between two AGVs (Automated Guided Vehicles) for a simplified road junction without traffic lights. The approach is based on the idea of zero-sum games. However, the replanning capability was also not considered in this work.

In [176], the authors look into a highly cooperative scenario, merging of vehicles onto a highway. It combines a cost-based driving strategy with a prediction model. Unfortunately, this approach assumes a simplified road geometry with a fixed position of where a merging vehicle can enter the highway and relies on more parameters than the one presented in this work. Furthermore, the mutual influence between traffic participants is not taken into account.

The approach in [94] considers the interaction for vehicle prediction and risk assessment at road intersections. The authors clearly separate a driver's high-level intention and interaction-aware prediction. With the help of Dynamic Bayesian Networks, high complexity is handled. Inspired by this work, [93] suggests a maneuver-based approach for high-way scenarios. The idea in this work is to consider the interaction between the road users by finding an optimal predicted scene in terms of minimizing the risk for all the traffic participants. It lacks, however, a prediction over multiple time steps as given in this chapter.

While inter-vehicle communication unarguably does bring benefits to cooperative driv-

ing, since crucial information will be available as a priori knowledge [96–98], there is also "need for significant penetration before [inter-vehicle communication systems] can become effective" [143]. However, the disadvantages due to the high cost of the required infrastructure, the scalability problem of the networks and the related security issues make its industrialization very difficult [125]. Furthermore, a cooperative interaction with older generation vehicles, which are not able of inter-vehicle communication, must be made possible. Therefore, a prediction and planning framework is required which enables a reliable cooperative driving in certain situations (e.g. highway entrance) without a specific need of inter-vehicle communication.

Nevertheless, [93] builds up the foundations on which the presented approach is based on. Both approaches share the use of an interaction-unaware and interaction-aware maneuver prediction. The most important difference is that this approach regards maneuver sequences over multiple time steps instead of a single next maneuver. Furthermore, in contrast to the numerous applications of game theory in traffic micro-behavior simulation (i.e. traffic situations, in which only few road users are in the "game" in a very limited space) [185], the concept of sequential games is applied here to the approach of cooperative behavioral strategy in order to consider the *replanning* capabilities of other traffic participants in the planning of the cognitive vehicle.

In this thesis, the problem of interactive scene prediction and planning is discussed and the novel approach is presented for merging onto a highway as an illustrative example, where a strong mutual interaction between vehicles occurs. The algorithm, however, can be applied to other scenarios as well.

5.2 Mathematical Backgrounds

This section outlines methods from literature relevant to the presented approach. As mentioned above, the derivation of the maneuver planning within the cooperative behavioral strategy is based on the game theory [122] methodology of *sequential games*, visualized in *extensive-form*. Mathematical game theory models entities that interact with each other. The entities are called *agents* or simply *players*. Games in which the goals of agents are in conflict are described as *adversarial search problems*. [134] introduces sequential games which describe games that consists of a sequence of turns. These games are represented graphically in extensive-form. Extensive-form, first defined generally in [89], presents a model of sequential games, that explicitly considers what information is available to an agent when selecting an action. Sequential games in extensive-form, called extensive-form games from here on, and relevant characteristics will be discussed in the following with examples.

Basic Extensive-form Game

The game considered in the following examples is a simple two player game. One player has an item in his left or right hand. The other player chooses one hand and wins if the item is in the chosen hand or looses otherwise. Win or loss of one player lead to the opposite event for the other player. This game can be defined as an extensive-form game

by the tuple $\Gamma_1 = (K, P, A(P), U)$, where

- K is the game tree with a initial state x^2 as the root state,
- $P = \{P_1, P_2\}$ are the players,
- $A\,(P) = \{l, r\}$ are the actions of the players,
- $U = \{1, -1\} \mathrel{\widehat{=}} \{\text{'win','loss'}\}$, is the payoff function.

Figure 5.1 shows the game tree in its extensive-form. The states show the index of the player whose turn it is, while the transitions between states are labeled with a chosen action. The payoff function is given next to the terminal state. The first entry corresponds to the payoff for player P_1 while the second entry corresponds to the payoff for P_2. Player P_2 has the first turn at the root state. The actions l and r correspond to hiding an item in the left or right hand. Afterwards the player P_1 chooses one hand and receives a payoff of 1 for the correct hand or a payoff of -1 for the other hand. The payoff for P_2 is the opposite.

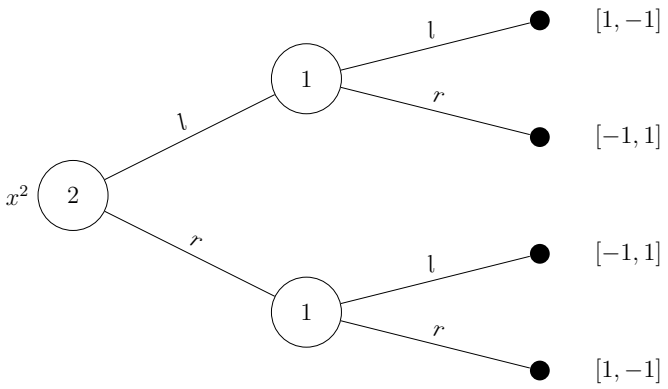

Fig. 5.1: Game tree of the extensive-form game defined by Γ_1.

The obvious strategy for P_1, to maximize the payoff, is to chose the same action as P_2. The player P_2 is at a clear disadvantage because the other player can observe his action. However, sequential games also offer the option to model a player not being able to observe a previous choice (graphically speaking) of another player.

Extensive-form Game with Information Sets

Information sets can be used to model limited information in extensive-form games. Information sets are defined as a set of states, where

- All states belong to one player,
- The player only knows that the information set has been reached, but not which state of the set.

This can be used to model simultaneous or hidden turns. A game with information sets consisting of more than one state is called a game with *imperfect information*. Opposed to a game with *perfect information*, a player does not always know in what state he currently is. Information sets can be used to model a slight variation of the previously presented game.

Information sets are used here to make the example game a little more realistic. Let's assume player P_2 is hiding an item in one of his hands without player P_1 observing which one. The example game can now be defined as an extensive-form game by the tuple $\Gamma_2 = (K, P, A(P), I, U)$, where

- K is the game tree with a initial state x^2 as the root state,
- $P = \{P_1, P_2\}$ are the players,
- $A(P) = \{l, r\}$ are the actions of the players,
- $I = I_1$ is a information set of player P_1,
- $U = \{1, -1\} \mathrel{\widehat{=}} \{\text{'win','loss'}\}$, is the payoff function.

Figure 5.2 shows the game tree in extensive-form, with a dashed box for the information set I_1. The game tree is otherwise equivalent to the previous game tree. Here, player P_1 is unable to observe the choice of P_2. P_1 can only determine that the information set I_1 has been reached.

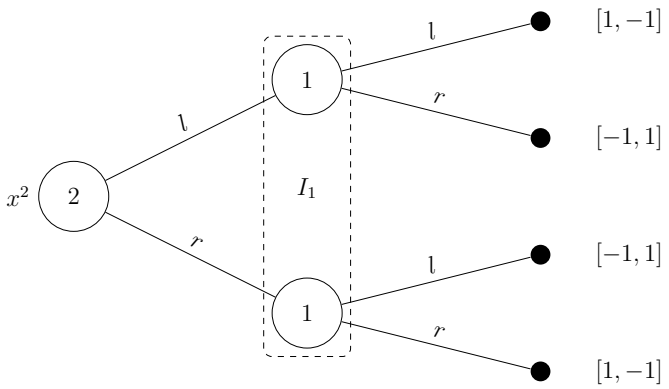

Fig. 5.2: Game tree of the extensive-form game defined by Γ_2 with a information set.

There is no obvious strategy for both players in this scenario. Player P_1 can not reason out a strategy for player P_2, because just as in the previous scenario there is no obvious strategy for player P_2. Neither is there an obvious strategy for maximizing the payoff of player P_1, as he can not determine the resulting terminal state reached by an action in the information set I_1. Extensive-form games offer a concept to model players with *indeterminable strategy*.

Extensive-form Game with Player Nature

The previous example showed that an obvious strategy for player 2 does not exists. The intended difficulty in determining a strategy for player 2 is important for this final example. In the example actions and payoff function were intentionally chosen so that a preference for an action of player 2 could not be determined. As the payoff function is not sufficient to determine a preference for an action, this situation is equal to player 1 not even knowing the payoff function of player 2. A game where the payoff function of one player is unknown to another player is a game of *incomplete information*. A game of incomplete information can be converted to a game of imperfect information by introducing a *player nature* [66]. A player nature can be used in an extensive-form game to model a player without payoffs and thus without a determinable strategy. The player nature makes probabilistic choices based on a distribution ρ.

The example game is still defined by a player hiding an item in one of his hands, unobserved by another player. However, now the player choosing the hand in which he suspects the item makes an educated guess. Having played this game countless times, he discovered a tendency for the left hand. Formally this would be modeled, by two types of players replacing the former player 2. One type of player would always choose the left hand and the other type would always choose the right hand. In the first turn of the game, a player nature would then choose the player, always choosing the left hand, with the probability representing the preference for the left hand. Likewise, a player nature would choose the player choosing the right hand with the complementary probability. This model is simplified in this chapter to replacing previous player 2 by a player nature with a probability distribution, expressing the probabilities of actions.

The extensive-form is now defined by a tuple $\Gamma_3 = (K, P, A(P), I, \rho, U)$, where

- K is the game tree with a initial state x^0 as the root state,
- $P = \{P_0, P_1\}$ are the players, with P_0 being the player nature,
- $A(P) = \{l, r\}$ are the actions of the players,
- $I = I_1$ is a information set of player P_1,
- $\rho(A(P_0))$ is the probability distribution over the actions of player nature, with $\rho(A(P_0) = l) = 0.6$ and $\rho(A(P_0) = r) = 0.4$,
- $U = \{1, -1\} \mathrel{\widehat{=}} \{$'win','loss'$\}$, is the payoff function.

Figure 5.3 shows the game tree in extensive-form, with the newly introduced player nature. The probabilistic choices of the player nature are depicted together with its actions. Player P_1 can now base his strategy on the predicted choice of player P_0. P_1 holds a *belief* of the information set I_1 has been reached, according to the distribution ρ. The *expected payoff* can be based on these beliefs. Based on the probability distribution ρ the best choice for player P_1 would be the more likely action of P_0, action 'l'.

Extensive-form games offer solutions, called equilibrium, based on assessing the optimal strategy of multiple players. These solutions were not presented, as they are not relevant

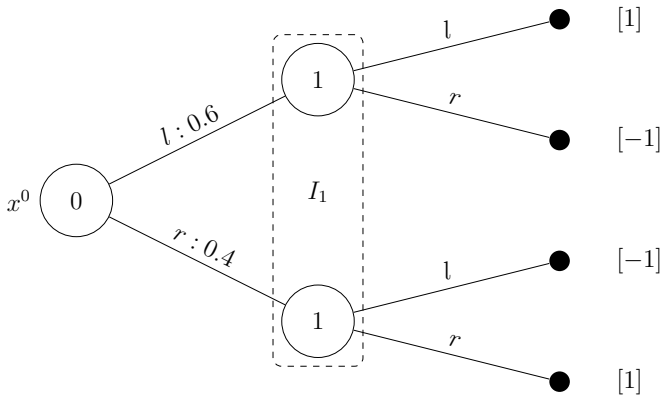

Fig. 5.3: Game tree of the extensive-form game defined by Γ_3 with player nature.

to the thesis. The concepts of information sets and the player nature are essential to the derivation of the maneuver planning within the cooperative behavioral strategy. Most importantly, the last example shows how probabilistic knowledge about another player can be used to find a strategy, when the best strategy of the player is unknown. The maneuver planning approach will be derived similar to the last example, based on beliefs, information sets and the expected payoffs.

5.3 Problem Formulation

Given a scene with multiple traffic participants, the task of prediction is to make statements about their future motion based on all observable states. The probabilistic nature of the prediction arises from non-observable states, e.g. the driver intention. The task of safe motion planning is to find a trajectory to act according to some cost function while avoiding collisions. Note, that prediction and planning must incorporate all affected traffic participants and cannot be done independently in certain traffic situations. This mutual influence of each other's decisions at each point in time has to be modelled in order to predict the scene as accurately as possible.

The approach in this chapter offers a prediction and planning algorithm which explicitly models the continuous mutual dependence of all traffic participants over multiple time steps. The following assumption describes the idea of this approach:

Assumption 5.1 *The motion planning of each traffic participant corresponds to its own most likely predicted maneuver in the prediction of the scene, taking into account the mutual dependencies. In other words, planning and prediction are equivalent problems.*

As the cognitive (host) vehicle is a part of the scene, the above assumption can be applied to it as well. Therefore, the most likely maneuver of the host vehicle will be at the same time its planned maneuver. The subsequent distinction between planning and prediction serves a better overview of the approach. In the following, the approach is referred to as *interactive maneuver planning*.

The task of the interactive maneuver planning is to find a *maneuver sequence* (resp. driving goals) π^{*T}_{Host} of the host vehicle up to the *planning horizon* T, which represents the

best trade-off between intention of the host vehicle and risk assessment with respect to the replanning ability of the other traffic. At the same time, this maneuver sequence is the most likely from the point of view of the surrounding traffic.

In contrast to the numerous applications of game theory in traffic micro-behavior simulation (i.e. traffic situations, in which only few road users are in the "game" in a very limited space) [185], the concept of sequential games is applied in this thesis to the approach of interactive driving strategy in order to model the *replanning* capabilities of each agent.

5.4 Approach

Figure 5.4 visualizes the idea of the approach. The goal is to plan a maneuver sequence over multiple discrete time steps for automated driving on highways that will be passed to the operational unit for execution. The planned maneuver sequence is interaction-aware, i.e. it depends on the prediction of other traffic participants (I). The prediction itself is interactive, as it depends on the prediction of the host vehicle by others (III). This interactive prediction implies interaction awareness, meaning the mutual dependence between traffic participants is considered.

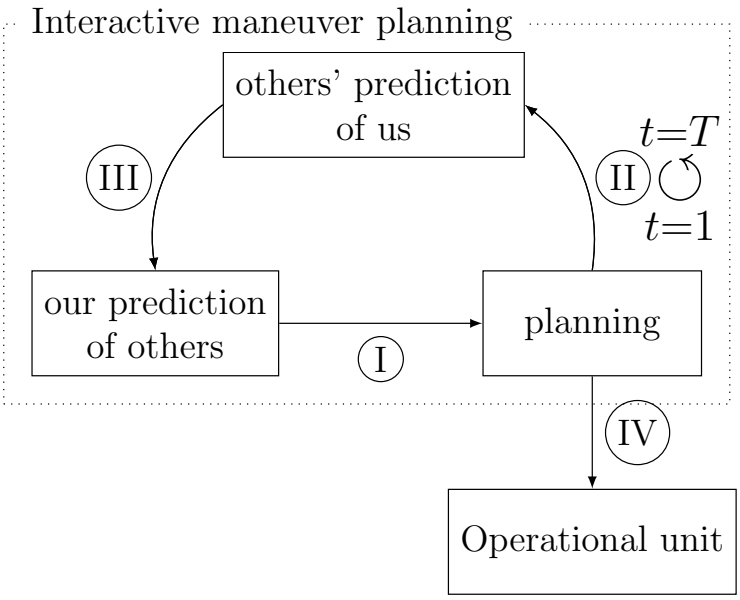

Fig. 5.4: Closed feedback loop of the interactive maneuver planning.

The essential contribution of the approach is that the cycle of prediction and planning is continued with respect to maneuver options previously determined by the planning module of the host vehicle (II). The main idea is that other traffic participants will observe the previous maneuver of the host vehicle and have the option of replanning themselves. The prediction and planning loop can thus be continued over multiple time steps up to the planning horizon T before passing the maneuver sequence with the highest interaction-aware probability (i.e. most likely maneuver sequence) as the driving goals to the operational unit (IV).

This maneuver sequence is the best trade-off between intention and collision avoidance in compliance with mutual interaction to other traffic participants. From a control perspective, prediction of multiple, partially cooperating vehicles is part of a closed feedback loop of acting, sensing and prediction of all traffic participants. As a consequence, prediction of other vehicles over reasonable time horizons has to incorporate own driving decisions as well. Thus, the maneuver planning based on this approach shows inherently a cooperative behavior towards the surrounding traffic.

In the following, the definitions and notations used in this chapter is first presented. Subsequently, the approach of the interactive maneuver planning is discussed in detail.

Definitions and Notations

According to the definitions from the Chapter 3, drivers are modeled in the following to a good approximation using a finite set of basic maneuvers $\mathcal{M}$. Thus, each j-th maneuver of the v-th vehicle at time step t belongs to a different set as, $m^t_{j,v} \in \mathcal{M}^t_v$.[2]

Basic maneuver sets are sufficient for planning over only a single time step, however, planning over multiple time steps requires the definition of maneuver sequences. The set of maneuver sequences of the v-th vehicle over several time steps is defined as the Cartesian product of its basic maneuver sets for all time steps up to t as

$$\Pi^t_v := \prod_{i=1}^{t} \mathcal{M}^i_v. \tag{5.1}$$

A maneuver sequence is defined as a t-tuple of maneuvers

$$\pi^t_v \in \Pi^t_v := \left(m^1_{j,v}, m^2_{k,v}, \ldots, m^t_{n,v}\right), \tag{5.2}$$

where each maneuver is of a different time step.

The focus on interaction requires a relation of maneuver sequences of multiple vehicles. The result of all vehicles performing a maneuver sequence is defined as a *scene*. The output scenes of the prediction module (see (I) in Figure 5.4) represent the prediction of surrounding traffic by the host vehicle. The *set of prediction scenes* $\mathcal{P}^t_{\text{Host}}$ is thus defined as the Cartesian product over entire sets of maneuver sequences, except the set of maneuver sequences of the host vehicle, as

$$\mathcal{P}^t_{\text{Host}} := \prod_{\substack{v \\ v \neq \text{Host}}} \Pi^t_v. \tag{5.3}$$

A prediction scene $p^t \in \mathcal{P}^t_{\text{Host}}$ represents therefore the expected reaction of traffic to the preceding planned maneuver sequence of the host vehicle. In Figure 5.5 the set of prediction scenes from perspective of the host vehicle is exemplarily illustrated.

The prediction scenes from perspective of other traffic participants (see (III) in Figure 5.4) differ from those of the host vehicle. It is based on a previously planned maneuver

[2] To simplify the notation, it is ignored that the set of basic maneuvers of each vehicle is dependent on its current state. However, this fact is taken into account in the implementation.

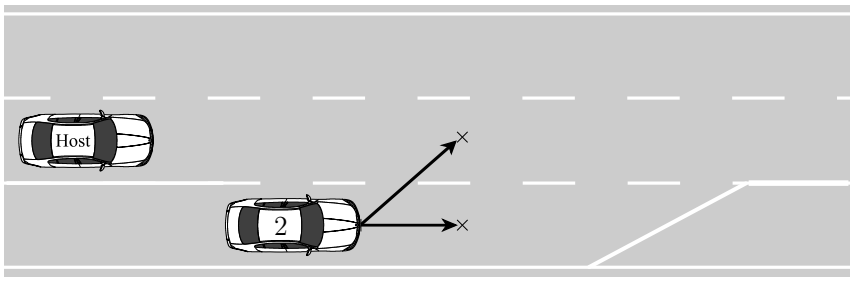

Fig. 5.5: The set of prediction scenes $\mathcal{P}^1_{\text{Host}}$ is described here by the predicted basic maneuvers of the vehicle 2.

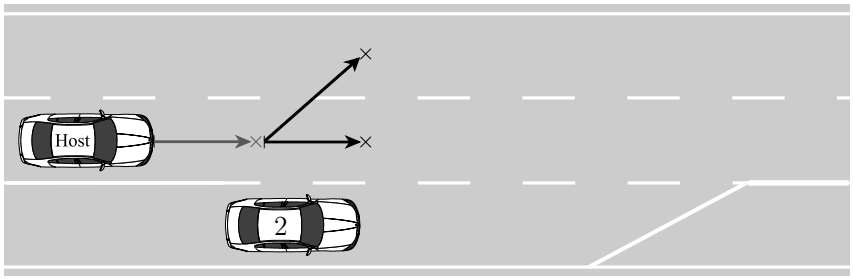

Fig. 5.6: The set of host-dependent prediction scenes $\mathcal{P}^2_{2,\pi^1_{\text{Host}}}$. The set of scenes is described by the maneuver options following the previous maneuver sequence of the cognitive vehicle (e.g. here lane keeping maneuver).

sequence of the host vehicle. This means that at time step t other traffic participants are assumed to have observed the planned maneuver sequence of the cognitive vehicle up to this point. It leads to the definition of the *set of host-dependent prediction scenes* $\mathcal{P}^t_{x,\pi_{\text{Host}}}$ of the traffic participant x. The set of scenes following a specific maneuver sequence π^{t-1}_{Host} of the host vehicle is defined as

$$\mathcal{P}^t_{x,\pi_{\text{Host}}} := \pi^{t-1}_{\text{Host}} \times \mathcal{M}^t_{\text{Host}} \times \prod_{\substack{v \\ v \neq \text{Host},x}} \Pi^t_v, \tag{5.4}$$

where $\pi^{t-1}_{\text{Host}} \times \mathcal{M}^t_{\text{Host}}$ expresses all maneuver options after a specific maneuver sequence π^{t-1}_{Host}. The Cartesian product, excluding the host vehicle as well as the traffic participant x, represents the possible maneuver sequences of all other traffic participants. An exemplary set of host-dependent prediction scenes at the second time step $\mathcal{P}^2_{2,\pi^1_{\text{Host}}}$ is visualized in Figure 5.6. Each maneuver option, following the planned single maneuver sequence of lane keeping π^1_{Host} by the host vehicle, expresses a host-dependent prediction scene by the vehicle 2.

Finally, the *set of planning scenes* $\mathcal{S}^t_{\pi_{\text{Host}}}$ is defined as

$$\mathcal{S}^t_{\pi_{\text{Host}}} := \Pi^t_{\text{Host}} \times \mathcal{P}^t_{\text{Host}}. \tag{5.5}$$

Here, any planning scene $s^t \in \mathcal{S}^t_{\pi_{\text{Host}}}$ expresses a set of one planned maneuver sequence with the predicted maneuver sequences of surrounding traffic. The single initial scene s^0 is the set of observed maneuvers of all other vehicles at the starting point of the planning

process.

As described before, the approach of interactive driving strategy will be reformulated in the following section as a problem which is solved by the tools of game theory, especially the extensive-form game formulation.

Interactive Maneuver Planning

The planning (resp. predicting) of the most likely maneuver sequence of the host vehicle π^{*T}_{Host} will be discussed in detail in this section. As mentioned above in Section 5.3, the approach is separated into the two modules of interactive planning and prediction. This serves only the purpose of clarity.

Replanning-aware Interactive Planning as Extensive-form Game

Applied to the presented planning problem, the host vehicle uses a prediction model to estimate the likelihood of future scenes (see Chapter 3). The information sets can be used to model the uncertainties of the scene prediction, without settling for a certain prediction. Moreover an extensive-form game allows representation of incomplete information in the form of probabilistic actions encoded as moves by nature. This feature will be used to model the other traffic participants.

The extensive-form game, which models the interactive maneuver planning of the host vehicle in this chapter, is defined by the quintuple $\Gamma = (K, P, I, \rho, U)$, where

- K is the game tree with the initial observed scene s^0 as the root node,
- P are the players:
  - P_0 is the player nature representing other traffic,
  - P_1 represents the host vehicle,
- I are the information sets, consisting of:
  - $\mathcal{P}^t_{\text{Host}}$, set of prediction scenes from (5.3),
  - $\mathcal{S}^t_{\pi_{\text{Host}}}$, set of planning scenes from (5.5),
- $\rho = P\left(p^t \in \mathcal{P}^t_{\text{Host}} | \mathcal{S}^{t-1}_{\pi_{\text{Host}}}\right)$ is the set of scene probabilities from the traffic and
- U^t is the set of payoffs belonging to each maneuver sequence of the host vehicle.

Figure 5.7 exemplarily shows a simple game tree cut after a single time step with two basic maneuver choices for the host and two possible evolutions of a second vehicle. The nodes are labeled with the player whose turn it currently is, while the transitions are labeled with the chosen action. The maneuvers of other traffic, i.e. the probability distribution over possible future scenes ρ, are supplied by the prediction module which will be discussed below. This limited knowledge about the current state is represented by the information set (dashed box around the two nodes of the host vehicle). Loosely speaking, this is the prediction of traffic from the perspective of the host vehicle $\mathcal{P}^1_{\text{Host}}$. Depending on the planned maneuver $m^1_{j,\text{Host}}$, the host vehicle arrives in the planning scene S^1_j. Consequently, the sets of planning

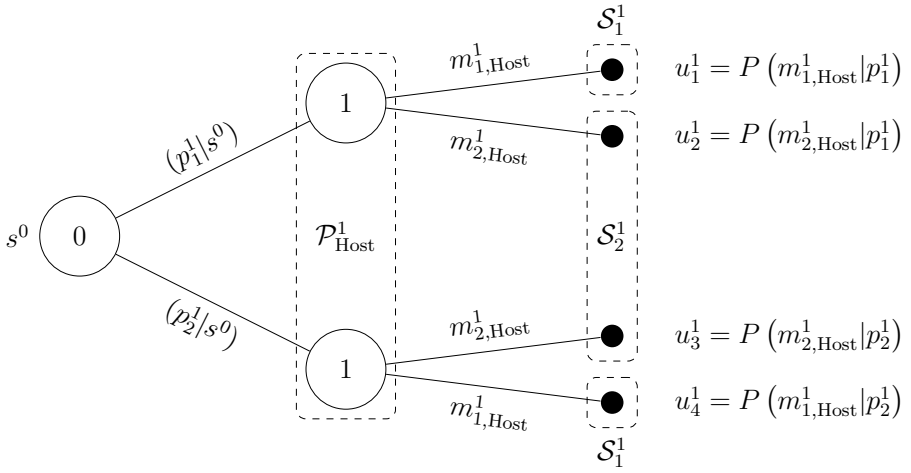

Fig. 5.7: Simple single time step extensive-form game tree.

scenes are also expressed as information sets for predicting the surrounding traffic in the next time step. The payoff $u^t \in U^t$ is expressed by the probability of the specified maneuver sequence, which represents a compromise between intention and risk assessment. The other traffic does not require a payoff function, since the exact strategy of other vehicles can not be determined (i.e. incomplete information).

The maneuver sequence with the maximum payoff is the most likely and, according to Assumption 5.1, is the expected decision of the host vehicle. Thus, the performance of the interactive maneuver planning is determined by the payoff function which will be derived in the following.

The payoff function for the single time step tree from Figure 5.7 is given as

$$u^1 = P\left(m_{j,\text{Host}}^1 | \mathcal{P}_{\text{Host}}^1\right) = P_{\nleftrightarrow}\left(m_{j,\text{Host}}^1\right) P_{\leftrightarrow}\left(m_{j,\text{Host}}^1 | \mathcal{P}_{\text{Host}}^1\right), \tag{5.6}$$

where $P_{\nleftrightarrow}\left(m_{j,\text{Host}}^1\right)$ is the interaction-unaware a priori probability which is independent from other traffic. It models the intention of the host vehicle. $P_{\leftrightarrow}\left(m_{j,\text{Host}}^1 | \mathcal{P}_{\text{Host}}^1\right)$ is the interaction-aware maneuver probability. It models the probability of performing a maneuver despite the collision risk associated with the set of predicted scenes $\mathcal{P}_{\text{Host}}^1$. While the prediction module estimates the probability for each scene $p^1 \in \mathcal{P}_{\text{Host}}^1$, the planning process can not assume that a certain scene will occur. In order to model this, the interaction-aware probability is conditioned on the full information set instead of only one predicted scene. The interaction-aware maneuver probability conditioned on the full prediction set is given as

$$\begin{aligned} P_{\leftrightarrow}\left(m_{j,\text{Host}}^1 | \mathcal{P}_{\text{Host}}^1\right) &= \sum_{p^1 \in \mathcal{P}_{\text{Host}}^1} P_{\leftrightarrow}\left(m_{j,\text{Host}}^1 | p^1\right) P\left(p^1 | s^0\right) \\ &= \sum_{p^1 \in \mathcal{P}_{\text{Host}}^1} \left(1 - R\left(m_{j,\text{Host}}^1, p^1\right)\right) P\left(p^1 | s^0\right). \end{aligned} \tag{5.7}$$

The term $R\left(m_{j,\text{Host}}^1, p^1\right) \in [0,1]$ represents the conditional collision risk of the maneuver $m_{j,\text{Host}}^1$ and each predicted scene p^1. This can be modeled by different approaches, e.g.

the ones presented in [62] or [92]. As per definition $\sum_{p^t \in \mathcal{P}^t_{\text{Host}}} P\left(p^t | \mathcal{S}^{t-1}_{\pi_{\text{Host}}}\right) = 1$, the last equation simplifies to

$$P_{\leftrightarrow}\left(m^1_{j,\text{Host}} | \mathcal{P}^1_{\text{Host}}\right) = \sum_{p^1 \in \mathcal{P}^1_{\text{Host}}} 1 - R\left(m^1_{j,\text{Host}}, p^1\right) P\left(p^1 | s^0\right). \tag{5.8}$$

$P\left(p^1 | s^0\right)$ is the probability of each predicted scene $p^1 \in \mathcal{P}^1_{\text{Host}}$ conditioned on the last set of planning scenes (i.e. in the single time step case, it is conditioned on the initial observed scene s^0). It follows from (5.8) that the payoff at the time step t is conditioned on the planning scenes from the previous time step $t-1$. Thus, (5.6) can be reformulated as

$$u^1 = P\left(m^1_{j,\text{Host}} | s^0\right) = P_{\nleftrightarrow}\left(m^1_{j,\text{Host}}\right) P_{\leftrightarrow}\left(m^1_{j,\text{Host}} | s^0\right). \tag{5.9}$$

The final step for evaluating maneuver sequences is to make the connection between consecutive maneuvers, extending the extensive-form from single to multiple time steps. Conditioning a basic maneuver $m^t_{j,\text{Host}}$ on a previous maneuver sequence π^{t-1}_{Host} is analog to taking account of all possible outcomes of the last maneuver sequence of the host vehicle when looking at the next basic maneuver. The scenes resulting from a host maneuver sequence π^{t-1}_{Host} have already been defined as the planning scenes $\mathcal{S}^{t-1}_{\pi_{\text{Host}}}$ (5.5). According to (5.9), the payoff of each consecutive basic maneuver is calculated as

$$u^t = P\left(m^t_{j,\text{Host}} | \mathcal{S}^{t-1}_{\pi_{\text{Host}}}\right) = P_{\nleftrightarrow}\left(m^t_{j,\text{Host}}\right) P_{\leftrightarrow}\left(m^t_{j,\text{Host}} | \mathcal{S}^{t-1}_{\pi_{\text{Host}}}\right). \tag{5.10}$$

For example, the payoff for a maneuver sequence of the host vehicle at the second time step is recursively calculated as

$$u^2_{j \to k} = P\big(m^2_{k,\text{Host}} | \mathcal{S}^1_j\big) P\left(m^1_{j,\text{Host}} | s^0\right), \tag{5.11}$$

where $\mathcal{S}^1_j$ is the set of planning scenes resulting from the basic maneuver $m^1_{j,\text{Host}}$ at the first time step. The interaction-aware maneuver probability based on the previous maneuver sequence is defined, similar to (5.8) in the general form, as

$$P_{\leftrightarrow}\left(m^t_{j,\text{Host}} | \mathcal{S}^{t-1}_{\pi_{\text{Host}}}\right) = \sum_{p^t \in \mathcal{P}^t_{\text{Host}}} 1 - R\left(m^t_{j,\text{Host}}, p^t\right) P\left(p^t | \mathcal{S}^{t-1}_{\pi_{\text{Host}}}\right). \tag{5.12}$$

Finally, the payoff for a maneuver sequence over t time steps is generally formulated as[3]

$$\begin{aligned} P\left(m^t_{j,\text{Host}} | \mathcal{S}^{t-1}_{\pi_{\text{Host}}}\right) &= P_{\nleftrightarrow}\left(m^t_{j,\text{Host}}\right) \cdot \\ &\qquad \sum_{p^t \in \mathcal{P}^t_{\text{Host}}} 1 - R\left(m^t_{j,\text{Host}}, p^t\right) P\left(p^t | \mathcal{S}^{t-1}_{\pi_{\text{Host}}}\right) \\ &= P\left(\mathcal{S}^t_{\pi_{\text{Host}}} | \mathcal{S}^{t-1}_{\pi_{\text{Host}}}\right). \end{aligned} \tag{5.13}$$

[3]The formulation $P\left(\mathcal{S}^t_{\pi_{\text{Host}}} | \mathcal{S}^{t-1}_{\pi_{\text{Host}}}\right)$ clearly shows the dependence of one set of planning scenes on the previous set. The set of planning scenes $\mathcal{S}^t_{\pi_{\text{Host}}}$ at the time step t is a state while the maneuver probability from (5.13) is used for the transition probability. Note that this satisfies the Markov property as the transition to each state only depends on the previous one.

Recalling the problem formulation from Sec. 5.3, the most likely maneuver sequence of the host vehicle expresses the best trade-off between intention and interaction with traffic and is given by

$$\pi_{\text{Host}}^{*T} = \underset{\mathcal{M}_{\text{Host}}^{t}}{\arg\max} \prod_{t=1}^{T} P\left(m_{j,\text{Host}}^{t} | \mathcal{S}_{\pi_{\text{Host}}}^{t-1}\right). \tag{5.14}$$

In order to reason about maneuver decisions, the planning module requires the likelihood of all possible host-dependent future evolutions of traffic $\rho = P\left(p^t | \mathcal{S}_{\pi_{\text{Host}}}^{t-1}\right)$. This incorporates the replanning ability of traffic participants which can react to the maneuvers of the host vehicle over one time step. The following prediction framework provides this required set of probability distributions. It is based on the proposed prediction framework discussed in Chapter 3.

Interactive Scene Prediction

The task of the interactive scene prediction module is to calculate the likelihood of all scenes $p^t \in \mathcal{P}_{\text{Host}}^{t}$, given the previously planed maneuver sequence of the host vehicle, as

$$P\left(p^t | \pi_{\text{Host}}^{t-1}\right) = P\left(p^t | \mathcal{S}_{\pi_{\text{Host}}}^{t-1}\right) = \prod_{\substack{\pi_v^t \in p^t \\ v \neq \text{Host}}} P\left(\pi_v^t | \pi_{\text{Host}}^{t-1}\right). \tag{5.15}$$

The maneuver sequences of different vehicles at each single time step are regarded as independent from each other, as during the planning process traffic participants are not aware of a certain maneuver sequence of others. Regarding the prediction and planning loop in Figure 5.4, each cycle considers one time step. The prediction in previous cycles has already been calculated and thus, out of a maneuver sequence, only the latest basic maneuver probability needs to be calculated. Equation (5.15) can be rewritten with respect to this recursion as

$$P\left(p^t | \pi_{\text{Host}}^{t-1}\right) = \prod_{\substack{\pi_v^t \in p^t \\ v \neq \text{Host}}} P\left(m_{j,v}^{t} | \pi_{\text{Host}}^{t-1}\right) P\left(\pi_v^{t-1} | \pi_{\text{Host}}^{t-2}\right), \tag{5.16}$$

where the probability $P\left(\pi_v^{t-1} | \pi_{\text{Host}}^{t-2}\right)$ has been calculated in the previous iteration or it is equal to one for $t = 1$.

The basic maneuver probabilities of other traffic participants combine the interaction-unaware as well as the interaction-aware probabilities, similar to the interactive planning module of the host vehicle. Equivalent to (5.10), the host-dependent probability of a maneuver $m_{j,v}^{t}$ of the v-th vehicle ($v \neq \text{Host}$) is calculated as

$$P\left(m_{j,v}^{t} | \pi_{\text{Host}}^{t-1}\right) = P_{\nleftrightarrow}\left(m_{j,v}^{t}\right) P_{\leftrightarrow}\left(m_{j,v}^{t} | \pi_{\text{Host}}^{t-1}\right). \tag{5.17}$$

The interaction-unaware maneuver prediction $P_{\nleftrightarrow}\left(m_{j,v}^{t}\right)$ of each vehicle is the result of a combination of the following two different maneuver probabilities. The initial prediction is an intention-based maneuver probability, $P_I\left(m_{j,v}^{t}\right)$, which models the unobservable intention of each traffic participant as in [93]. This probability is refined here by the output of the proposed maneuver prediction framework presented in Chapter 3.

With the assumption of rational drivers, the task of calculating an interaction-aware maneuver probability is inevitably associated with risk assessment. The risk is modeled based on multiple possible future evolutions of traffic. Equivalent to (5.12), the interaction-aware maneuver probability of each evaluated vehicle is given by

$$\begin{aligned} P_{\leftrightarrow}\left(m_{j,v}^{t}|\pi_{\text{Host}}^{t-1}\right) &= \sum_{p^t \in \mathcal{P}_{\text{Host}\setminus v}^{t}} P_{\leftrightarrow}\left(m_{j,v}^{t}|p^t\right) P\left(p^t|\pi_{\text{Host}}^{t-1}\right) \\ &= \sum_{p^t \in \mathcal{P}_{\text{Host}\setminus v}^{t}} 1 - R\left(m_{j,v}^{t}, p^t\right) P\left(p^t|\pi_{\text{Host}}^{t-1}\right). \end{aligned} \tag{5.18}$$

$\mathcal{P}_{\text{Host}\setminus v}^{t}$ is the set of predicted scenes from the perspective of the host vehicle, excluding the evaluated vehicle v.

According to (5.18), the interactive prediction of the v-th vehicle depends on the prediction of the traffic (including the host vehicle) from perspective of this evaluated vehicle $P_{\leftrightarrow}\left(m_{j,v}^{t}|p^t\right)$ and the planned maneuver of the host vehicle from the previous step through $P\left(p^t|\pi_{\text{Host}}^{t-1}\right)$. Note that the last terms includes the mutual dependence of maneuver probabilities of different vehicles at each time step on each other.

An intuitive solution to resolve this mutual dependency would be to use the interaction-unaware maneuver probabilities of other traffic to calculate the interaction-aware prediction of the evaluated vehicle v', as in

$$P\left(p^t|\pi_{\text{Host}}^{t-1}\right) = \prod_{\substack{v \\ v \neq v'}} P_{\nleftrightarrow}\left(m_{j,v}^{t}\right). \tag{5.19}$$

If possible, extracting a hierarchy from traffic rules results in a solution that respects the structure of the traffic. With this solution, the mutual dependence between traffic participants can be resolved as well. In Figure 5.8 the developed interactive scene prediction framework is presented exemplarily for two vehicles by its different modules and the two different data flows. Path I is not taken into account if a clear hierarchy exists. For example in the merge scenario from Figure 5.5, vehicle 2 is supposed to yield the right-of-way of the host vehicle when driving on the highway. In situations where a hierarchy could not be extracted, however, path II is neglected.

After the likelihood of all possible host-dependent scenes ρ is calculated, the most likely maneuver sequence of the host vehicle from (5.14) is determined. The presented interactive maneuver planning determines how mutual influences between vehicles are evaluated over multiple time steps. In the following, an an exemplary implementation of the presented approach, applied to highway entry ramp merging scenarios, will be briefly outlined.

Definition of Basic Maneuver

Similar to the definition presented in Chapter 3, each basic maneuver $m_{j,v}^{t} \in \mathcal{M}_v$ is defined through the set of pairs of a longitudinal motion m_{long} and a lateral motion m_{lat},

$$m_{j,v}^{t} = \{m_{\text{long}}, m_{\text{lat}}\}. \tag{5.20}$$

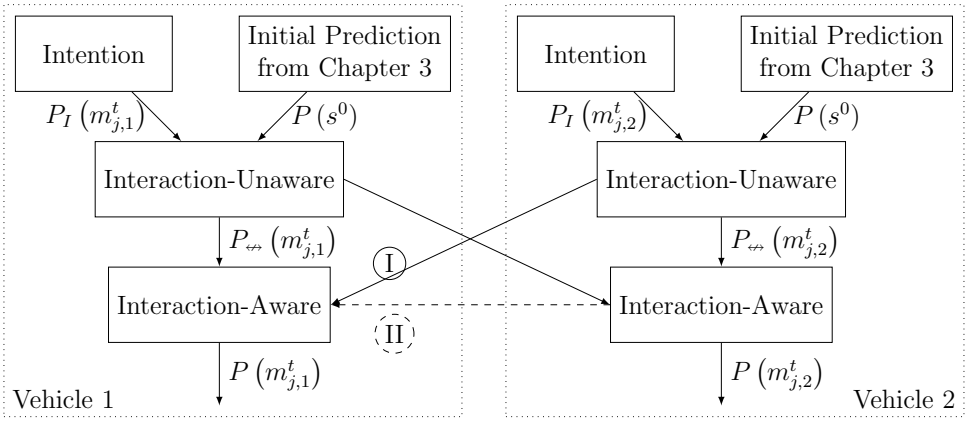

Fig. 5.8: The diagram of the developed interactive scene prediction framework. Depending on the hierarchy assumption, two possible data flows exist. The approach can be applied without restriction to any number of vehicles.

The longitudinal motion is an element from the discrete set of feasible longitudinal accelerations (resp. decelerations) $\mathcal{M}_{\text{long}}$ given by

$$m_{\text{long}} \in \mathcal{M}_{\text{long}} := \{a_{\min}, \ldots, 0, \ldots, a_{\max}\}. \tag{5.21}$$

The lateral motion is an element from the discrete set of feasible lateral movements, $\mathcal{M}_{\text{lat}}$, given by

$$m_{\text{lat}} \in \mathcal{M}_{\text{lat}} := \{-1, 0, +1\} \mathrel{\widehat{=}} \{\text{LCL, LK, LCR}\}, \tag{5.22}$$

corresponding to a lane change to the left, keeping the lane or a lane change to the right. The basic maneuver set of the v-th vehicle at the time step t is thus defined by the Cartesian product of its motion sets as

$$\mathcal{M}^t_v = \{m^t_{1,v}, m^t_{2,v}, \ldots\} := \mathcal{M}_{\text{long}} \times \mathcal{M}_{\text{lat}}. \tag{5.23}$$

The interactive maneuver planning in the upcoming examples evaluates $|\mathcal{M}_{\text{Host}}| = 15$ possible maneuvers. Five maneuvers per lane change intent cover constant velocity, maximal acceleration and three decelerating maneuvers. The maximal number of lane changes up to the planning horizon of $T = 6$ seconds is limited to one.

Intention-based Maneuver Probability

This maneuver probability models the intent of each driver (including the host vehicle). The lateral and longitudinal motions in this thesis are assumed statistically independent for reason of simplification and combined to the intention-based maneuver probability, as

$$P_I\left(m^t_{j,v}\right) = P_I\big(\{m_{\text{long}}, m_{\text{lat}}\}\big) = P_{I_1}\big(m_{\text{long}}\big) P_{I_2}\big(m_{\text{lat}}\big). \tag{5.24}$$

The intent of the host vehicle is based on preferring a given desired velocity. The desired velocity of other vehicles is assumed as their highest velocity since the first observation. The host vehicle prefers keeping the current lane, while it assumes a merging vehicle will

tend to change to the left hand lane proportional to the distance to the end of the highway entry ramp (the information is provided by the prior digital maps). These assumptions specify different distributions for the host and merge vehicle for this example.

Risk Assessment

The interaction-aware maneuver probabilities from (5.12) and (5.18) require calculating collision risk. As proposed in [62], the collision risk in the current implementation is a heuristic of time to collision (TTC) and intervehicular time (TIV) values. Within the cooperative behavioral strategy, the overall risk is approximated as the maximum risks between the specific maneuver $m_{j,v}^t$ and every maneuver sequence belonging to the predicted scene p^t as

$$R\left(m_{j,v}^t, p^t\right) = \max_{\pi_{v'}^t \in p^t} r_{\mathrm{TTC}}\left(m_{j,v}^t, \pi_{v'}^t\right) \max_{\pi_{v'}^t \in p^t} r_{\mathrm{TIV}}\left(m_{j,v}^t, \pi_{v'}^t\right). \tag{5.25}$$

Interaction Hierarchy

As discussed before, an interaction hierarchy model for using a more sophisticated a priori probability is applied. As an overview, Figure 5.9 shows the dependencies when using the interaction-aware probability as an a priori probability. This method differentiates between lane changing and lane keeping maneuvers. The first underlying assumption is that vehicles changing lane submit to the intent of vehicles already on the target lane. This means that vehicles changing a lane try not to interfere with the intended movement of other vehicles. This justifies assessing the risk of lane change maneuvers based on the intention-based maneuver probabilities of other vehicles. This assumption also justifies assessing the risk of lane keeping maneuvers based on the previously calculated interaction-aware lane change maneuver probabilities. For the lane keeping maneuvers it is also important, that the risk from rear vehicles on the same lane is neglected, as they are assumed to be responsible for keeping a safe distance. This means that the dependence of lane keeping maneuvers is from leading vehicles to following vehicles and can be calculated iterative from front to back.

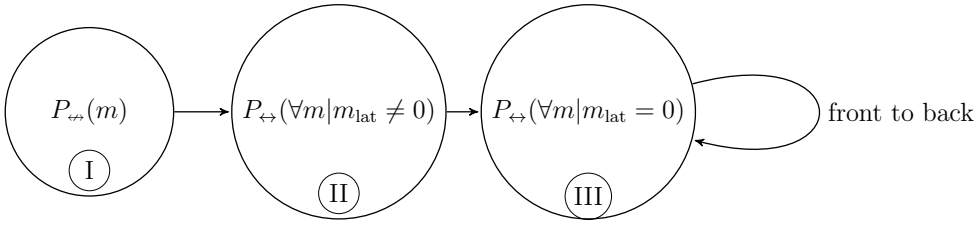

Fig. 5.9: Dependencies between interaction-unaware maneuver probabilities (I) and interactive lane change (II) and lane keeping (III) maneuver probabilities.

With this setup, the potential of the developed replanning-aware interactive scene prediction and planning is evaluated in the following section.

5.5 Evaluation

The performance of the presented approach has been evaluated in a MATLAB® simulated environment which is developed for simulating arbitrary highway scenarios.

The advantages of the approach are demonstrated by three scenarios that demand different cooperative behaviors. The first scenario focuses on the benefits of planning over multiple time steps. It compares the developed approach with two other maneuver planning approaches. The second scenario shows the effects of the replanning-aware prediction of the traffic. The last scenario shows another cooperative reaction. Here, the host vehicle yields by decelerating, to improve the overall safety of the traffic scene. The merging vehicle is simulated with a similar implementation of the introduced interactive driving strategy, but planning just the next maneuver. The behavioral parameters are different and unknown to the host vehicle. The result is a maneuver sequence over three time steps ($T = 6\,\mathrm{s}$), of which only the first maneuver is executed before replanning of the host vehicle.

Yield by Lane Change Scenario

The host vehicle using the developed interactive maneuver planning will be referred in the following as c_{AI1}. Its behavior is compared to a maneuver planning approach c_{AI2} which considers interaction solely over one time step (similar to [93]). Finally, the driving strategy c_{AI3} is introduced to show the difference to a naïve approach which uses a host-independent prediction of the traffic. Here, the basic behavioral strategy based on combinatorial optimization, described in the previous chapter, is applied.

The performed trajectories of the three maneuver planning approaches during the entire simulation time are given in Figure 5.10. It is important to note that the merging vehicle has not even started to merge, i.e. the observation-based prediction does not predict a lane change maneuver. The vehicle c_{AI1} yields early to the merging vehicle by changing to the left hand lane. In comparison, the vehicle c_{AI2} changes the lane at a later point in time and vehicle c_{AI3} keeps the lane and thus does not show any cooperative behavior.

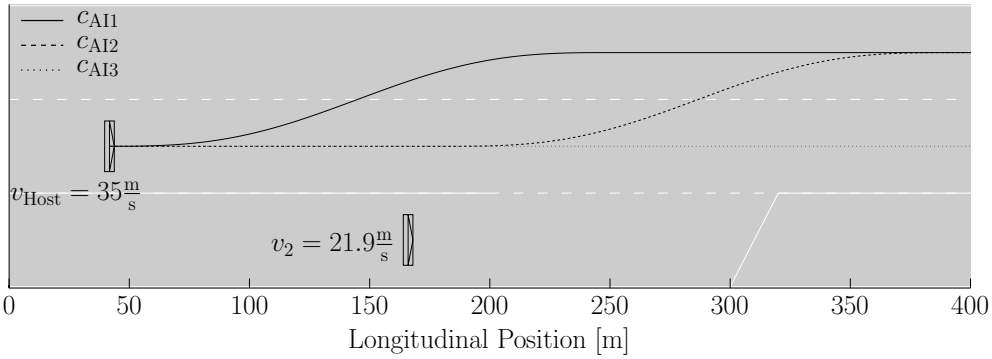

Fig. 5.10: The yield by lane change scenario driven with the three different driving strategies.

This scenario clearly shows how planning over multiple time steps results in an earlier reaction than one-step planning despite the same behavioral parameters. It also indicates how the performance of the planning depends greatly on the prediction approach. Thus, the host vehicle c_{AI1} yields early to the merging vehicle to reduce the risk for its

Tab. 5.1: Relevant maneuver sequences for the first scenario. The sequence probabilities of increasing time steps are depicted top to bottom. Each time step represents an interval of 2 s in the current implementation. The table also shows the interaction-ware maneuver probabilities. The most likely maneuver sequence is highlighted at each time step.

$t=1$	$P\left(m_4^1\right)$	13.89%	$P\left(m_9^1\right)$	**18.51%**		
	$P_{\leftrightarrow}\left(m_4^1\right)$	100%	$P_{\leftrightarrow}\left(m_9^1\right)$	99.99%		
$t=2$	$P\left(m_4^1, m_4^2\right)$	3.21%	$P\left(m_9^1, m_4^2\right)$	3.17%	$P\left(m_9^1, m_9^2\right)$	**4.12%**
	$P_{\leftrightarrow}\left(m_4^2 \mid m_4^1\right)$	100%	$P_{\leftrightarrow}\left(m_4^2 \mid m_9^1\right)$	98.24%	$P_{\leftrightarrow}\left(m_9^2 \mid m_9^1\right)$	95.06%
$t=3$	$P\left(m_4^1, m_4^2, m_4^3\right)$	**0.96%**	$P\left(m_9^1, m_4^2, m_4^3\right)$	0.91%	$P\left(m_9^1, m_9^2, m_9^3\right)$	0.73%
	$P_{\leftrightarrow}\left(m_4^3 \mid m_4^1, m_4^2\right)$	100%	$P_{\leftrightarrow}\left(m_4^3 \mid m_9^1, m_4^2\right)$	96.53%	$P_{\leftrightarrow}\left(m_9^3 \mid m_9^1, m_9^2\right)$	60.38%

consecutive maneuvers at a later point in time. In contrast, c_{AI3} which uses a simple host-independent prediction does not even consider interaction with the merging vehicle. This shows that using intention and mutual interaction for the prediction module instead of only an observation-based approach is essential.

In order to present the reasoning of the replanning-aware interactive maneuver planning, a context relevant selection of maneuver sequences and the associated probabilities is listed in Table 5.1. The sequence probabilities of increasing time steps are depicted top to bottom, with the probabilities of previous sequence sections above the probabilities at a later time step. Each time step represents an interval of 2 s in the current implementation. Note that the probabilities decrease over time because they represent the probabilities of maneuver sequences. As such, with multiple time steps they are a multiplication of multiple basic maneuver probabilities. The table also shows the interaction-aware maneuver probabilities $P_{\leftrightarrow}()$. As discussed before, the latter denotes the probability of a maneuver despite the assessed risks (5.25). It is finally multiplied with the intention-based probability, in order to calculate the total maneuver probability $P()$ (5.17). The most likely maneuver sequence is highlighted at each prediction time step.

Table 5.1 shows that keeping the lane with constant velocity (m_9) is the most likely maneuver sequence choice for the first two time steps. The lane keeping maneuver sequence (m_9^1, m_9^2, m_9^3) becomes unlikely in the third time step due to a comparatively low interaction-aware probability. In the last time step the maneuver sequence of consecutive left lane change maneuvers with constant velocity (m_4^1, m_4^2, m_4^3) becomes most likely. Starting the lane change process at a later time step than the first time step (m_9^1, m_4^2, m_4^3) comes with a lower interaction-aware probability.

No-Yield Scenario

The second scenario explains the advantage of combining planning and prediction in order to model the mutual dependence between maneuvers of different vehicles over time. The host vehicle is again approaching a highway entry ramp with a merging vehicle while the adjacent left lane is blocked by other traffic. Changing to the left lane in order to let the merging vehicle merge onto the highway is thus not a safe option. Consequently, the cognitive vehicle faces the choice of letting the merging vehicle merge in front or behind

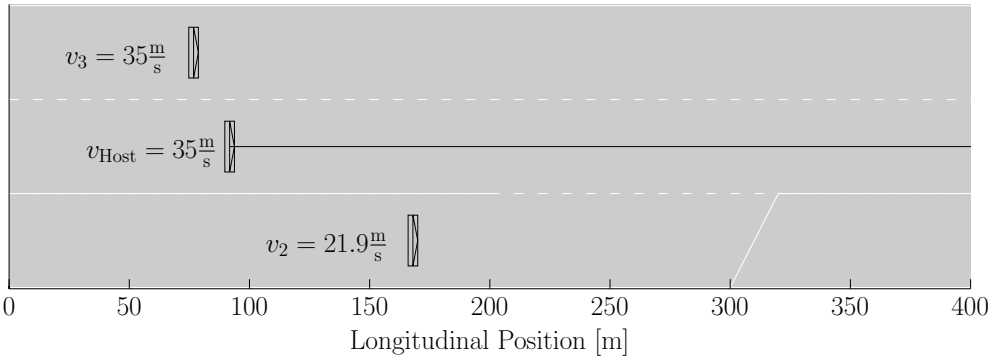

Fig. 5.11: The second merge scenario. Due to the host-dependent prediction over multiple time steps, the host vehicle prefers the current lane and velocity.

Tab. 5.2: Relevant maneuver sequences for the second scenario. Notations similar to Table 5.1.

$t=1$	$P\left(m_7^1\right)$	13.46%			$P\left(m_9^1\right)$	**28.85%**
	$P_{\leftrightarrow}\left(m_7^1\right)$	99.99%			$P_{\leftrightarrow}\left(m_9^1\right)$	99.98%
$t=2$	$P\left(m_7^1, m_8^2\right)$	2.67%	$P\left(m_7^1, m_{10}^2\right)$	4.39%	$P\left(m_9^1, m_9^2\right)$	**8.87%**
	$P_{\leftrightarrow}\left(m_8^2 \mid m_7^1\right)$	95.43%	$P_{\leftrightarrow}\left(m_{10}^2 \mid m_7^1\right)$	*82.23%*	$P_{\leftrightarrow}\left(m_9^2 \mid m_9^1\right)$	*95.76%*
$t=3$	$P\left(m_7^1, m_8^2, m_9^3\right)$	1.01%	$P\left(m_7^1, m_{10}^2, m_9^3\right)$	0.75%	$P\left(m_9^1, m_9^2, m_9^3\right)$	**1.14%**
	$P_{\leftrightarrow}\left(m_9^3 \mid m_7^1, m_8^2\right)$	58.44%	$P_{\leftrightarrow}\left(m_9^3 \mid m_7^1, m_{10}^2\right)$	22.76%	$P_{\leftrightarrow}\left(m_9^3 \mid m_9^1, m_9^2\right)$	15.73%

Tab. 5.3: Probability of the start of merging, conditioned on the last maneuver of the host vehicle for the second scenario.

Host maneuver (t=1)	m_6^1	m_7^1	m_8^1	m_9^1	m_{10}^1
Merge probability (t=2)	37.53%	32.71%	25.32%	17.51%	11.29%

itself by decelerating or just continuing on the lane. Figure 5.11 visualizes the relevant situation while Table 5.2 shows selected maneuver sequence probabilities related to the depicted situation.

The maneuver m_9 represents keeping constant velocity while a higher index represents an accelerating maneuver and lower indices represent decelerating maneuvers. The driving strategy favors overtaking the merging vehicle by keeping constant velocity (m_9^1, m_9^2, m_9^3) over decelerating (m_7^1, m_8^2, m_9^3) and letting the vehicle merge in front of it.

In order to better understand this reasoning, the risk and host-dependent prediction of the merging vehicle requires a closer look. Table 5.3 shows the probabilities of the merging vehicle starting a merge maneuver at the second time step, conditioned on the latest maneuver choice of the host vehicle. The values are the sum of the probabilities of all scenes, following the previous maneuver choice of the host vehicle. The probabilities show, that decelerating in the first time step causes a higher merge probability in the second time step. This has an effect on the interaction-aware maneuver probability of the host vehicle, which is based on the collision risk as well as the probability of the scene itself (see (5.12)).

For example, the velocity after the maneuver sequence of m_7^1 and m_{10}^2 is lower than after the one of m_9^1 and m_9^2. This does not directly imply a higher interaction-aware maneuver probability for the former sequence (italic values in Table 5.2). In contrast, the

probability of performing the maneuver despite the risk is still lower for the first maneuver sequence. The reason is that the probability of the merging vehicle starting a merge maneuver conditioned on m_7^1 is about double as high as for m_9^1. In summary, the effect of the host vehicle decreasing the risk by decreasing its velocity is overcome by the higher chance of the merging vehicle changing the lane.

This effect cannot be observed anymore in the last time step. The maneuver sequence (m_9^1, m_9^2, m_9^3) has a lower interaction-aware maneuver probability than the sequence (m_7^1, m_8^2, m_9^3) because this maneuver sequence results in an overall riskier situation. However, due to the intention of the host vehicle for keeping the lane with constant velocity, this maneuver sequence is still preferred.

Yield by Deceleration Scenario

This scenario shows the third cooperative solution. Compared to the previous scenario, the distance to the merging vehicle is now increased. Figure 5.12 visualizes the relevant situation while Table 5.4 shows that this scenario is resolved by decelerating and letting the vehicle to merge in front. Afterwards, the host vehicle chooses to change the lane in order to reduce risk and accelerate to its desired velocity. This is possible because the distance to the vehicle on the left hand lane increases as the host vehicle decelerates.

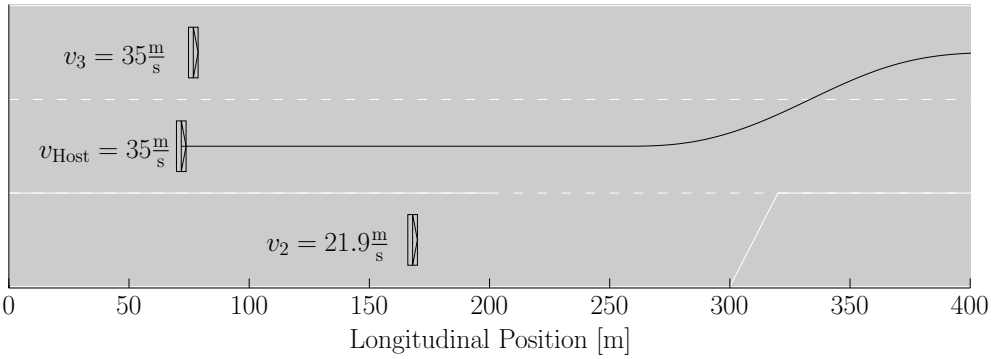

Fig. 5.12: The yield by deceleration scenario. The situation is resolved by decelerating and letting the vehicle to merge in front.

Tab. 5.4: Relevant maneuver sequences for the last scenario. Notations similar to Table 5.1.

$t=1$	$P(m_8^1)$	19.99%			$P(m_9^1)$	**27.26%**
	$P_{\leftrightarrow}(m_8^1)$	99.99%			$P_{\leftrightarrow}(m_9^1)$	99.99%
$t=2$	$P(m_8^1, m_8^2)$	3.75%			$P(m_9^1, m_9^2)$	**7.49%**
	$P_{\leftrightarrow}(m_8^2 \mid m_8^1)$	95.54%			$P_{\leftrightarrow}(m_9^2 \mid m_9^1)$	97.48%
$t=3$	$P(m_8^1, m_8^2, m_9^3)$	0.86%	$P(m_8^1, m_8^2, m_{10}^3)$	**0.87%**	$P(m_9^1, m_9^2, m_9^3)$	0.86%
	$P_{\leftrightarrow}(m_9^3 \mid m_8^1, m_8^2)$	60.29%	$P_{\leftrightarrow}(m_{10}^3 \mid m_8^1, m_8^2)$	56.78%	$P_{\leftrightarrow}(m_9^3 \mid m_9^1, m_9^2)$	25.16%

The three scenarios clearly show the advantages of the interactive planning framework over multiple time steps and using a host-dependent maneuver prediction of traffic. Furthermore, it is shown that the same interactive maneuver planning leads to different cooperative behaviors depending on the initial traffic situation. In cases where the mutual

dependence between maneuver choices is negligible (e.g. in regular highway scenarios), the cooperative behavioral strategy will be disabled

The presented approach was developed and evaluated in a simulated environment. The next section analyzes the complexity of the cooperative behavioral strategy and introduces an algorithm from game theory to reduce the computational time and to achieve an on-line capability of the algorithm.

5.6 Complexity Analysis

The approach described in this chapter evaluates a multitude of possibilities. This section will outline the complexity of the developed interactive maneuver planning.

The number of possible maneuver sequences increases exponentially with time steps,

$$N^t_{m,\text{planning}} = |\Pi^t_{\text{Host}}| = |\mathcal{M}_{\text{Host}}|^t. \tag{5.26}$$

The interaction-unaware probabilities have to be evaluated for each maneuver. However, the more relevant factor are the interaction-aware probabilities as they require risk assessment with the predicted maneuvers of other traffic. The risk assessment for each maneuver has to be evaluated with respect to $|p_t|$ maneuvers of $|\mathcal{P}^t_{\text{Host}}|$ predicted scenes (5.25). Based on the definition of $\mathcal{P}^t_{\text{Host}}$, the number of risks to be evaluated for each single basic maneuver is

$$\begin{aligned} N^t_{R,\text{planning}} &= |p_t| \cdot |\mathcal{P}^t_{\text{Host}}|, \text{ with} \\ |\mathcal{P}^t_{\text{Host}}| &= |\Pi^t_v|^{V-1}, \\ |p_t| &= V - 1, \end{aligned} \tag{5.27}$$

where V is the number of vehicles and thus $V-1$ is the number of traffic participants besides the host vehicle. The number of maneuver sequences of other vehicles $|\Pi^t_v|$ is calculated just as (5.26), but the differentiation allows a different number of basic maneuver options for the host vehicle and other traffic participants. In order to determine the full complexity of the interactive maneuver planning, the complexity of calculating the prediction probabilities of $\mathcal{P}^t_{\text{Host}}$ needs to be examined.

To calculate the probability of the predicted scenes, the prediction modules multiplies $|p_t|$ maneuver probabilities for all $|\mathcal{P}^t_{\text{Host}}|$ prediction scenes. The number of calculated maneuver probabilities for one set of prediction scenes is thus equal to $N^t_{R,\text{planning}}$, the number of collision to be evaluated in the planning process. However, the whole idea of the regarding the mutual dependence of vehicles is to have more than one set of prediction scenes, depending on the previously evaluated maneuver sequence of the host vehicle. It means that $|\Pi^{t-1}_{\text{Host}}|$ sets of prediction scenes have to be considered at the time step t. The number of basic maneuvers to be evaluated for prediction is thus determined as

$$\begin{aligned} N^t_{m,\text{prediction}} &= |\Pi^{t-1}_{\text{Host}}| \cdot |p_t| \cdot |\mathcal{P}^t_{\text{Host}}|, \text{ with} \\ |\mathcal{P}^t_{\text{Host}}| &= |\Pi^t_v|^{V-1}, \\ |p_t| &= V - 1. \end{aligned} \tag{5.28}$$

Similar to the planning, this requires the calculation of interaction-unaware and interaction-aware maneuver probabilities. For the latter, each maneuver has to be evaluated with respect to $|p_t|$ maneuvers of $\mathcal{P}^t_{\text{Host}\setminus v}$ predicted scenes (5.18). Thus, the number of risks to be evaluated for each single maneuver is

$$\begin{aligned} N^t_{R,\text{prediction}} &= |p_t| \cdot |\mathcal{P}^t_{\text{Host}\setminus v}|, \text{ with} \\ |\mathcal{P}^t_{\text{Host}\setminus v}| &= |\mathcal{M}_{\text{Host}}|^t \cdot |\Pi^t_v|^{V-2}, \\ |p_t| &= V-1, \end{aligned} \tag{5.29}$$

where $V-2$ is the number of all vehicles besides the host vehicle and the currently evaluated prediction candidate v.

The total number of evaluated maneuvers is finally calculated as

$$\begin{aligned} N^t_m &= N^t_{m,\text{planning}} + N^t_{m,\text{prediction}} \\ &= |\mathcal{M}_{\text{Host}}|^t + |\mathcal{M}_{\text{Host}}|^{t-1} \cdot (V-1) \cdot |\mathcal{M}_v|^{t(V-1)}. \end{aligned} \tag{5.30}$$

Likewise, the total number of evaluated risks is

$$\begin{aligned} N^t_R &= N^t_{m,\text{planning}} \cdot N^t_{R,\text{planning}} + N^t_{m,\text{prediction}} \cdot N^t_{R,\text{prediction}} \\ &= |\mathcal{M}_{\text{Host}}|^t \cdot (V-1) \cdot |\mathcal{M}_v|^{t(V-1)} + \\ &\quad (V-1)^2 \cdot |\mathcal{M}_{\text{Host}}|^t \cdot |\mathcal{M}_v|^{t(2V-3)}. \end{aligned} \tag{5.31}$$

Equation (5.31) shows an exponential dependence on time as well as number of traffic participants. However, in most cases where a cooperative behavior should be performed, it is sufficient to consider only the most relevant traffic participant (i.e. $V = 2$). This reduces the complexity of the algorithm to $\mathcal{O}(|\mathcal{M}_{\text{Host}}|^{2t})$. In order to further reduce the computational complexity and thus the computing time, alpha-beta pruning [134] is used. This concept from game theory eliminates the maneuver possibilities from the search-tree which are guaranteed to not be the best solution.

Figure 5.13 shows the computing time results for the three scenarios from the last section. The exemplary single-threaded MATLAB® implementation was run on an Intel® Core i5-2540M@2.6 GHz. The time values were averaged over 10 executions that led to the resulting maneuver sequences previously presented for the scenarios. The pruning algorithm was able to eliminate more than 70% of the maneuver options in the last time step. The computing time does not increase for the latter two scenarios even though the number of vehicles increases. This can be explained by the host vehicle using directly the output of the prediction framework for the non-merging vehicle (i.e. neglecting explicit modeling of the mutual dependence to non-merging vehicle), since the focus of the exemplary implementation was on the interaction between the host and the merging vehicle. Put simply, the computational complexity does not increase with the number of vehicles since the mutual dependence of other traffic besides the interesting one (here the merging vehicle) will be neglected. The parallel computing nature of the proposed algorithm enables a native GPGPU, e.g. CUDA C implementation [136], in order to minimize the required computing time.

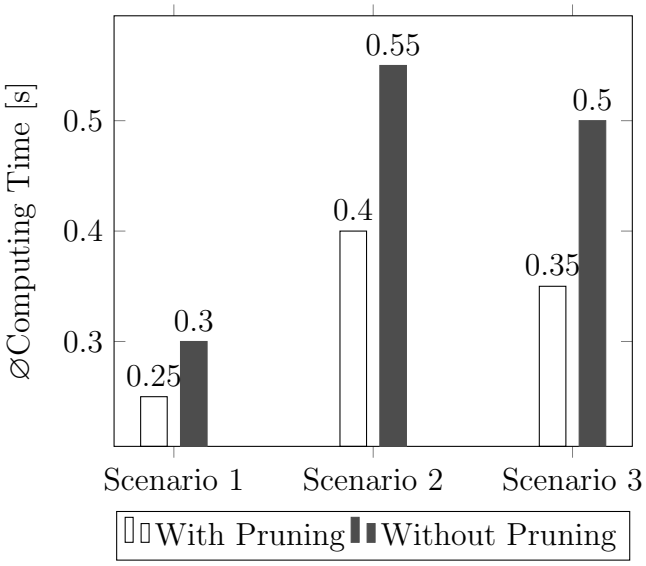

Fig. 5.13: The average computing time for each execution of the interactive maneuver planning with and without pruning for the scenarios.

As explained before the algorithm presented in this chapter predicts the future behavior of other traffic participants at a high-level base. Concerning execution time, the algorithm in its current state offers a close-to-online prediction and will be sped up further in future works. The current state serves as a proof-of-concept, demonstrating its prediction capabilities with a -compared the complex problem- low computational demand.

The merging traffic scenario has been chosen for demonstration because it offers the clearest isolation of a strong interaction in a everyday environment. Further test, however, also show similar benefits at other scenes.

5.7 Conclusion and Discussion

This chapter presented a novel on-line capable approach to the cooperative behavioral strategy in highly-automated driving based on game theory. The introduced prediction and planning loop of the host vehicle captures the mutual dependence between maneuver choices of all traffic participants over multiple time steps. The replanning ability of other vehicles was thus integrated into the planning of a reasonable interactive maneuver sequence for the host vehicle. It was shown that the approach is able to realize different proactive and cooperative driving behaviors in various simulated highway scenarios. Furthermore, this approach can be used as a sophisticated prediction module in other advanced driver assistance systems. It evaluates the effects of own maneuver on surrounding traffic and predicts their motion over multiple time steps.

For the mathematical modeling of the problem and its solution, methods from game theory have been applied. The planning and prediction framework regards the future evolution of traffic in such an extent that analysis of the problem complexity was also necessary. Nevertheless, the on-line capability of the presented approach has been shown.

The precision of the proposed prediction and planning framework can certainly be im-

proved if relevant information such as intended maneuvers of other traffic participants are a priori known to the framework. This can be achieved in the future through inter-vehicle communication. Future researches should be done with focus on improving the computing time. Moreover, evaluating of the approach with real data and its advantages in more complex interactive situations has to be be investigated.

In the next chapter, the driver take over behavioral strategy during autonomous driving based on model-predictive approach will be discussed in detail.

6 Driver Take Over Behavioral Strategy

During autonomous driving, in particular conditional or highly automated driving, a critical part of the system is the driver take over request. Little focus has been given to this important aspect in an automated driving journey. A driver take over request, or TOR, can happen for various reasons and under varying circumstances. Once a TOR occurs, as defined in conditional or highly automated driving, the driver has a finite amount of time in order to take over manual control of the vehicle before the automated driving system deactivates. This chapter presents a detailed analysis of why a TOR can occur, how the automated driving system should react during the TOR phase and what should happen at the end of a TOR in order to realize a safe and comfortable TOR for the driver[1]. Various behavioral strategies during a TOR are presented and evaluated for a single-lane highway scenario. Similar to the previous behavioral strategies, the maneuver planning here is based on the model predictive approach.

6.1 Introduction and State of the Art

As one can quickly see, it is not simple to develop an automated driving system which may at times still have technical limits and will require the driver to take over control under certain situations. Regarding the automation levels as defined by SAE (see Chapter 1), the driver's responsibilities during an automated driving mode between Level 2-4 (i.e. partial, conditional and high automation) is not easy to understand and will be an unfamiliar aspect of autonomous driving to new drivers confronted with such systems. Unfortunately, communication in the media about autonomous driving may be setting high expectations on future users of such technology and its limits, where the need for the driver to take over control in certain situations is rarely covered. How real drivers (not test drivers) react to such a system at different automation levels and how the system itself should behave in each of the automation levels during a take over scenario is not well researched in the literature, but is a very critical aspect of the new automated driving applications which will appear in the near future.

Some studies in the area of human-machine-interaction (HMI) have been carried out in order to learn how long it takes for a driver to take over control during conditional or high automation [63]. Preliminary results show that a driver is capable of safely retaking control of the vehicle within about 7 seconds whilst being distracted with a secondary task during the automated driving mode, although the shorter the take over time, the worse the driver's performance. Therefore it is desirable to give the driver as much time as possible. Level 2 automation has been well studied in the European Union funded project HAVEIt [67]. New steps are being made today in the European Union funded

[1]Parts of the results in this chapter have been pre-published in [194].

project AdaptiVe [3] in order to gain new insights on the technological and HMI challenges of the higher automation levels. As part of this project, the BMW Group Research and Technology will research automated driving at Level 2 and Level 3 in city and highway scenarios, respectively. One aspect of this research is the behavior of the vehicle during the critical driver take over scenario.

This chapter will consider the driver take over request scenario for Level 3 and Level 4 automation, where the driver is not responsible for continuously monitoring the system and the environment. The detailed problem and its variables facing an automated driving system in such a scenario, and its implications, is first described. A novel approach using model predictive control for maneuver planning during the take over phase is subsequently presented. Finally, Results of the proposed approach is evaluated using the simulated environment.

6.2 Problem Formulation

The main problem with Level 3 and 4 automation is that the vehicle must operate under the assumption that the driver cannot immediately take over the driving task, as in Level 2 automation, and requires a certain amount of time in order to retake control of the vehicle. In this section, the implications of this fundamental problem on the automated driving system is analyzed.

Before considering the problem in detail, some states for the automated driving system are defined. The automated driving system is at any time in a given state s defined by

$$s \in \mathcal{S}, \text{ where } \mathcal{S} = \{S_{\text{Auto}}, S_{\text{TOR}}, S_{\text{Safe}}, S_{\text{Manuel}}\} \tag{6.1}$$

where the state S_{Auto} defines the automated driving mode, the state S_{TOR} is the time during which the vehicle finds itself in the TOR phase after a TOR has been initiated by the system, S_{Safe} is the safe state of the vehicle in case the driver does not retake control and S_{Manuel} is the state for the manual driving mode.

There are many reasons for which a TOR should be initiated by the system. The goal of this chapter is to construct a general TOR strategy which, given the constraints of the TOR, is valid for all TOR situations. The most obvious reason to initiate a TOR is to signal the end of the automated driving route, for example before exiting a highway, where the driver will need to retake control due to the fact that the vehicle cannot drive automated beyond the defined route. This is also the easiest situation, as no further unknown variables come into play which may effect the TOR strategy. Other situations deal with an unexpected change in the vehicle's environment, a change with which the automated driving system may not be able to fully cope with, for example a sudden detection of an unknown stationary object. In such situations, the variables describing the situation need to be formulated in a general manner for the TOR strategy, such that safe vehicle operation is guaranteed until the driver has retaken control. Other reasons, such as sensor or hardware failure may also lead to initiating a TOR; these reasons, however, will be ignored here and the system is assumed to function without failure.

TOR Time Interval

The most obvious variable in the TOR problem is the time required for the driver to take over control. This time interval will be designated as $T_{\mathrm{TOR}} = [t_{\mathrm{TOR,s}}, t_{\mathrm{TOR,e}}]$, where $t_{\mathrm{TOR,s}}$ and $t_{\mathrm{TOR,e}}$ is the start and end time of the TOR phase, respectively. The TOR time interval is the most critical input to the TOR problem, as it defines the minimum time that the automated driving system must be able to operate safely after giving a TOR at $t_{\mathrm{TOR,s}}$ until the driver has retake control of the vehicle at a time $\leq t_{\mathrm{TOR,e}}$. All other restrictions during the TOR phase will be derived using the TOR interval as the key variable. Note that the value of T_{TOR} itself is not yet known and still requires more research in the HMI field in order to learn how long it takes for an average driver to take over control of the vehicle. Preliminary research, however, puts T_{TOR} probably around 10 seconds [63].

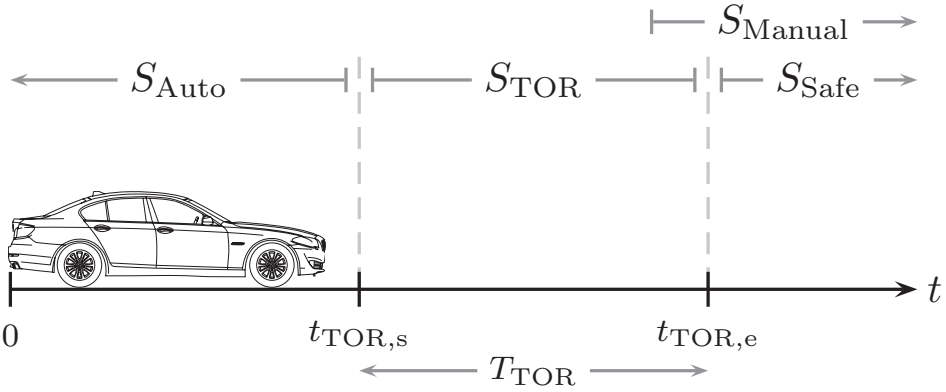

Fig. 6.1: Time line of the driver take over process through the various states of the automated driving system. From the automated driving mode S_{Auto}, the vehicle may make a driver take over request (TOR) at $t_{\mathrm{TOR,s}}$. The TOR phase, with a duration of T_{TOR}, gradually brings the vehicle to a stop, thereby reaching S_{Safe} at the end of the TOR phase. Ideally, any time during the TOR phase, the driver takes over manual control (S_{Manuel}).

Based on T_{TOR}, two key goals are defined, either of which must occur at the end of the TOR phase $t_{\mathrm{TOR,e}}$:

- The driver must have successfully retaken manual control of the vehicle (the primary goal). This state is designed as S_{Manuel}.
- The vehicle must have come to a complete stop and have reached $v = 0$, without disturbing the surrounding traffic (the secondary goal). This state is known as the safe state and is designed by S_{Safe}.

Overall, the primary goal should be reached as comfortably as possible. The challenge is in developing a driving behavior which does not disturb the driver during the TOR phase, allowing him/her to comfortably retake control of the vehicle, but at the same time still controlling the vehicle in a manner such that the secondary goal can at all times be reached in the case that the driver fails to take over control. The time line of the TOR phase with the respective automated driving modes s is shown in Figure 6.1. Note that either the

states S_{Safe} or S_{Manuel} may occur from the state S_{TOR}, where ideally S_{Manuel} occurs first when the driver has successfully taken over manual control.

Assuming a simple strategy of coming to a complete stop with a constant deceleration a during S_{TOR}, the resulting TOR time interval and distance required is shown in Figure 6.2. As can be seen, for low decelerations and high initial velocities at $t_{\text{TOR,s}}$, unrealistic TOR times (well over 15-20 seconds) and traveled distances of over 500 m must be realized. Therefore, a more complex vehicle behavior and strategy must be developed in order to meet the requirements of coming to a stop before a potential obstacle and before the end of the defined TOR phase is reached.

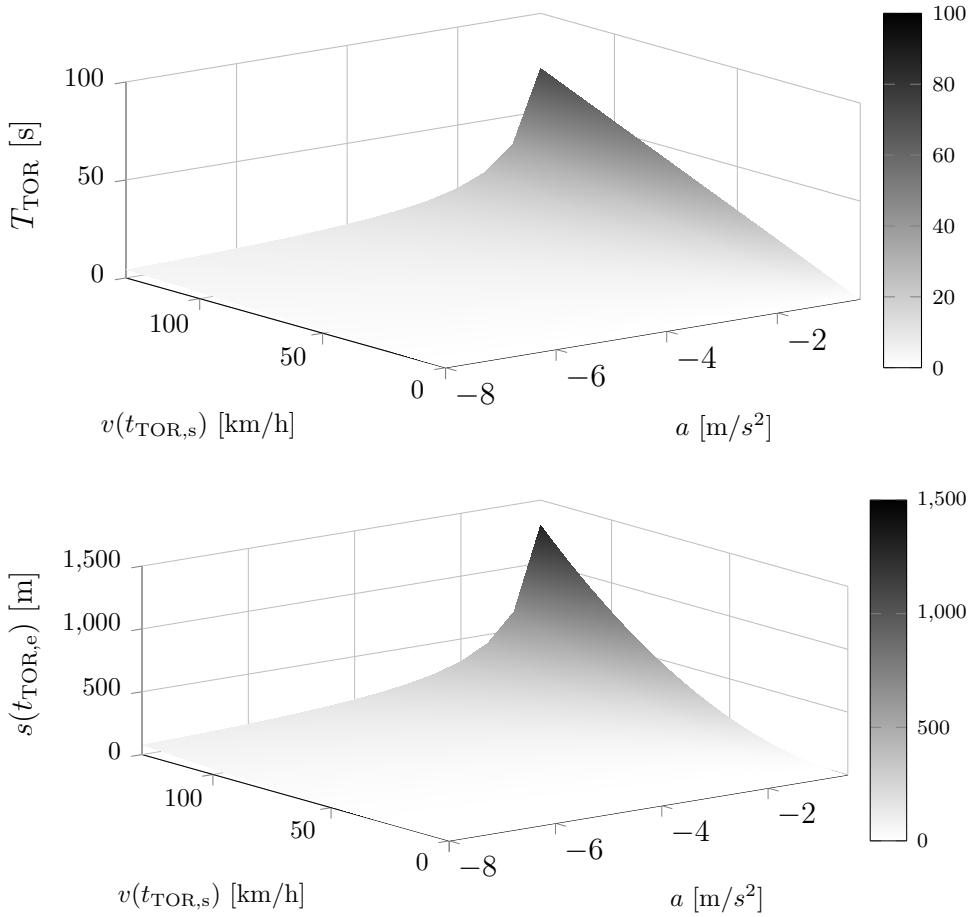

Fig. 6.2: Depiction of a simple constant deceleration TOR maneuver planning and the resulting time T_{TOR} and distance $s(t_{\text{TOR,e}})$ required to come to a complete stop for various initial velocities $v(t_{\text{TOR,s}})$.

Stationary Object Constraint

In addition to the TOR interval, the vehicle's environment plays a critical role in the driver take over problem, especially in guaranteeing that the secondary goal of coming to a complete stop is met. Under the assumption that the driver is able to better resolve a critical driving situation, it may be favorable that the automated driving mode initiate a TOR when an unknown stationary object is detected within the driving path.

The stationary object constraint is one of the important constraints in the TOR problem, as the vehicle must guarantee the secondary goal of not colliding with an unknown object and coming to a complete stop in case the driver does not respond to the TOR. In the TOR problem, this distance to such a stationary object, which restricts the traveled distance before reaching the primary or secondary goal, will be denoted as d_{TOR}. In the case of a stationary object, d_{TOR} is equal to the distance to the stationary object such that

$$d_{\text{TOR}} = s_{\text{TOR},O_i^{\text{stat}}} = s_{O_i^{\text{stat}}} \tag{6.2}$$

where $s_{\text{TOR},O_i^{\text{stat}}}$ is the distance along the lane to the stationary object O_i^{stat} given in the host vehicle relative lane coordinate system. In case no stationary object exists at the time of the TOR, then $d_{\text{TOR}} = \infty$.

Lead Vehicle Constraint

Most of the time while driving on the highway, an automated driving system is probably in an active cruise control situation, requiring to keep a safe distance to the vehicle in front [12]. For the TOR, it is necessary to derive a lead vehicle constraint such that a maximum stopping distance $s_{\text{TOR},O_i^{\text{lead}}}$ can be calculated for this situation. It is assumed that a sudden deceleration of the lead vehicle is automatically handled by the basic behavioral strategy which is active during S_{Auto}. For $s_{\text{TOR},O_i^{\text{lead}}}$, a situation is defined where a virtual stationary object is placed in front of the lead vehicle, and that the lead vehicle keeps a certain safe distance to this virtual stationary object. At any point in time, it may occur that the lead vehicle suddenly swerves out of the lane, revealing such a stationary object, reducing the problem to the stationary object constraint, such that $s_{\text{TOR},O_i^{\text{lead}}}$ is analog to $s_{\text{TOR},O_i^{\text{stat}}}$. The situation is depicted in Figure 6.3.

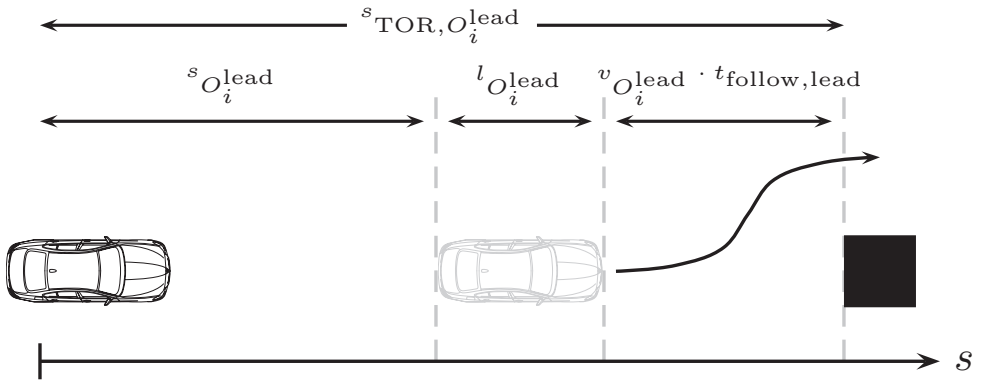

Fig. 6.3: Visual derivation of the lead vehicle constraint, where an imaginary stationary object is placed in front of the lead vehicle in order to calculate the TOR distance constraint $s_{\text{TOR},O_i^{\text{lead}}}$ for a lead vehicle.

Given the above mentioned situation, a different d_{TOR} can be calculated such that a stopping distance to a virtual stationary object behind the lead vehicle can be reached.

This new stopping distance $s_{\text{TOR},O_i^{\text{lead}}}$ is defined as

$$d_{\text{TOR}} = s_{\text{TOR},O_i^{\text{lead}}} = s_{O_i^{\text{lead}}} + l_{O_i^{\text{lead}}} + v_{O_i^{\text{lead}}} \cdot t_{\text{follow,lead}} \tag{6.3}$$

where $s_{O_i^{\text{lead}}}$ is the distance to the vehicle in front (the lead vehicle), $v_{O_i^{\text{lead}}}$ is the current speed of the lead vehicle and $t_{\text{follow,lead}}$ is the assumed time-gap to the stationary object from the lead vehicle.

Environment Observability Constraint

A further constraint on the TOR problem is that of environment observability. At any given time, the automated driving vehicle is able to only observe a certain area around the vehicle, restricted by the vehicle's sensors and their current performance, which may depend on external factors such as the weather. The observability of the vehicle's environment is pre-calculated into a distance s_{obs} describing the current observability of the automated driving vehicle transformed into a host vehicle relative lane coordinate system, such that an observability distance along the current lane is available. The assumption is made that at any time, directly behind the observability distance, may lie a stationary object, in front of which the automated driving system must come to a complete stop during S_{TOR}. Therefore, a new d_{TOR} is defined

$$d_{\text{TOR}} = s_{\text{TOR,obs}} = s_{\text{obs}} \tag{6.4}$$

where $s_{\text{TOR,obs}}$ is the required stopping distance based on the environment observability constraint, which directly is the environment observability along the current lane s_{obs}.

Applying the Constraints

The above mentioned constraints are reevaluated at every time step and the minimum of the distance constraints

$$d_{\text{TOR}} = \min\{s_{\text{TOR},O_i^{\text{stat}}}, s_{\text{TOR},O_i^{\text{lead}}}, s_{\text{TOR,obs}}\} \tag{6.5}$$

is used in the approach presented in the following section. In addition to simply using the distance constraints in the optimization problem for generating a TOR behavior during S_{TOR}, they can further be used during S_{Auto} in conjunction with a desired TOR behavior in order to adjust the speed of the automated driving system such that at all times a comfortable TOR can be experienced by the driver in case an activation of S_{TOR} occurs.

6.3 Approach

In the previous section, a time constraint, the TOR time interval T_{TOR} and a distance constraint d_{TOR} were defined for the TOR problem. As the primary goal is to give the driver ample time to take over manual control of the vehicle, and doing so in a comfortable fashion, additional constraints will be defined in this section in order to construct a favorable

deceleration profile during S_{TOR}. In this section, an approach using model predictive control (MPC) is presented, which solves for a deceleration profile that is able to bring the vehicle to a complete stop under the defined constraints.

A discrete dynamic optimization problem with respect to defined constraints is solved in order to calculate an optimal 1-dimensional trajectory profile for bringing the vehicle to a complete stop before $t_{\text{TOR,e}}$ is reached and doing so in a comfortable fashion. The state space $\mathbf{x}(k)$ and input space $u(k)$ of the discrete dynamic system are defined as

$$\mathbf{x}(k) \in \mathbb{R}^2 = \begin{pmatrix} v(k) \\ s(k) \end{pmatrix} = \begin{pmatrix} \text{longitudinal velocity} \\ \text{traveled distance} \end{pmatrix} \tag{6.6}$$

$$u(k) \in \mathbb{R} = a(k) = \text{acceleration} \tag{6.7}$$

where k is the discrete time variable sampled from the continuous time space t.

The basis for this problem is a dynamic model, which in this case is a linear system assuming a uniform acceleration, resulting in

$$\mathbf{x}(k+1) = A\mathbf{x}(k) + Bu(k) \tag{6.8}$$

with

$$A = \begin{pmatrix} 1 & 0 \\ t_s & 1 \end{pmatrix}, \; B = \begin{pmatrix} t_s \\ \frac{1}{2}t_s^2 \end{pmatrix} \tag{6.9}$$

where t_s is the discretization time for the problem.

The goal is to find an optimal sequence of decelerations during T_{TOR} such that the value of the objective function is optimized over the time horizon with respect to the constraints:

$$J_N^*(\mathbf{x}(0)) = \min_{u^*(0),\cdots,u^*(k)} \sum_{k=0}^{K=T_{\text{TOR}}} \phi(\mathbf{x}(k), u(k)). \tag{6.10}$$

One difficulty with this optimization problem is that, in practice, the sequence of decelerations which is obtained by the optimizer can not be simply applied due to the fact that the model of the system predicting its evolution is inaccurate (from the uniform assumption) and, additionally, the effects of subsequent trajectory planning and controller outputs are not regarded. Furthermore, external disturbances are not considered. Thus, the receding horizon approach is realized, which makes it possible to newly solve the dynamic optimization problem again, starting with the actual measured state as the new initial condition, and repeating for every new replanning time instance.

The objective function which is to be optimized is defined as

$$\phi(\mathbf{x}(k), u(k)) = \|\mathbf{Q}\mathbf{x}(k)\|_2 + \|Ru(k)\|_2 + \|W\Delta u(k)\|_2 \tag{6.11}$$

where $\mathbf{Q}, R, W \geq 0$ represent user-defined weights on the states, input and input change. Given the TOR problem, the goal is to reach the safe state ($v(K) = 0$ and $x_2(K) \leq d_{\text{TOR}}$ with $K = t_{\text{TOR,e}}$) within the minimum possible distance traveled. Additionally, the required deceleration should also be minimized, in order to avoid disrupting traffic and to increase comfort. For maximum comfort, the longitudinal jerk should also be minimized.

The state-constraints of the MPC-Problem are defined as

$$0 \leq x_1(k) \leq 130\,{}^{\mathrm{km}}/_{\mathrm{h}} \tag{6.12}$$

$$x_1(K) = 0 \tag{6.13}$$

$$0 \leq x_2(k) \leq d_{\mathrm{TOR}} \tag{6.14}$$

where they define the possible speed of the vehicle, the speed which should be reached at K and restriction on the distance traveled with respect to d_{TOR}.

In order to meet the requirement of giving the driver an ample amount of time, in a comfortable fashion (minimal braking), to take over manual control of the vehicle during the TOR phase, additional time-varying constraints are defined on the input $u(k)$. The TOR phase T_{TOR} is therefore divided into three intervals $t_{\mathrm{TOR1,\cdots,3}}$ ($T_{\mathrm{TOR}} = t_{\mathrm{TOR1}} + t_{\mathrm{TOR2}} + t_{\mathrm{TOR3}}$). The constraints of maximum deceleration and longitudinal jerk can then be defined to vary in these intervals, thereby escalating over time in order to reach S_{Safe}. This defines the following additional constraints regarding acceleration and jerk as

$$a_{\mathrm{decel,max}}(k) \leq u(k) \leq a_{\mathrm{accel,max}}(k) \tag{6.15}$$

$$\mathrm{Jerk}_{\mathrm{decel,max}}(k) \leq \Delta u(k) \leq \mathrm{Jerk}_{\mathrm{accel,max}}(k). \tag{6.16}$$

The quadratic cost function (6.11) with the linear equality and the affine inequality constraints (6.14,6.16), together define a convex optimization problem. The formulated problem here is a special case of model predictive control with a fixed end constraint, and with a diminishing rather than receding horizon (i.e. the trajectory is only planned to intercept) [114].

Given these time-dependent constraints, a strategy must now be proposed for how the constraints should vary over time. In this thesis, two such strategies are proposed, both of which operate on the concept of three escalation levels, or phases, as described above by $t_{\mathrm{TOR1,\cdots,3}}$. For each of the three escalation levels, different values for acceleration and jerk are defined, such that $a_{\mathrm{accel,max/min}}(k)$ and $\mathrm{Jerk}_{\mathrm{decel,max/min}}(k)$ are step functions. The proposed strategies are:

1. Maximize the time with the minimum escalation level, i.e:

$$t_{\mathrm{TOR1}} \rightarrow \max \tag{6.17}$$

2. Minimize the following further constraint (prefer less escalation):

$$\alpha_1 t_{\mathrm{TOR1}} + \alpha_2 t_{\mathrm{TOR2}} + \alpha_3 t_{\mathrm{TOR3}} \rightarrow \min \tag{6.18}$$

   with $\alpha_1 < \alpha_2 < \alpha_3$.

Note that other strategies are also possible by means of additional or modified constraints, thereby making the presented approach quite universal for solving the TOR problem with different desired behaviors during S_{TOR}.

In order to assure a real time execution of the proposed approach, the solution of the optimization problem for all possible inputs is pre-computed offline and made available

online by means of a piecewise affine feedback policy [70]. This eliminates the need for solving the solution of a quadratic or linear problem in real time.

6.4 Evaluation

The proposed approach using the previously described optimization problem is evaluated by showing the generated deceleration and velocity profiles and the traveled distance given different initial velocities of the automated driving vehicle. These profiles are then used to generate inputs in each processing cycle for further motion planning algorithms in the automated driving system, thereby realizing the desired behavior during S_{TOR}.

For simplicity, all of the results use $T_{\text{TOR}} = 10\,\text{s}$. However, the approach works just the same for different values of T_{TOR}. Note that the selection of $T_{\text{TOR}} = 10\,\text{s}$ has little real-world significance, as the minimum required time for a TOR is still an active topic of research. For all of the results, the maximum change in acceleration is chosen as $\text{Jerk}_{\text{decel,max}} = -2$ and $\text{Jerk}_{\text{accel,max}} = 1\ \forall k$. The maximum acceleration is also chosen to be $a_{\text{accel,max}} = 0\ \forall k$, as no acceleration is desired and the maximum deceleration is chosen as the step function

$$a_{\text{decel,max}}(k) = \begin{cases} -1\,\text{m/s}^2 & k \leq t_{\text{TOR1}} \\ -3\,\text{m/s}^2 & t_{\text{TOR1}} < k \leq t_{\text{TOR2}} \\ -8\,\text{m/s}^2 & k > t_{\text{TOR3}} \end{cases} \tag{6.19}$$

over k where $k = 0$ represents the beginning of S_{TOR} such that $k = 0 = t_{\text{TOR,s}}$. This step function is used to define the three TOR intervals $t_{\text{TOR1,}\cdots\text{,3}}$, where the actual selection of the length $t_{\text{TOR1,}\cdots\text{,3}}$ is done by the optimization algorithm presented in the previous section. The weighting parameters $\mathbf{Q}, R, W$ are chosen as

$$\mathbf{Q} = \begin{bmatrix} 1 & 0 \\ 0 & 0.1 \end{bmatrix} \tag{6.20}$$

$$R = 10 \tag{6.21}$$

$$W = 100. \tag{6.22}$$

Even though the presented results rely on the above defined parameters, all of the parameters can be freely chosen in order to obtain the desired behavior. The goal is to demonstrate the approach and not optimize for the best TOR behavior, as that is a very subjective evaluation requiring input from extensive driver studies. The results are shown for initial velocities in the range $v(0) = [40 \ldots 130]\,\text{km/h}$.

Figure 6.4 shows the results with the above mentioned parameters for a TOR distance of $d_{\text{TOR}} = \infty$. The large value for d_{TOR} signifies that a potential obstacle is non-existent and the vehicle may come to a stop within any amount of distance traveled. The top row shows the resulting deceleration and velocity profiles and total distance traveled of the vehicle during S_{TOR} for various initial velocities using strategy 1 (maximize minimum escalation level). The boundaries between the TOR intervals is depicted by the green and yellow lines. The bottom row shows the same results using strategy 2 (weighted preference of the TOR intervals). In both cases, the vehicles successfully comes to a complete stop within

10 s and for the maximum velocity of 130 km/h does so within a traveled distance of roughly 250 m. Both strategies show that larger decelerations from the 2nd and 3rd TOR interval are delayed, such that the driver experiences mostly the deceleration of t_{TOR1}. With the maximum initial velocity of 130 km/h, for strategy 1 t_{TOR2} begins at $t = 8\,\text{s}$, whereas for strategy 2 at $t = 5\,\text{s}$, giving the driver ample amount of time to take over control during t_{TOR1}, where the deceleration is minimal. The 3rd TOR interval is only present for the last 2 s of S_{TOR} for strategy 1 and does not occur at all in strategy 2. In general, the lower the initial velocity, the less deceleration is necessary.

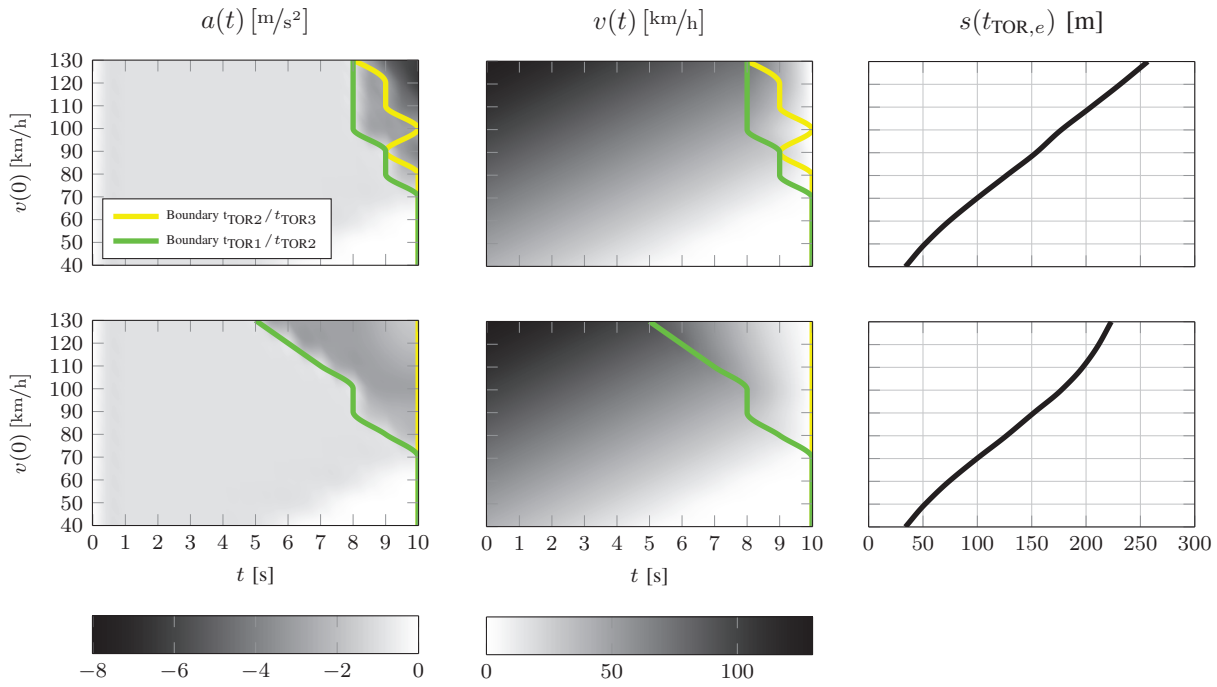

Fig. 6.4: Vehicle behavior during S_{TOR} for various initial velocities with $T_{\text{TOR}} = 10\,\text{s}$. Top row shows the results for TOR strategy 1 (maximize time of first TOR interval) and bottom row shows the results for TOR strategy 2 (weighted optimization of TOR intervals). Acceleration and velocity profiles as well as distance traveled is shown. Note that a TOR distance of $d_{\text{TOR}} = \infty$ is used, such that the distance traveled does not play a role in the generated behavior.

Figure 6.5 shows the results using a TOR distance of $d_{\text{TOR}} = 100\,\text{m}$. This simulates the case in which the sensors detect and classify a potentially dangerous situation fairly close to the vehicle, where it is determined by the system to be a relevant situation for initiating a driver TOR. Again, the top row of the figure shows the results for strategy 1 and the bottom row for strategy 2. Due to the close proximity of the obstacle in the lane, t_{TOR1} is only $t = 1\,\text{s}$ long for both strategies at the maximum initial velocity of 130 km/h, where stronger braking is necessary much earlier in order to bring the vehicle to a stop. At about $t = 5\,\text{s}$, the vehicle comes to a complete stop before reaching the object, but does so before the complete TOR time duration of $t = 10\,\text{s}$ is reached. For both strategies and for all velocities, the vehicle successfully comes to a top before the obstacle, traveling precisely a

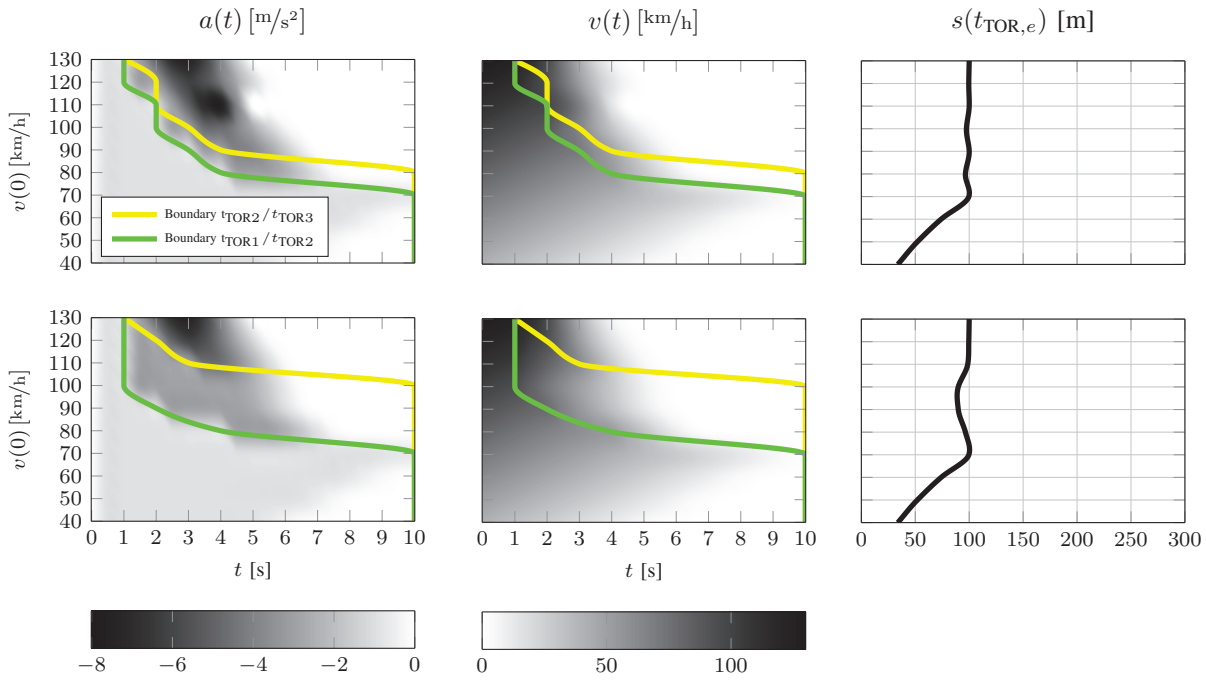

Fig. 6.5: Vehicle behavior during S_{TOR} for various initial velocities with $T_{\mathrm{TOR}} = 10\,\mathrm{s}$ and a TOR distance of $d_{\mathrm{TOR}} = 100\,\mathrm{m}$, simulating a TOR during a situation where an obstacle obstructing the lane requires the driver to take over. As in Figure 6.4, top row shows the results for TOR strategy 1 and bottom row TOR strategy 2.

distance of 100 m.

6.5 Conclusion and Discussion

This chapter presented an approach for dealing with a driver take over request during autonomous driving based on model predictive control. Simulation results were presented for different strategies in order to show the effects of different constraints in the optimization problem. All of the presented strategies, however, achieve the goal of bringing the vehicle to a safe stop within the allotted TOR time or before a potentially stationary obstacle or critical situation in the lane.

The next step is to integrate these strategies into a prototype vehicle for autonomous driving and test various TOR scenarios with the different strategies. What makes this difficult is that the results of such tests not only depend on quantitative results, but also from qualitative feedback from drivers, as the impression of the vehicle's behavior on the driver during the TOR phase plays a crucial role in the acceptance of a certain strategy. Additionally, the vehicle's TOR behavior also plays a critical role in drivers' acceptance of autonomous driving in general and should therefore be designed to be as comfortable as possible while still guaranteeing safety in case the driver fails to take over. The maneuver planning approach in this chapter, however, presents a general framework where, based on the feedback of field tests with real drivers, constraints can be modified and/or added in

order to develop the best possible and most acceptable behavior.

In the last five chapters the functional architecture of the tactical decision-making process, the novel traffic scene prediction module and the different behavioral strategies were discussed in detail. All these together provides the complex artificial intelligence of the automated driving function. During the development phase of this tactical level, the following two important issues has to be investigated:

- How can the effect of parameter changes within the tactical decision-making process be objectively evaluated?
- What is the impact of automated driving with actual implementation of its tactical level on traffic safety and traffic efficiency?

For these reasons, a novel framework for impact assessment based on microscopic traffic simulation is developed which allows the study of the above questions. In the early stage of the development, the proposed framework can be applied to steadily examine the effect of each modification within the tactical decision-making process on the traffic. Consequently, the enormous costs related to the time-consuming and partly safety-critical real world tests on highways can be saved. This framework will be discussed in detail in the next section.

7 Impact Assessment Based on Microscopic Traffic Simulation Framework

As discussed in the previous chapters, highly automated driving on highways requires a complex artificial intelligence that makes optimal decisions based on the ongoing measurements. Notably no attempt has been performed to evaluate the impacts of such a sophisticated system on traffic. Another important point is the impact of continuous increase in the number of highly automated vehicles on future traffic safety and traffic efficiency. This chapter introduces a novel framework to evaluate these impacts in a developed microscopic traffic simulation environment. This framework is used on the one hand to ensure the functionality of the tactical decision-making process in the early development stage. On the other hand, the impacts of increasing automation rates, up to hundred percent, on traffic safety and traffic flow is evaluated[1].

7.1 Introduction and State of the Art

Many automobile manufacturers and research institutes across the world have been developing prototype vehicles for automated driving. Since then, thousands of kilometers of automated driving experience on highways have been achieved. But there is a little research on the impact of highly automated vehicles (HAV) on traffic characteristics and especially when the traffic is a mix of human drivers and highly automated vehicles. Microscopic traffic simulation enables the prediction of what the impact of the new technology might be on traffic characteristics before the new technology is actually in place [47]. The outcomes help to pursue legal and political confirmation for the highly automated driving functions as well.

Traffic based evaluations of advanced driver assistance systems (ADAS) have been performed in many research works. For instance, the evaluation of Adaptive Cruise Control (ACC) is studied in [111] on motorway capacity. In this study ACC was implemented in the car following model of the microscopic simulation tool in a way that ACC equipped vehicles have shorter reaction delay comparing to the standard vehicles. The result indicates that the ACC headway setting can basically influence the achievable highway capacity. In [112] the same researchers investigated the effects of ACC on TTC and TTC-based safety indicators. Outcome of this study shows that the safety aspects of traffic are mainly influenced by the design of ACC system and in some cases they are more critical in terms of safety than the investigated baseline scenario. Other Examples include works of [42, 43, 102, 104, 164]. In the majority of these studies, longitudinal ADAS is considered. In most of them the longitudinal control ADAS is modeled simply by modifications of the car-following model of the simulation tool.

[1] Parts of the results in this chapter have been pre-published in [190, 191, 198].

In the study by [68], the effects of overtaking assistant as a lateral ADAS system, on traffic efficiency, safety and comfort is investigated by means of microscopic traffic simulations. In this study the willingness to overtake of assisted drivers is influenced by the assistant. For equipped vehicles stochastic overtaking probability functions in the simulation tool is replaced by a deterministic procedure. The result of this study shows that the effect on traffic efficiency is rather small and there is an improvement in individual driver comfort. Regarding safety aspects the conclusion shows that specifications of the overtaking assistance systems are directly influencing the safety indicators.

Considering that highly automated driving is identified as a sophisticated advanced driving assistance systems with a specified artificial intelligence, notably, no attempt has been performed to evaluate this combination. It is of importance to evaluate the effects of highly automated vehicles in traffic flow early in the development so that, if they are discovered to unintentionally create problems, the tactical decision-making process can be adjusted accordingly. Apart from that, the implementation of highly automated driving in a traffic simulation environment can provide an opportunity to compare different parameterization to achieve the optimum point in system design.

The objective of this chapter is to introduce a novel framework to evaluate the impact of highly automated vehicles in traffic flow in terms of safety and efficiency, regarding different indicators within various scenarios by means of microscopic traffic simulation. Thus, the proposed basic behavioral strategy based on combinatorial optimization with greedy search, as discussed in Chapter 4.4, is evaluated in the microscopic traffic simulation tool PELOPS$^{©fka}$ [29] which has been extended for this task.

In the following, the description of applied microscopic traffic simulation tool PELOPS is first provided. Subsequently, the setup of simulation and its results are explained. Finally, the results are discussed and the conclusion is provided.

7.2 Microscopic Traffic Simulation Tool PELOPS

Use of an appropriate tool is essential to confirm that it can support the purpose, needs, and scope of the work [47]. The microscopic, vehicle-orientated traffic simulation program PELOPS (Program for the DEvelopment of LOngitudinal Traffic Processes in System Relevant Environment) is developed by IKA/FKA[2] in cooperation with the BMW AG. "PELOPS represents a combination of detailed sub-microscopic vehicle model and microscopic traffic model. This allows for the analytical investigation of the vehicle longitudinal dynamic behavior as well as traffic flow. Advantage of this method is that it considers all of interactions that take place between the driver, vehicle and traffic" [29].

As illustrated in Figure 7.1, PELOPS considers three significant components of traffic system and applies a model for each: vehicle model, environment model and driver model. The vehicle model presented in high level of details regarding components simulates the vehicle dynamic characteristics. The simulation is based on actuating variables, such as pedal position and gear selection. It also provides precise determination of the efficiency and fuel consumption parameters. The environment model gives the possibility to design

[2]Institute für Kraftfahrzeug Aachen /Forschungsgesellschaft Kraftfahrwesen mbH Aachen.

the intended route with desired curvatures, number and width of lanes and transitions in lateral and longitudinal directions. In addition, traffic signs and other environmental parameters can also be simulated. To realize the connection of vehicle model and environmental model, a driver model is applied. This model is subdivided into a behavior and an action model. According to current driving status and surroundings traffic situation provided by environmental model, behavior model determines the driving strategy. The action model delivers the intended driving strategy to vehicle model.

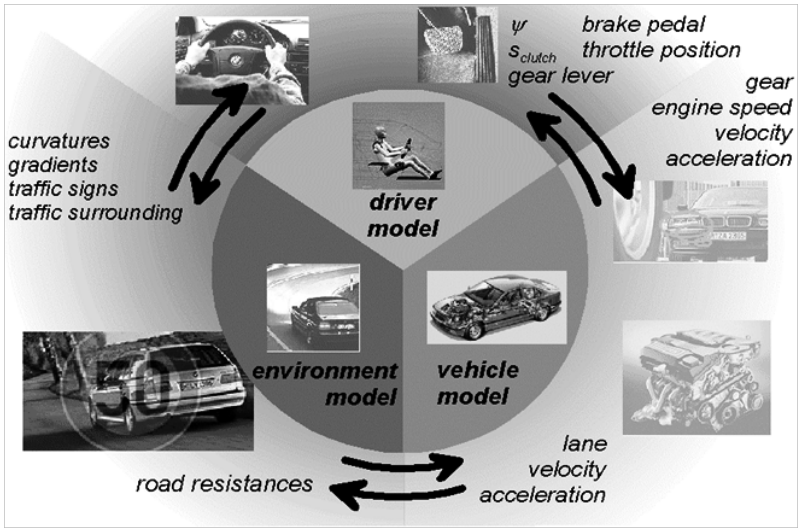

Fig. 7.1: PELOPS Structure. Image source [29].

Determination of driving strategy by behavior model is based on two important submodels: longitudinal car following model, which is based on the psychophysical approach of Wiedemann and lateral behavior model (lane change model). Furthermore, an external driver by means of a feature in PELOPS can override these two models. The feature allows implementing an external driver model either as software in the loop (SIL) or by embedding the algorithms. This makes PELOPS suitable for exploring the impact of different highly automated driving models in traffic flow. This two features are described in the following.

Software in the loop (SIL)

This SIL feature is basically made for rapid prototyping for development of assistance systems. In this feature there is no need to implement the algorithms and functions directly in PELOPS as source code. Software programs can be operated with PELOPS in a coupled simulation. In this project the software that is coupled is Simulink®, in which the model of highly automated vehicle's controller is developed. The model is coupled via Xface[3] to the interface in PELOPS (Co-Simulation mode). By means of this interface the model functions as a controller for only one vehicle. This vehicle is selected in the built traffic scenario and the Simulink model overrides the vehicle's driver model in PELOPS. Figure 7.2 provides the data flow diagram of this feature.

[3]Xface denotes a standardized interface to driving environment and vehicle data.

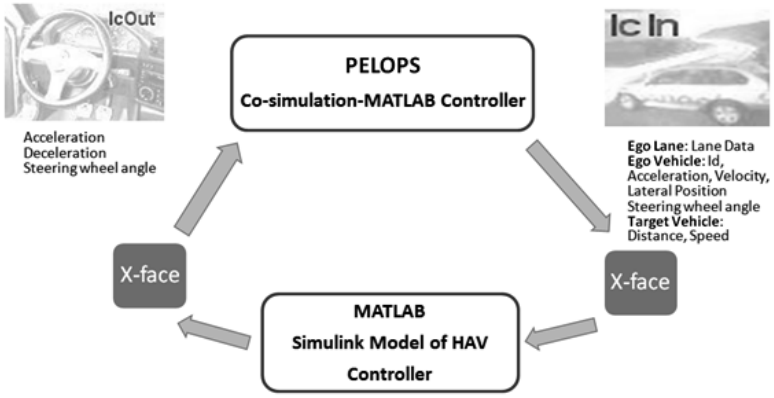

Fig. 7.2: SIL feature of PELOPS [198].

For instance, a vehicle model designed with different longitudinal and lateral controllers in MATLAB/Simulink receives several signals as input via Xface interface from PELOPS. These signals include data regarding relative speed and the distance to the surrounding traffic. With this data, the vehicle controller model calculates a value for acceleration and steering wheel angle and sends it back to PELOPS. The result is updated vehicle position and acceleration in PELOPS.

Embedding process

At the first stages of implementing the HAD model in PELOPS, it was intended to implement only one vehicle model using SIL feature, to make sure that the basic behavioral strategy with the selected parameters functions as expected. For further stages in order to have several highly automated vehicles simultaneously in a traffic scenario, the HAD model was embedded into the source code of the program as a driver model. This was realized by means of generating the C-Code of the model using Real-Time Workshop© and compiling the vehicle code within PELOPS source code. The implemented code can be called independently for each vehicle as a controller unit which override the driver model on PELOPS. With this method, it is possible to build a scenario with up to 100 percent highly automated vehicles with different tactical decision-making process. In the following, the setup for the designed scenario is described in more details.

7.3 Simulation Setup

After proper implementation and verification of the highly automated vehicle's controller model, the simulation scenarios are designed and built in PELOPS. Considering that the applied microsimulation tool is used as a deterministic tool and no randomness is involved during the simulation. Therefore, only one simulation run will provide the desired data. The basic configuration used in this thesis is a four-lane highway with a length of 6000 m. A measurement loop is placed in every 500 m to collect the macroscopic data.

In the current implementation approach, the controller model overrides the driver model

during the entire simulation horizon. Thus, the design of the simulated route shall be adapted to the controller model capabilities. In some situations (e.g. traffic congestion with high traffic density) the existing highly automated driving controller model requests the driver to take the control of the vehicle. Therefore in the scope of this research work, lane ends and traffic congestion are avoided in the simulation setup. In other words, only the impact of basic behavioral strategy is investigated here since this strategy is active in most of the time.

For the traffic generation, the data from the highway section close to the Elbe tunnel in the south direction near Hamburg in Germany is used. By means of this macroscopic data the vehicles with defined driver characteristics are generated. The PELOPS behavior for the driver population was previously calibrated. The simulation time is 1800 s per simulation run. Three scenarios with these basic configurations are built by zero, fifty and hundred percent of vehicles equipped with the presented highly automated driving model from Chapter 4.

7.4 Simulation Results

One of the main outcomes of the impact evaluation is the case of accidents in the scenarios. Microscopic traffic simulation tool PELOPS is developed in a way that collisions are avoided by the vehicles that are controlled by applied the lateral and longitudinal behavior models. The results also show that the collisions occur only between two highly automated vehicles. A study of these cases can beneficially contribute to the improvement of tactical decision-making process. Collision cases are happened in the simulation mostly due to simultaneous lane changing of two highly automated vehicles to the same target (see Table 7.1).

Tab. 7.1: Summery of accident cases in different scenarios.

Scenario / Accident Type	0% HAV	50% HAV	100% HAV
Simultaneous lane changing	0	7	2

The most important cause of accidents revealed in the simulation is when two HAVs are driving on two different lanes with lateral distance of one lane in between and both decide simultaneously to change to the lane in between. There are two main reasons that explain the occurrence of this type of collision. First reason is related to the provided data range of the sensors implemented on the two sides of the highly automated vehicle at application level. Regarding the environment model discussed in 4.4, the sensors provide only the data of one adjacent lane to the host vehicle at application level. This means that two vehicles do not recognize each other when they are located on two different lanes with a lateral distance of one lane between them. This case of accident can be avoided by the extension of the data range at the application level. It is worth mentioning that this type of accident has never occurred during the simulation of the highly automated vehicles in driving simulator; considering that in the driving simulator only one highly automated vehicle can

be simulated. Therefore, the interactions between two highly automated vehicles with the same tactical decision-making process could not be investigated.

Second type of the accident case generated only by the reactive highly automated vehicle presented in [11] is mainly due to the lack of maneuver prediction of other traffic (more than 5 accidents by the 50% HAV). A vehicle in front of the highly automated vehicle will be here recognized in the same lane with the host vehicle when at least half of the vehicle's width passes the lane marking of the ego lane. This preliminary strategy is applied for the Adaptive Cruise Control system implemented to select the proper target vehicle to adapt the velocity accordingly. However, this recognition strategy causes critical situations when a vehicle in adjacent lane performs a cut-in maneuver to the ego lane in a small longitudinal distance. The result of accident cases after implementing the proposed model predictive basic behavioral strategy improved highly automated vehicle model with the prediction framework shows that no cases of collision due to prediction problem have occurred and only the first type of accident is happening. It should be noted that the vehicles that collide are removed from the simulation right after the collision to avoid the accident side effects on the simulated traffic scenario.

Impact Evaluation

In the scope of this work the impact evaluation concentrates mainly on traffic safety and efficiency. This safety aspect is evaluated by measurement of following indicators:

1. Time To Collision
2. Time Exposed TTC (TET)
3. Time Integrated TTC (TIT)

The authors in [71] reported the TTC threshold that identifies the relatively safe and critical encounters as three seconds. In the scope of this research the same threshold is applied. Table 7.2 shows the results for TTC values. Significant reduction in the total number of critical cases can be observed comparing the baseline scenario with 1440 critical encounters to the other two scenarios with 729 and only 16 critical situations for the scenario with 50 and 100 percent penetration rates of highly automated vehicles respectively. This is an obvious result thanks to the same desired speed and the reaction time for highly automated vehicles which consequences in fewer vehicle-vehicle interactions in traffic flow; thus, much fewer critical situations. In the scenario with fifty percent of HAV the frequency of the critical situation below 1.5 seconds that is defined as the sufficient safety distance [76] is remarkably increased comparing to the baseline scenario. Therefore, conclusions regarding safety aspect in the mixed scenario are better be drawn from the other TTC based indicators.

The authors in [112] define Time Exposed Time-to-collision (TET) as follows: "It is the summation of all moments that a driver approaches a front vehicle with a TTC value below the threshold TTC". Therefore the lower the TET value, the more safe the scenario. TET value has decreased by increasing the penetration rate of the highly automated vehicles. 144.1 second is the total time exposed to safety critical situation in the baseline scenario,

Tab. 7.2: TTC frequency in scenarios with different penetration rates (F=Frequency, RF=Relative Frequency).

Scenario	0% HAV		50% HAV		100% HAV	
TTC (s)	F	RF%	F	RF%	F	RF%
< 0.8	0	0.00	79	10.71	0	0.00
$0.8 - 1.5$	31	2.15	128	17.58	0	0.00
$1.5 - 2.0$	102	7.08	133	18.27	4	25.00
$2.0 - 2.5$	404	28.06	149	20.47	7	43.75
$2.5 - 3.0$	903	62.71	240	32.97	5	31.25
Total	1440	100	729	100	16	100

whereas the exposition time in scenario with 50 percent penetration rate of HAV equals to 72.9 seconds. The TET value for the scenario with 100 percent HAV penetration rate is only 1.6 seconds.

The disadvantage of TET is that it does not show the severity of the critical situations. Therefore, another indicator to take the impact of TTC value into account is developed. "Time Integrated Time-to-collision (TIT) indicator uses the integral of the time to collision profile of drivers to express the level of safety (in s^2). A high TIT value means a large exposition time to duration weighted unsafe TTC-values, which is negative for road safety" [112]. Considering this statement it can be concluded that the scenario with 50 percent penetration rate of HAV with a TIT value of 76.29 square second is in lower level of safety comparing to the baseline scenario with TIT value equal to 66 square second. The highest level of safety belongs to the scenario with 100 percent HAV with only 1.10 square second TIT.

The scenario with fifty percent penetration rate of highly automated vehicles is thus studied in more details. Evaluation of safety indicators is carried out regarding the type of the vehicle's driver model (HAD vs. human driver). By this evaluation a detailed view on HAV and human driver interactions is achieved. Table 7.3 depicts how each group contributes to generation of critical situations. The results show that highly automated vehicles as used in this study have the tendency to get closer to the leading vehicle to generate a critical situation and react faster to clear the situation. This basically happens thanks to the faster reaction time of HAV comparing to human drivers. Thus, the frequency of critical cases in which highly automated vehicle is involved as a following vehicle is higher camparing to the frequency of the situation where a PELOPS driver is a following vehicle.

Tab. 7.3: TET and TIT values for different scenarios.

Scenario	TET (s)	TIT (s^2)
0% HAV	144.1	66.16
50% HAV	72.9	76.29
100% HAV	1.6	1.10

Regarding the outcome for TET values, it can be interpreted that in mixed traffic highly automated vehicles have higher exposition to critical situations than PELOPS vehicles as a follower. Which means that as a follower the HAV is contributing to longer critical situations than PELOPS driver. In addition from the results for TIT values, it can be concluded that among all critical situations the critical cases that take place between two HAV vehicles have the highest level of criticality in terms of safety among all the other categories.

The term traffic efficiency may cover a variety of aspects. The author in [27] defines the efficiency of traffic flow on a highway as "production per time unit". The more vehicle kilometer produced in a highway per hour, the greater is the efficiency. Moreover, the higher average travel speed contributes to more efficient traffic. Within the scope of this impact evaluation, traffic efficiency is evaluated by measurement of set of relevant indicators such as travel time and average travel speed, which are characterizing traffic efficiency. In the following, results of the impact evaluation according to these indicators are provided.

The outcome of travel time calculation for the whole simulation track (6 km) is shown in Table 7.4. As expected the higher rate of highly automated vehicles consequences in shorter travel time. This happens thanks to higher percentage of vehicles with higher desired speed.

Tab. 7.4: Travel time and distance traveled in different scenarios.

Scenario	Total Travel Time (s)	Average (s)	Total Distance Traveled (km)
0% HAV	613, 872	265	13, 696.80
50% HAV	505, 173	217	13, 690.48
100% HAV	415, 890	174	14, 128.93

In the simulation horizon of 1800 s in the baseline scenario 13 696.80 km are traveled in 613 872 s (resp. 170.52 h). The average of the travel time in the baseline scenario equals to 265 s. No significant difference in total distance travelled is observed comparing the baseline scenario and the scenario with 50 percent penetration rate of highly automated vehicles; however the total travel time has decreased remarkably. The reason is that in the scenario with fifty percent penetration rate of highly automated vehicles more than fifty percent of the fleet has the desired speed of 130 $\frac{\text{km}}{\text{h}}$ which consequences in shorter travel time. Furthermore, the relatively short reaction time of highly automated vehicles results in less vehicle-vehicle interactions, thus shorter time to travel the whole track. Significant increase in the total distance traveled, approximately 432 km, and respectively 197 982 s decrease in total travel time in the scenario with 100 percent HAV is the consequence of high frequency of vehicles with higher desired speed and less vehicle-vehicle interactions in this scenario. The result of evaluation shows that the highly automated vehicle can contribute to more efficient traffic in terms of reducing the travel time and production of more veh.km travelled according to the definition of traffic efficiency by [27].

The average travel speed by time and space are calculated based on the microscopic data of each vehicle in each simulation time step. Table 7.5 displays these two values in different scenarios regarding time and space. Average travel speed as an indicator for efficiency shows that the higher penetration rate of Highly Automated Vehicle contribute

Tab. 7.5: Average travel speed in different scenarios.

Scenario	Average Travel Speed by Time ($\frac{km}{h}$)	Average Travel Speed by Space ($\frac{km}{h}$)
0% HAV	82.8	80.3
50% HAV	99.0	98.5
100% HAV	122.1	122.9

to higher efficiency in traffic in terms of increasing the overall average speed of traffic flow.

Macroscopic variables such as traffic flow, density, speed reflect the average state of the overall traffic flow in contrast to the microscopic traffic flow variables. An important relation in traffic flow theory is the continuity equation $q = k \cdot u$ (traffic flow equals density times the speed). Fundamental diagram describes the relation between the macroscopic traffic flow variables based on continuity equation [73]. Macroscopic variables are calculated by means of data provided by measurement loops implemented in every five hundred meter distance in the simulated track. Each measurement loop calculates the density, flow and speed in a 60 s time interval.

Figure 7.3 illustrates the traffic flow by traffic density for all scenarios. Different scenarios are differentiated by various colors. In Flow-Density diagram gradient of the line fitting the data set and passing the axes intersection defines the desired speed [157]. Gradients of the lines (a), (b) and (c) are representative of the desired speed in each scenario. The steepest gradient belongs to the line (a) which is fitting the data of the scenario with 100 percent Highly Automated Vehicles. The higher desired speed consequences in higher average speed as discussed in section.

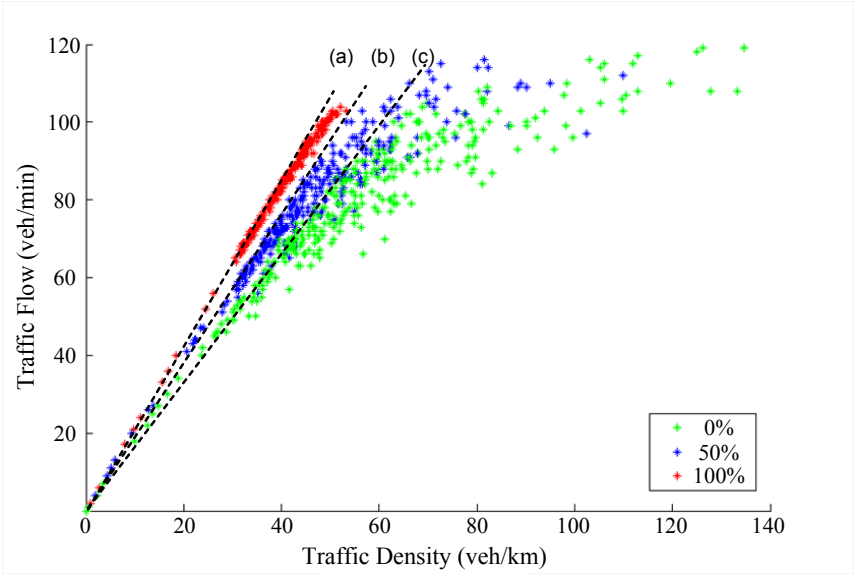

Fig. 7.3: Fundamental Diagram of Traffic Density vs. Traffic Flow [198].

Another outcome of this figure can be explained as a harmonization effect by increasing HAV penetration rate. Green points depicting the data for the baseline scenario are more scattered than the blue ones illustrating the scenario with 50 percent penetration rate and red points have the highest level of harmonization. This phenomenon can be explained by

higher frequency of vehicles having high desired speed and equal reaction time in scenarios with 50 and 100 percent penetration rate of HAV respectively.

7.5 Conclusion and Discussion

Within this thesis, highly automated vehicles are evaluated in traffic flow on highways by means of microscopic traffic simulation. Microscopic traffic simulation models study individual vehicles in traffic flow. It is therefore feasible to include advanced driver assistance systems functionality in the driver models of the simulation. A microscopic traffic simulation tool to be used for simulation of traffic including highly automated vehicles should enable the complete substitution of driver model and its sub-models. SIL feature in PELOPS enables the implementation of the highly automated vehicle's model by fully overriding the driver model and thus ensures its functionality and parameter tuning.

The implementation methodology applied in this chapter is rather a new attempt in impact evaluation of ADAS in traffic flow, which is also considered as one of the main achievements of this thesis. In case that a new strategy is applied in a module of HAV controller model, or alteration of a parameter in the model is investigated, this methodology allows the easy implementation of the improved model. Furthermore, the impact of this model improvements on traffic can be also evaluated.

Within the scope of the first research study, impacts of highly automated vehicles on traffic safety and efficiency are studied by measurement of a set of indicators that are characterizing these aspects. In addition, PELOPS is used as a deterministic traffic simulation model. Thus, the evaluation process in terms of defined indicators is only performed on the result of one validated simulation run. Improving PELOPS to perform stochastic simulations by involving random number seeds during the simulation can achieve a broader representative variety of traffic situations. Performing the required statistical analysis can ensure statistical validity of the results.

In summary, this chapter introduces an implementation methodology for evaluation of advanced driver assistance systems, particularly highly automated driving in microscopic traffic simulation. With this methodology the impacts of a new tactical decision-making process applied in the model can be investigated. Moreover, adjustment of model parameters can be performed systematically. The results of impact evaluation in this study with the applied environment model and the basic behavioral strategy show that the increase in the penetration rate of the highly automated vehicle together with proper adjustment of model parameter may result in considerate improvements of safety in traffic in terms of defined indicators. Furthermore, the developed methodology gives the opportunity to compare traffic efficiency and safety measures with different penetration rates in various scenarios by means of microscopic traffic simulation.

8 Conclusion and Future Directions

Within this thesis, a highly automated driving system for highways has been described. The main contribution is development of a novel *hierarchical decision network* which implements the continuous decision-making process of a human driver by determining a discrete set of different behavioral strategies. Each behavior implements a suitable *model predictive maneuver planning* for the specific traffic situation, regarding the overall requirements as well as the certain objectives of the corresponding behavioral strategy. The novel approach offers benefits in terms of flexible and modular functional development and allowing distributed computing. Further improvements of the intelligence can be done by defining a new behavior and adapting its decision-making process to handle its specific requirements and objectives. In the following, concluding remarks and an outlook are presented.

8.1 Concluding Remarks

In Chapter 2, the state-of-the-art frameworks concerning the tactical decision-making process of automated driving have been discussed. It has been revealed that the division of the continuous driving task into a finite set of discrete driving states is the most effective way to master this complex task. However, lack of flexibility and modular expandability as well as the mostly insufficient consideration of the future state of the surrounding traffic in the decision-making process are major shortcomings of the state-of-the-art approaches. Based on the results of the evaluation in this chapter, a novel framework for the tactical decision-making process, the so-called hierarchical decision network, has been presented. One of the main advantages of the proposed framework is the centralization of the interaction-aware traffic scene prediction module and applying its outcomes to ensure a reactive and anticipatory decision-making. Furthermore, introducing the concept of high-level behavioral strategies with their specific objectives and well-defined input/output interfaces simplifies the complex driving task and enables a modular expandability of the system. In addition, thanks to the arbitration layer, which performs the task of situation classification, an intelligent managing of the behavioral strategies in a distributed manner is allowed.

A novel on-line capable approach to maneuver prediction of highway traffic is presented in Chapter 3. The proposed traffic scene prediction module provides the subsequent behavioral strategies with the required information about the future state of the environment. The approach is based on the idea of multi-agent simulation which models the interaction between the future planned maneuvers of all traffic participants over multiple time steps. It was shown that the sophisticated combination of the model-based intention estimation with the learning-based motion prediction has benefits in terms of native extensibility by expert knowledge and reduction of difficulties associated with the curse of dimensionality. Furthermore, the achieved precision and average prediction horizon can be greatly

improved.

In this thesis, three behavioral strategies are developed for highly automated driving in highway applications to accomplish the most of complex traffic situations: Basic Behavioral Strategy, Cooperative Behavioral Strategy and Driver Take Over Behavioral Strategy. In Chapter 4, a novel model predictive maneuver planning for the basic behavioral strategy was presented. The motivation was to develop a maneuver planning which determines the "global optimum" in terms of the above-mentioned definitions and which satisfies the requirements for reactivity and anticipatory. It allows comfortable and safe driving for all the traffic participants. Additionally, the traffic rules are also considered. The non-linear model was first approximated with a hybrid system formulation. To determine the optimal driving goals, two different approaches were applied and evaluated: A mixed-integer quadratic program with an approximated linear objective function and a combinatorial optimization with partly non-linear objective functions.

The combinatorial formulation of the problem achieves the on-line requirement and the freedom in problem formulation to get the "optimal driving behavior", but holds the risk of getting stuck in a local optimum. Thanks to the separation in levels with different priorities, the approach allows a straightforward extension to additional costs. Solving the problem by the mixed-integer quadratic program provides in most cases the same or at least a similar driving behavior, but guarantees to find the global optimum. It could be used to ensure the functionality of the driving behavior and the solution exactness of the combinatorial optimization.

In Chapter 5 a novel on-line capable approach to the cooperative behavioral strategy based on game theory was presented. The introduced prediction and planning loop of the host vehicle captures the mutual dependence between maneuver choices of all traffic participants over multiple time steps. The replanning ability of other vehicles was thus integrated into the planning of a reasonable interactive maneuver sequence for the host vehicle. It was shown that the approach is able to realize different proactive and cooperative driving behaviors in various simulated highway scenarios. For the mathematical modeling of the problem and its solution, methods from game theory have been applied.

Chapter 6 presented an approach for dealing with a driver take over request during autonomous driving based on model predictive control with diminishing horizon. Simulation results were presented for different strategies in order to show the effects of different constraints in the optimization problem. All of the presented strategies, however, achieve the goal of bringing the vehicle to a safe stop within the allotted take over request time or before a potentially stationary obstacle or critical situation in the lane.

In the last five chapters the functional architecture of the tactical decision-making process, the novel traffic scene prediction module and the different behavioral strategies were discussed in detail. All these together provides the complex artificial intelligence of the automated driving function. During the development phase of the tactical level, the following two important issues has to be investigated:

- How can the effect of parameter changes within the tactical decision-making process be objectively evaluated?
- What is the impact of automated driving with actual implementation of its tactical level on traffic safety and traffic efficiency?

For these reasons, a novel framework for impact assessment based on microscopic traffic simulation was developed in Chapter 7 which allows the study of the above questions. In the early stage of the development, the proposed framework can be applied to steadily examine the effect of each modification within the tactical decision-making process on the traffic. Consequently, the enormous costs related to the time-consuming and partly safety-critical real world tests on highways can be saved.

8.2 Outlook

Over the past few years, a lot of progress has been made in automated driving applications. BMW has been testing automated driving on highways in Germany since 2011. „The HAD prototypes are still on going testing and are being continuously improved. Although there have been major improvements in the last decade, all aspects of the automated driving system, including perception, localization, decision-making and path planning algorithms, still need to be further developed in order to bridge the gap between robotics research and a customer-ready system. The next big steps will be to focus on the industrialization of HAD technology: what needs to be done to get such technology into production vehicles? In this area, there is still a lot of work to be done, especially in the area of validation and certification [189].“

Besides the usage for long distance traffic on highways, private vehicles or public buses are operated in urban environments most of the time. Statistics of the United Nations show that the urban population in 2014 accounted for 54% of the total global population. It is predicted that by 2050 about 64% of the developing countries and 86% of the developed countries will be urbanized [161]. As a result, introducing highly automated resp. autonomous driving in urban environments will be the next step for future mobility.

The promising results of the developed methodology attract continuation of this research activity. Two main directions have to be pursued in the future:

1. Future work should focus on improving the current implementation, especially enhancement of the situation assessment and the arbitration process. Here, the machine learning approaches are very promising. On the other side, improvement of the interaction-aware scene prediction module thanks to increasing number of training data is essential, in order to implement an even more human-like predictive decision-making.

2. Application and adaption of the introduced central decision-making process for the urban scenarios. The first successful concept has been developed within a supervised student project [202].

A Implementation Details of the Interaction-aware Traffic Scene Prediction

This chapter gives a detailed overview about the most important implementation details of the interaction-aware traffic scene prediction framework.

A.1 Trajectory Generation

Depending on the results of the developed situation prediction module, the most likely future trajectory of each vehicle in the current traffic scene for the next $T = 5\,\mathrm{s}$ will be generated. The following n-th degree polynomial is a suitable model for this task [178]

$$p(x) = \sum_{i=0}^{n} \alpha_i x^i = \alpha_n x^n + \alpha_{n-1} x^{n-1} + \ldots + \alpha_0. \tag{A.1}$$

The boundary conditions of $p(x)$ are determined by the polynomial coefficients α_i. The calculation is performed in a lane-relative coordinate system. Thus, the trajectory generation is also valid in curves. The lateral offset $y(x)$ along the trajectory is given at the position x by

$$y(x) = p(x). \tag{A.2}$$

The orientation $\theta(x)$ and curvature $\kappa(x)$ along the trajectory at the position x are determined by derivatives of the polynomial [24]

$$\theta(x) = \tan\left(p'\left(x\right)\right) \tag{A.3}$$

$$\kappa(x) = \frac{p''\left(x\right)}{\left(1 + \left(p'\left(x\right)\right)^2\right)^{\frac{3}{2}}}. \tag{A.4}$$

The orientation of the trajectory at the initial position $x_0 = 0$ corresponds to the heading angle of the vehicle relative to its lane, θ_0. The orientation of the end position x_1 as well as the curvature at the start and end positions of the trajectory are set to zero. The end position itself depends on the predicted interaction-aware longitudinal motion of the corresponding vehicle. Based on the most likely predicted lateral motion, the generated trajectory guides the measured initial lateral offset y_0 to the end offset y_1. The polynomial

boundary conditions can thus be summarized as

$$\begin{aligned} p(x_0) &= y_0 \\ p'(x_0) &= \arctan(\theta_0) \\ p''(x_0) &= 0 \\ p(x_1) = y_1 &= \begin{cases} -y_0 & \text{if } P_v(m_{\text{lat}} = 0, \mathcal{F}_v, \mathcal{I}_v) \geq 50\% \\ \pm w_l & \text{else} \end{cases} \\ p'(x_1) &= 0 \\ p''(x_1) &= 0, \end{aligned} \tag{A.5}$$

where w_l is the width of the lane change maneuver. Figure A.1 shows an example of the generated trajectory for a predicted lane change to the left maneuver and the associated coordinate system.

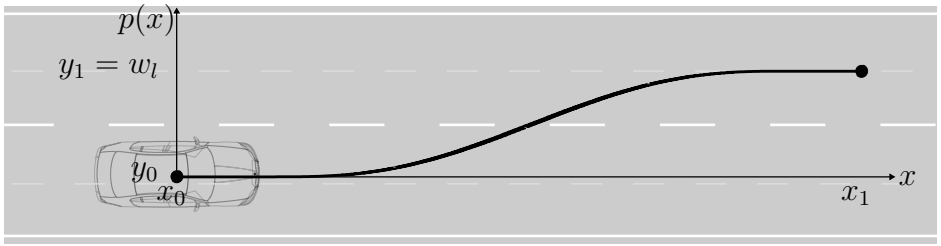

Fig. A.1: Example of a generated lane change trajectory.

Through the use of a quintic function (polynomial of fifth degree), which is C^2 continuous, the polynomial coefficients can be calculated on-line by solving the following linear equation

$$\begin{bmatrix} \alpha_0 \\ \alpha_1 \\ \alpha_2 \\ \alpha_3 \\ \alpha_4 \\ \alpha_5 \end{bmatrix} = \begin{bmatrix} 1 & 0 & 0 & 0 & 0 & 0 \\ 0 & 1 & 0 & 0 & 0 & 0 \\ 0 & 0 & 2 & 0 & 0 & 0 \\ 1 & x_1 & x_1^2 & x_1^3 & x_1^4 & x_1^5 \\ 0 & 1 & 2x_1 & 3x_1^2 & 4x_1^3 & 5x_1^4 \\ 0 & 0 & 2 & 6x_1 & 12x_1^2 & 20x_1^3 \end{bmatrix}^{-1} \begin{bmatrix} y_0 \\ \arctan(\theta_0) \\ 0 \\ y_1 \\ 0 \\ 0 \end{bmatrix}. \tag{A.6}$$

A.2 Prototype Lane Change Trajectory

As discussed in the Section 3.3, one of the features of the proposed Bayesian classifier is to consider the history in the data. To realize it, different prototype lane change trajectories has been recorded from real traffic on highways. These recordings are shown in Figure A.2. Consequently, the current measurements will be compared to these prototype trajectories. The maximum similarity will be used as the third feature to predict the future lateral movement of vehicles.

Regarding to 3.3, the optimal length of the trajectory comparison, n, has to be found. The minimum length for n is two, as with the length of one the feature would be almost the same as the first two features. On the other hand, lane changes should be detected as early

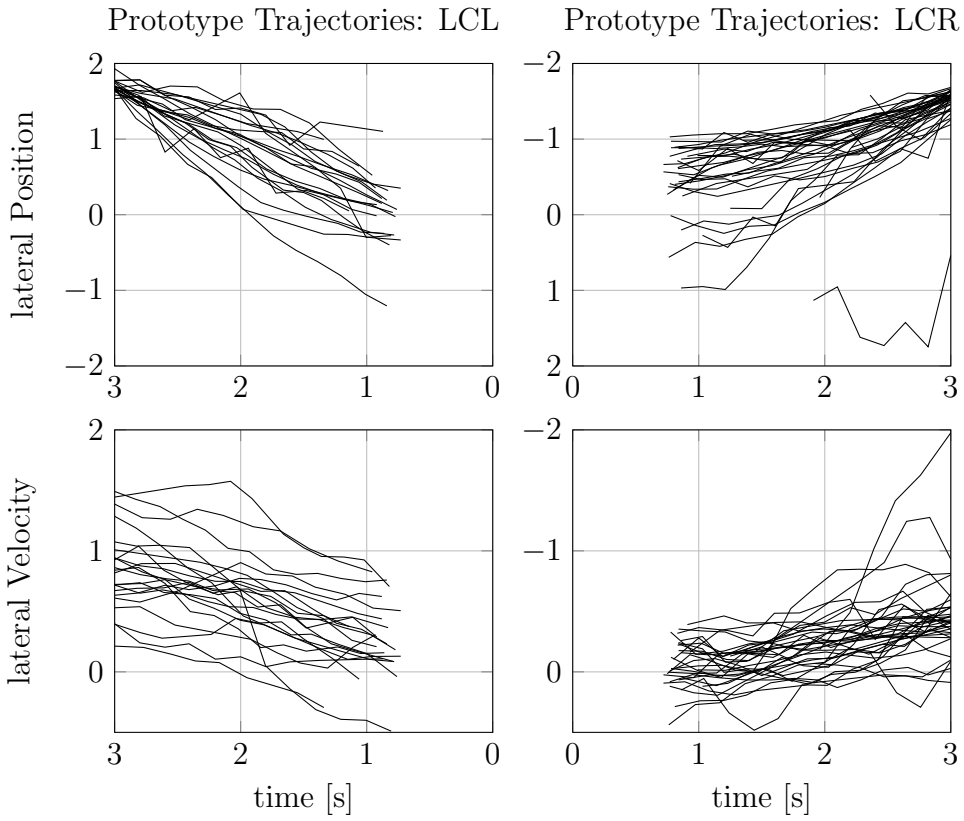

Fig. A.2: The prototype trajectories of different lane change maneuvers with their lateral positions and velocities before a lane change event. The lane change events happen here at the third second.

as possible. The larger n is, the later the Bayesian classifier will detect the lane change. Based on the actual implementation, the trajectory comparison with $n = 3$ (approximately last 0.6 s) shows the best classification performance in terms of the Fisher's criterion.

A.3 Bayesian Classifier Parameters

In the following, the correlation of the different features is calculated over the complete training data to determine if the approach of considering independent features is legit.

	f_1	f_2	f_3
f_1	1.0	0.2827	0.2129
f_2	0.2827	1.0	0.2924
f_3	0.2129	0.2924	1.0

Tab. A.1: Correlation matrix of the three proposed features.

As it can be seen in Table A.1, the correlation ranges from 21% between feature f_1 and f_3 up to nearly 30% between feature f_2 and f_3. Therefore, the normal distribution is also estimated as multivariate. The multivariate normal distribution for a given feature vector

$\mathcal{F}$ is defined as

$$p(\mathcal{F}) = \frac{1}{\sqrt{2\pi|\mathbf{\Sigma}|}} \cdot \exp^{-\frac{1}{2}(\mathcal{F}-\mu)^T \mathbf{\Sigma}^{-1}(\mathcal{F}-\mu)}, \tag{A.7}$$

where $\mathbf{\Sigma}$ is the covariance matrix and μ is the vector of mean values. To enable an on-line computation, the determinant $|\mathbf{\Sigma}|$ and the inverse $\mathbf{\Sigma}^{-1}$ are precomputed. The following tables summarizes the estimated μ and $\mathbf{\Sigma}$ for the three lateral motions.

LCL	μ	$\mathbf{\Sigma}$	f_1	f_2	f_3
f_1	1.5234	f_1	0.9886	0.1295	0.0845
f_2	0.5859	f_2	0.1295	0.1381	0.0465
f_3	0.5426	f_3	0.0845	0.0465	0.0891

Tab. A.2: Multivariate normal distribution of the class: lane change left.

LK	μ	$\mathbf{\Sigma}$	f_1	f_2	f_3
f_1	-0.3141	f_1	0.7627	0.0399	0.0398
f_2	0.0801	f_2	0.0399	0.0307	0.0160
f_3	-0.1666	f_3	0.0398	0.0160	0.1059

Tab. A.3: Multivariate normal distribution of the class: lane keeping.

LCR	μ	$\mathbf{\Sigma}$	f_1	f_2	f_3
f_1	-1.6538	f_1	0.5336	0.0706	0.0686
f_2	-0.2289	f_2	0.0706	0.0599	0.0280
f_3	-0.5604	f_3	0.0686	0.0280	0.0977

Tab. A.4: Multivariate normal distribution of the class: lane change right.

Bibliography

[1] Firebird III. [Online], http://www.carstyling.ru/resources/concept/large/1958_GM_Firebird-III.jpg.

[2] Tobias Achterberg. Scip: solving constraint integer programs. *Mathematical Programming Computation*, 1(1):1–41, 2009.

[3] AdaptiVe. AdaptiVe. [Online], http://www.adaptive-ip.eu/, 2015.

[4] S. B. Adiprasito. *Fahrzeuglängsführung im Niedergeschwindigkeitsbereich*. PhD thesis, Technische Universität Braunschweig, 2004.

[5] Michael Aeberhard, Stefan Schlichthärle, Nico Kaempchen, and Torsten Bertram. Track-to-track fusion with asynchronous sensors using information matrix fusion for surround environment perception. *IEEE Transactions on Intelligent Transportation Systems*, 13(4):1717–1726, December 2012.

[6] G. Agamennoni, J.I. Nieto, and E.M. Nebot. Estimation of multivehicle dynamics by considering contextual information. *Robotics, IEEE Transactions on*, 28(4):855–870, Aug 2012.

[7] A.A. Albousefi, Hao Ying, D. Filev, F. Syed, K.O. Prakah-Asante, F. Tseng, and Hsin-Hsiang Yang. A support vector machine approach to unintentional vehicle lane departure prediction. In *Intelligent Vehicles Symposium Proceedings, 2014 IEEE*, pages 299–303, June 2014.

[8] M. Althoff and A. Mergel. Comparison of markov chain abstraction and monte carlo simulation for the safety assessment of autonomous cars. *Intelligent Transportation Systems, IEEE Transactions on*, 12(4):1237–1247, Dec 2011.

[9] S. Ammoun and F. Nashashibi. Real time trajectory prediction for collision risk estimation between vehicles. In *Intelligent Computer Communication and Processing, 2009. ICCP 2009. IEEE 5th International Conference on*, pages 417–422, Aug 2009.

[10] G.S. Aoude, V.R. Desaraju, L.H. Stephens, and J.P. How. Driver behavior classification at intersections and validation on large naturalistic data set. *Intelligent Transportation Systems, IEEE Transactions on*, 13(2):724–736, June 2012.

[11] M. Ardelt. *Hybrid Control Strategies for Advanced Safety- and Driver Assistance Systems*. PhD thesis, München, Technische Universität, 2012.

[12] M. Ardelt, C. Coester, and N. Kämpchen. Highly automated driving on freeways in real traffic using a probabilistic framework. *Intelligent Transportation Systems, IEEE Transactions on*, 13:1576–1585, 2012.

[13] M. Ardelt, P. Waldmann, F. Homm, and N. Kaempchen. Strategic decision-making process in advanced driver assistance systems. In *6th IFAC Symposium Advances in Automotive Control*, Munich, Germany, July 2010.

[14] S. Arora, A.K. Raina, and A.K. Mittal. Collision avoidance among agvs at junctions. In *Intelligent Vehicles Symposium, 2000. IV 2000. Proceedings of the IEEE*, pages 585–589, 2000.

[15] AutoNOMOS Labs Berlin. Autonomos labs. [Online], 2011. Accessed: 2015-07-13.

[16] C. R. Baker and J. M. Dolan. Traffic interaction in the urban challenge: Putting boss on its best behavior. *IEEE/RSJ International Conference on Intelligent Robots and Systems*, pages 1752–1758, September 2008.

[17] Tirthankar Bandyopadhyay, KokSung Won, Emilio Frazzoli, David Hsu, WeeSun Lee, and Daniela Rus. Intention-aware motion planning. In Emilio Frazzoli, Tomas Lozano-Perez, Nicholas Roy, and Daniela Rus, editors, *Algorithmic Foundations of Robotics X*, volume 86 of *Springer Tracts in Advanced Robotics*, pages 475–491. Springer Berlin Heidelberg, 2013.

[18] C. Basarke, C. Berger, K. Berger, K. Cornelsen, M. Doering, J. Effertz, T. Form, T. Gülke, F. Graefe, P. Hecker, K. Homeier, F. Klose, C. Lipski, M. Magnor, J. Morgenroth, T. Nothdurft, S. Ohl, F. Rauskolb, B. Rumpe, W. Schuhmacher, J. Wille, and L. Wolf. Team CarOLO – Technical Paper. Informatik-Bericht, Technische Universität Braunschweig, 2008.

[19] BBC Technology. Toyota sneak previews self-drive car ahead of tech show. [Online], 2013. Accessed: 2015-07-13.

[20] A. Bemporad, W.P.M.H. Heemels, and B. De Schutter. On hybrid systems and closed-loop mpc systems. *Automatic Control, IEEE Transactions on*, 47(5):863–869, May 2002.

[21] Alberto Bemporad and Manfred Morari. Control of systems integrating logic, dynamics, and constraints. *Automatica*, 35(3):407–427, March 1999.

[22] M. Benmimoun, A. Pütz, A. Zlocki, and L Eckstein. Effects of acc and fcw on speed, fuel consumption, and driving safety. In *Vehicular Technology Conference (VTC Fall), 2012 IEEE*, pages 1–6, 2012.

[23] BMW Group PressClub Global. Ready for takeover! [Online], August 2011. Accessed: 2015-07-13.

[24] I.N. Bornstein, K.A. Semendjajew, G. Musiol, and H. Mühlig. *Taschenbuch der Mathematik*. Verlag Harri Deutsch, 2001.

[25] F. Borrelli. *Constrained Optimal Control of Linear and Hybrid Systems*. Lecture Notes in Control and Information Sciences. Springer Berlin Heidelberg, 2003.

[26] F. Borrelli, A. Bemporad, and M. Morari. *Predictive Control for linear and hybrid systems*. to be published, 2015.

[27] Werner Brilon. Traffic flow analysis beyond traditional methods. In *Proceedings of the 4th International Symposium on Highway Capacity*, pages 26–41, 2000.

[28] A. Broadhurst, S. Baker, and T. Kanade. Monte carlo road safety reasoning. In *Intelligent Vehicles Symposium, 2005. Proceedings. IEEE*, pages 319–324, June 2005.

[29] M. Bröckerhoff. Pelops whitepaper. Technical report, Forschungsgesellschaft Kraftfahrwesen mbH Aachen (FKA), Aachen, Germany, 2007.

[30] K.H. Brodersen, Cheng Soon Ong, K.E. Stephan, and J.M. Buhmann. The balanced accuracy and its posterior distribution. In *Pattern Recognition (ICPR), 2010 20th International Conference on*, 2010.

[31] Statistisches Bundesamt. Verkehrsunfälle 2013. Technical Report 7, Statistisches Bundesamt, Wiesbaden, 2014.

[32] Andrej Cacilo, Sarah Schmidt, Philipp Wittlinger, Florian Herrmann, Wilhelm Bauer, Oliver Sawade, Hannes Doderer, Matthias Hartwig, and Volker Scholz. Hochautomatisiertes fahren auf autobahnen - industriepolitische schlussfolgerungen. Technical report, Fraunhofer-Institut Für Arbeitswirtschaft und Organisation IAO, 2015.

[33] David D. Clarke, Patrick J. Ward, and Jean Jones. Overtaking road-accidents: differences in manoeuvre as a function of driver age. In *Accident Analysis and Prevention, Elsevier science Ltd*, 1998.

[34] CNET. Volvo details autonomous Drive Me cars, on sale in 2017. [Online], 2015. Accessed: 2015-07-13.

[35] European Commission. EU Commission White Paper on Transport 2050 . [Online], http://fevr.org/welcome-to-eu-commission-white-paper/, 2011. Accessed: 2015-04-10.

[36] European Commission. Mobility and Transport - Road Safety - Statistics - accidents data. [Online], http://ec.europa.eu/transport/road_safety/specialist/statistics/index_en.htm, Oct 2013. Accessed: 2015-04-10.

[37] T. H. Cormen, C. E. Leiserson, R. L. Rivest, and C. Stein. *Introduction to Algorithms*. The MIT Press, 2009.

[38] Ismail Dagli, Michael Brost, and Gabi Breuel. Action recognition and prediction for driver assistance systems using dynamic belief networks. In *Agent Technologies, Infrastructures, Tools, and Applications for E-Services*, volume 2592 of *Lecture Notes in Computer Science*, pages 179–194. Springer Berlin Heidelberg, 2003.

[39] DARPA. GRAND CHALLENGE 2004. [Online], http://archive.darpa.mil/grandchallenge04/, 2004. Accessed: 2015-04-20.

[40] DARPA. GRAND CHALLENGE 2005. [Online], http://archive.darpa.mil/grandchallenge05/, 2005. Accessed: 2015-04-20.

[41] DARPA. URBAN CHALLENGE. [Online], http://archive.darpa.mil/grandchallenge/, 2007. Accessed: 2015-07-13.

[42] L. C. Davis. Effect of adaptive cruise control systems on traffic flow. *Phys. Rev. E*, 69, 2004.

[43] L.C. Davis. Effect of adaptive cruise control systems on mixed traffic flow near an on-ramp. *Physica A: Statistical Mechanics and its Applications*, 379(1):274–290, 2007.

[44] Definition from Wordreference. Definition from Wordreference. [Online], http://www.wordreference.com/definition/maneuver, 2015. Accessed: 2015-04-14.

[45] U. Dogan, J. Edelbrunner, and I. Iossifidis. Autonomous driving: A comparison of machine learning techniques by means of the prediction of lane change behavior. In *Robotics and Biomimetics (ROBIO), 2011 IEEE International Conference on*, pages 1837–1843, Dec 2011.

[46] Edmund Donges. A conceptual framework for active safety in road traffic. *Vehicle System Dynamics*, 32(2-3):113–128, 1999.

[47] R. Dowling, A. Skabardonis, and Alexiadis V. *Traffic Analysis Toolbox Volume III: Guidelines for Applying Traffic Microsimulation Software.* US Department of Transportation-Federal Highway Administration, 2004.

[48] Yaoqiong Du, Yizhou Wang, and Ching-Yao Chan. Autonomous lane-change controller. In *Intelligent Vehicles Symposium (IV), 2015 IEEE International Conference on*, 2015.

[49] A. E. Eiben and J. E. Smith. *Introduction to Evolutionary Computing.* Springer, 2007.

[50] Kalan Elliott. The Original Futurama: The Legacy of the 1939 World's Fair. [Online], http://www.popularmechanics.com/technology/design/a5322/4345790/, 2010. Accessed: 2015-04-10.

[51] Tom Fawcett. An introduction to roc analysis. *Pattern Recogn. Lett.*, 27(8):861–874, 2006.

[52] Kevin Fitchard. Ford is ready for the autonomous car. Are drivers? [Online], https://gigaom.com/2012/04/09/ford-is-ready-for-the-autonomous-car-are-drivers/, 2012. Accessed: 2015-07-13.

[53] C. Frese and J. Beyerer. A comparison of motion planning algorithms for cooperative collision avoidance of multiple cognitive automobiles. In *Intelligent Vehicles Symposium (IV), 2011 IEEE*, pages 1156–1162, June 2011.

[54] Christian Frese. *Planung kooperativer Fahrmanöver für kognitive Automobile*. PhD thesis, Karlsruhe Institute of Technology, 2012.

[55] H. Fritz, A. Gern, H. Schiemenz, and C. Bonnet. Chauffeur assistant: a driver assistance system for commercial vehicles based on fusion of advanced acc and lane keeping. In *Intelligent Vehicles Symposium, 2004 IEEE*, pages 495–500, June 2004.

[56] A. Furda and L. Vlacic. Enabling safe autonomous driving in real-world city traffic using multiple criteria decision making. *Intelligent Transportation Systems Magazine, IEEE*, 3(1):4–17, 2011.

[57] GCDC. Grand Cooperative Driving Challenge. [Online], http://www.gcdc.net/, 2011. Accessed: 2015-04-20.

[58] N.B. Geddes. *Magic Motorways*. Read Books, 2009.

[59] A. Geiger, M. Lauer, F. Moosmann, B. Ranft, H. Rapp, C. Stiller, and J. Ziegler. Team annieway's entry to the 2011 grand cooperative driving challenge. *Intelligent Transportation Systems, IEEE Transactions on*, 13(3):1008–1017, 2012.

[60] T. Gindele, S. Brechtel, and R. Dillmann. A probabilistic model for estimating driver behaviors and vehicle trajectories in traffic environments. In *Intelligent Transportation Systems (ITSC), 2010 13th International IEEE Conference on*, pages 1625–1631, Sept 2010.

[61] Tobias Gindele, Daniel Jagszent, Benjamin Pitzer, and Rüdiger Dillmann. Design of the planner of team annieway's autonomous vehicle used in the darpa urban challenge 2007. In *Intelligent Vehicles Symposium, 2008 IEEE*, pages 1131–1136, June 2008.

[62] S. Glaser, B. Vanholme, S. Mammar, D. Gruyer, and L. Nouveliere. Maneuver-based trajectory planning for highly autonomous vehicles on real road with traffic and driver interaction. *Intelligent Transportation Systems, IEEE Transactions on*, 11(3):589–606, 2010.

[63] Christian Gold, Daniel Damböck, Lutz Lorenz, and Klaus Bengler. "Take Over!" How long does it take to get the driver back into the loop? In *57th Human Factors and Ergonomics Society (HFES) International Annual Meeting*, San Diego (CA), USA, September 2013.

[64] B. Gutjahr and M. Werling. Automatic collision avoidance during parking and maneuvering - an optimal control approach. In *Intelligent Vehicles Symposium Proceedings, 2014 IEEE*, pages 636–641, June 2014.

[65] Isabelle Guyon and André Elisseeff. An introduction to variable and feature selection. *Journal of Machine Learning Research*, 3, 2003.

[66] J. C. Harsanyi. Games with incomplete information played by "bayesian" players, i-iii. *Manage. Sci.*, 50(12 Supplement):1804–1817, December 2004.

[67] HAVEit. HAVEit. [Online], http://www.haveit-eu.org/, 2010.

[68] G. Hegeman, A. Tapani, and S. Hoogendoorn. Overtaking assistant assessment using traffic simulation. *Transportation Research Part C: Emerging Technologies*, 17(6):617–630, 2009.

[69] F. Heimes and H.-H. Nagel. Towards active machine-vision-based driver assistance for urban areas. *International Journal of Computer Vision*, 50(1):5–34, 2002.

[70] M. Herceg, M. Kvasnica, C.N. Jones, and M. Morari. Multi-Parametric Toolbox 3.0. In *Proc. of the European Control Conference*, pages 502–510, July 2013.

[71] Stephen Hirst and Robert Graham. The format and presentation of collision warnings. In Y. Ian Noy, editor, *Ergonomics and Safety of Intelligent Driver Interfaces*, page 1997. L. Erlbaum Associates Inc., 1997.

[72] F. Homm, N. Kaempchen, and D. Burschka. Fusion of laserscannner and video based lanemarking detection for robust lateral vehicle control and lane change maneuvers. In *Intelligent Vehicles Symposium*, pages 969–974, Baden-Baden, Germany, June 2011.

[73] S.P. Hoogendoorn and V.L. Knoop. *The Transport System and Transport Policy: An Introduction*, chapter Traffic flow theory and modelling. Edward Elgar, 2013.

[74] C. Howson and P. Urbach. *Scientific Reasoning: The Bayesian Approach*. Philosophy Series. Open Court, 2006.

[75] IEEE SPECTRUM. How Google's Autonomous Car Passed the First U.S. State Self-Driving Test. [Online], 2014. Accessed: 2015-07-13.

[76] Helmut Janker, editor. *Straßenverkehrsordnung (StVO)*. Deutscher Taschenbuch Verlag, 2015.

[77] László A. Jeni, Jeffrey F. Cohn, and Fernando De La Torre. Facing imbalanced data–recommendations for the use of performance metrics. In *Proceedings of the 2013 Humaine Association Conference on Affective Computing and Intelligent Interaction, IEEE*. IEEE Computer Society, 2013.

[78] Leslie Pack Kaelbling, Michael L Littman, and Anthony R Cassandra. Planning and acting in partially observable stochastic domains. *Artificial intelligence*, 101(1):99–134, 1998.

[79] Nico Kaempchen, Michael Aeberhard, Peter Waldmann, Michael Ardelt, and Sebastian Rauch. Der bmw nothalteassistent: Hochautomatisiertes fahren für mehr sicherheit im straßenverkehr. *Elektronik Automotive*, 8/9:26–29, September 2011.

[80] Sören Kammel, Julius Ziegler, Benjamin Pitzer, Moritz Werling, Tobias Gindele, Daniel Jagzent, Joachim Schröder, Michael Thuy, Matthias Goebl, Felix von Hundelshausen, Oliver Pink, Christian Frese, and Christoph Stiller. Team annieway's autonomous system for the 2007 darpa urban challenge. *Journal of Field Robotics*, 25(9):615–639, 2008.

[81] Nico Kämpchen, Michael Aeberhard, Michael Ardelt, and Sebastian Rauch. Technologies for highly automated driving on highways. *ATZ worldwide*, 114(6):34–38, 2012.

[82] Nico Kämpchen, Michael Aeberhard, Peter Waldmann, Michael Ardelt, and Sebastian Rauch. Der BMW Nothalteassistent: Hochautomatisiertes Fahren für mehr Sicherheit im Straßenverkehr. *Elektronik Automotive*, 8/9:26–29, September 2011.

[83] D. Kasper, G. Weidl, T. Dang, G. Breuel, A. Tamke, A. Wedel, and W. Rosenstiel. Object-oriented bayesian networks for detection of lane change maneuvers. *Intelligent Transportation Systems Magazine, IEEE*, 4(3):19–31, 2012.

[84] Alex Keel. *Statistik II, Wahrscheinlichkeit*. Verlag Wilhelm Surbir Wittenbach/St. Gallen, 2004.

[85] E. C. Kerrigan and J. M. Maciejowski. Soft constraints and exact penalty functions in model predictive control. In *Proc. UKACC International Conference (Control 2000)*, 2000.

[86] N. Kirby. *Introduction to Game AI*. Course Technology/Cengage Learning, 2011.

[87] Ko-FAS. Kooperative Fahrzeugsicherheit. [Online], http://www.ko-fas.de, 2009-2013. Accessed: 2015-04-20.

[88] Thorsten Koch, Tobias Achterberg, Erling Andersen, Oliver Bastert, Timo Berthold, Robert E. Bixby, Emilie Danna, Gerald Gamrath, Ambros M. Gleixner, Stefan Heinz, Andrea Lodi, Hans Mittelmann, Ted Ralphs, Domenico Salvagnin, Daniel E. Steffy, and Kati Wolter. MIPLIB 2010. *Mathematical Programming Computation*, 3(2):103–163, 2011.

[89] H.W. Kuhn, K.J. Arrow, and A.W. Tucker. *Contributions to the Theory of Games*. Number Bd. 2 in Annals of mathematics studies. Princeton University Press, 1953.

[90] P. Kumar, Mathias Perrollaz, Stéphanie Lefèvre, and Christian Laugier. Learning-based approach for online lane change intention prediction. In *Intelligent Vehicles Symposium (IV), 2013 IEEE*, pages 797–802, June 2013.

[91] Damon Lavring. Google's Autonomous Prius Drives Blind Man to Taco Bell. [Online], http://www.wired.com/2012/03/googles-autonomous-prius-drives-blind-man-to-taco-bell/, 2012. Accessed: 2015-04-10.

[92] A. Lawitzky, D. Wollherr, and M. Buss. Maneuver-based risk assessment for high-speed automotive scenarios. In *Intelligent Robots and Systems (IROS), 2012 IEEE/RSJ International Conference on*, pages 1186–1191, Oct 2012.

[93] Andreas Lawitzky, Daniel Althoff, Christoph F. Passenberg, Georg Tanzmeister, Dirk Wollherr, and Martin Buss. Interactive scene prediction for automotive applications. In *Intelligent Vehicles Symposium (IV), 2013 IEEE*, pages 1028–1033, 2013.

[94] S. Lefèvre, C. Laugier, and J. Ibanez-Guzman. Evaluating risk at road intersections by detecting conflicting intentions. In *Intelligent Robots and Systems (IROS), 2012 IEEE/RSJ International Conference on*, pages 4841–4846, Oct 2012.

[95] S. Lefèvre, D. Vasquez, and C. Laugier. A survey on motion prediction and risk assessment for intelligent vehicles. *ROBOMECH Journal*, 1(1):1–14, 2014.

[96] L. Li and Fei-Yue Wang. *Advanced Motion Control and Sensing for Intelligent Vehicles*. Springer US, 2007.

[97] Li Li, Fei-Yue Wang, and H. Kim. Cooperative driving and lane changing at blind crossings. In *Intelligent Vehicles Symposium, 2005. Proceedings. IEEE*, pages 435–440, June 2005.

[98] Li Li, Ding Wen, and Danya Yao. A survey of traffic control with vehicular communications. *Intelligent Transportation Systems, IEEE Transactions on*, 15(1):425–432, Feb 2014.

[99] G. Lidoris, K. Klasing, A. Bauer, Tingting Xu, K. Kuhnlenz, D. Wollherr, and M. Buss. The autonomous city explorer project: aims and system overview. In *ntelligent Robots and Systems, 2007. IROS 2007. IEEE/RSJ International Conference on*, pages 560–565, Oct 2007.

[100] G. Lidoris, D. Wollherr, and M. Buss. *Bayesian Framework for State Estimation and Robot Behaviour Selection in Dynamic Environments*. INTECH Open Access Publisher, 2008.

[101] G. Lidoris, D. Wollherr, and M. Buss. Bayesian state estimation and behavior selection for autonomous robotic exploration in dynamic environments. In *Intelligent Robots and Systems, 2008. IROS 2008. IEEE/RSJ International Conference on*, pages 1299–1306, Sept 2008.

[102] R. Liu and J. Tate. Network effects of intelligent speed adaptation systems. *Transportation*, 31(3):297–325, 2004.

[103] L.N. Long, S.D. Hanford, O. Janrathitikarn, G.L. Sinsley, and J.A. Miller. A review of intelligent systems software for autonomous vehicles. In *IEEE Symposium on Computational Intelligence in Security and Defense Applications, 2007. CISDA 2007*, pages 69–76, 2007.

[104] W. J R Louwerse and S.P. Hoogendoorn. Adas safety impacts on rural and urban highways. In *Intelligent Vehicles Symposium, 2004 IEEE*, pages 887–890, 2004.

[105] J. Maciejowski. *Predictive Control with Constraints*. Prentice Hall, 2002.

[106] Aaron Martinez and Enrique Fernández. *Learning ROS for Robotics Programming*. Packt Publishing, sep 2013.

[107] David Mayne. Nonlinear model predictive control:challenges and opportunities. In Frank Allgöwer and Alex Zheng, editors, *Nonlinear Model Predictive Control*, volume 26 of *Progress in Systems and Control Theory*, pages 23–44. Birkhäuser Basel, 2000.

[108] Mercedes-Benz next. Autonom auf den Spuren von Bertha Benz. [Online], http://next.mercedes-benz.com/autonom-auf-den-spuren-von-bertha-benz/, 2013. Accessed: 2015-04-10.

[109] D. Meyer-Delius, C. Plagemann, and W. Burgard. Probabilistic situation recognition for vehicular traffic scenarios. In *Robotics and Automation, 2009. ICRA '09. IEEE International Conference on*, pages 459–464, May 2009.

[110] Zbigniew Michalewicz and David B. Fogel. *How to solve it: modern heuristics*. Springer, 2004.

[111] M. Minderhoud and P. Bovy. Impact of Intelligent Cruise Control on Motorway Capacity. *Transportation Research Record*, 1679:1–9, 1999.

[112] M. Minderhoud and P. Bovy. Extended time-to-collision measures for road traffic safety assessment. *Accident Analysis and Prevention*, 33:89–97, 2001.

[113] Michael Montemerlo, Jan Becker, Suhrid Bhat, Hendrik Dahlkamp, Dmitri Dolgov, Scott Ettinger, Dirk Haehnel, Tim Hilden, Gabe Hoffmann, Burkhard Huhnke, Doug Johnston, Stefan Klumpp, Dirk Langer, Anthony Levandowski, Jesse Levinson, Julien Marcil, David Orenstein, Johannes Paefgen, Isaac Penny, Anna Petrovskaya, Mike Pflueger, Ganymed Stanek, David Stavens, Antone Vogt, and Sebastian Thrun. Junior: The stanford entry in the urban challenge. *Journal of Field Robotics*, 25(9):569–597, 2008.

[114] M.W. Mueller and R D'Andrea. A model predictive controller for quadrocopter state interception. In *Control Conference (ECC), 2013 European*, pages 1383–1389, 2013.

[115] R.B. Myerson. *GAME THEORY*. Harvard University Press, 1997.

[116] J.E. Naranjo, C. Gonzalez, R. Garcia, and T. de Pedro. Lane-change fuzzy control in autonomous vehicles for the overtaking maneuver. *Intelligent Transportation Systems, IEEE Transactions on*, 9(3):438–450, Sept 2008.

[117] D. C K Ngai and N. H C Yung. A multiple-goal reinforcement learning method for complex vehicle overtaking maneuvers. *Intelligent Transportation Systems, IEEE Transactions on*, 12(2):509–522, 2011.

[118] T. Niimura and K. Tanaka. *An Introduction to Fuzzy Logic for Practical Applications*. Springer New York, 1996.

[119] J. Nilsson and J. Sjoberg. Strategic decision making for automated driving on two-lane, one way roads using model predictive control. In *Intelligent Vehicles Symposium (IV), 2013 IEEE*, pages 1253–1258, June 2013.

[120] N. Oliver and A.P. Pentland. Graphical models for driver behavior recognition in a smartcar. In *Intelligent Vehicles Symposium, 2000. IV 2000. Proceedings of the IEEE*, pages 7–12, 2000.

[121] Sylvie C. W. Ong, Shao Wei Png, David Hsu, and Wee Sun Lee. Planning under uncertainty for robotic tasks with mixed observability. *International Journal of Robotics Research*, 29(8):1053–1068, July 2010.

[122] M.J. Osborne. *An Introduction to Game Theory*. Oxford University Press, Incorporated, 2009.

[123] Christos Papadimitriou and John N. Tsitsiklis. The complexity of markov decision processes. *Mathematics of Operations Research*, 12(3):441–450, Aug 1987.

[124] M Papageorgiou, M. Leibold, and M. Buss. *Optimierung. Statische, dynamische, stochastische Verfahren für die Anwendung*. Springer Vieweg, 2012.

[125] V. Paruchuri. Inter-vehicular communications: Security and reliability issues. In *ICT Convergence (ICTC), 2011 International Conference on*, pages 737–741, Sept 2011.

[126] M. Pellkofer. *Verhaltensentscheidung für autonome Fahrzeuge mit Blickrichtungssteuerung*. PhD thesis, Universität der Bundeswehr München, 2003.

[127] Sebastian Rauch, Thomas Schaller, Artem Savkin, and Peter Hecker. Hochgenaue Fahrzeugeigenlokalisierung und kollektives Erlernen hochgenauer digitaler Karten. In *12. Symposium Automatisierungssysteme, Assistenzsysteme und eingebettete Systeme für Transportmittel*, Braunschweig, Germany, Februar 2011.

[128] Fred W. Rauskolb, Kai Berger, Christian Lipski, Marcus A. Magnor, Karsten Cornelsen, Jan Effertz, Thomas Form, Fabian Graefe, Sebastian Ohl, Walter Schumacher, Jörn-Marten Wille, Peter Hecker, Tobias Nothdurft, Michael Doering, Kai Homeier, Johannes Morgenroth, Lars C. Wolf, Christian Basarke, Christian Berger, Tim Gülke, Felix Klose, and Bernhard Rumpe. Caroline: An autonomously driving vehicle for urban environments. *Journal of Field Robotics*, 2008.

[129] re/code. Google's new self-driving car ditches the steering wheel. [Online], http://recode.net/2014/05/27/googles-new-self-driving-car-ditches-the-steering-wheel/, 2014. Accessed: 2015-07-13.

[130] T. Rehder, Z. Georgiev, L. Louis, D. Schramm, and D. Burschka. Effektive nutzung von hochdimensionalen kontinuierlichen umfelddaten zur prädiktion von fahrverhalten mit bayesschen netzen. In *16. Braunschweiger Symposium AAET 2015: Automatisierungs-, Assistenzsysteme und eingebettete Systeme für Transportmittel*, 2015.

[131] Ian Riches. Automotive Ethernet Market Growth Outlook. [Online], `http://www.google.com/url?sa=t&rct=j&q=&esrc=s&source=web&cd=1&ved=0CCEQFjAA&url=http%3A%2F%2Fstandards.ieee.org%2Fevents%2Fautomotive%2F2014%2F00_Automotive_Ethernet_Market_Growth_Outlook.pdf&ei=_LwnVcrgG8uzswGKoIKIAw&usg=AFQjCNFKV3y80xtFdow3FDmOWAHmrmSk6w&bvm=bv.90491159,d.bGg&cad=rja`, 2014. Accessed: 2015-04-10.

[132] ROS. Robot Operating System. [Online], http://www.ros.org, 2015. Accessed: 2015-04-10.

[133] J. K. Rosenblatt. Damn: a distributed architecture for mobile navigation. *Journal of Experimental & Theoretical Artificial Intelligence*, 9:339–360, 1997.

[134] S. J. Russell and P. Norvig. *Artificial Intelligence: A Modern Approach*. Pearson Education, 2 edition, 2010.

[135] SAE International. Taxonomy and definitions for terms related to on-road motor vehicle automated driving systems. Technical Report SAE J 3016, SAE International, January 2014.

[136] Jason Sanders and Edward Kandrot. *CUDA by Example: An Introduction to General-Purpose GPU Programming*. Addison Wesley, 2010.

[137] J. Schlechtriemen, A. Wedel, J. Hillenbrand, G. Breuel, and K.-D. Kuhnert. A lane change detection approach using feature ranking with maximized predictive power. In *Intelligent Vehicles Symposium Proceedings, 2014 IEEE*, pages 108–114, June 2014.

[138] Miranda A. Schreurs and Sibyl D. Steuwer. *Autonomes Fahren: Technische, rechtliche und gesellschaftliche Aspekte*, chapter 8, pages 151–173. Springer Berlin Heidelberg, 2015.

[139] R. Schubert, E. Richter, and G. Wanielik. Comparison and evaluation of advanced motion models for vehicle tracking. In *Information Fusion, 2008 11th International Conference on*, pages 1–6, June 2008.

[140] R. Schubert, K. Schulze, and G. Wanielik. Situation assessment for automatic lane-change maneuvers. *Intelligent Transportation Systems, IEEE Transactions on*, 11(3):607–616, Sept 2010.

[141] Wilko Schwarting and Patrick Pascheka. Recursive conflict resolution for cooperative motion planning in dynamic highway traffic. In *Intelligent Transportation Systems (ITSC), 2014 IEEE 17th International Conference on*, 2014.

[142] Yoav Shoham and Kevin Leyton-Brown. *Multiagent Systems: Algorithmic, Game-Theoretic, and Logical Foundations*. Cambridge University Press, 2008.

[143] M. L. Sichitiu and M. Kihl. Inter-vehicle communication systems: A survey. *Communications Surveys Tutorials, IEEE*, 10(2):88–105, Feb 2008.

[144] B. Siciliano and O. Khatib. *Springer Handbook of Robotics*. Gale virtual reference library. Springer, 2008.

[145] SIMTD. Sichere Intelligente Mobilität Testfeld Deutschland. [Online], http://www.simtd.de, 2008-2013. Accessed: 2016-07-09.

[146] Stanford Report. Stanford's robotic Audi to brave Pikes Peak without a driver. [Online], http://news.stanford.edu/news/2010/february1/shelley-pikes-peak-020310.html, 2010. Accessed: 2015-07-13.

[147] T. Gasser et al. Rechtsfolgen zunehmeder fahrzeugautomatisierung. Technical Report Fahrzeugtechnik Heft F 83, Bundesanstalt für Straßenwesen, January 2012.

[148] G. Tanzmeister, M. Friedl, D. Wollherr, and M Buss. Path planning on grid maps with unknown goal poses. In *Intelligent Transportation Systems - (ITSC), 2013 16th International IEEE Conference on*, pages 430–435, Oct 2013.

[149] The New York Times. G.M. EN-V: Sharpening the Focus of Future Urban Mobility. [Online], http://wheels.blogs.nytimes.com/2010/03/24/g-m-en-v-sharpening-the-focus-of-future-urban-mobility/?_r=0, 2010. Accessed: 2015-07-13.

[150] The New York Times. Elon Musk Says Self-Driving Tesla Cars Will Be in the U.S. by Summer. [Online], 2015. Accessed: 2015-07-13.

[151] The Verge. This is Tesla's D: an all-wheel-drive Model S with eyes on the road. [Online], http://www.theverge.com/2014/10/9/6955357/this-is-tesla-s-d-an-all-wheel-drive-car-with-eyes-on-the-road, 2014. Accessed: 2015-07-13.

[152] J. Thomas. Höllen Trip - Freihändig durch die grüne Hölle der Nürburgring Nordschleife. *Auto Motor Sport*, 25:138–139, 2009.

[153] Sebastian Thrun, Wolfram Burgard, and Dieter Fox. *Probabilistic Robotics*. The MIT Press, Cambridge, MA, 2005.

[154] Sebastian Thrun, Mike Montemerlo, Hendrik Dahlkamp, David Stavens, Andrei Aron, James Diebel, Philip Fong, John Gale, Morgan Halpenny, Gabriel Hoffmann, Kenny Lau, Celia Oakley, Mark Palatucci, Vaughan Pratt, Pascal Stang, Sven Strohband, Cedric Dupont, Lars-Erik Jendrossek, Christian Koelen, Charles Markey, Carlo Rummel, Joe van Niekerk, Eric Jensen, Philippe Alessandrini, Gary Bradski, Bob Davies, Scott Ettinger, Adrian Kaehler, Ara Nefian, and Pamela Mahoney.

Stanley: The robot that won the darpa grand challenge. *Journal of Field Robotics*, 23(9):661–692, 2006.

[155] International Business Times. Google Inc. Says Self-Driving Car Will Be Ready By 2020. [Online], 2014. Accessed: 2015-07-13.

[156] P. Trautman and A. Krause. Unfreezing the robot: Navigation in dense, interacting crowds. In *Intelligent Robots and Systems (IROS), 2010 IEEE/RSJ International Conference on*, pages 797–803, Oct 2010.

[157] Martin Treiber and Arne Kesting. *Traffic Flow Dynamics: Data, Models and Simulation*. Springer Berlin Heidelberg, 2013.

[158] A. Turnwald, W. Olszowy, D. Wollherr, and M. Buss. Interactive navigation of humans from a game theoretic perspective. In *Intelligent Robots and Systems (IROS 2014), 2014 IEEE/RSJ International Conference on*, 2014.

[159] S. Ulbrich and M. Maurer. Probabilistic online pomdp decision making for lane changes in fully automated driving. In *Intelligent Transportation Systems - (ITSC), 2013 16th International IEEE Conference on*, pages 2063–2067, Oct 2013.

[160] S. Ulbrich and M. Maurer. Evaluation einer taktischen verhaltensentscheidungsfindung für fahrstreifenwechsel beim vollautomatisierten fahren in städten. In *9. Workshop Fahrerassistenzsysteme (FAS2014), Walting, Deutschland*, 2014.

[161] United Nations, Department of Economic and Social Affairs, Population Division. World Urbanization Prospects: The 2014 Revision, Highlights (ST/ESA/SER.A/352). Technical report, New York, 2014.

[162] Chris Urmson, Joshua Anhalt, Drew Bagnell, Christopher Baker, Robert Bittner, M. N. Clark, John Dolan, Dave Duggins, Tugrul Galatali, Chris Geyer, Michele Gittleman, Sam Harbaugh, Martial Hebert, Thomas M. Howard, Sascha Kolski, Alonzo Kelly, Maxim Likhachev, Matt McNaughton, Nick Miller, Kevin Peterson, Brian Pilnick, Raj Rajkumar, Paul Rybski, Bryan Salesky, Young-Woo Seo, Sanjiv Singh, Jarrod Snider, Anthony Stentz, William Whittaker, Ziv Wolkowicki, Jason Ziglar, Hong Bae, Thomas Brown, Daniel Demitrish, Bakhtiar Litkouhi, Jim Nickolaou, Varsha Sadekar, Wende Zhang, Joshua Struble, Michael Taylor, Michael Darms, and Dave Ferguson. Autonomous driving in urban environments: Boss and the urban challenge. *Journal of Field Robotics*, 25(8):425–466, 2008.

[163] P. Vadakkepat, Kay Chen Tan, and Wang Ming-Liang. Evolutionary artificial potential fields and their application in real time robot path planning. In *Evolutionary Computation, 2000. Proceedings of the 2000 Congress on*, volume 1, pages 256–263, 2000.

[164] Bart van Arem, Cornelie J.G. van Driel, and Ruben Visser. The impact of cooperative adaptive cruise control on traffic-flow characteristics. *IEEE Transactions on Intelligent Transportation Systems*, 7(4):429–436, December 2006.

[165] Sabine Verboven and Mia Hubert. Matlab library libra. *Wiley Interdisciplinary Reviews: Computational Statistics*, 2(4):509–515, 2010.

[166] Michel Verleysen and Damien Francois. The curse of dimensionality in data mining and time series prediction. In Joan Cabestany, Alberto Prieto, and Francisco Sandoval, editors, *Computational Intelligence and Bioinspired Systems*, volume 3512 of *Lecture Notes in Computer Science*, pages 758–770. Springer Berlin Heidelberg, 2005.

[167] VisLab. The VisLab Intercontinental Autonomous Challenge. [Online], http://viac.vislab.it/, 2010. Accessed: 2015-07-13.

[168] Volkswagen. Temporary Auto Pilot. [Online], `http://www.volkswagenag.com/content/vwcorp/content/de/innovation/driver_assistance/Temporary_Auto_Pilot.html`, 2012. Accessed: 2015-07-13.

[169] F. Wagner, R. Schmuki, T. Wagner, and P. Wolstenholme. *Modeling Software with Finite State Machines: A Practical Approach*. CRC Press, 2006.

[170] P. Waldmann, N. Kämpchen, M. Ardelt, and F. Homm. Der nothalteassistent - abgesichertes anhalten bei plötzlicher fahrunfähigkeit des fahrzeugführers. In *Proc. of the 3rd Deutscher AAL-Kongress - Ambient Assisted Living*, 2010.

[171] Peter Waldmann and Daniel Niehues. Der BMW Track Trainer - automatisiertes Fahren im Grenzbereich auf der Nürburgring Nordschleife. In *4. Tagung Sicherheit durch Fahrerassistenz*, Garching, Germany, April 2010.

[172] M. Walmsley. *Multi-threaded Programming in C++*. Springer, 2000.

[173] Marc Weber. Where to? A History of Autonomous Vehicles. [Online], http://www.computerhistory.org/atchm/where-to-a-history-of-autonomous-vehicles/, 2014. Accessed: 2015-04-10.

[174] Junqing Wei and J.M. Dolan. A robust autonomous freeway driving algorithm. In *Intelligent Vehicles Symposium, 2009 IEEE*, pages 1015–1020, June 2009.

[175] Junqing Wei, J.M. Dolan, and B. Litkouhi. A prediction- and cost function-based algorithm for robust autonomous freeway driving. In *Intelligent Vehicles Symposium (IV), 2010 IEEE*, pages 512–517, June 2010.

[176] Junqing Wei, J.M. Dolan, and B. Litkouhi. Autonomous vehicle social behavior for highway entrance ramp management. In *Intelligent Vehicles Symposium (IV), 2013 IEEE*, pages 201–207, June 2013.

[177] Moritz Werling. *Ein neues Konzept für die Trajektoriengenerierung und -stabilisierung in zeitkritischen Verkehrsszenarien*. PhD thesis, KIT Scientific Publishing, 2010.

[178] Moritz Werling, Sören Kammel, Julius Ziegler, and Lutz Gröll. Optimal trajectories for time-critical street scenarios using discretized terminal manifolds. *The International Journal of Robotics Research*, 2011.

[179] J. Wille, F. Saust, and M. Maurer. Stadtpilot: Driving autonomously on Braunschweig's inner ring road. In *IEEE Intelligent Vehicles Symposium*, pages 506–511, San Diego (CA), USA, June 2010.

[180] J. M. Wille, K. Homeier, R. Matthaei, T. Nothdurft, S. Ohl, A. Sasse, F. Saust, P. Hecker, M. Maurer, W. Schuhmacher, and L. Wolf. Der Stadtpilot - Autonomes Fahren auf dem Braunschweiger Stadtring. *Technische Universität Braunschweig*, 2011.

[181] H. Winner, S. Hakuli, and G. Wolf, editors. *Handbuch Fahrerassistenzsysteme Grundlagen, Komponenten und Systeme für aktive Sicherheit und Komfort*. GWV Fachverlage GmbH, 2009.

[182] Michael T. Wolf and J.W. Burdick. Artificial potential functions for highway driving with collision avoidance. In *Robotics and Automation, IEEE International Conference on*, 2008.

[183] M. Wooldridge. *An Introduction to MultiAgent Systems*. Wiley, 2009.

[184] Harry Zhang. The Optimality of Naive Bayes. In Valerie Barr and Zdravko Markov, editors, *FLAIRS Conference*. AAAI Press, 2004.

[185] He Zhang, Yuelong Su, Lihui Peng, and Danya Yao. A review of game theory applications in transportation analysis. In *Computer and Information Application (ICCIA), 2010 International Conference on*, pages 152–157, Dec 2010.

[186] J. Ziegler, P. Bender, M. Schreiber, H. Lategahn, T. Strauss, C. Stiller, Thao Dang, U. Franke, N. Appenrodt, C.G. Keller, E. Kaus, R.G. Herrtwich, C. Rabe, D. Pfeiffer, F. Lindner, F. Stein, F. Erbs, M. Enzweiler, C. Knoppel, J. Hipp, M. Haueis, M. Trepte, C. Brenk, A. Tamke, M. Ghanaat, M. Braun, A. Joos, H. Fritz, H. Mock, and M. Hein. Making bertha drive – an autonomous journey on a historic route. *Intelligent Transportation Systems Magazine, IEEE*, 6(2):8–20, Summer 2014.

[187] J. Ziegler and C. Stiller. Fast collision checking for intelligent vehicle motion planning. In *Intelligent Vehicles Symposium (IV), 2010 IEEE*, pages 518–522, June 2010.

[188] Julius Ziegler, Philipp Bender, Henning Lategahn, Markus Schreiber, Tobias Strauß, and C Stiller. Kartengestütztes automatisiertes fahren auf der bertha-benz-route von mannheim nach pforzheim. In *9. Workshop Fahrerassistenzsysteme (FAS2014), Walting, Deutschland*, 2014.

Own Publications and Supervised Student Projects

[189] M. Aeberhard, S. Rauch, M. Bahram, G. Tanzmeister, J. Thomas, Y. Pilat, F. Homm, W. Huber, and N. Kaempchen. Experience, results and lessons learned from automated driving on germany's highways. *Intelligent Transportation Systems Magazine, IEEE*, 7(1):42–57, Spring 2015.

[190] M. Bahram, Z. Ghandeharioun, P. Zahn, M. Baur, W. Huber, and F. Busch. Microscopic traffic simulation based evaluation of highly automated driving on highways. In *Intelligent Transportation Systems (ITSC), 2014 IEEE 17th International Conference on*, pages 1752–1757, Oct 2014.

[191] M. Bahram, Z. Ghandeharioun, P. Zahn, M. Baur, W. Huber, and F. Busch. *Impact Evaluation of Highly Automated Vehicles in Traffic Flow on Highways by means of Microscopic Traffic Simulation*, chapter Fahrerassistenz und Aktive Sicherheit. Wirksamkeit - Beherrschbarkeit - Absicherung, pages 67–80. expert verlag, 2015.

[192] M. Bahram, C. Hubmann, A. Lawitzky, M. Aeberhard, and D Wollherr. A Combined Model- and Learning-based Framework for Interaction-aware Maneuver Prediction. *IEEE Transactions on Intelligent Transportation Systems*, 17(6), 2016.

[193] M. Bahram, A. Lawitzky, J. Friedrichs, M. Aeberhard, and D. Wollherr. A Game Theoretic Approach to Replanning-aware Interactive Scene Prediction and Planning. *IEEE Transactions on Vehicular Technology*, 65(6), 2016.

[194] Mohammad Bahram, Michael Aeberhard, and Dirk Wollherr. Please Take Over! An Analysis and Strategy For a Driver Take Over Request During Autonomous Driving. In *IEEE Intelligent Vehicles Symposium*, Seoul, Korea, June 2015.

[195] Mohammad Bahram, Artur Lohrer, and Michael Aeberhard. Generatives Prädiktionsmodell zur frühzeitigen Spurwechselerkennung. In *9. FAS-Workshop Fahrerassistenzsysteme Walting*, pages 47–54, 2014.

[196] Mohammad Bahram, Anton Wolf, Michael Aeberhard, and Dirk Wollherr. A Prediction-Based Reactive Driving Strategy for Highly Automated Driving Function on Freeways. In *IEEE Intelligent Vehicles Symposium*, pages 400–406, Dearborn (MI), USA, June 2014.

[197] Jasper Friedrichs. Replanning-aware interactive scene prediction and planning. Master's thesis, Lehrstuhl für Steuerungs- und Regelungstechnik, Technische Universität München, 2014.

[198] Zahra Ghandeharioun. Impact evaluation of highly automated vehicles in traffic flow on highways by means of microscopic traffic simulation. Master's thesis, Lehrstuhl Für Verkehrstechnik, Technische Universität München, 2014.

[199] Constantin Hubmann. An interaction and observation based maneuver prediction framework. Master's thesis, Institute for Data Processing, Technische Universität München, 2014.

[200] Artur Lohrer. Prediction and planning for highly automated driving. Master's thesis, Institut für Informatik VI, Technische Universität München, 2014.

[201] Anton Wolf. Development and validation of a prediction-based, reactive driving strategy for highly automated driving on freeways. Master's thesis, Lehrstuhl für Steuerungs- und Regelungstechnik, Technische Universität München, 2014.

[202] Yupeng Wu. Intention-aware motion planning for highly automated driving at urban intersections. Master's thesis, Institute for Human-Machine Communication, Technische Universität München, 2015.